2/6183
02

NASA TECHNICAL NOTE

NASA TN D-1644

c. 1

NASA TN D-1644

Corrected Copy

NOTE: This is CORRECTED COPY for NASA TN D-1644, originally released 6-12-1963.

ASCENT FROM THE LUNAR SURFACE

by Rowland E. Burns and Larry G. Singleton

George C. Marshall Space Flight Center
Huntsville, Ala.

NATIONAL AERONAUTICS AND SPACE ADMINISTRATION • WASHINGTON, D. C. • AUGUST 1965

NASA TN D-1644

Corrected Copy

ASCENT FROM THE LUNAR SURFACE

By Rowland E. Burns and Larry G. Singleton

George C. Marshall Space Flight Center
Huntsville, Ala.

NATIONAL AERONAUTICS AND SPACE ADMINISTRATION

For sale by the Clearinghouse for Federal Scientific and Technical Information
Springfield, Virginia 22151 – Price $5.00

TABLE OF CONTENTS

LIST OF ILLUSTRATIONS

List of Illustrations, Continued

LIST OF TABLES

List of Tables, Continued

List of Tables, Concluded

LIST OF SYMBOLS

A	Constant of Integration (tan I)
a	Semi-Major Axis of Orbit
$\mathbf{a}$	Vector Acceleration
C	Constant of Integration
E	Energy of Vehicle Per Unit Mass
$\mathcal{E}$	Eccentric Anomaly
e	Orbital Eccentricity
F	Fundamental Function Appearing in the Euler Equations
f	Indicates Functional Form
G	Universal Gravitation Constant
$\mathbf{g}$	Vector Acceleration of Gravity
g	Magnitude of Gravitational Acceleration
I	Orbital Inclination
I_{sp}	Specific Impulse
$\hat{i}, \hat{j}, \hat{k}$	Space Fixed Unit Vectors
J_i	One of the Various Constraint Equations Appearing in F ($i = 1,\ldots,6$)
K	Intermediate Quantities of Integration Process
l_1, l_2	Angular Momenta Per Unit Mass
M	Mass of the Moon
m	Vehicle Mass
$\dot{m}$	Vehicle Mass Flow Rate
R	Mass Ratio
$\mathbf{r}$	Radius Vector
r	Scalar Radius
s	Dummy Variable
$\mathbf{T}$	Thrust Vector
T	Scalar Thrust
t	Time
u	Characteristic Velocity and Dummy Integration Variable
$\hat{u}_r, \hat{u}_\theta, \hat{u}_\phi$	Vehicle Fixed Unit Vectors
$\mathbf{v}$	Vector Velocity
v	Scalar Velocity
x	Either of the Control Variables
y	Any of the Position or Velocity Coordinates

LIST OF SYMBOLS (Concluded)

a	Lunar Referenced Thrust-to-Weight Ratio
β	Central Angle Traversed During Ascent
Γ	Quantity to be Minimized Plus End Point Constraints
γ	Thrust Orientation Angle
Δ	Finite Increment in Numerical Integration
δ	Thrust Orientation Angle
η	True Anomaly in Transfer Orbit
θ	Latitude Position Angle of the Vehicle
κ	The Sum of the Quantity to be Maximized and all Applicable Constraints
λ_i	Time Dependent Lagrange Multipliers ($i = 1,\ldots,6$)
ν_i	Constant Lagrange Multipliers ($i=1, 2, 3$)
ρ	$\dot{r}$
σ	$\dot{\phi}$
ϕ	Longitudinal Position Angle of the Vehicle
χ	Azimuth
Ω	Angular Velocity of the Moon
ω	$\dot{\theta}$

SUBSCRIPTS

a	Apogee Condition
c	Cutoff Condition (Elliptical or Parabolic Orbits)
f	Final Condition in Low Circular Orbit
i	Dummy Subscript
m	Dummy Subscript
n	Dummy Subscript
p	Perigee Condition
s	Dummy Subscript
0	Initial Condition (Lunar Surface)
$\oplus$	Astronomical Subscript for the Earth
☾	Astronomical Subscript for the Moon

Arabic number subscripts indicate various integration constants or members of a set. Time derivatives are indicated by the dot notation.

ASCENT FROM THE LUNAR SURFACE

By
Rowland E. Burns
and
Larry G. Singleton

SUMMARY

The problem of three-dimensional optimal ascent from the lunar surface is discussed in the report using the techniques of variational calculus. The Moon is assumed to be spherical and rotating, but perturbational effects from all other bodies are neglected. Final orbital inclination is calculated under the assumption that the angular displacement of the moon is negligible during ascent. Only single stage vehicles are considered and are subdivided into propellant and final mass in orbit, i.e., there is no consideration of payload dependencies upon structural mass, etc. Furthermore, both the thrust and mass flow rate are assumed constant throughout the powered flight for a given vehicle.

SECTION I. EQUATIONS OF MOTION

The equations of motion will be derived in a spherical coordinate system. As shown in FIG 1, θ is the latitude angle (measured from the equatorial plane positive toward the north) and ϕ is the longitude angle (measured from the Moon's prime meridian positive in the direction of rotation). Let $\mathbf{r}$ be the radius vector from the center of the Moon to the vehicle. At the tip of the radius vector let us define an orthogonal system of unit vectors, $\hat{u}_r$, $\hat{u}_\theta$, $\hat{u}_\phi$. Let $\hat{u}_r$ be collinear with $\mathbf{r}$ (positive in the same direction as $\mathbf{r}$); let $\hat{u}_\theta$ be perpendicular to $\hat{u}_r$ in a plane containing $\hat{u}_r$ and the polar axis (positive in the direction of increasing θ): let $\hat{u}_\phi$ be perpendicular to both $\hat{u}_r$ and $\hat{u}_\theta$ and chosen to form a right-handed system with $\hat{u}_r$ and $\hat{u}_\theta$.

By trigonometry we can express $\hat{u}_r$, $\hat{u}_\theta$, and $\hat{u}_\phi$ in terms of $\hat{i}$, $\hat{j}$, and $\hat{k}$ as

$$\hat{u}_r = \cos\theta\cos\phi\ \hat{i} + \cos\theta\sin\phi\ \hat{j} + \sin\theta\ \hat{k} \tag{1}$$

$$\hat{u}_\theta = -\sin\theta\cos\phi\ \hat{i} - \sin\theta\sin\phi\ \hat{j} + \cos\theta\ \hat{k} \tag{2}$$

$$\hat{u}_\phi = -\sin\phi\ \hat{i} + \cos\phi\ \hat{j} \tag{3}$$

Equations (1) through (3) may be differentiated to yield

$$\dot{\hat{u}}_r = \dot{\theta}\ \hat{u}_\theta + \dot{\phi}\cos\theta\ \hat{u}_\phi \tag{4}$$

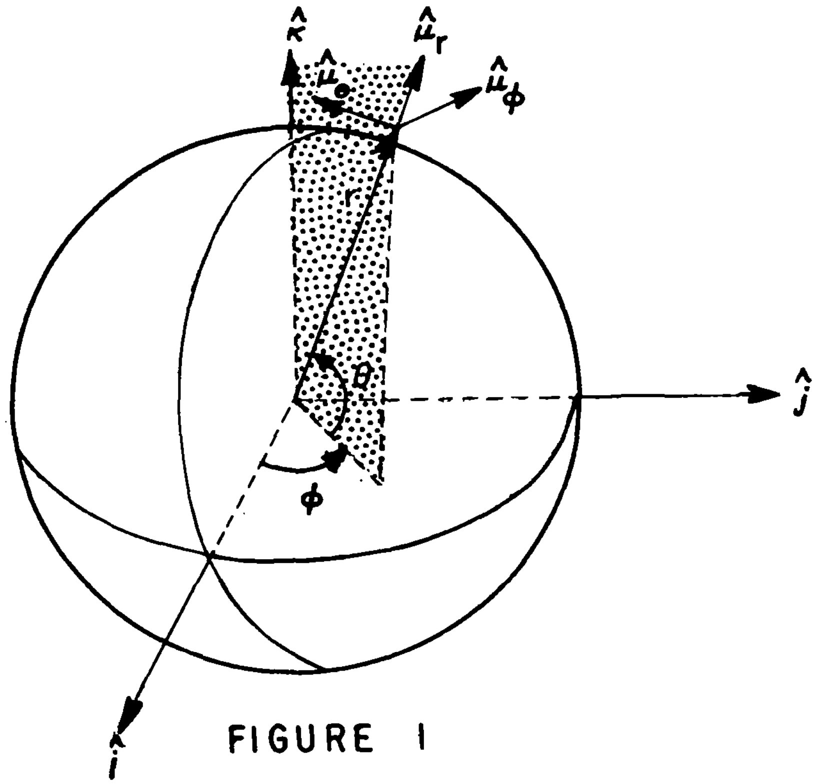

FIGURE 1

COORDINATE SYSTEM

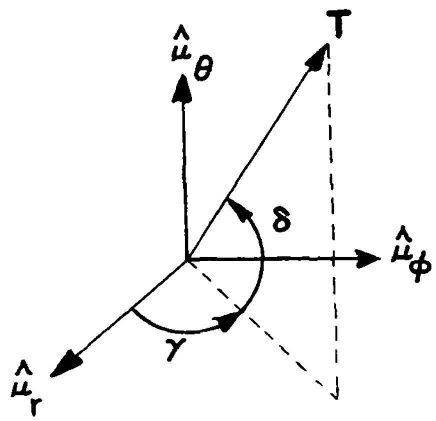

FIGURE 2

GIMBAL ANGLE COORDINATES

$$\dot{\hat{u}}_\theta = -\dot{\theta}\,\hat{u}_r - \dot{\phi}\,\sin\theta\,\hat{u}_\phi \tag{5}$$

$$\dot{\hat{u}}_\phi = -\,(\cos\theta\,\hat{u}_r - \sin\theta\,\hat{u}_\theta)\,\dot{\phi} \tag{6}$$

The radius vector, $\mathbf{r}$, may be expressed as

$$\mathbf{r} = r\,\hat{u}_r \tag{7}$$

The velocity may now be defined as

$$\mathbf{v} \equiv \dot{\mathbf{r}} = \dot{r}\,\hat{u}_r + r\,\dot{\hat{u}}_r = \dot{r}\,\hat{u}_r + r\,\dot{\theta}\,\hat{u}_\theta + r\,\dot{\phi}\cos\theta\,\hat{u}_\phi \tag{8}$$

The acceleration is given as the time derivative of velocity as

$$\begin{aligned} \mathbf{a} \equiv \dot{\mathbf{v}} &= \ddot{r}\,\hat{u}_r + 2\,\dot{r}\,\dot{\hat{u}}_r + r\,\ddot{\hat{u}}_r = \\ &[\ddot{r} - r(\dot{\theta}^2 + \dot{\phi}^2\cos^2\theta)]\,\hat{u}_r + [r\,\ddot{\theta} + 2\dot{r}\dot{\theta} + r\,\dot{\phi}^2\sin\theta\cos\theta]\,\hat{u}_\theta \\ &+ [r\,\ddot{\phi}\cos\theta - 2r\,\dot{\phi}\,\dot{\theta}\sin\theta + 2\,\dot{r}\,\dot{\phi}\cos\theta]\,\hat{u}_\phi \end{aligned} \tag{9}$$

The thrust vector, shown in FIG 2, has direction cosines γ and δ. From FIG 2 we may write the thrust as

$$\mathbf{T} = T\cos\delta\cos\gamma\,\hat{u}_r + T\sin\delta\,\hat{u}_\theta + T\cos\delta\sin\gamma\,\hat{u}_\phi \tag{10}$$

The remaining force, gravity, is always directed along the radius. If we denote the acceleration of gravity as $\mathbf{g}$, the mass of the Moon as M and the universal gravitational constant as G we can write

$$\mathbf{g} = -\frac{MG}{r^2}\,\hat{u}_r \tag{11}$$

By Newton's second law we may now write

$$m\,\mathbf{a} = \mathbf{T} + m\,\mathbf{g} \tag{12}$$

where m is the mass of the vehicle.

Inserting equations (9), (10) and (11) into (12), equating components, and dividing by m gives

$$\ddot{r} - r(\dot{\theta}^2 + \dot{\phi}^2\cos^2\theta) = \frac{T}{m}\cos\delta\cos\gamma - \frac{MG}{r^2} \tag{13}$$

$$r\,\ddot{\theta} + 2\,\dot{r}\,\dot{\theta} + r\,\dot{\phi}^2\sin\theta\cos\theta = \frac{T}{m}\sin\delta \tag{14}$$

$$r\,\ddot{\phi}\cos\theta - 2r\,\dot{\phi}\,\dot{\theta}\sin\theta + 2\,\dot{r}\,\dot{\phi}\cos\theta = \frac{T}{m}\cos\delta\sin\gamma \quad * \tag{15}$$

We may now state the problem as follows: Subject to constraints (13), (14) and (15), as well as specified initial and final conditions, determine the functions γ and δ as functions of time such that the maximum payload is injected into orbit.

---

* An alternative derivation of these equations is given in reference 4.

The solution of this problem requires the use of the calculus of variations. As equations (13), (14) and (15) now stand we would have to make use of second order Lagrange equations. To avoid this, we make the following kinematical substitutions: define

$$\dot{r} = \rho \tag{16}$$

$$\dot{\theta} = \omega \tag{17}$$

$$\dot{\phi} = \sigma \tag{18}$$

Substituting (16), (17) and (18) into (13), (14) and (15) and isolating all derivative terms gives

$$\dot{\rho} - \frac{T}{m} \cos \delta \cos \gamma + \frac{MG}{r^2} - r\ (\omega^2 + \sigma^2 \cos^2 \theta) = 0 \tag{19}$$

$$\dot{\omega} - \frac{T}{mr} \sin \delta + \frac{2\rho\omega}{r} + \sigma^2 \sin \theta \cos \theta = 0 \tag{20}$$

$$\dot{\sigma} - \frac{T}{m\, r \cos \theta} \cos \delta \sin \gamma - 2\omega\sigma \tan \theta + \frac{2\rho\sigma}{r} = 0 \tag{21}$$

One further relationship is required. Since the vehicle is assumed to have a constant mass flow rate, $\dot{m}$, we may write

$$m = m_0 - \dot{m}\, t \tag{22}$$

where m is the instantaneous mass, m_0 the initial mass, and t is the time since lift-off.

SECTION II. BOUNDARY CONDITIONS

Before proceeding to the actual variational formulation of the ascent, it will be advantageous to determine the boundary conditions associated with the problem. We shall denote initial values by a zero subscript and final values by an f subscript. At the initial point, $t = t_0 = 0$, the vehicle will be assumed to be at rest on the lunar surface. The launch longitude, ϕ_0, is arbitrary since we have assumed a spherical Moon. The simplest assumption on ϕ_0 is that it be chosen equal to zero. Furthermore, the first derivative of ϕ_0, $\dot{\phi}_0$, is simply given by the angular rate of rotation of the Moon which we shall denote by Ω. The latitude of launch, θ_0, is arbitrary.* Since $\hat{u}_\phi$ and $\hat{u}_\theta$ are perpendicular, the lunar rotation induces no motion in $\hat{u}_\theta$ direction and we may set $\dot{\theta}_0 = 0$.

In summary, we have the following set of initial conditions:

$$t = t_0 = 0 \tag{23}$$

---

* Except for $\pm \frac{\pi}{2}$. The coordinate system chosen is degenerate with respect to $\theta = \pm \frac{\pi}{2}$. If launches into polar orbit are of interest, the rotations which produce equations (1), (2) and (3) may be reversed in order of application. The resulting equations will be degenerate with respect to equatorial launch, $\theta_0 = 0$, but acceptable to study launch into polar orbits.

$$m = m_0 \tag{24}$$

$$r = r_0 = r_☾ \quad \text{(radius of the Moon)} \tag{25}$$

$$\dot{r} = \dot{r}_0 = \rho_0 = 0 \tag{26}$$

$$\theta = \theta_0 \quad \left(\text{arbitrary, but} \neq \frac{\pi}{2}\right) \tag{27}$$

$$\dot{\theta} = \dot{\theta}_0 = \omega_0 = 0 \tag{28}$$

$$\phi = \phi_0 = 0 \tag{29}$$

$$\dot{\phi} = \dot{\phi}_0 = \sigma_0 = \Omega \quad \text{(angular velocity of the Moon)} \tag{30}$$

At the final point we require a circular orbit of specified inclination. From equation (8) we may write the square of the velocity as

$$\mathbf{v} \cdot \mathbf{v} = \dot{\mathbf{r}} \cdot \dot{\mathbf{r}} = \dot{r}^2 + r^2 (\dot{\theta}^2 + \dot{\phi}^2 \cos^2 \theta) = \rho^2 + r^2(\omega^2 + \sigma^2 \cos^2 \theta) \tag{31}$$

The condition for circularity may be stated as

$$\dot{\mathbf{r}} \cdot \dot{\mathbf{r}} = \frac{MG}{r} \tag{32}$$

Thus

$$\rho^2 + r^2 (\omega^2 + \sigma^2 \cos^2 \theta) = \frac{MG}{r} \tag{33}$$

or

$$MG - r\rho^2 - r^3 (\omega^2 + \sigma^2 \cos^2 \theta) = 0 \tag{34}$$

But, for a circular orbit we must also have at cutoff

$$\dot{r} = \rho = 0 \tag{35}$$

Thus (34) becomes

$$MG - r^3 (\omega^2 + \sigma^2 \cos^2 \theta) = 0 \tag{36}$$

Equations (35) and (36) must be fulfilled at $t = t_f$.

We now digress slightly to determine the orbital inclination as a function of the cutoff parameters.

Assuming that the rotation of the Moon is negligible during ascent,* the final inclination is

---

* The actual amount of rotation is less than two tenths of a second of arc for the trajectories considered. Reference 5 presents a detailed treatment of the effect because of rotation of the primary on orbital inclination.

readily derivable from spherical trigonometry, if we assume the orbit to be planar. From FIG 3 we have

$$\tan I = \frac{\sqrt{\sin^2 (\theta_f - \theta_0) + \tfrac{1}{2} \sin 2\theta_0 \sin 2\theta_f (1 - \cos \theta_f)}}{\cos \theta_0 \cos \theta_f \sin \phi_f} \tag{37}$$

For $\theta_c = 0$ (equatorial launch) we have

$$\tan I = \frac{\tan \theta_f}{\sin \phi_f} \tag{38}$$

A more exact equation can be derived for non-planer trajectories by noting that the inclination is defined as the angle between the (instantaneous) orbital plane and the equator. A vector perpendicular to the orbital plane is

$$\mathbf{r} \times \mathbf{v} = r^2 \left(- \dot{\theta}\, \hat{u}_\phi + \dot{\phi} \cos \theta\, \hat{u}_\theta\right) \tag{39}$$

while a unit vector perpendicular to the equatorial plane is

$$\hat{k} = \sin \theta\, \hat{u}_r + \cos \theta\, \hat{u}_\theta \tag{40}$$

Then

$$\cos I = \frac{\hat{k} \cdot \mathbf{r} \times \mathbf{v}}{|\mathbf{r} \times \mathbf{v}|} = \frac{\dot{\phi} \cos \theta}{(\dot{\theta}^2 + \dot{\phi}^2 \cos^2 \theta)^{1/2}}$$

giving

$$\tan I = \frac{\sqrt{\dot{\theta}^2 + \dot{\phi}^2 \sin^2 \theta \cos^2 \theta}}{\dot{\phi} \cos^2 \theta} \tag{41}$$

Equation (37) will be used in the formulation rather than the more exact form given by equation (41). This will be justified as an acceptable simplification later in the report. (see p. 22, para. 2.)

SECTION III. VARIATIONAL FORMULATION

In this section we shall formulate the necessary conditions to maximize the gross weight placed in orbit. The problem may be rephrased to read: determine the optimum steering program that will minimize propellant consumption for ascent from a given initial point to a prescribed set of end conditions.

The mass of propellant expended may be written as

$$m_p = m_0 - m_f = m_0 - (m_0 - \dot{m}\, t_f) = \dot{m}\, t_f \tag{42}$$

Equation (42) shows that minimizing the propellant consumption is equivalent to minimizing the time required to attain orbit, as is intuitively apparent for the case of a vehicle with constant mass flow rate.

Let us now make the following definitions: define J_i $(i = 1,\ldots,6)$ as

$$J_1 = \dot{\rho} - \frac{T \cos \delta \cos \gamma}{m} + \frac{MG}{r^2} - r(\omega^2 + \sigma^2 \cos^2 \theta) = 0 \tag{43}$$

$$J_2 = \dot{\omega} - \frac{T \sin \delta}{m r} + \frac{2 \rho \omega}{r} + \sigma^2 \sin \theta \cos \theta = 0 \tag{44}$$

$$J_3 = \dot{\sigma} - \frac{T \cos \delta \sin \gamma}{m r \cos \theta} - 2 \omega \sigma \tan \theta + \frac{2 \rho \sigma}{r} = 0 \tag{45}$$

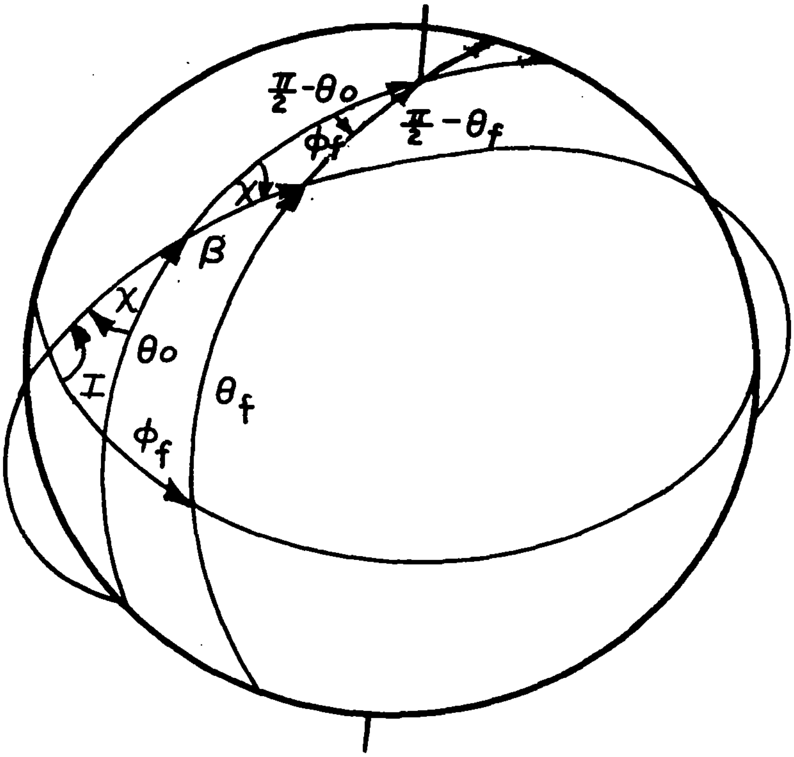

FIGURE 3

INCLINATION

$$J_4 = \dot{r} - \rho = 0 \tag{46}$$

$$J_5 = \dot{\theta} - \omega = 0 \tag{47}$$

$$J_6 = \dot{\phi} - \sigma = 0 \tag{48}$$

Let λ_i $(i = 1, \ldots, 6)$ be time dependent Lagrange multipliers and write

$$F = \lambda_i \; J_i \text{ (sum on } i) \tag{49}$$

Also, define

$$\Gamma = \dot{m}\, t_f + \nu_1 \left[M G - r_f^3 (\omega_f^2 + \sigma_f^2 \cos^2 \theta_f) \right] + \nu_2 \rho_f$$
$$+ \nu_3 \left[\tan I - \frac{\sqrt{\sin^2(\theta_f - \theta_0) + \frac{1}{2} \sin 2\theta_0 \sin 2\theta_f (1 - \cos \phi_f)}}{\cos \theta_0 \cos \theta_f \sin \phi_f} \right] \tag{50}$$

where the ν's are constant Lagrange multipliers.

Let y_s denote any member of the set ρ, ω, σ, r, θ, ϕ and x_s either of the control variables γ, δ.

We have the problem of finding the steering program, $\gamma(t)$, $\delta(t)$, which minimizes the propellant expenditure required to ascend from a given point on the lunar surface into a prespecified lunar orbit. This is equivalent to the problem stated in the following theorem which is proved in reference 2.

Given

$$\kappa = \Gamma + \int_{t_0}^{t_1} F(x_s, y_s, \dot{y}_s, t)\, dt \tag{51}$$

The necessary conditions to minimize κ are given by

$$\frac{\partial F}{\partial x_s} = 0 \text{ (all time values)} \tag{52}$$

$$\frac{\partial F}{\partial y_s} - \frac{d}{dt}\left(\frac{\partial F}{\partial \dot{y}_s}\right) = 0 \text{ (all time values)} \tag{53}$$

For any y_s's not fixed at $t = t_0$

$$\frac{\partial \Gamma}{\partial y_{s_0}} - \left(\frac{\partial F}{\partial \dot{y}_s}\right)_0 = 0 \tag{54}$$

For any y_s's not fixed at $t = t_f$

$$\frac{\partial \Gamma}{\partial y_{s_f}} + \left(\frac{\partial F}{\partial \dot{y}_{s_f}}\right) = 0 \tag{55}$$

For the final time point, $t = t_f$ (never fixed)

$$\frac{\partial \Gamma}{\partial t_f} - \left(\dot{y}_s \frac{\partial F}{\partial \dot{y}_s}\right)_f = 0 \quad \text{(sum on } s\text{)} \tag{56}$$

Since the form of equations (43) through (48) gives explicit representation for the $\dot{y}_s$ terms we find that

$$\frac{\partial F}{\partial \dot{y}_s} = \lambda_s \tag{57}$$

and

$$\frac{d}{dt}\left(\frac{\partial F}{\partial \dot{y}_s}\right) = \dot{\lambda}_s \tag{58}$$

Equation (53) may be rewritten in the form

$$\dot{\lambda}_s - \left(\frac{\partial F}{\partial y_s}\right) = 0 \tag{59}$$

SECTION IV. VARIATIONAL EQUATIONS

The expression for F, defined by equation (49), is given in expanded form by

$$\begin{aligned} F = {} & \lambda_1 \left[\dot{\rho} - \frac{T \cos\delta \cos\gamma}{(m_0 - \dot{m} t)} + \frac{MG}{r^2} - r(\omega^2 + \sigma^2 \cos^2\theta)\right] \\ & + \lambda_2 \left[\dot{\omega} - \frac{T \sin\delta}{(m_0 - \dot{m} t) r} + \frac{2\rho\omega}{r} + \sigma^2 \sin\theta \cos\theta\right] \\ & + \lambda_3 \left[\dot{\sigma} - \frac{T \cos\delta \sin\gamma}{(m_0 - \dot{m} t) r \cos\theta} - 2\omega\sigma \tan\theta + \frac{2\rho\sigma}{r}\right] \\ & + \lambda_4 [\dot{r} - \rho] + \lambda_5 [\dot{\theta} - \omega] + \lambda_6 [\dot{\phi} - \sigma] \end{aligned} \tag{60}$$

Applying equation (52) to the control variable γ

$$\frac{\partial F}{\partial \gamma} = \frac{T}{(m_0 - \dot{m} t)} \cos\delta \left[\lambda_1 \sin\gamma - \frac{\lambda_3}{r \cos\theta} \cos\gamma\right] = 0 \tag{61}$$

For a constant thrust single stage vehicle

$$\frac{T}{(m_0 - \dot{m} t)} \neq 0 \tag{62}$$

Thus we must have either

$$\cos\delta = 0 \tag{63}$$

or

$$\lambda_1 \sin \gamma - \frac{\lambda_3}{r \cos \theta} \cos \gamma = 0 \tag{64}$$

Equation (63) cannot be true at $t = t_0$ since polar orbits have been ruled out by our choice of the coordinate system. At other time points where equation (63) is not fulfilled* we have

$$\tan \gamma = \frac{\lambda_3}{\lambda_1 r \cos \theta} \tag{65}$$

The Euler equation corresponding to the control variable δ is

$$\frac{\partial F}{\partial \delta} = \frac{T}{(m_0 - \dot{m} t)} \left[\lambda_1 \sin \delta \cos \gamma - \frac{\lambda_2}{r} \cos \delta + \frac{\lambda_3}{r \cos \theta} \sin \delta \sin \gamma \right] = 0 \tag{66}$$

or

$$\left[\lambda_1 \cos \gamma + \frac{\lambda_3}{r \cos \theta} \sin \gamma \right] \sin \delta = \frac{\lambda_2}{r} \cos \delta \tag{67}$$

From equation (65)

$$\sin \gamma = \pm \frac{\lambda_3}{\sqrt{\lambda_3^2 + (\lambda_1 r \cos \theta)^2}} \tag{68}$$

and

$$\cos \gamma = \pm \frac{\lambda_1 r \cos \theta}{\sqrt{\lambda_3^2 + (\lambda_1 r \cos \theta)^2}} \tag{69}$$

Inserting (68) and (69) into (67) and solving for $\tan \delta$ gives

$$\tan \delta = \frac{\pm \lambda_2 \cos \theta}{\sqrt{\lambda_3^2 + (\lambda_1 r \cos \theta)^2}} \tag{70}$$

Since they will be needed later we solve equation (70) for

$$\sin \delta = \frac{\pm \lambda_2 \cos \theta}{\sqrt{(\lambda_1^2 r^2 + \lambda_2^2) \cos^2 \theta + \lambda_3^2}} \tag{71}$$

and

$$\cos \delta = \pm \sqrt{\frac{\lambda_1^2 r^2 \cos^2 \theta + \lambda_3^2}{(\lambda_1^2 r^2 + \lambda_2^2) \cos^2 \theta + \lambda_3^2}} \tag{72}$$

---

* During the numerical integration of the set of equations that will result, the probability that equation (63) will actually be fulfilled is negligible since $\cos \delta = 0$ occurs only for discrete points. It is a simple matter to insert a flag into the computer program to indicate that equation (63) is satisfied and thus equation (64) is no longer fulfilled. With this understanding (which is sloppy mathematics, but standard engineering) we may proceed under the assumption that equation (63) is never satisfied.

Turning now to the application of equation (59) we consider the variables y_s in the order $\rho, \omega, \sigma, r, \theta, \phi$.

$$\dot{\lambda}_1 - \frac{\partial F}{\partial \rho} = \dot{\lambda}_1 - \frac{2}{r}(\lambda_2 \omega + \lambda_3 \sigma) + \lambda_4 = 0 \tag{73}$$

$$\dot{\lambda}_2 - \frac{\partial F}{\partial \omega} = \dot{\lambda}_2 + 2(\lambda_1 r\omega - \frac{\lambda_2 \rho}{r} + \lambda_3 \sigma \tan \theta) + \lambda_5 = 0 \tag{74}$$

$$\dot{\lambda}_3 - \frac{\partial F}{\partial \sigma} = \dot{\lambda}_3 + 2 [(\lambda_1 r \cos \theta - \lambda_2 \sin \theta) \sigma \cos \theta + \lambda_3 (\omega \tan \theta - \frac{\rho}{r})] + \lambda_6 = 0 \tag{75}$$

$$\dot{\lambda}_4 - \frac{\partial F}{\partial r} = \dot{\lambda}_4 + \lambda_1 \left[\frac{2MG}{r^3} + (\omega^2 + \sigma^2 \cos^2 \theta)\right] + \frac{2\rho}{r^2} [\lambda_2 \omega + \lambda_3 \sigma]$$
$$- \frac{T}{(m_0 - \dot{m} t) r^2} \left[\lambda_2 \sin \delta + \frac{\lambda_3 \cos \delta \sin \gamma}{\cos \theta}\right] = 0 \tag{76}$$

$$\dot{\lambda}_5 - \frac{\partial F}{\partial \theta} = \dot{\lambda}_5 - \sigma^2 [2\lambda_1 r \sin \theta \cos \theta + \lambda_2 (\cos^2 \theta - \sin^2 \theta)]$$
$$+ 2 \lambda_3 \omega \sigma \sec^2 \theta + \left[\frac{T \cos \delta \sin \gamma}{(m_0 - \dot{m} t) r}\right] \lambda_3 \tan \theta \sec \theta = 0 \tag{77}$$

$$\dot{\lambda}_6 - \frac{\partial F}{\partial \phi} = \dot{\lambda}_6 = 0 \tag{78}$$

Equation (78) may immediately be integrated to give

$$\lambda_6 = C_1 \tag{79}$$

where C_1 is some constant of integration.

SECTION V. SUMMARY OF ANALYTICAL RESULTS

The equations of motion, (43) through (48) along with the equations of the turn program, (65) and (70), and equations (73) through (77) and (79) (which determine the Lagrange multipliers that are included in the turn program), completely specify the optimal three-dimensional steering program of a single-stage constant-thrust vehicle except for initial conditions. While the initial conditions specifying position and velocity at $t = t_0$ as well as desired end conditions may easily be stated, the initial values of $\lambda_1, \ldots, \lambda_6$ are very difficult to determine. Once these values are chosen, no degree of freedom is left in the system. The determination of $(\lambda_1)_0, \ldots, (\lambda_6)_0$ to obtain desired end conditions is discussed below.

The equations developed in the preceding sections may be reduced in number by inserting the expressions for ρ, ω, σ from equations (16), (17) and (18) into equations (73) through (77) and eliminating the control variables (γ, δ) by use of equations (65) and (70).* Equation (79)

* The sign ambiguity involved in the sine and cosine functions of the control variables will be resolved by choosing an upward launch, toward the north, in the direction of the lunar rotation. With these restrictions the positive sign should be chosen in each case. Further considerations of sign choice will be given in Section VI.

will be used to eliminate λ_6 from equation (75).

Before making the above substitutions, one further step will be taken to eliminate m_0 from the equations of motion.

The term for thrust to mass ratio may be written

$$\frac{T}{m_0 - \dot{m}\,t} = \frac{(T/m_0)}{1 - \frac{\dot{m}}{m_0}\,t} \tag{80}$$

Now the mass flow rate, $\dot{m}$, is related to specific impulse, I_{sp}, by the equation

$$\dot{m} = \frac{T}{(g_0)_\oplus\, I_{sp}} \tag{81}$$

where $(g_0)_\oplus$ is the acceleration of gravity at the Earth's surface. Substituting equation (81) into equation (80) we have

$$\frac{T}{m_0 - \dot{m}\,t} = \frac{(T/m_0)}{1 - \frac{T}{(g_0)_\oplus\, I_{sp}}\,\frac{t}{m_0}} = \frac{(T/m_0)}{1 - \frac{T}{m_0}\,\frac{t}{(g_0)_\oplus\, I_{sp}}} \tag{82}$$

Dividing numerator and denominator of equation (82) by the acceleration of gravity at the Moon's surface, $(g_0)_☾$, we have

$$\frac{T}{m_0 - \dot{m}\,t} = \frac{[\,T/m_0\,(g_0)_☾\,]}{\frac{1}{(g_0)_☾} - \frac{T}{m_0\,(g_0)_☾}\,\frac{t}{(g_0)_\oplus\, I_{sp}}} \tag{83}$$

The term $[\,T/m_0\,(g_0)_☾\,]$ can now be recognized as the initial thrust-to-weight of the vehicle evaluated at the lunar surface. We shall abbreviate this term as a. Thus

$$\frac{T}{m_0 - \dot{m}\,t} = \frac{a}{\frac{1}{(g_0)_☾} - \frac{a}{(g_0)_\oplus\, I_{sp}}\,t} = \frac{a\,(g_0)_☾\,(g_0)_\oplus\, I_{sp}}{(g_0)_\oplus\, I_{sp} - a\,(g_0)_☾\,t} \tag{84}$$

The right-hand member of equation (84) is preferable to the left-hand member since it shows direct dependence on the important parameters of initial thrust-to-weight and specific impulse. The left-hand member masks this dependence by the inclusion of the lift-off mass.

Performing the above indicated modifications, we now summarize the results of the preceding work with the following set of equations as the final form of equations (13) through (15) and (73) through (78).

$$\ddot{r} = \left[\frac{a(g_0)_☾\,(g_0)_\oplus\, I_{sp}}{(g_0)_\oplus\, I_{sp} - a\,(g_0)_☾\,t}\right] \frac{\lambda_1 r\cos\theta}{\sqrt{(\lambda_1^2 r^2 + \lambda_2^2)\cos^2\theta + \lambda_3^2}} - \frac{MG}{r^2} + r(\dot{\theta}^2 + \dot{\phi}^2\cos^2\theta) \tag{85}$$

$$\ddot{\theta} = \left[\frac{a(g_0)_{\langle} (g_0)_{\oplus} I_{sp}}{(g_0)_{\oplus} I_{sp} - a(g_0)_{\langle}\, t}\right] \frac{\lambda_2 \cos\theta}{r\sqrt{(\lambda_1^2 r^2 + \lambda_2^2)\cos^2\theta + \lambda_3^2}} - \frac{2\dot{r}\dot{\theta}}{r} - \dot{\phi}^2 \sin\theta\cos\theta \tag{86}$$

$$\ddot{\phi} = \left[\frac{a(g_0)_{\langle} (g_0)_{\oplus} I_{sp}}{(g_0)_{\oplus} I_{sp} - a(g_0)_{\langle}\, t}\right] \frac{\lambda_3}{r\cos\theta\sqrt{(\lambda_1^2 r^2 + \lambda_2^2)\cos^2\theta + \lambda_3^2}} + 2\dot{\theta}\dot{\phi}\tan\theta - \frac{2\dot{r}\dot{\phi}}{r} \tag{87}$$

$$\dot{\lambda}_1 - \frac{2}{r}(\lambda_2\dot{\theta} + \lambda_3\dot{\phi}) + \lambda_4 = 0 \tag{88}$$

$$\dot{\lambda}_2 + 2\left(\lambda_1 r\dot{\theta} - \frac{\lambda_2\dot{r}}{r} + \lambda_3\dot{\phi}\tan\theta\right) + \lambda_5 = 0 \tag{89}$$

$$\dot{\lambda}_3 + 2\,[(\lambda_1 r\cos\theta - \lambda_2\sin\theta)\dot{\phi}\cos\theta + \lambda_3(\dot{\theta}\tan\theta - \dot{r}/r)] + C_1 = 0 \tag{90}$$

$$\dot{\lambda}_4 + \lambda_1\left[\frac{2MG}{r^3} + (\dot{\theta}^2 + \dot{\phi}^2\cos^2\theta)\right] + \frac{2\dot{r}}{r^2}(\lambda_2\dot{\theta} + \lambda_3\dot{\phi})$$
$$-\left[\frac{a(g_0)_{\langle} (g_0)_{\oplus} I_{sp}}{(g_0)_{\oplus} I_{sp} - a(g_0)_{\langle}\, t}\right]\left[\frac{(\lambda_2^2\cos^2\theta + \lambda_3^2)}{r^2\cos\theta\sqrt{(\lambda_1^2 r^2 + \lambda_2^2)\cos^2\theta + \lambda_3^2}}\right] = 0 \tag{91}$$

$$\dot{\lambda}_5 - \dot{\phi}^2(\lambda_1 r\sin 2\theta + \lambda_2\cos 2\theta) + 2\lambda_3\dot{\theta}\dot{\phi}\sec^2\theta$$
$$+ \left[\frac{a(g_0)_{\langle} (g_0)_{\oplus} I_{sp}}{(g_0)_{\oplus} I_{sp} - a(g_0)_{\langle}\, t}\right]\left[\frac{\lambda_3^2\tan\theta\sec\theta}{r\sqrt{(\lambda_1^2 r^2 + \lambda_2^2)\cos^2\theta + \lambda_3^2}}\right] = 0 \tag{92}$$

The above equations can be further reduced in number by differentiation of equations (88) and (89) followed by insertion of the expressions for $\dot{\lambda}_4$ and λ_5. This alternative form is shown in Appendix A.

SECTION VI. CHOICE OF SIGN CONVENTION

Equations (68), (69), (71) and (72) indicate that there is a certain amount of freedom in choosing the sign convention to be adopted in numerical integration of the equations of motion. This choice can be investigated either by consideration of the physical parameters (trigonometric functions of the gimbal angles) or the mathematical parameters (Lagrange multipliers) with equivalent results. We choose the former method.

We may consider all possible cases by giving the functions cos δ, sin δ, sin γ, cos γ either plus or minus signs in all possible combinations, and listing the results in tabular form. For reasons that will become apparent below, we also list the product cos δ cos γ.

Case Number	$\cos\delta$	$\sin\delta$	$\sin\gamma$	$\cos\gamma$	$\cos\delta\cos\gamma$
1	+	+	+	+	+
2	+	+	+	–	–
3	+	+	–	+	+
4	+	+	–	–	–
5	+	–	+	+	+
6	+	–	+	–	–
7	+	–	–	+	+
8	+	–	–	–	–
9	–	+	+	+	–
10	–	+	+	–	+
11	–	+	–	+	–
12	–	+	–	–	+
13	–	–	+	+	–
14	–	–	+	–	+
15	–	–	–	+	–
16	–	–	–	–	+

Insertion of the sign conventions 9 through 16 into equations 85 through 92 show that they correspond, mathematically, to cases 4, 3, 2, 1, 8, 7, 6, and 5, respectively. Thus we immediately reduce the number of cases to be considered by a factor of two.

Furthermore, in cases 2, 4, 6, and 8 the sign of the product $\cos\delta\cos\gamma$ is negative on the radial thrust term. If the initial value of λ_1 were chosen negative then the resultant force would be in alignment with the positive radius vector for at least a portion of the powered flight. A few numerical experiments were conducted to check this possibility, and it was found that the corresponding trajectories did exist.

An analagous situation is found in cases 5 and 7. For case 5 we can obtain a positive inclination by first setting the thrust term on the $\ddot{\theta}$ equation negative (the signs on the thrust terms are, of course, arbitrary) and then forcing a negative value of $\sin\delta$. Thus, we obtain another possible solution.

Finally, cases 1 and 3 will be considered. Case 1 is the most physically reasonable of possible choices. The first of these two cases is equivalent to firing with the planetary rotation to the north in an outward direction (i.e., in the direction of increasing radius vector). Case 3, with $\tan\delta$ negative, corresponds exactly, except that we now fire against the planetary rotation.

The choice of which of the above cases to be studied will now be discussed. Cases 1 and 3 are, of course, of the most importance. Case 1 is studied in detail and case 3 was given less consideration. In order to check the possible solutions corresponding to the other remaining cases, case 5 was carried out in equivalent detail to case 1 and case 7 in a manner similar to case 3. Cases 2, 4, 6, and 8 were given only a cursory check and the results are not presented.

Another point of consideration before closing this section is symmetry under θ reflection. From physical considerations it is fairly obvious that if the initial latitude is θ_0 and an orbit of inclination I achieved from ascent from this point, the equivalent physical results must be obtained if the launch latitude is $-\theta_0$ and the resulting inclination is $-I$. As is well known, the free-flight equations possess this symmetry. We may then require that the powered-flight equations, including the equations governing the Lagrange multipliers, possess this same symmetry.

The problem may be approached by replacing θ by $-\theta$ in equations (85) through (92) and observing the results. This procedure shows that our principle holds only if the multipliers λ_1, λ_3, and λ_4 are symmetric with respect to θ reflection, while the multipliers λ_2 and λ_5 are antisymmetric with respect to this reflection. This result might have been predicted since the latter two multipliers are those associated with non-planar flight.

We may now essentially double the amount of data available from our results by the above principle. Suppose, for example, that we have numerical data corresponding to the initial conditions $\theta = 0$, and a final inclination of 5°. We may then obtain identical results by reversing the sign on the inclination and the signs on the Lagrange multipliers λ_2 and λ_5.

In the numerical data presented below, the sign convention used in preparation of the data will be specified by use of the case numbers given above, i.e., "sign convention for case number 1," "sign convention for case number 3," etc.

One final remark is in order before proceeding to the numerical integration procedure. A comment was made above about "forcing" a negative value of sin δ, and the immediate question that comes to mind is just how this may be done in practice.

More generally we may consider the problem of arbitrarily fixing the signs of the trigonometric functions of the two thrust orientation angles. We consider the signs of the sines to demonstrate the involved principles. Equation (68) shows that sin γ will be positive or negative according to the sign of λ_3 if the radical is always taken as positive. Likewise, for cos θ positive and the radical of equation (71) positive, the sign of sin δ will agree with the sign of λ_2.

Thus the problem is reduced to fixing the signs of λ_2 and λ_3. The procedure for doing this is not immediately obvious. It was found, numerically, that λ_5 and C_1 exerted such strong dominance over all other terms in equations (89) and (90) that λ_2 and λ_3 always have the opposite sign of λ_5 and C_1, respectively. The large values of λ_5 that were necessary to give even low inclinations, as well as the large value of C_1 that was chosen, ensured that this sign asymmetry was maintained throughout the powered flight.

In summary, then, reversing the sign of the initial value of λ_5 reverses the sign on the final value of the inclination with no other changes. Reversing the sign of C_1 changes the direction of launch with respect to the lunar rotation. In the latter case other parameters also change, because there does not exist an east-west symmetry on a rotating sphere.

VII. NUMERICAL INTEGRATION PROCEDURE

Since the resulting set of Euler equations, along with the equations of motion, could not be solved by analytical methods it was necessary to resort to numerical integration techniques.

In order to obtain some feel for the results that can be obtained, we note that at the initial point the variables r_0, $\dot{r}_0$, θ_0, $\dot{\theta}_0$, ϕ_0, $\dot{\phi}_0$, λ_1^0, λ_2^0, λ_3^0, λ_4^0, λ_5^0, C_1, I_{sp}, and a (thrust-to-weight ratio) must be specified. The first six of these (r, $\dot{r}$, θ, $\dot{\theta}$, ϕ, $\dot{\phi}$) are fixed by our choice of launch site. The final two (I_{sp} and a) are fixed either by technological feasibility or optimization criterion.

The λ's are further restricted by two considerations. Once λ_1 has been chosen, the lift-off angles γ_0 and δ_0 then determine λ_2 and λ_3. Furthermore, one of the multipliers acts only as a scaling factor since equations (88) through (92) are homogeneous*

Thus, we are left with only λ_1, λ_4, and λ_5 as arbitrary initial parameters.

At the end point there are numerous conditions that it would be convenient to specify. Restricting our discussion to circular orbits,** the first such requirement is that circular energy is obtained. Secondly, the requirement that $\dot{r}_f = 0$ must be invoked to insure circularity (this corresponds to a flight path angle of 90 degrees from the vertical in body-fixed coordinates). Thirdly, the requirements on the final orbital inclination must be attained. From stability of guidance considerations the thrust vector must be aligned with the velocity vector at injection. (This puts endpoint requirements on γ_f and δ_f.) Finally, the altitude should be a predetermined variable.

We are apparently faced with the problem of mapping three initial conditions into six end point conditions. One further degree of freedom is available, however, namely the choice of cutoff time. This parameter serves very nicely to determine circular energy.

The problem may now be stated as:

Given r_0, $\dot{r}_0$, θ_0, $\dot{\theta}_0$, ϕ_0, $\dot{\phi}_0$, γ_0 (or λ_3), δ_0 (or λ_2), I_{sp} and a, determine

λ_1, λ_4, λ_5 and t_f

such that cutoff energy, zero radial velocity, specified inclination, specified altitude, and final alignment of the thrust vector with the velocity vector are obtained.*** By elementary considerations it is not possible to map four initial conditions into six end point conditions.

In practice, circular energy, zero radial velocity and desired inclination are always required. This leaves one free parameter, and a choice of the most desirable remaining end point to be obtained must be made.****

It is interesting to note that there is not a one-to-one control correspondence between initial and final conditions. That is, one cannot state that λ_1 controls final radial velocity, λ_4 controls final gamma, etc. In reality, the situation is much more complex and there is a complicated interrelationship between initial conditions and end conditions. The method employed was, first of all, to check which initial parameters could iterate which end conditions. It was found that λ_1 could iterate final altitude, radial velocity, or final gamma. λ_4 was good for isolating final radial

---

* The multiplier chosen to be arbitrary was C_1 (or λ_6). As was noted previously, a negative C_1 corresponds to firing with the lunar rotation and positive C_1 corresponds to firing against the lunar rotation. No orbit could be attained with $C_1 = 0$. The value chosen for C_1 was -10^5.

** The problem of non-circular orbits will be discussed in APPENDIX B.

*** It is very important to realize, at this point, that *the angles* ϕ *and* θ *at cutoff* (ϕ_f, θ_f) *are fixed (though unknown).* This fact is very important in connection with the necessary end point conditions.

****From this point on we refer to isolating final gamma ($= \pi/2$ in all cases) as an equivalence to isolating the angle between the thrust and velocity vectors.

velocity, less adept at final altitude and very poor for final gamma. Only λ_5 was used to determine inclination--and it was used for nothing else. Checks were also made to determine the applicability of λ_3 and C_1 as iteration parameters. λ_3 was found to isolate final gamma and nothing else. C_1 can be used as an iteration parameter (if another λ is frozen) and was found to be acceptable (but not good) for isolating final radial velocity and final gamma, but very poor for isolating final altitude.

The iteration parameters were then chosen and a "forced" one-to-one correspondence was used. For example, λ_1 was chosen to isolate a final gamma of 90 degrees, λ_4 was chosen to force the final radial velocity to be zero, and λ_5 was chosen to determine final inclination. Once the desired gamma was obtained in a first order isolation, the computer incremented λ_4, reconverged λ_1, etc., until both final gamma and radial velocity matched specified end conditions. Then the inclination was attached in a third order isolation. Thus, one-to-one correspondence is only a surface artiface and the computer, in reality, searches out a single three-dimensional initial point which corresponds to the prespecified final point. This method is generally referred to as the "cruddy creeper". Another method of approach is to attempt a complete run with guessed initial multipliers and record the end conditions. One of the multipliers is then modified, and the end conditions again recorded. The multipliers are then reset to the initial guesses and the above procedure is repeated until all multipliers have been changed and the results noted. The machine then performs a multi-dimensional interpolation for the initial conditions which yield the desired end conditions. This procedure was finally chosen in preference to the "cruddy creeper" since its convergence time is between one and two orders of magnitude faster.

It was found that there also exist initial values of the thrust-to-weight ratio which produce maximum values for the mass fraction, if the final altitude is specified, and maximum final altitudes, if the final value of gamma is specified to be 90°. Besides the isolation of an "optimum" thrust-to-weight ratio, it was also found that there exist initial values of the lift-off angles, gamma and delta, which maximize mass ratio for the second sort of trajectory. We could thus have trajectories which isolate four end conditions and three initial conditions. Such trajectories would require a prohibitively long running time, even on the fastest available computers.

The trajectories which maximize mass fraction via choice of initial thrust-to-weight ratio are relatively easy to isolate since the maxima are rather flat and the burning times are short. The isolation of the thrust-to-weight ratio which maximizes final altitude (for the case of $\gamma_f = \pi/2$) are extremely difficult to isolate and these trajectories are quite unstable. The isolation of initial values of gamma and delta which maximize the mass fraction at cutoff is also difficult but is of less practical importance.

The choice of the time increment used in numerical integration is a very important quantity. A previous version of this report (Ref. 3) presented data obtained by using a value of 64 seconds for numerical integration. (These data are included here.) This time increment was initially chosen by comparison of trajectories run with varying time increments. Unfortunately, the initial thrust-to-weight ratio used for the comparative runs was low and false results as to the relative accuracies were obtained. The difference in end conditions has since been found to vary strongly with high time increments for trajectories which have a high initial thrust-to-weight ratio. This is because these trajectories have shorter burning times and thus fewer segments are used during the numerical integration than in the low initial thrust-to-weight ratio cases.

Thus far the problem is simply one of accuracy. The final values of the several variables corresponding to the higher thrust-to-weight ratios were found to be enough in error that false maxima were introduced into the resultant graphs of mass fraction (ratio of initial mass to final mass) as a function of initial thrust-to-weight ratio for those trajectories which align thrust and velocity at cutoff.

Restricting ourselves to this case, for the moment, trajectories were studied which maximized m_f/m_0 as a function of T/W_0 for various values of the time increment used in numerical integrations. FIG 4 shows the results of this study. It may be seen that, as the time increment approaches zero, the optimum initial lunar thrust-to-weight ratio apparently becomes unbounded.

This result may be predicted in retrospect. As is well known, the optimal burning program to maximize mass fraction (exclusive of atmospheric drag) is impulsive. We might thus expect that if the vehicle is launched in the direction of the lunar rotation at an arbitrarily high thrust level, we would obtain a maximum mass fraction, since gravity losses have vanished. It is not immediately apparent that this argument is applicable since the cases treated assume non-horizontal lift-off and it is not possible to launch in the direction of lunar rotation. It should be remembered, however, that the equations of motion are derived under the assumption of a point vehicle, which is equivalent to assuming vanishing moments of inertia. The turning rate of the vehicle is, thus, governed by only the momentum of the point mass, which is negligible at lift-off.

The above result is, then, the consequence of the assumption of a point vehicle in any area where this approximation is invalid. The question arises as to whether the mass fraction may be maximized via a choice of initial thrust-to-weight ratio if the altitude is prespecified rather than alignment of thrust and velocity vectors. Such maxima were found to exist. In this case these maxima were essentially independent of the time increment used in integration for values of the increment of four seconds or less.

The actual time increment finally chosen was four seconds. This gave accuracy of at least five significant figures by comparison with time increments of one second. The numerical data given in a previous version of this report (Ref. 3) were run at a time increment of 64 seconds and are also included. The purpose for this inclusion is to provide a large amount of useful data that is sufficiently accurate for preliminary design purposes. A duplication of these data at a lower time increment was made only for cases which were considered to be of particular importance. Furthermore, the entire set of data which deals with ascent to a 15-kilometer orbit was not included in the previous publication.

The technological range considered was chosen to give a broad brush outline of what values may be of interest rather than a detailed study of a given configuration. The specific impulses considered were 300, 350, 400, and 450 sec. The thrust-to-weight ratios chosen were 1, 1.1, 1.3, 1.5, 2, 3, 4, 5, 6, and 7 (lunar reference).*

The launch site was arbitrarily chosen to be the lunar equator at the lunar prime meridian ($\phi_0 = \theta_0 = 0$) and the final orbital inclination was chosen to be 5 degrees.

The lift-off angle, γ_0, was varied from 0° to 40° in steps of 10°. The angle δ was always set equal to zero. For the special case of $\gamma_0 = 0°$, the initial thrust-to-weight ratio was considered for the range between 1 and 2.

A few cases are given in the next section to illustrate the procedure for obtaining orbits of inclination higher than 5°, as well as the effects of non-equatorial launch.

Below is a resumé of the constants used in the program. These values were the best available at inception of this report, but probably can be improved upon due to more recent measurements of various constants.

$$(MG)_{☾} = 4.899996 \times 10^{12} \; m^3/\text{sec}^2$$
$$(r_0)_{☾} = 1.738 \times 10^6 \; m$$
$$(g_0)_{☾} = 1.622169 \; m/\text{sec}^2$$
$$(g_0)_{\oplus} = 9.81 \; m/\text{sec}^2$$

APPENDIX C shows a block diagram of the final form of the computer program.

---

* To convert from lunar referenced thrust-to-weight to a corresponding value referenced to the Earth's surface it is necessary only to multiply by

$$g_{☾}/g_{\oplus} = .1653587$$

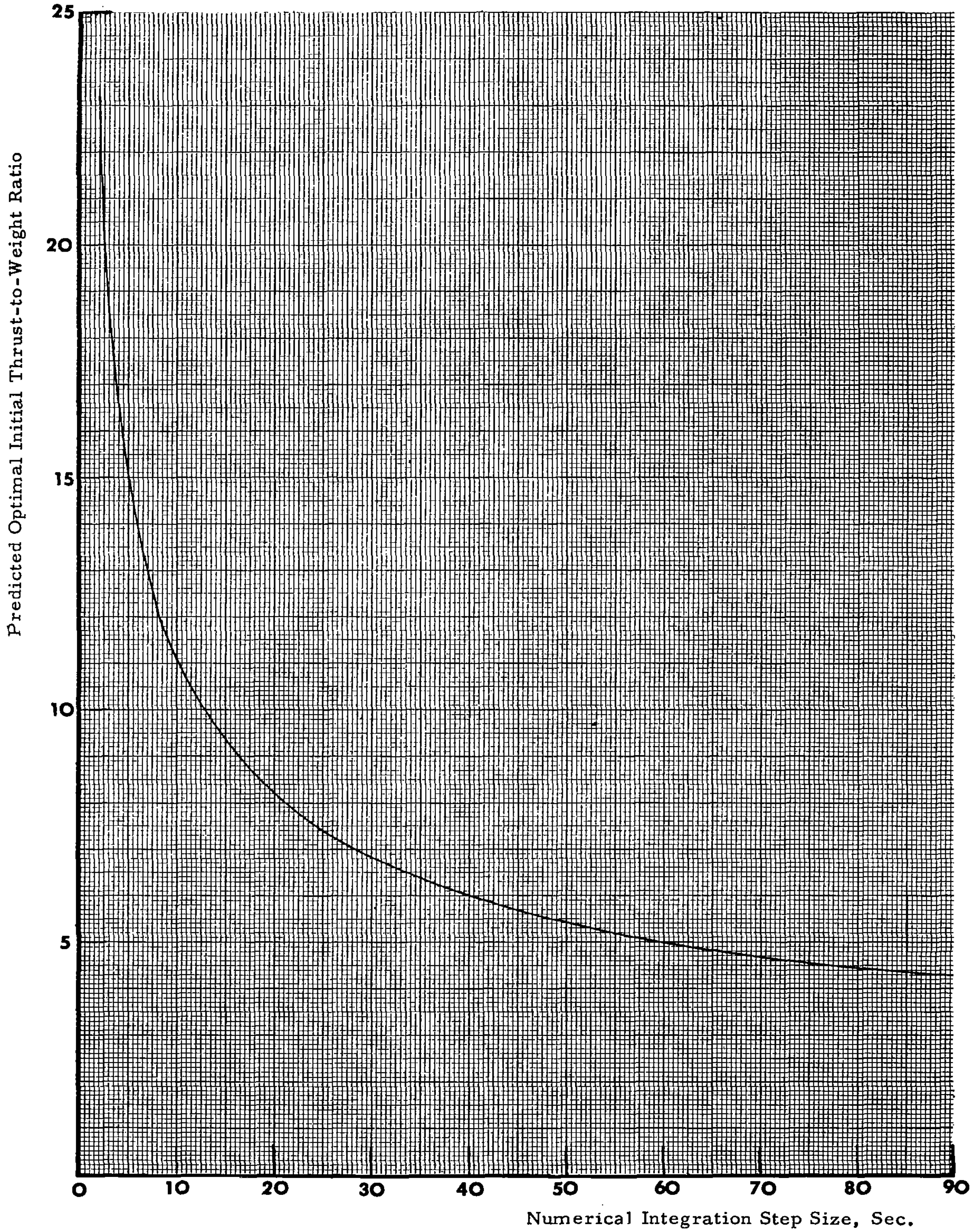

FIGURE 4. PREDICTED OPTIMAL INITIAL THRUST-TO-WEIGHT RATIO VS TIME INCREMENT USED IN NUMERICAL INTEGRATION; THRUST AND VELOCITY VECTORS ALIGNED AT ORBIT.

SECTION VIII. NUMERICAL RESULTS

In this section, we present the results of numerical integrations performed on the set of simultaneous equations (85) through (92). These results, contained in Tables 1 through 52 will be prefaced by a short introduction on the assumptions made, and an explanation of the purpose of each Table.

A few general remarks can be made about the Tables:

1. The initial value of the longitude, ϕ_0, is always set equal to zero. Since the assumption of rotational symmetry was invoked in the derivation of the equations of motion, this in no way further restricts the validity of our solutions.
2. With the exception of Table 34, the initial value of the latitude, θ_0, is always zero.
3. The initial value of the thrust orientation angle δ is always zero.
4. With the exception of Tables 1 through 11, 35, 36, 37, 50, 51, and 52 the final value of the thrust orientation angle γ is always $\pi/2$. (The final value of δ was usually within 2° of the value of the inclination angle.)
5. The value of C_1 was always set at -10^5 for inclinations angles in the range $3\pi/2 < I < \pi/2$ and $+10^5$ for inclinations in the range $\pi/2 < I < 3\pi/2$.
6. The time increment for numerical integration was 4 seconds for Tables 1 through 21 and 64 seconds for Tables 22 through 52.
7. The final value of $\dot{r}$ is always zero and circular energy is always achieved. ($\ddot{r}$ is also zero by the conditions of circular energy if $\gamma_f = \pi/2$.)
8. Tables 1 through 37 correspond to the sign convention of case 1 except for the second half of Table 33 which corresponds to the sign convention of case 3. Tables 38 through 52 correspond to the sign convention of case 5 except for the second half of Table 49 which corresponds to the sign convention of case 7. It should be noted that analogues of each of Tables 22 through 37 are given in Tables 38 through 52 except for Table 37. This Table would be identical for either sign convention 1 or 5.*
9. Altitudes are presented in meters, velocities in meter/sec., etc.

We proceed, now, to a more detailed discussion of the individual tables. Those remarks referenced directly to Tables 22 through 37 apply equally well to the analogous Tables 38 through 52

Tables 1 through 11 present data for trajectories which ascend to a 15-kilometer orbit under the assumption of vertical lift-off. These tables are the result of numerical integration of the equations of motion using a time step increment of four seconds. These tables list the final value of gamma at orbit and it may be seen that these values are usually near 90°. Those trajectories with initial thrust-to-weight ratio of less than four "hump" during the ascent; i.e., the final altitude is not the maximum altitude.

Table 1 contains thrust-to-weight ratios which maximize the percentage of initial mass which achieves orbit for each listed specific impulse.

Tables 12 through 21 always have thrust and velocity alignment at orbit. For this reason the altitudes are not constant, but vary over a range of almost 100 kilometers. (It may be noted that, for a given specific impulse, there exists an initial thrust-to-weight ratio which produces a given altitude. We could thus specify both a final value of gamma and a final altitude, provided the initial thrust-to-weight ratio was not fixed. This is reasonable in that another degree of freedom has opened up.)

---

* See Section VI for a discussion of sign conventions.

This set of tables also provides a basis of comparison for later tables which present data from a study of the same vehicles with a larger value of the time increment, used in numerical integration. These later tables (discussed below) cover a much wider range of initial conditions than is presented in the first 21 tables.

Tables 22 through 25 present data for initial thrust-to-weight ratios of 1, 1.1, 1.3, and 1.5, respectively, under the assumption of vertical lift-off. There is a direct correlation between the initial thrust-to-weight ratio and the largest lift-off angle that may be used. In the case of vertical lift-off, the initial thrust-to-weight ratio may, theoretically, be as low as one. On the other hand, for an initial lift-off angle of 40° the initial thrust-to-weight ratio was found to have an asymptotic limit at about 1.4. For initial thrust-to-weight ratios of less than 2, only vertical lift-off was considered because of practical considerations. The reason for inclusion of these low values of thrust-to-weight ratios for even vertical lift-off is not immediately apparent. More will be said about this in Section X, but for the present it is interesting to note that a maximum altitude exists in the vicinity of an initial thrust-to-weight ratio of 1.2.

Tables 26 through 31 constitute the bulk of the numerical work. Each of these tables has a given initial thrust-to-weight ratio, and contains data for varying the specific impulse and initial lift-off angle.

As was noted previously, there is some thrust-to-weight value (for a given specific impulse) that produces a maximum altitude. This statement is limited to vertical lift-off, insofar as it is investigated here, but is probably more generally applicable. Furthermore, we must bear in mind that there is a constraint placed on the final value of γ. Under these restrictions, Table 32 presents initial thrust-to-weight values that produce maximum final altitudes.

Table 33 is much more specialized than the preceding tables, in that it presents data only for the special case of an initial thrust-to-weight ratio of 2, a specific impulse of 300 sec., and vertical lift-off. In this table, the vehicle is assumed to lift-off from the equator and ascend to circular orbits of various inclinations. It can easily be seen that as we approach the singular point of a 90° inclination, the Lagrange multipliers increase at a frightening rate. For this reason the inclination values were not studied between 89° and 91° (the time required to isolate even these values was quite high). This table is split in half by a dashed line. The data above the dotted line $(0^\circ < I_f < 89^\circ)$ have a C_1 value of -10^5, and those below $(91^\circ < I_f < 180^\circ)$ have a C_1 value of $+10^5$ (corresponding to sign conventions of cases 1 and 3, respectively). The physical parameters corresponding to an inclination of 90° may be found by interpolation. In the event that polar orbits are of importance, it would be easier to rewrite the equations of motion with this singularity built into an inclination of little importance, or set up the equations in a non-trigonometric form which avoids singularities.

Table 34 is a short presentation of data obtained for the same vehicle used in Table 33. In this case, the lift-off latitude was varied, and λ_5 was always set equal to zero.

In Table 35, the final value of γ is not constrained to be 90°. The vehicle under consideration is assumed to have an initial thrust-to-weight ratio of 5, and a specific impulse of 450 sec. The reference case from which this table was constructed was entry number 16 of Table 29. The initial lift-off angle was varied, and λ_1° was used to maintain the same altitude found for the case of vertical ascent.

Table 36 shows the data obtained when the final mass fraction was optimized with respect to the initial lift-off angle for the same vehicle used in Table 35. No restriction was placed on either the final altitude or final value of gamma. Since two end points were free, one of the initial multipliers (in addition to C_1) was arbitrary. The multiplier chosen was λ_4°. Several of the trajectories in the middle of this table exhibit the phenemonon of "humping". Below these values, the vehicle "falls" the whole way into orbit, and the "humping" effect vanishes. The increase in mass fraction obtained by optimizing the initial value of gamma is about 1.3 per cent.

Table 37 optimizes the initial value of gamma to obtain maximum mass fraction in orbit under the restriction that the final altitude was constant. The final value of gamma was, of course, unconstrainable since λ_1^o was used to isolate final altitude. In each of the two cases presented, the increase in mass fraction was about 1 per cent.

As a final point, we comment on the accuracy of using equation (38) (or (37) for non-equatorial launch). It was found that for those trajectories achieving an inclination of 5°, that equation (38) introduced an error of less than .02°. Even for the case of a final inclination of 89°, the error introduced by this approximation was only 0.2°. Since the original data was obtained via equation (38), it was not felt that this small error was significant enough to justify recomputing all trajectories.

TABLE 1. Optimum Initial Lunar Thrust-to-Weight Ratios

$\theta_0 = \phi_0 = 0$; $I_f = 5°$; $r_f - r_0 = 15{,}000$ m.

I_{sp}	$(T/W)_0$	γ_f	m_f/m_0	λ_1^0	λ_4^0	λ_5^0	t_f
300	3.9718	91.034	.54633	1.39727	.0126960	-8805.6	207.23
350	4.0840	90.811	.59580	1.33974	.0122601	-8804.6	209.49
400	4.1740	90.650	.63577	1.29741	.0119506	-8803.8	211.09
450	4.2437	90.517	.66867	1.26597	.0117115	-8803.3	212.47

TABLE 2. Initial Lunar Thrust-to-Weight Ratio = 1

$\theta_0 = \phi_0 = 0$; $I_f = 5°$; $\gamma_0 = 0°$; $r_f - r_0 = 15{,}000$ m

I_{sp}	γ_f	m_f/m_0	λ_1^0	λ_4^0	λ_5^0	t_f
300	80.106	.44723	65.09321	.1066590	-8792.8	1002.85
350	79.155	.49268	75.01276	.1195080	-8787.7	1073.81
400	78.409	.53053	84.84919	.1323969	-8783.0	1135.63
450	77.813	.56258	94.59077	.1452506	-8778.7	1190.37

TABLE 3. Initial Lunar Thrust-to-Weight Ratio = 1.1

$\theta_0 = \phi_0 = 0$; $I_f = 5^\circ$; $\gamma_0 = 0^\circ$; $r_f - r_0 = 15{,}000$ m

I_{sp}	γ_f	m_f/m_0	λ_1°	λ_4°	λ_5°	t_f
300	77.918	.47404	35.99196	.0628207	-8800.2	867.47
350	76.725	.52170	39.79936	.0674281	-8797.4	920.34
400	75.752	.56126	43.31592	.0717841	-8795.0	964.83
450	74.943	.59461	46.56987	.0758766	-8792.0	1002.91

TABLE 4. Initial Lunar Thrust-to-Weight Ratio = 1.3

$\theta_0 = \phi_0 = 0$; $I_f = 5^\circ$; $\gamma_0 = 0^\circ$; $r_f - r_0 = 15{,}000$ m

I_{sp}	γ_f	m_f/m_0	λ_1°	λ_4°	λ_5°	t_f
300	77.621	.50289	16.15442	.0316771	-8804.4	693.75
350	76.459	.55180	17.20222	.0325911	-8802.8	729.75
400	75.518	.59202	18.11438	.0334556	-8801.5	759.14
450	74.741	.62566	18.91465	.0342560	-8800.4	783.63

TABLE 5. Initial Lunar Thrust-to-Weight Ratio = 1.5

$\theta_0 = \phi_0 = 0$; $I_f = 5^\circ$; $\gamma_0 = 0^\circ$; $r_f - r_0 = 15{,}000$ m

I_{sp}	γ_f	m_f/m_0	λ_1^0	λ_4^0	λ_5^0	t_f
300	78.772	.51793	9.42197	.0207388	-8805.4	583.06
350	77.727	.56710	9.84948	.0208316	-8804.0	610.86
400	76.889	.60732	10.21344	.0209669	-8803.0	633.27
450	76.202	.64077	10.52648	.0211175	-8802.2	651.72

TABLE 6. Initial Lunar Thrust-to-Weight Ratio = 2

$\theta_0 = \phi_0 = 0$; $I_f = 5^\circ$; $r_f - r_0 = 15{,}000$ m

I_{sp}	γ_f	m_f/m_0	λ_1^0	λ_4^0	λ_5^0	t_f
300	82.188	.53508	4.11135	.0124421	-8805.6	421.74
350	81.359	.58429	4.19652	.0120772	-8804.5	439.95
400	80.705	.62427	4.26921	.0118226	-8803.7	454.44
450	80.176	.65735	4.33149	.0116363	-8803.0	466.24

TABLE 7. Initial Lunar Thrust-to-Weight Ratio = 3

$\theta_0 = \phi_0 = 0$; $I_f = 5^\circ$; $r_f - r_0 =$ 15,000 m

I_{sp}	γ_f	m_f/m_0	λ_1°	λ_4°	λ_5°	t_f
300	87.384	.54522	1.91021	.0109303	-8805.5	275.02
350	86.738	.59443	1.90315	.0103782	-8804.4	286.14
400	86.237	.63425	1.90020	.0099785	-8803.7	294.92
450	85.837	.66706	1.89934	.0096760	-8803.1	302.02

TABLE 8. Initial Lunar Thrust-to-Weight Ratio = 4

$\theta_0 = \phi_0 = 0$; $I_f = 5^\circ$; $r_f - r_0 = 15{,}000$ m

I_{sp}	γ_f	m_f/m_0	λ_1°	λ_4°	λ_5°	t_f
300	91.126	.54658	1.38907	.0127624	-8805.6	205.65
350	90.535	.59593	1.36368	.0120715	-8804.6	213.81
400	90.082	.63581	1.34631	.0115732	-8803.8	220.24
450	89.723	.66865	1.33379	.011970	-8803.2	225.43

TABLE 9. Initial Lunar Thrust-to-Weight Ratio = 5

$\theta_0 = \phi_0 = 0$; $I_f = 5°$; $r_f - r_0 = 15{,}000$ m

I_{sp}	γ_f	m_f/m_0	λ_1^0	λ_4^0	λ_5^0	t_f
300	94.177	.54517	1.20759	.0154050	-8805.9	165.04
350	93.590	.59472	1.17344	.0145543	-8804.8	171.57
400	93.144	.63475	1.14949	.0139442	-8804.0	176.71
450	92.794	.66772	1.13181	.0134852	-8803.5	180.85

TABLE 10. Initial Lunar Thrust-to-Weight Ratio = 6

$\theta_0 = \phi_0 = 0$; $I_f = 5°$; $r_f - r_0 = 15{,}000$ m

I_{sp}	γ_f	m_f/m_0	λ_1^0	λ_4^0	λ_5^0	t_f
300	96.856	.54275	1.14167	.0184201	-8806.3	138.26
350	96.249	.59248	1.10105	.0173855	-8805.1	143.76
400	95.792	.63270	1.07241	.0166474	-8804.4	148.08
450	95.434	.66583	1.05117	.0160941	-8803.7	151.57

TABLE 11. Initial Lunar Thrust-to-Weight Ratio = 7

$\theta_0 = \phi_0 = 0$; $I_f = 5°$; $r_f - r_0 = 15{,}000$ m

I_{sp}	γ_f	m_f/m_0	λ_1°	λ_4°	λ_5°	t_f
300	99.307	.53979	1.12683	.0216784	-8806.7	119.27
350	98.668	.58978	1.08040	.0204370	-8805.5	124.04
400	98.188	.63021	1.04766	.0195552	-8804.7	127.79
450	97.815	.66354	1.02335	.0188964	-8804.1	130.80

TABLE 12. Initial Lunar Thrust-to-Weight Ratio = 1

$\theta_0 = \phi_0 = 0$; $I_f = 5°$; $\gamma_0 = 0°$; $\gamma_f = \pi/2$

I_{sp}	$r_f - r_0$	m_f/m_0	λ_1°	λ_4°	λ_5°
300	54154	.42877	97.33660	.1603670	-8786.2
350	59664	.47291	114.60499	.1829909	-8778.7
400	64282	.50999	131.65260	.2053368	-8771.8
450	68191	.54162	148.46797	.2274060	-8765.3

TABLE 13. Initial Lunar Thrust-to-Weight Ratio = 1.1

$\theta_0 = \phi_0 = 0$; $I_f = 5°$; $\gamma_0 = 0°$; $\gamma_f = \pi/2$

I_{sp}	$r_f - r_0$	m_f/m_0	λ_1^o	λ_4^o	λ_5^o
300	62931	.45185	62.95928	.1128095	-8796.3
350	69847	.49814	72.00603	.1246639	-8791.7
400	75796	.53692	80.44945	.1356819	-8787.7
450	80968	.56990	88.34058	.1459543	-8784.2

TABLE 14. Initial Lunar Thrust-to-Weight Ratio = 1.3

$\theta_0 = \phi_0 = 0$; $I_f = 5°$; $\gamma_0 = 0$; $\gamma_f = \pi/2$

I_{sp}	$r_f - r_0$	m_f/m_0	λ_1^o	λ_4^o	λ_5^o
300	62420	.48068	32.51963	.0693737	-8804.2
350	68994	.52859	36.13233	.0743249	-8801.8
400	74597	.56840	39.32520	.0786480	-8799.8
450	79426	.60199	42.16431	.0824576	-8798.1

TABLE 15. Initial Lunar Thrust-to-Weight Ratio = 1.5

$\theta_0 = \phi_0 = 0$; $I_f = 5°$; $\gamma_0 = 0$; $\gamma_f = \pi/2$

I_{sp}	$r_f - r_0$	m_f/m_0	λ_1^o	λ_4^o	λ_5^o
300	55626	.49807	19.70747	.0497318	-8806.7
350	61178	.54649	21.58605	.0525388	-8805.0
400	65863	.58648	23.20294	.0549127	-8803.7
450	69864	.62003	24.60780	.0569473	-8802.6

TABLE 16. Initial Lunar Thrust-to-Weight Ratio = 2

$\theta_0 = \phi_0 = 0$; $I_f = 5°$; $\gamma_f = \pi/2$

I_{sp}	$r_f - r_0$	m_f/m_0	λ_1^o	λ_4^o	λ_5^o
300	39045	.52145	7.99520	.0290282	-8807.6
350	42606	.57010	8.61537	.0302629	-8806.4
400	45567	.60993	9.13358	.0312711	-8805.6
450	48064	.64309	9.57261	.0321097	-8804.9

TABLE 17. Initial Lunar Thrust-to-Weight Ratio = 3

$\theta_0 = \phi_0 = 0$; $I_f = 5^\circ$; $\gamma_f = \pi/2$

I_{sp}	$r_f - r_0$	m_f/m_0	λ_1°	λ_4°	λ_5°
300	20985	.54028	2.55822	.0157716	-8806.3
350	22742	.58879	2.72493	.0163452	-8805.4
400	24186	.62822	2.86142	.0168046	-8804.7
450	25392	.66085	2.97511	.0171806	-8804.2

TABLE 18. Initial Lunar Thrust-to-Weight Ratio = 4

$\theta_0 = \phi_0 = 0$; $I_f = 5^\circ$; $\gamma_f = \pi/2$

I_{sp}	$r_f - r_0$	m_f/m_0	λ_1°	λ_4°	λ_5°
300	12954	.54828	1.20225	.0107577	-8805.2
350	13995	.59665	1.27440	.0111352	-8804.4
400	14847	.63586	1.33297	.0114358	-8803.8
450	15555	.66822	1.38143	.0116807	-8803.3

TABLE 19. Initial Lunar Thrust-to-Weight Ratio = 5

$\theta_0 = \phi_0 = 0$; $I_f = 5^\circ$; $\gamma_f = \pi/2$

I_{sp}	$r_f - r_0$	m_f/m_0	λ_1°	λ_4°	λ_5°
300	8784	.55266	.68292	.0081228	-8804.6
350	9474	.60094	.72190	.0084052	-8803.8
400	10036	.64001	.75340	.0086295	-8803.2
450	10502	.67222	.77935	.0088118	-8802.7

TABLE 20. Initial Lunar Thrust-to-Weight Ratio = 6

$\theta_0 = \phi_0 = 0$; $I_f = 5^\circ$; $\gamma_f = \pi/2$

I_{sp}	$r_f - r_0$	m_f/m_0	λ_1°	λ_4°	λ_5°
300	6352	.55539	.43458	.0065027	-8804.1
350	6843	.60361	.45855	.0067285	-8803.3
400	7243	.64283	.47786	.0069076	-8802.7
450	7573	.67470	.49373	.0070530	-8802.3

TABLE 21. Initial Lunar Thrust-to-Weight Ratio = 7

$\theta_0 = \phi_0 = 0$; $I_f = 5°$; $\gamma_f = \pi/2$

I_{sp}	$r_f - r_0$	m_f/m_0	λ_1^0	λ_4^0	λ_5^0
300	4811	.55726	.29831	.0054087	-8803.8
350	5178	.60543	.31435	.0055967	-8803.0
400	5477	.64435	.32724	.0057458	-8802.4
450	5724	.67638	.33782	.0058667	-8801.9

TABLE 22. Initial Lunar Thrust-to-Weight Ratio = 1

$\theta_0 = \phi_0 = 0$; $I_f = 5°$; $\gamma_0 = 0°$; $\gamma_f = \pi/2$

I_{sp}	$r_f - r_0$	m_f/m_0	λ_1^0	λ_4^0	λ_5^0
300	54154	.42876	97.337	.1603	-8786.1
350	59666	.47290	114.604	.1829	-8778.7
400	64285	.50999	131.652	.2053	-8771.7
450	68194	.54161	148.467	.2274	-8765.2

TABLE 23. Initial Lunar Thrust-to-Weight Ratio = 1.1

$\theta_0 = \phi_0 = 0$; $I_f = 5°$; $\gamma_0 = 0°$; $\gamma_f = \pi/2$

I_{sp}	$r_f - r_0$	m_f/m_0	λ_1°	λ_4°	λ_5°
300	62929	.45185	62.958	.1128	-8796.2
350	69847	.49814	72.005	.1246	-8791.7
400	75796	.53692	80.449	.1356	-8787.7
450	80968	.56990	88.339	.1459	-8784.1

TABLE 24. Initial Lunar Thrust-to-Weight Ratio = 1.3

$\theta_0 = \phi_0 = 0$; $I_f = 5°$; $\gamma_0 = 0$; $\gamma_f = \pi/2$

I_{sp}	$r_f - r_0$	m_f/m_0	λ_1°	λ_4°	λ_5°
300	62420	.48067	32.519	.069373	-8804.2
350	68994	.52859	36.132	.074324	-8801.7
400	74596	.56840	39.324	.078647	-8799.7
450	79427	.60198	42.164	.082457	-8798.0

TABLE 25. Initial Lunar Thrust-to-Weight Ratio = 1.5

$\theta_0 = \phi_0 = 0$; $I_f = 5°$; $\gamma_0 = 0$; $\gamma_f = \pi/2$

I_{sp}	$r_f - r_0$	m_f / m_0	λ_1°	λ_4°	λ_5°
300	55625	.49806	19.707	.049730	-8806.7
350	61182	.54649	21.586	.052539	-8805.0
400	65867	.58648	23.203	.054913	-8803.6
450	69869	.62002	24.608	.056948	-8802.5

TABLE 26. Initial Lunar Thrust-to-Weight Ratio = 2

$\theta_0 = \phi_0 = 0$; $I_f = 5^\circ$; $\gamma_f = \pi/2$

γ_0	I_{sp}	$r_f - r_0$	m_f/m_0	λ_1°	λ_4°	λ_5°
0	300	39048	.52146	7.994	.02902	-8807.5
10	300	34493	.52793	9.197	.03314	-10701.6
20	300	29599	.53339	11.076	.03935	-13400.1
30	300	24114	.53810	14.484	.05040	-17998.2
40	300	17657	.54221	22.834	.07723	-28863.9
0	350	42611	.57010	8.614	.03026	-8806.3
10	350	37496	.57659	9.916	.03460	-10766.6
20	350	32062	.58203	11.973	.04121	-13578.0
30	350	26019	.58670	15.757	.05312	-18425.9
40	350	18949	.59074	25.287	.08284	-30190.4
0	400	45572	.60993	9.133	.03127	-8805.4
10	400	39975	.61633	10.517	.03579	-10819.3
20	400	34080	.62167	12.724	.04273	-13723.0
30	400	27568	.62623	16.830	.05537	-18778.3
40	400	19986	.63017	27.411	.08763	-31318.3
0	450	48070	.64309	9.572	.03210	-8804.7
10	450	42053	.64935	11.025	.03679	-10862.8
20	450	35761	.65455	13.360	.04401	-13843.4
30	450	28850	.65897	17.746	.05727	-19073.6
40	450	20835	.66277	29.267	.09177	-32288.7

TABLE 27. Initial Lunar Thrust-to-Weight Ratio = 3

$\theta_0 = \phi_0 = 0$; $I_f = 5^\circ$; $\gamma_f = \pi/2$

γ_0	I_{sp}	$r_f - r_0$	m_f/m_0	λ_1°	λ_4°	λ_5°
0	300	20756	.54070	2.5629	.015804	-8806.1
10	300	19185	.54412	2.8351	.017161	-9891.4
20	300	17471	.54714	3.2058	.018967	-11257.9
30	300	15508	.54988	3.7620	.021638	-13183.5
40	300	13155	.55236	4.7249	.026229	-16379.0
0	350	22544	.58916	2.7260	.016364	-8805.2
10	350	20780	.59257	3.0173	.017777	-9922.0
20	350	18877	.59557	3.4163	.019667	-11332.2
30	350	16719	.59826	4.0183	.022475	-13327.8
40	350	14149	.60069	5.0689	.027338	-16664.3
0	400	24012	.62855	2.8600	.016814	-8804.6
10	400	22084	.63190	3.1667	.018273	-9946.6
20	400	20022	.63483	3.5887	.020229	-11391.6
30	400	17702	.63744	4.2286	.023148	-13443.8
40	400	14953	.63980	5.3524	.028236	-16895.1
0	450	25236	.66115	2.9720	.017184	-8804.1
10	450	23168	.66441	3.2912	.018679	-9966.7
20	450	20973	.66725	3.7324	.020691	-11440.4
30	450	18515	.66977	4.4039	.023702	-13539.1
40	450	15616	.67204	5.5899	.028977	-17085.6

TABLE 28. Initial Lunar Thrust-to-Weight Ratio = 4

$\theta_0 = \phi_0 = 0$; $I_f = 5°$; $\gamma_f = \pi/2$

γ_0	I_{sp}	$r_f - r_0$	m_f/m_0	λ_1^o	λ_4^o	λ_5^o
0	300	12492	.54730	1.2649	.01104	-8805.5
10	300	11897	.54989	1.3542	.01165	-9575.3
20	300	11167	.55228	1.4769	.01246	-10494.1
30	300	10264	.55447	1.6575	.01362	-11699.6
40	300	9132	.55643	1.9489	.01546	-13501.0
0	350	13511	.59594	1.3349	.01140	-8804.6
10	350	12838	.59842	1.4317	.01204	-9594.1
20	350	12029	.60071	1.5641	.01289	-10538.8
30	350	11041	.60280	1.7588	.01410	-11781.8
40	350	9811	.60468	2.0735	.01602	-13647.2
0	400	14350	.63534	1.3914	.01169	-8804.0
10	400	13609	.63770	1.4944	.01235	-9609.2
20	400	12734	.63988	1.6348	.01322	-10574.5
30	400	11674	.64187	1.8410	.01448	-11847.5
40	400	10362	.64367	2.1750	.01647	-13764.4
0	450	15045	.66784	1.4379	.01192	-8803.5
10	450	14251	.67009	1.5460	.01260	-9621.6
20	450	13318	.67217	1.6931	.01350	-10603.6
30	450	12197	.67406	1.9090	.01479	-11901.2
40	450	10817	.67576	2.2591	.01684	-13806.4

TABLE 29. Initial Lunar Thrust-to-Weight Ratio = 5

$\theta_0 = \phi_0 = 0$; $I_f = 5^\circ$; $\gamma_f = \pi/2$

γ_0	I_{sp}	$r_f - r_0$	m_f/m_0	λ_1°	λ_4°	λ_5°
0	300	8855	.54797	.7394	.008376	-8805.9
10	300	8545	.55080	.7711	.008685	-9411.7
20	300	8107	.55346	.8218	.009127	-10109.8
30	300	7529	.55589	.9017	.009777	-10988.5
40	300	6793	.55802	1.0301	.010790	-12230.2
0	350	9489	.59687	.7827	.008678	-8805.0
10	350	9143	.59953	.8174	.009002	-9425.1
20	350	8666	.60203	.8719	.009461	-10141.3
30	350	8047	.60430	.9571	.010134	-11045.0
40	350	7262	.60630	1.0942	.011182	-12325.7
0	400	10009	.63644	.8172	.008914	-8804.3
10	400	9632	.63893	.8543	.009251	-9435.9
20	400	9123	.64127	.9119	.009723	-10166.5
30	400	8469	.64340	1.0015	.010414	-11090.0
40	400	7644	.64527	1.1458	.011492	-12402.1
0	450	10442	.66904	.8453	.009104	-8803.7
10	450	10039	.67139	.8845	.009451	-9444.7
20	450	9503	.67359	.9447	.009935	-10187.0
30	450	8819	.67558	1.0380	.010641	-11126.7
40	450	7960	.67734	1.1883	.011744	-12464.4

TABLE 30. Initial Lunar Thrust-to-Weight Ratio = 6

$\theta_0 = \phi_0 = 0$; $I_f = 5^\circ$; $\gamma_f = \pi/2$

γ_0	I_{sp}	$r_f - r_0$	m_f/m_0	λ_1°	λ_4°	λ_5°
0	300	7210	.54645	.44334	.006420	-8806.4
10	300	6997	.54974	.45414	.006584	-8311.0
20	300	6648	.55288	.48018	.006868	-9877.8
30	300	6166	.55577	.52620	.007317	-10571.4
40	300	5550	.55832	.60107	.008015	-11518.3
0	350	7633	.59555	.47506	.006705	-8805.5
10	350	7397	.59863	.48693	.006876	-9321.2
20	350	7025	.60156	.51433	.007167	-9901.6
30	350	6516	.60426	.56244	.007623	-10613.2
40	350	5871	.60663	.64091	.008335	-11586.9
0	400	7987	.63530	.50030	.006927	-8804.9
10	400	7733	.63818	.51309	.007105	-9329.6
20	400	7341	.64092	.54166	.007401	-9921.0
30	400	6812	.64343	.59156	.007864	-10647.2
40	400	6143	.64564	.67309	.008587	-11642.8
0	450	8284	.66807	.52078	.007104	-8804.3
10	450	8014	.67076	.53435	.007287	-9336.5
20	450	7605	.67332	.56393	.007588	-9936.9
30	450	7058	.67566	.61534	.008057	-10675.0
40	450	6369	.67772	.69946	.008790	-11688.6

TABLE 31. Initial Lunar Thrust-to-Weight Ratio = 7

$\theta_0 = \phi_0 = 0$; $I_f = 5^\circ$; $\gamma_f = \pi/2$

γ_0	I_{sp}	$r_f - r_0$	m_f/m_0	λ_1^0	λ_4^0	λ_5^0
0	300	6440	.54395	.24488	.004774	-8807.6
10	300	6264	.54774	.24755	.004859	-9242.2
20	300	5942	.55140	.26462	.005072	-9720.9
30	300	5482	.55480	.29840	.005442	-10294.1
40	300	4892	.55783	.35322	.006018	-11057.7
0	350	6761	.59330	.27071	.005066	-8806.6
10	350	6569	.59685	.27358	.005154	-9250.6
20	350	6230	.60026	.29099	.005368	-9740.6
30	350	5751	.60343	.32549	.005736	-10328.3
40	350	5141	.60625	.38186	.006312	-11112.9
0	400	7024	.63326	.29105	.005289	-8805.8
10	400	6818	.63658	.29413	.005381	-9257.5
20	400	6466	.63976	.31185	.005595	-9756.5
30	400	5972	.64271	.34699	.005963	-10355.9
40	400	5344	.64533	.40469	.006541	-11157.2
0	450	7240	.66622	.30747	.005465	-8804.5
10	450	7023	.66932	.31077	.005560	-9262.4
20	450	6661	.67227	.32876	.005775	-9769.4
30	450	6155	.67503	.36446	.006143	-10378.3
40	450	5513	.67747	.42329	.006723	-11193.4

TABLE 32. Maximum Final Altitudes

$\theta_0 = \phi_0 = 0$; $I_f = 5°$; $\gamma_0 = 0°$; $\gamma_f = \pi/2$

I_{sp}	T/W_0	$r_f - r_0$	m_f/m_0	λ_1^o	λ_4^o	λ_5^o
300	1.1808	64341	.46552	46.961	.09028	-8800.6
350	1.1785	71340	.51236	53.349	.09878	-8797.1
400	1.1756	77359	.55126	59.465	.10687	-8794.0
450	1.1732	82585	.58422	65.137	.11432	-8791.3

TABLE 33. Variation of Inclination

$\theta_0 = \phi_0 = 0$; $\gamma_0 = 0$; $\gamma_f = \pi/2$; $T/W_0 = 2$; $I_{sp} = 300$ sec

Inclination	$r_f - r_0$	m_f/m_0	λ_1°	λ_4°	λ_5°
0	39047	.52146	7.9633	.02891	0
10	39051	.52145	8.0883	.02936	-17752.3
20	39061	.52140	8.4835	.03797	-36656.4
30	39077	.52133	9.2179	.03345	-58182.7
40	39096	.52124	10.4418	.03788	-84641.1
50	39122	.52113	12.4810	.04526	-120417.2
60	39151	.52099	16.1172	.05842	-175538.9
70	39183	.52085	23.7483	.08605	-280200.0
80	39218	.52069	47.7772	.17302	-589750.8
85	39238	.52061	99.2107	.35919	-1237639.6
85.5	39240	.52060	111.2294	.40269	-1388474.1
86	39242	.52059	126.5797	.45825	-1580976.2
86.5	39244	.52058	146.8550	.53164	-1835102.2
87	39246	.52057	174.9114	.63319	-2186562.6
87.5	39248	.52057	216.1803	.78257	-2703334.1
88	39250	.52056	282.9471	1.02424	-3539137.5
88.5	39253	.52055	409.4504	1.48213	-5122344.4
89	39252	.52054	740.9142	2.68191	-9270169.5
91	39259	.52051	331.4204	1.19952	-4145244.2
91.5	39261	.52050	243.4064	.88094	-3043532.6
92	39263	.52049	192.3460	.69612	-2404207.7
92.5	39265	.52049	159.0078	.57545	-1986636.1
93	39266	.52048	135.5252	.49045	-1692445.1
93.5	39271	.52047	118.1147	.42743	-1474075.4
94	39269	.52046	104.6433	.37868	-1305127.8
94.5	39272	.52045	93.9484	.33996	-1170881.4
95	39275	.52045	85.2774	.30858	-1061915.8
100	39291	.52037	44.3983	.16061	-546091.3
110	39327	.52021	23.0019	.08316	-269483.1
120	39361	.52006	15.8560	.05730	-170922.7
130	39390	.51993	12.3879	.04474	-117949.0
140	39416	.51982	10.4251	.03764	-83183.5
150	39436	.51973	9.2400	.03335	-57292.2
160	39451	.51966	8.5272	.03077	-36139.5
170	39465	.51962	8.1436	.02938	-17513.2
180	39463	.51961	8.0212	.02894	0

TABLE 34. Variation of Lift-off Latitude

$\phi_0 = 0;\ \gamma_0 = 0;\ \gamma_f = \pi/2;\ \lambda_5 = 0;\ (T/W)_0 = 2;\ I_{sp} = 300$ sec

θ_0	$r_f - r_0$	m_f / m_0	λ_1^0	λ_4^0	Inclination
0	39048	.52146	7.9634	.02891	0
30	39076	.52133	9.1998	.03338	30.000000
60	39148	.52099	15.9552	.05784	60.000000

TABLE 35. Variation of Initial Gamma for Constant Final Altitude

$r_f - r_0 =$ 10443 m. ; $\phi_0 = \theta_0 = 0$; $I_f = 5°$; $(T/W)_0 = 5$; $I_{sp} = 450$ sec

γ_0	m_f / m_0	γ_f	λ_1^0	λ_4^0	λ_5^0
357	.66836	89.933	.82829	.008908	-8623.7
358	.66859	89.954	.83368	.008971	-8683.1
359	.66882	89.976	.83936	.009036	-8743.1
0	.66904	90.000	.84535	.009104	-8803.7
1	.66937	90.024	.85164	.009176	-8865.2
2	.66950	90.049	.85828	.009250	-8927.4
3	.66982	90.075	.86525	.009328	-8990.6

TABLE 36. Maximization of Mass Fraction With Respect to Initial Gamma

$I_f = 5^\circ$; $\lambda_4 = .0090090081$; $(T/W)_0 = 5$; $I_{sp} = 450$

γ_0	$r_f - r_0$	m_f/m_0	γ_f	λ_1	λ_5	$(r - r_0)_{max}$
20°	9503	.67359	90.000	.9447	-10187.0	Cutoff Value
30°	8389	.67574	89.657	.9798	-11031.3	Cutoff Value
40°	7057	.67766	89.207	1.0323	-12097.6	Cutoff Value
50°	5414	.67931	88.596	1.1114	-13596.8	Cutoff Value
60°	3348	.68067	87.714	1.2397	-16074.0	Cutoff Value
62°	2844	.68090	87.487	1.2758	-16800.9	3018
65°	2080	.68122	87.009	1.3406	-18145.5	2332
70°	579	.68168	86.284	1.4941	-21518.5	1166
74°	-860	.68196	85.201	1.6987	-26349.9	354
75°	-1263	.68201	85.133	1.7719	-28151.0	Cutoff Value
79°	-3108	.68213	83.780	2.2802	-41301.3	Cutoff Value
79.573848	-3409	.68214	83.536	2.4101	-44779.0	Cutoff Value
80°	-3641	.68213	83.345	2.5245	-47865.0	Cutoff Value

TABLE 37. Maximization of Mass Fraction With Respect to Initial Gamma for Constant Final Altitude

$\theta_0 = \phi_0 = 0$; $I_f = 5^\circ$

$(T/W)_0$	I_{sp}	γ_0	$r_f - r_0$	m_f/m_0	γ_f	λ_1°	λ_4°	λ_5°
2	300	0	39048	.52146	90°	7.9943	.02902	-8807.5
2	300	38.299998	39052	.53160	103.854°	190.2039	.65559	-143626.4
3	350	0	22544	.58916	90°	2.7260	.01636	-8805.2
3	350	49.0088013	22545	.59719	100.633°	44.2443	.23481	-83828.6

TABLE 38. Initial Lunar Thrust-to-Weight Ratio = 1

$\theta_0 = \phi_0 = 0$; $I_f = 5°$; $\gamma_0 = 0°$; $\gamma_f = \pi/2$

I_{sp}	$r_f - r_0$	m_f/m_0	λ_1°	λ_4°	λ_5°
300	53927	.42889	96.887	.15952	7400.2
350	59415	.47303	114.069	.18202	7203.9
400	64011	.51012	131.027	.20425	7024.3
450	67903	.54174	147.756	.22621	6859.1

TABLE 39. Initial Lunar Thrust-to-Weight Ratio = 1.1

$\theta_0 = \phi_0 = 0$; $I_f = 5°$; $\gamma_0 = 0°$; $\gamma_f = \pi/2$

I_{sp}	$r_f - r_0$	m_f/m_0	λ_1°	λ_4°	λ_5°
300	62700	.45198	62.650	.11215	7761.8
350	69591	.49827	71.645	.12393	7632.0
400	75518	.53705	80.039	.13488	7516.7
450	80671	.57003	87.884	.14509	7413.6

TABLE 40. Initial Lunar Thrust-to-Weight Ratio = 1.3

$\theta_0 = \phi_0 = 0$; $I_f = 5^\circ$; $\gamma_0 = 0^\circ$; $\gamma_f = \pi/2$

I_{sp}	$r_f - r_0$	m_f/m_0	λ_1°	λ_4°	λ_5°
300	62206	.48081	32.347	.06890	8165.6
350	68755	.52872	35.936	.07382	8096.8
400	74336	.56853	39.107	.07811	8037.6
450	79146	.60212	41.926	.08189	7986.2

TABLE 41. Initial Lunar Thrust-to-Weight Ratio = 1.5

$\theta_0 = \phi_0 = 0$; $I_f = 5^\circ$; $\gamma_0 = 0^\circ$; $\gamma_f = \pi/2$

I_{sp}	$r_f - r_0$	m_f/m_0	λ_1°	λ_4°	λ_5°
300	55438	.49819	19.598	.04936	8376.0
350	60970	.54662	21.463	.05214	8333.8
400	65636	.58661	23.068	.05450	8298.1
450	69622	.62015	24.463	.05651	8267.6

TABLE 42. Initial Lunar Thrust-to-Weight Ratio = 2

$\theta_0 = \phi_0 = 0$; $I_f = 5°$; $\gamma_f = \pi/2$

γ_0	I_{sp}	$r_f - r_0$	m_f/m_0	λ_1^o	λ_4^o	λ_5^o
0	300	38910	.52157	7.947	.02878	8606.2
10	300	34358	.52802	9.132	.03281	10450.6
20	300	29469	.53346	10.979	.03888	13067.2
30	300	23990	.53816	14.312	.04963	17501.3
40	300	17546	.54224	22.402	.07549	27871.9
0	350	42476	.57021	8.567	.03002	8589.1
10	350	37347	.57669	9.844	.03425	10494.5
20	350	31919	.58211	11.864	.04070	13215.6
30	350	25883	.58676	15.560	.05228	17879.7
40	350	18829	.59078	24.775	.08086	29070.5
0	400	45402	.61004	9.076	.03099	8576.0
10	400	39814	.61643	10.438	.03542	10529.7
20	400	33927	.62175	12.604	.04220	13335.9
30	400	27423	.62629	16.613	.05447	18190.4
40	400	19858	.63020	26.828	.08545	30086.6
0	450	47889	.64320	9.512	.03182	8562.7
10	450	41882	.64944	10.941	.03640	10558.5
20	450	35600	.65462	13.231	.04345	13435.3
30	450	28697	.65902	17.510	.05632	18450.0
40	450	20701	.66280	28.617	.08940	30958.2

TABLE 43. Initial Lunar Thrust-to-Weight Ratio = 3

$\theta_0 = \phi_0 = 0$; $I_f = 5°$; $\gamma_f = \pi/2$

γ_0	I_{sp}	$r_f - r_0$	m_f/m_0	λ_1^o	λ_4^o	λ_5^o
0	300	20692	.54077	2.5500	.01567	8735.5
10	300	19106	.54418	2.8164	.01698	9806.4
20	300	17395	.54720	3.1815	.01875	11151.3
30	300	15437	.54992	3.7284	.02135	13041.3
40	300	13088	.55239	4.6723	.02583	16166.8
0	350	22454	.58925	2.7096	.01620	8729.7
10	350	20693	.59264	2.9968	.01759	9831.0
20	350	18794	.59563	3.3896	.01943	11217.7
30	350	16640	.59830	3.9811	.02217	13174.7
40	350	14076	.60072	5.0101	.02690	16434.3
0	400	23914	.62864	2.8424	.01665	8725.1
10	400	21991	.63197	3.1446	.01807	9850.6
20	400	19934	.63489	3.5600	.01998	11270.8
30	400	17618	.63749	4.1883	.02283	13281.8
40	400	14876	.63983	5.2884	.02778	16650.3
0	450	25132	.66123	2.9534	.01701	8721.3
10	450	23070	.66448	3.2678	.01847	9866.6
20	450	20879	.66730	3.7019	.02044	11314.2
30	450	18426	.66982	4.3611	.02337	13369.5
40	450	15534	.67207	5.5215	.02850	16828.4

TABLE 44. Initial Lunar Thrust-to-Weight Ratio = 4

$\theta_0 = \phi_0 = 0$; $I_f = 5°$; $\gamma_f = \pi/2$

γ_0	I_{sp}	$r_f - r_0$	m_f/m_0	λ_1^0	λ_4^0	λ_5^0
0	300	12446	.54734	1.2578	.01093	8771.0
10	300	11851	.54992	1.3457	.01153	9535.9
20	300	11122	.55232	1.4665	.01232	10444.9
30	300	10221	.55450	1.6443	.01345	11635.1
40	300	9090	.55646	1.9308	.01525	13409.2
0	350	13460	.59598	1.3272	.01129	8770.0
10	350	12787	.59846	1.4225	.01191	9552.0
20	350	11980	.60075	1.5528	.01274	10485.9
30	350	10993	.60283	1.7444	.01392	11712.4
40	350	9765	.60471	2.0536	.01580	13548.3
0	400	14293	.63538	1.3832	.01157	8767.6
10	400	13554	.63774	1.4845	.01222	9564.9
20	400	12680	.63992	1.6227	.01307	10518.8
30	400	11622	.64190	1.8256	.01429	11774.3
40	400	10313	.64369	2.1536	.01624	13659.9
0	450	14986	.66788	1.4294	.01180	8765.7
10	450	14192	.67013	1.5357	.01246	9575.4
20	450	13261	.67220	1.6804	.01334	10545.6
30	450	12142	.67409	1.8927	.01460	11824.9
40	450	10765	.67579	2.2365	.01660	13751.2

TABLE 45. Initial Lunar Thrust-to-Weight Ratio = 5

$\theta_0 = \phi_0 = 0$; $I_f = 5^\circ$; $\gamma_f = \pi/2$

γ_0	I_{sp}	$r_f - r_0$	m_f/m_0	λ_1°	λ_4°	λ_5°
0	300	8828	.54798	.7347	.008289	8789.7
10	300	8519	.55081	.7658	.008589	9391.4
20	300	8080	.55347	.8158	.009020	10083.6
30	300	7502	.55590	.8945	.009657	10953.4
40	300	6766	.55803	1.0210	.010647	12180.3
0	350	9471	.59688	.7789	.008603	8786.9
10	350	9113	.59955	.8117	.008902	9403.3
20	350	8636	.60204	.8653	.009349	10113.2
30	350	8017	.60432	.9493	.010006	11007.3
40	350	7233	.60631	1.0843	.011031	12272.2
0	400	9990	.63645	.8133	.008837	8785.2
10	400	9599	.63895	.8483	.009147	9412.8
20	400	9091	.64129	.9050	.009607	10136.8
30	400	8437	.64342	.9932	.010282	11050.3
40	400	7612	.64529	1.1353	.011335	12345.7
0	450	10407	.66906	.8399	.009009	8783.9
10	450	10004	.67141	.8783	.009345	9420.6
20	450	9468	.67360	.9374	.009815	10156.1
30	450	8785	.67560	1.0293	.010505	11085.4
40	450	7926	.67735	1.1773	.011581	12405.6

TABLE 46. Initial Lunar Thrust-to-Weight Ratio = 6

$\theta_0 = \phi_0 = 0$; $I_f = 5°$; $\gamma_f = \pi/2$

γ_0	I_{sp}	$r_f - r_0$	m_f/m_0	λ_1^0	λ_4^0	λ_5^0
0	300	7194	.54646	.43990	.006347	8799.6
10	300	6981	.54975	.45036	.006504	9302.2
20	300	6632	.55289	.47598	.006781	9865.2
30	300	6149	.55578	.52144	.007221	10552.9
40	300	5533	.55833	.59543	.007906	11490.4
0	350	7614	.59556	.47140	.006628	8797.1
10	350	7379	.59864	.48289	.006793	9310.6
20	350	7006	.60157	.50984	.007076	9886.8
30	350	6498	.60427	.55733	.007522	10591.9
40	350	5852	.60664	.63483	.008220	11555.3
0	400	7967	.63531	.49647	.006847	8795.6
10	400	7713	.63819	.50885	.007018	9317.9
20	400	7321	.64093	.53693	.007306	9904.9
30	400	6792	.64344	.58616	.007759	10624.3
40	400	6122	.64565	.66664	.008467	11609.0
0	450	8262	.66807	.51681	.007022	8794.4
10	450	7992	.67077	.52995	.007198	9324.0
20	450	7584	.67333	.55901	.007491	9919.8
30	450	7037	.67567	.60971	.007949	10650.9
40	450	6347	.67773	.69271	.008667	11653.1

TABLE 47. Initial Lunar Thrust-to-Weight Ratio = 7

$\theta_0 = \phi_0 = 0$; $I_f = 5^\circ$; $\gamma_f = \pi/2$

γ_0	I_{sp}	$r_f - r_0$	m_f/m_0	λ_1°	λ_4°	λ_5°
0	300	6429	.54395	.24210	.004709	8805.0
10	300	6253	.54774	.24459	.004790	9238.1
20	300	5931	.55140	.26143	.004998	9713.5
30	300	5471	.55480	.29489	.005361	10282.0
40	300	4881	.55783	.34922	.005928	11038.3
0	350	6749	.59331	.26776	.004998	8804.1
10	350	6557	.59685	.27044	.005082	9245.9
20	350	6218	.60026	.28758	.005290	9732.5
30	350	5739	.60343	.32174	.005651	10315.3
40	350	5128	.60625	.37758	.006218	11092.1
0	400	7010	.63327	.28797	.005219	8802.3
10	400	6805	.63658	.29084	.005306	9252.3
20	400	6452	.63976	.30828	.005514	9747.8
30	400	5958	.64271	.34304	.005875	10342.0
40	400	5331	.64533	.40017	.006443	11135.2
0	450	7225	.66622	.30428	.005394	8802.6
10	450	7009	.66932	.30736	.005483	9259.0
20	450	6647	.67228	.32505	.005692	9760.3
30	450	6140	.67503	.36035	.006053	10363.8
40	450	5499	.67747	.41859	.006622	11170.5

TABLE 48. Maximum Final Altitudes

$\theta_0 = \phi_0 = 0$; $I_f = 5°$; $\gamma_0 = 0°$; $\gamma_f = \pi/2$

I_{sp}	T/W_0	$r_f - r_0$	m_f/m_0	λ_1^0	λ_4^0	λ_5^0
300	1.1799	64117	.46553	46.862	.08992	7959.0
350	1.1787	71090	.51253	53.036	.09811	7857.8
400	1.1757	77094	.55141	59.145	.10619	7763.1
450	1.1731	82294	.58434	64.821	.11365	7678.2

TABLE 49. Variation of Inclination

$\theta_0 = \phi_0 = 0;\ \gamma_0 = 0;\ \gamma_f = \pi/2;\ T/W_0 = 2;\ I_{sp} = 300$ sec

Inclination	$r_f - r_0$	m_f/m_0	λ_1^0	λ_4^0	λ_5^0
0	39084	.52146	7.9634	.02891	0
10	38499	.52189	7.9020	.02838	17346.5
20	36900	.52314	7.7333	.02682	35808.2
30	34405	.52506	7.5051	.02427	56809.4
40	31259	.52744	7.3057	.02079	82594.9
50	27810	.53000	7.2914	.01645	117410.4
60	24469	.53240	7.7751	.01121	171002.0
70	21654	.53433	9.6067	.00467	272688.4
80	19797	.53552	17.0322	-.00581	573156.6
85	19323	.53577	34.1366	-.02002	1200490.6
85.5	19294	.53579	38.1739	-.02298	1346132.0
86	19268	.53580	43.3448	-.02670	1532195.5
86.5	19245	.53581	50.1701	-.03153	1777283.9
87	19228	.53581	59.6053	-.03809	2115272.7
87.5	19212	.53581	73.4779	-.04762	2611524.3
88	19200	.53582	95.8423	-.06279	3410439.2
88.5	19189	.53582	137.9604	-.09114	4913670.9
89	19185	.53581	264.8541	-.16394	8796812.9
91	19196	.53577	114.6169	-.07569	4080896.4
91.5	19208	.53576	83.9815	-.05499	2987115.2
92	19223	.53574	66.3109	-.04294	2355459.3
92.5	19244	.53572	54.8189	-.03499	1943959.2
93	19264	.53570	46.7488	-.02934	1654612.6
93.5	19286	.53568	40.7939	-.02510	1440671.6
94	19317	.53565	36.1891	-.02174	1274701.9
94.5	19350	.53562	32.5525	-.01904	1143284.9
95	19382	.53559	29.6027	-.01680	1036449.3
100	19915	.53514	15.9585	-.00490	532394.4
110	21876	.53361	9.3945	+.00500	262603.8
120	24769	.53137	7.7242	.01141	166609.5
130	28173	.52869	7.3000	.01660	115036.6
140	31656	.52592	7.3410	.02091	81174.6
150	34817	.52339	7.5534	.02435	55936.9
160	37318	.52136	7.7879	.02688	35297.6
170°	38915	.52006	7.9591	.02842	17109.9
180°	39463	.51961	8.0212	.02894	0.0

TABLE 50. Variation of Initial Gamma for Constant Final Altitude

$r_f - r_0 = 10407$ m ; $\phi_0 = \theta_0 = 0$; $I_f = 5°$; $(T/W)_0 = 5$; $I_{sp} = 450$ sec

γ_0	m_f/m_0	γ_f	λ_1^0	λ_4^0	λ_5^0
357	.66838	89.933	.82302	.008813	8605.6
358	.66861	89.954	.82834	.008875	8664.6
359	.66884	89.976	.83395	.008940	8724.2
0	.66906	90.000	.83995	.009009	8783.9
1	.66929	90.023	.84608	.009077	8845.5
2	.66951	90.048	.85263	.009151	8907.4
3	.66974	90.074	.85953	.009228	8970.1

TABLE 51. Maximization of Mass Fraction With Respect to Initial Gamma

$I_f = 5°$; $\lambda_4 = .0090090081$; $(T/W)_0 = 5$; $I_{sp} = 450$ sec

γ_0	$r_f - r_0$	m_f/m_0	γ_f	λ_1^0	λ_5^0	$(r - r_0)_{max}$
20°	8914.9	.67381	89.574	.8736	10089.5	Cutoff Value
30°	7884.6	.67592	89.266	.9067	10883.9	Cutoff Value
40°	6620.8	.67780	88.857	.9563	11885.3	Cutoff Value
50°	5065.5	.67941	88.299	1.0315	13291.9	Cutoff Value
60°	3101.0	.68073	87.488	1.1534	15615.1	Cutoff Value
65°	1891.1	.68127	86.920	1.2493	17558.6	2194.3
70°	453.2	.68171	86.164	1.3955	20731.4	1100.9
79.470782°	-3358.5	.68214	83.615	2.2486	42087.4	Cutoff Value
80°	-3638.7	.68214	83.389	2.3833	45669.0	Cutoff Value

TABLE 52. Maximization of Mass Fraction With Respect to Initial Gamma for Constant Final Altitude

$\theta_0 = \phi_0 = 0$; $I_f = 5°$

$(T/W)_0$	I_{sp}	γ_0	$r_f - r_0$	m_f/m_0	γ_f	λ_1^0	λ_4^0	λ_5^0
2	300	0°	38910	.52157	90°	7.947	.028726	8606.2
2	300	38.365062	38911	.53168	103.87545	184.693	.635524	136385.7
3	350	0°	22454	.58925	90°	2.709	.016209	8729.7
3	350	49.175259°	22453	.59725	100.65028	43.677	.231310	82208.2

SECTION IX. GRAPHICAL PRESENTATION OF RESULTS

To present the data given in Section VIII in a more readily useable form, and to aid interpolation, a number of graphs are presented. Section X will deal with specific methods of using the graphs (as well as the tables of the preceding section) for sample calculations.

All of the graphs presented below correspond to the sign convention of case number 1, unless otherwise stated (i.e., FIG 60, 61, 62, 63, 64, and 65).

FIG 5 and 6 are a graphical presentation of the most important parameters of Table 1. The initial thrust-to-weight ratios shown in FIG 5 are those which maximize mass fraction in orbit. The only remaining independent parameter, specific impulse, is shown as the abscissa of these graphs.

FIG 7 through 14 are plotted from Tables 2 through 11. In each case the initial lunar thrust-to-weight ratio is chosen as the independent variable since most other quantities depend strongly on this quantity. The specific impulse values (which exert less influence) are used as parameters on graphs having multiple curves.

FIG 15 through 22 are taken from Tables 12 through 21. These graphs are later repeated for corresponding data which were calculated using the large numerical integration interval; e.g., FIG 15 "corresponds" to FIG 25 and 26. It may be noted that the mass fraction at orbit continues to increase with an increasing initial thrust-to-weight ratio in FIG 15, but reaches a well-defined maximum in FIG 26. FIG 15 is correct; the peak shown in FIG 26 is introduced by the large time step used in numerical integration.

FIG 23 through 33 cover the tabular data for the case of $\gamma_0 = 0°$. FIG 23 is similar to FIG 5, but in this case the thrust-to-weight values are chosen to produce maximum altitudes. FIG 24, along with FIG 28, 29, 30, 31, 32, and 33 present Lagrange multipliers as functions of specific impulse or thrust-to-weight ratios with specific impulse as a parameter. FIG 24 corresponds to the same thrust-to-weight assumption as FIG 23.

FIG 25 and 26 present altitude and mass fraction as functions of initial lunar thrust-to-weight ratio with specific impulse as a parameter; they differ only in the range of thrust-to-weight ratio that is covered.

FIG 27 shows a plot of mass fraction vs final altitude with both specific impulse and thrust-to-weight ratios as parameters. The data covered are the same as FIG 26.

FIG 34 through 53 cover the same data as FIG 23 through 33 (but now $\gamma_0 = 10°, 20°, 30°$, or $40°$) except that in these cases no data are presented for initial lunar thrust-to-weight ratios of less than 2.

FIG 54 to 59 are plots of mass fraction and final altitude as functions of the initial thrust orientation angle (γ_0). In these figures, the thrust-to-weight ratio is different for each graph (T/W_0) = 2, 3, 4, 5, 6, or 7).

FIG 60 through 65 show the behavior of $r_f - r_0$, m_f/m_0 λ_1°, λ_4°, and λ_5° (respectively) as functions of final inclination for a vehicle with an initial thrust-to-weight ratio of 2, and a specific impulse of 300 sec. The sign conventions of cases 1, 3, 5, and 7 (see Section VI) are presented in these graphs. The sign convention influences the final altitudes and mass fractions very strongly as can be seen from FIG 50 and 51. Although the magnitudes of λ_1°, λ_4°, and λ_5° apparently are unbounded as we approach an inclination of 90°, there appears to be a discontinuity at infinity. This could be expected from the fact that C_1 has a jump discontinuity across polar orbit inclination.

FIG 66 through 71 do not correspond to any of the tables of Section VIII, but were prepared from a special detailed trajectory printout. These graphs show the time history of various parameters along the trajectory. It is interesting to note that θ and ϕ (as well as their first and second derivatives) are "parallel" throughout the flight. This "parallelism" also occurs for the gimbal angles γ and δ. Note that both γ and δ slightly "overshoot" their final values just prior to orbital injection. As can be seen from FIG 71, inclination increases very rapidly during the early portion of the flight when the thrust is turning a small velocity vector.

FIG 72 presents variations in final altitude, mass fraction, and final inclination as a function of lift-off latitude. FIG 73 shows λ_1^o and λ_5^o for the same variation of latitude. The assumptions about the vehicle are an initial thrust-to-weight ratio of 2 and a specific impulse of 300 sec.

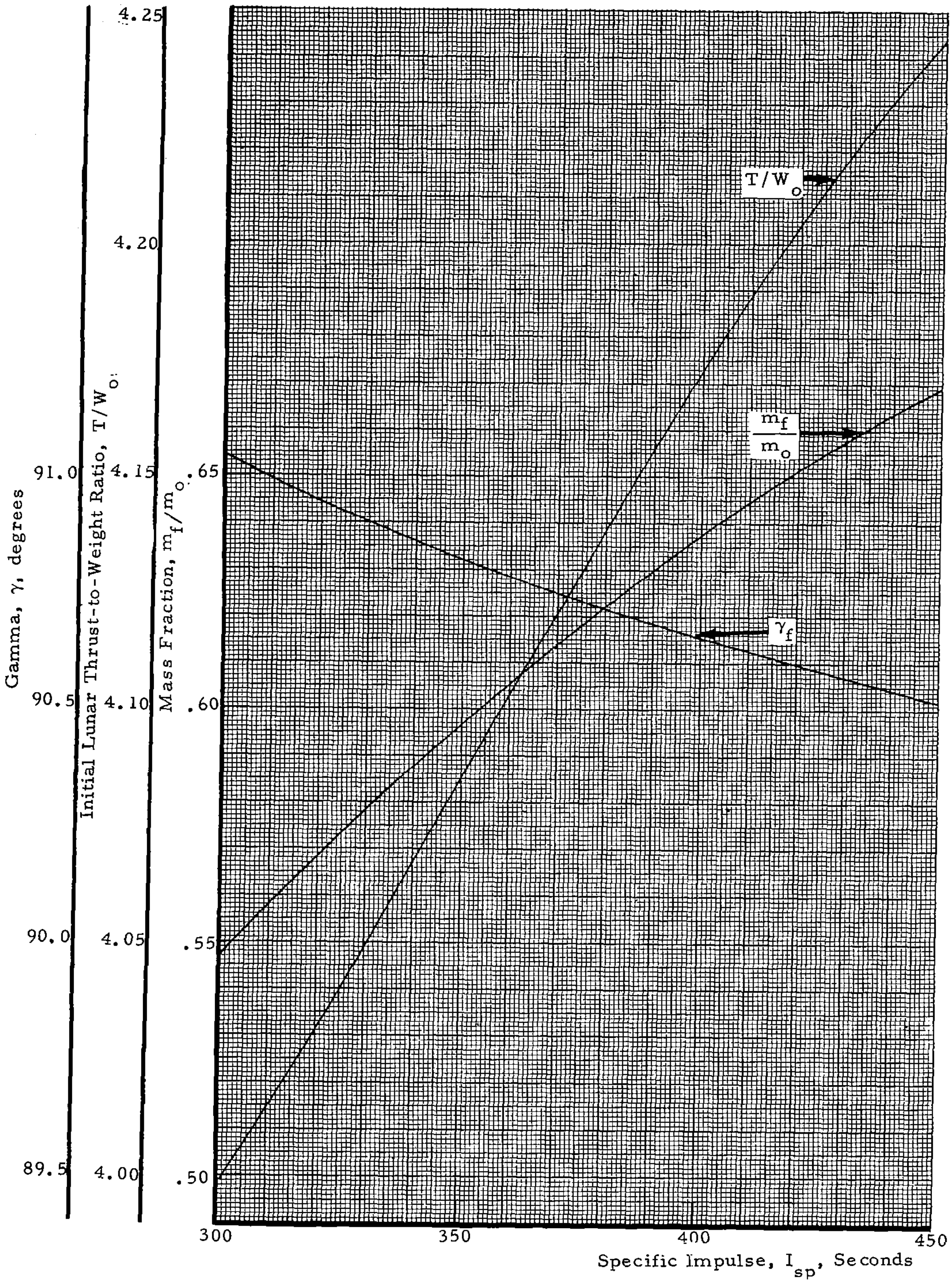

FIGURE 5. FINAL VALUE OF GAMMA, OPTIMAL INITIAL LUNAR-TO-WEIGHT RATIO AND MASS FRACTION VS SPECIFIC IMPULSE FOR ASCENT TO 15 KILOMETER ORBIT (Δt=4 SEC)

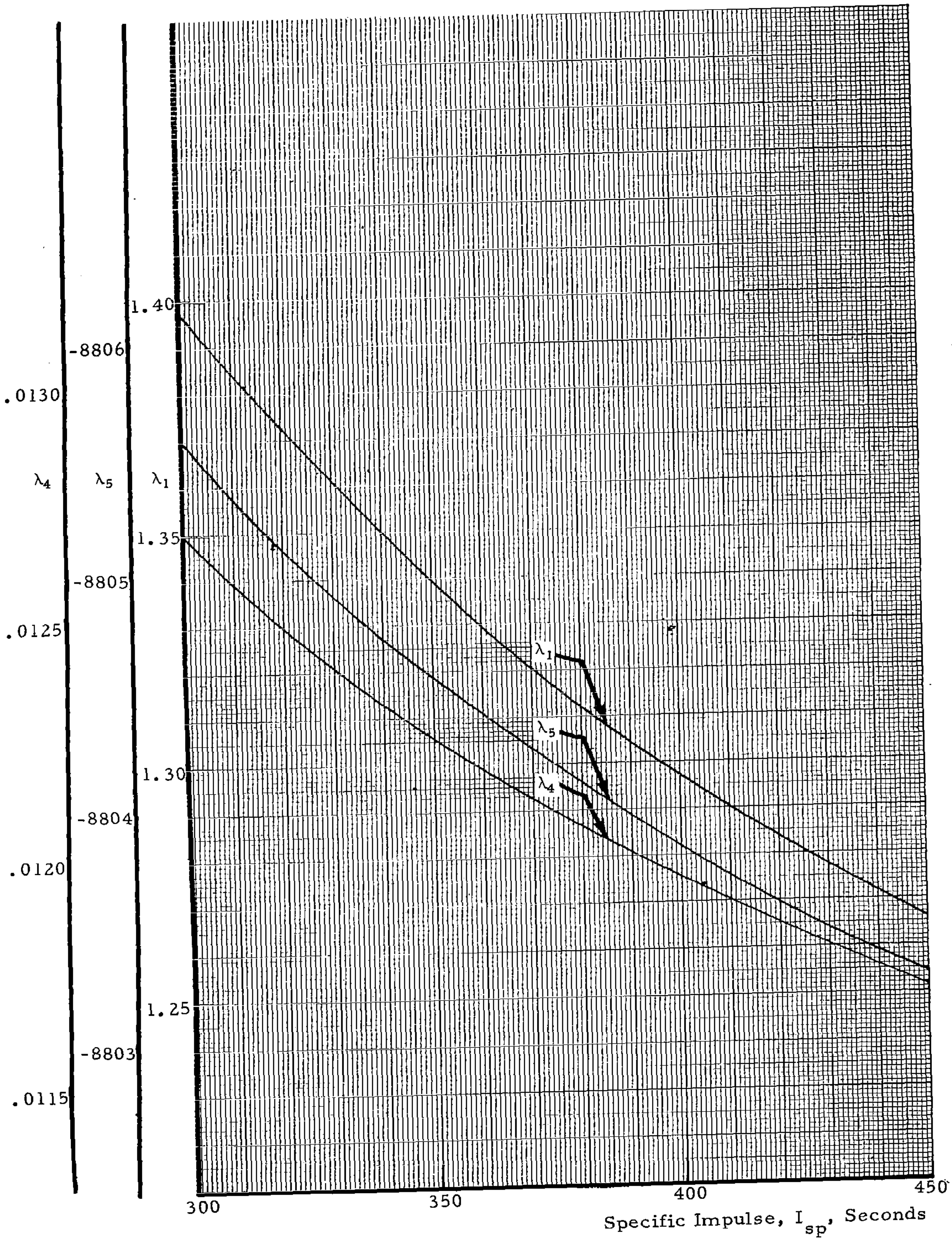

FIGURE 6. λ_1, λ_4, and λ_5 VS SPECIFIC IMPULSE FOR OPTIMAL INITIAL LUNAR THRUST-TO-WEIGHT RATIO: ASCENT TO 15 KILOMETER ORBIT (Δt=4 SEC)

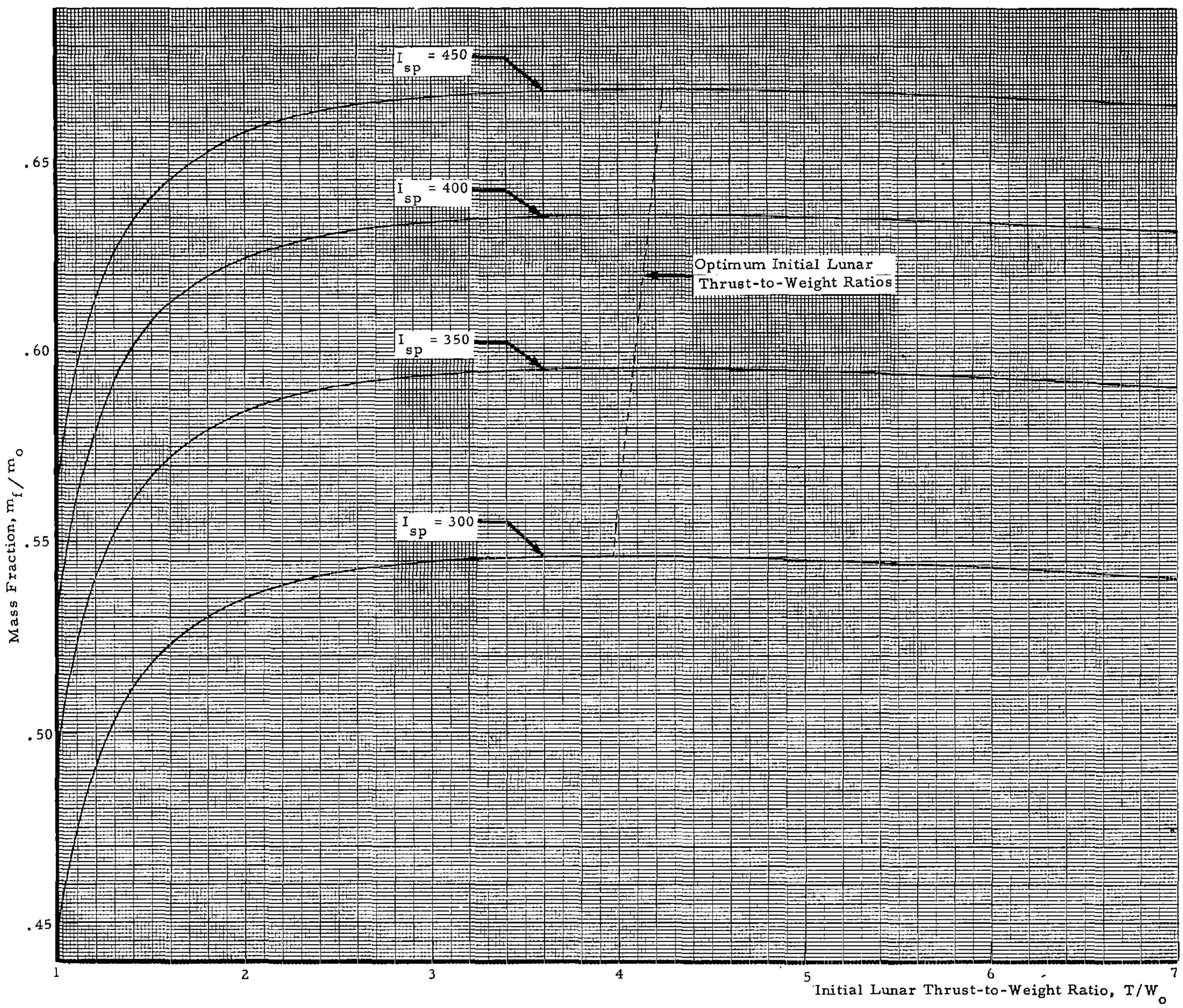

FIGURE 7. MASS FRACTION VS INITIAL LUNAR THRUST-TO-WEIGHT RATIO FOR ASCENT TO 15 KILOMETER ORBIT (Δt=4 SEC)

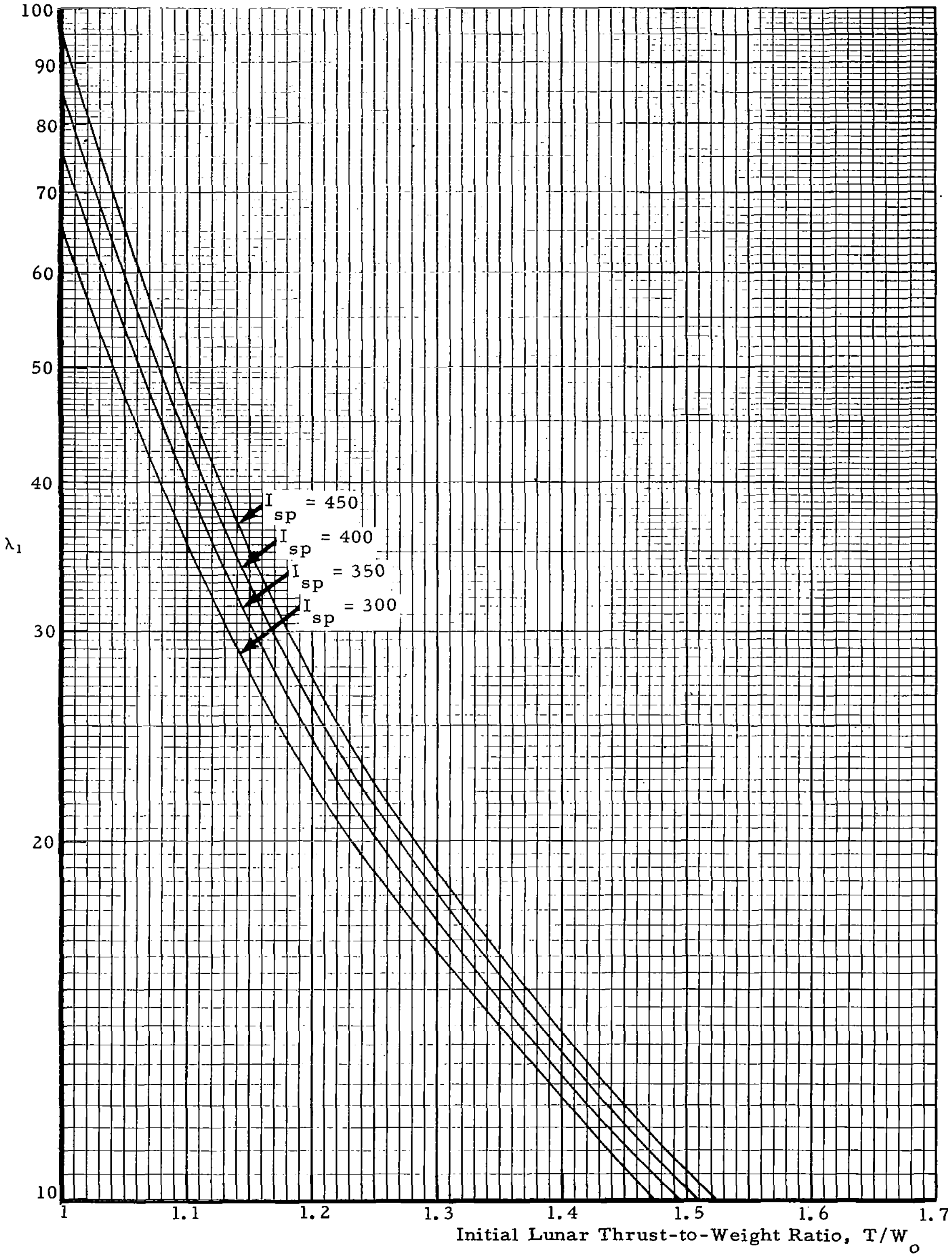

FIGURE 8. λ_1 VS INITIAL LUNAR THRUST-TO-WEIGHT RATIO FOR ASCENT TO 15 KILOMETER ORBIT (Δt=4 SEC)

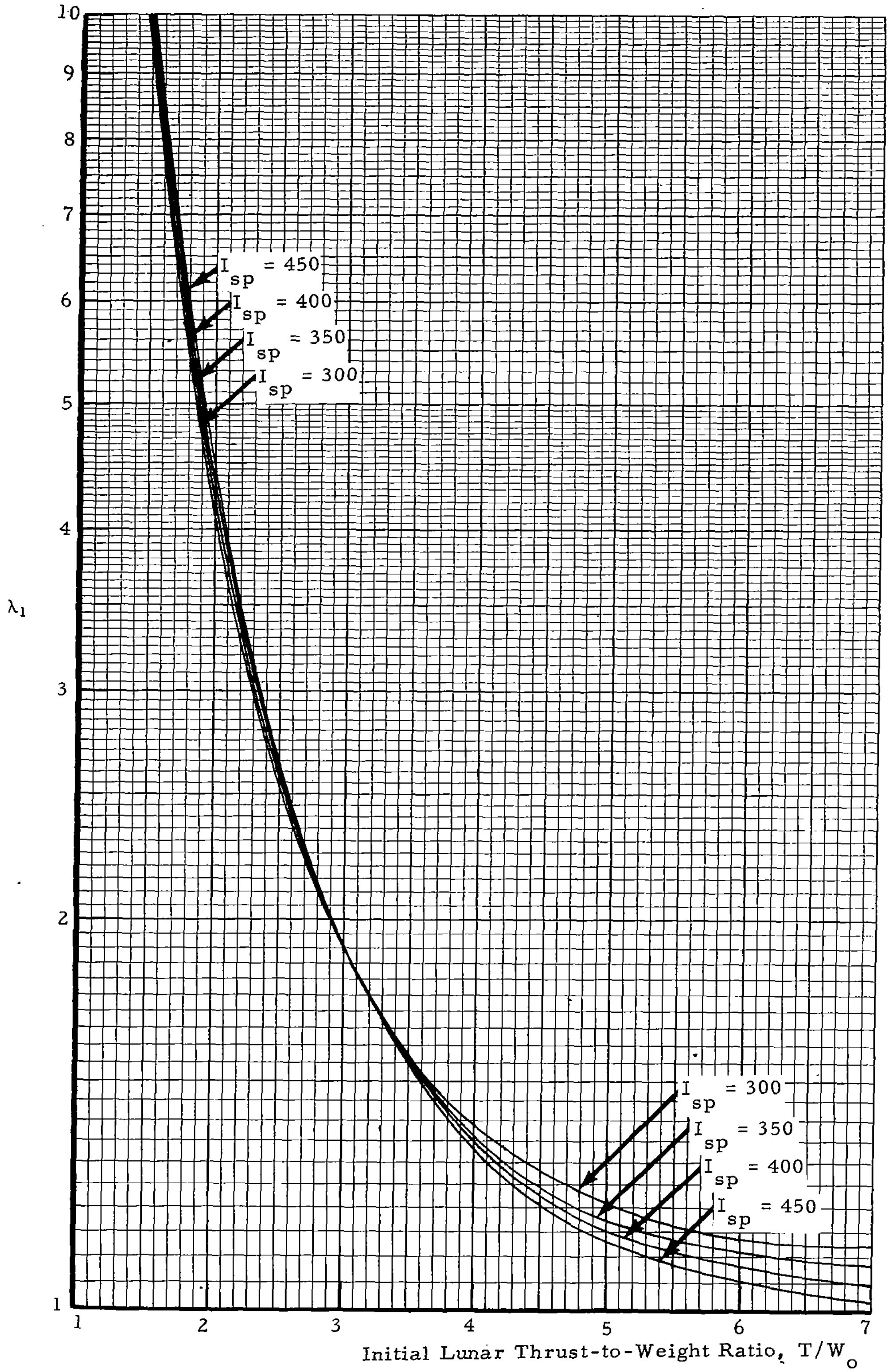

FIGURE 9. λ_1 VS INITIAL LUNAR THRUST-TO-WEIGHT RATIO FOR ASCENT TO 15 KILOMETER ORBIT (Δt=4 SEC)

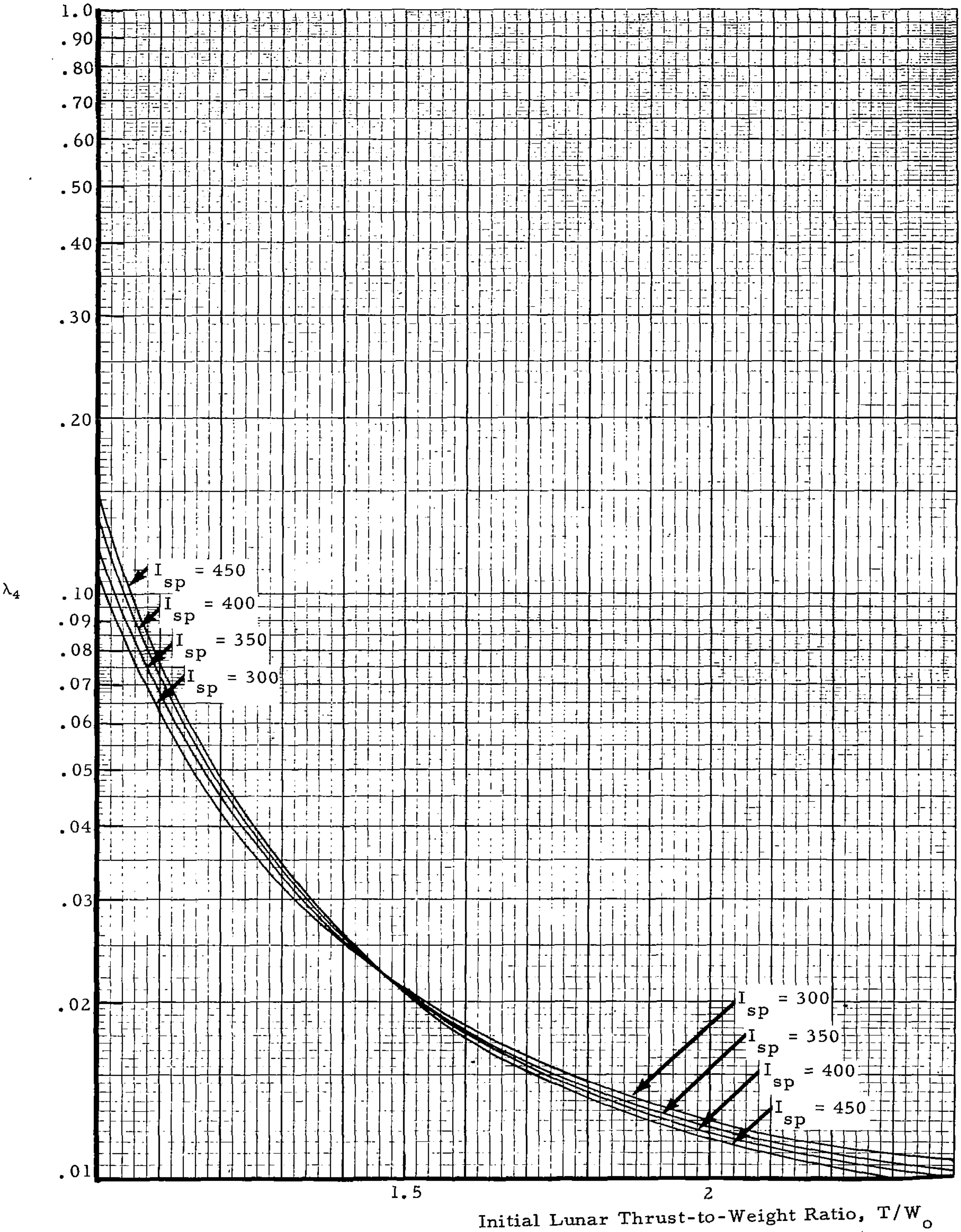

FIGURE 10. λ_4 VS INITIAL LUNAR THRUST-TO-WEIGHT RATIO FOR ASCENT TO 15 KILOMETER ORBIT (Δt=4 SEC)

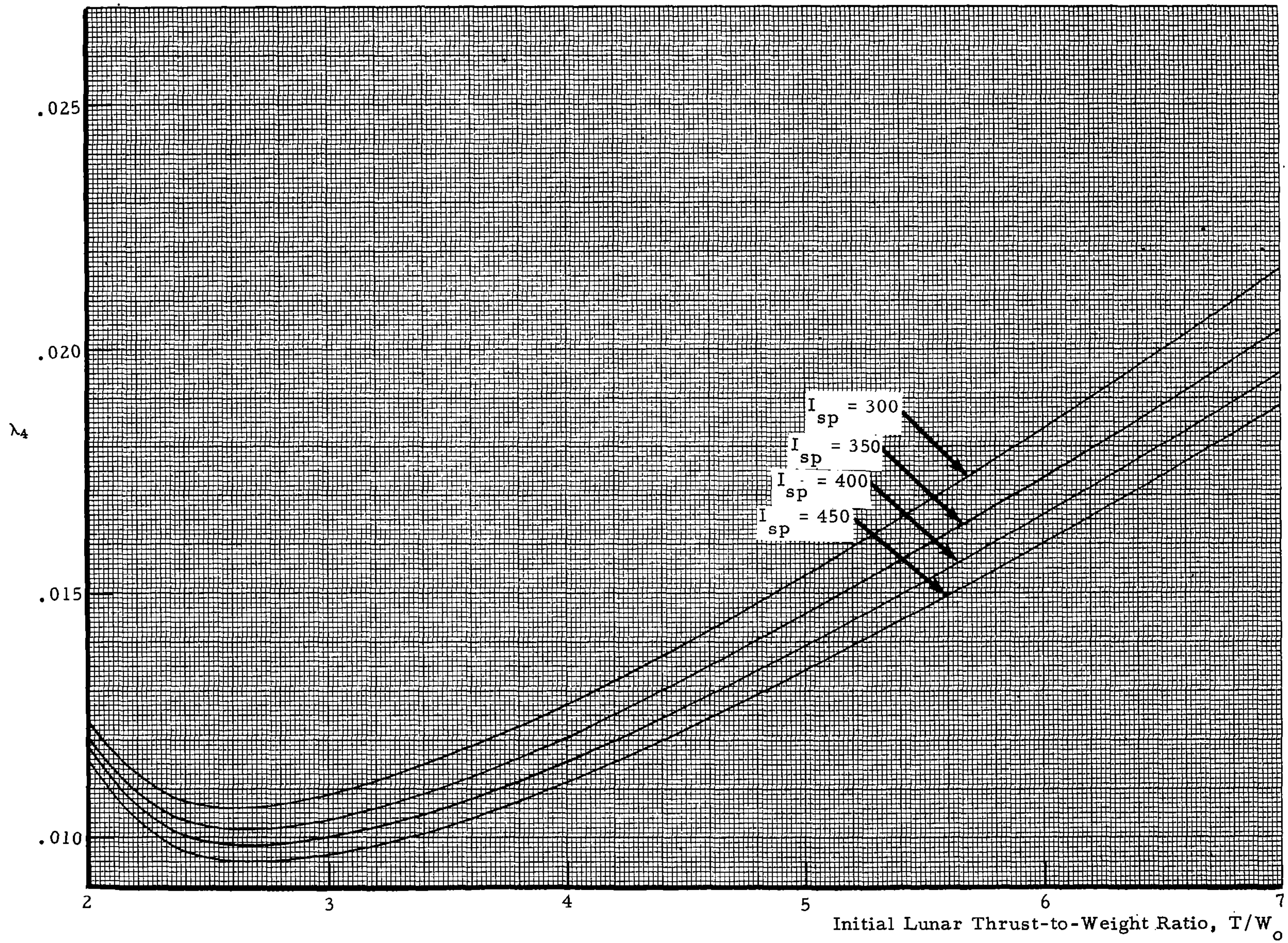

FIGURE 11. λ_4 VS INITIAL LUNAR THRUST-TO-WEIGHT RATIO FOR ASCENT TO 15 KILOMETER ORBIT (Δt=4 SEC)

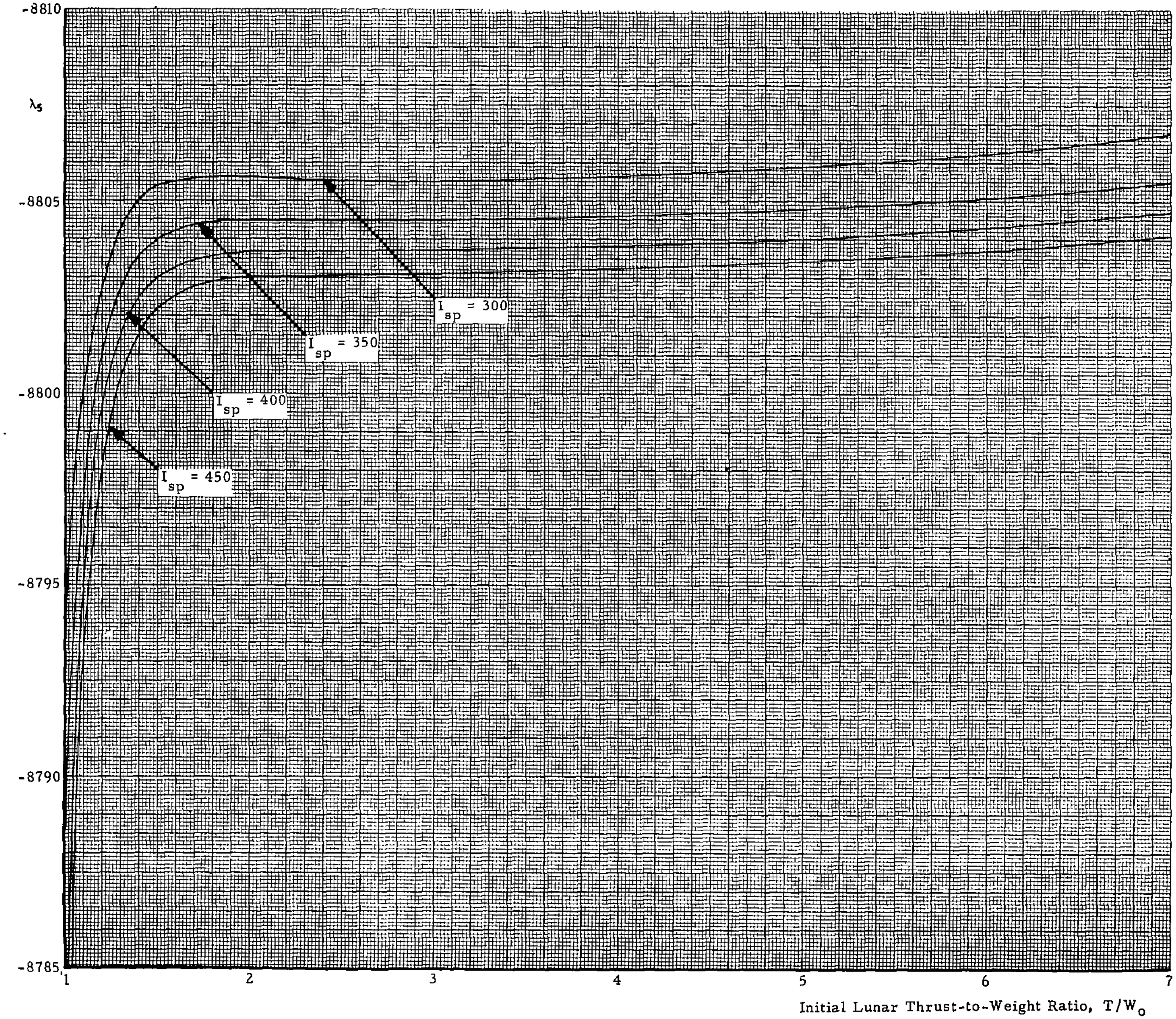

FIGURE 12. λ_4 VS INITIAL LUNAR THRUST-TO-WEIGHT RATIO FOR ASCENT TO 15 KILOMETER ORBIT (Δt=4 SEC)

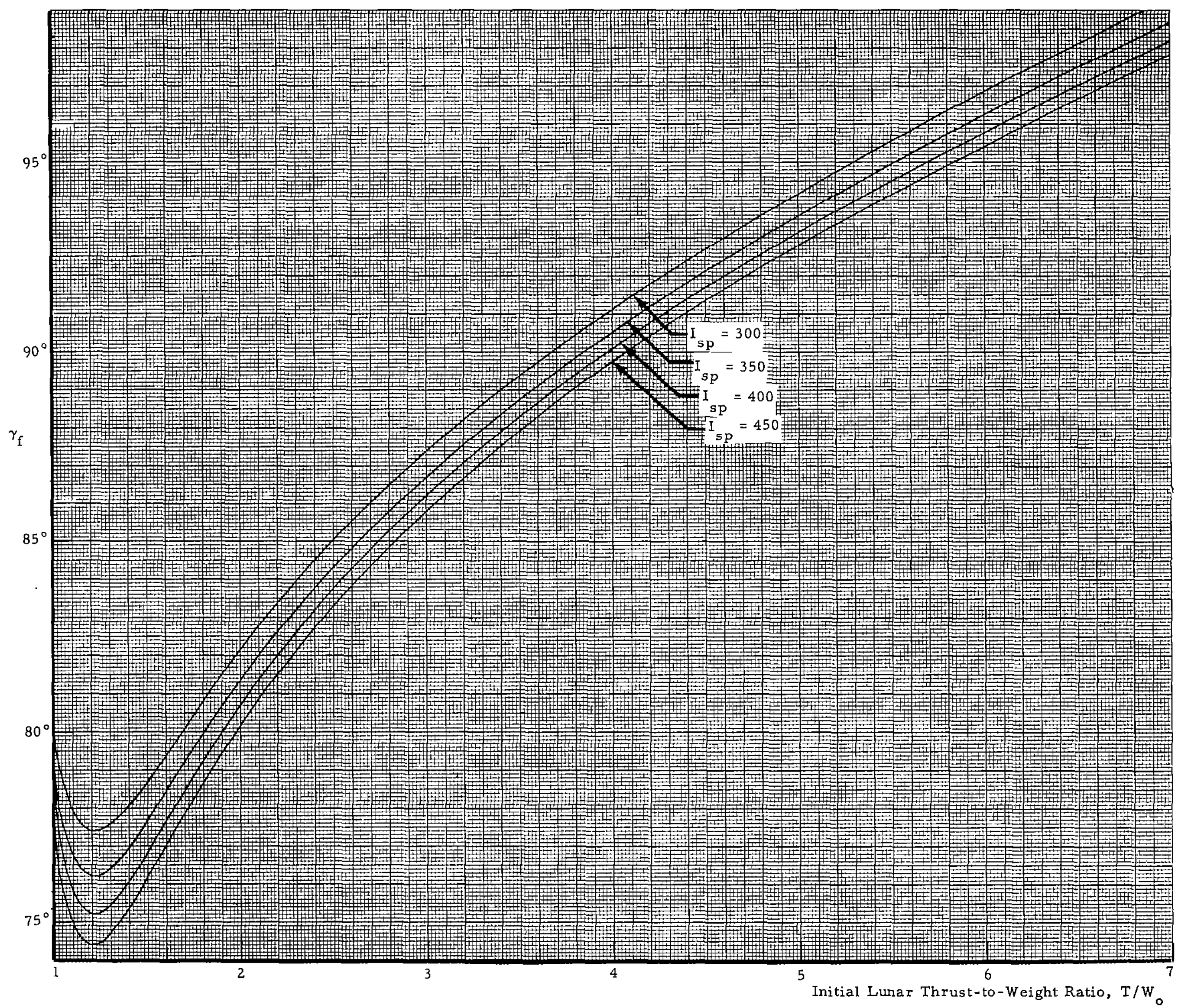

FIGURE 13. FINAL VALUE OF GAMMA VS INITIAL LUNAR THRUST-TO-WEIGHT RATIO FOR ASCENT TO 15 KILOMETER ORBIT (Δt=4 SEC)

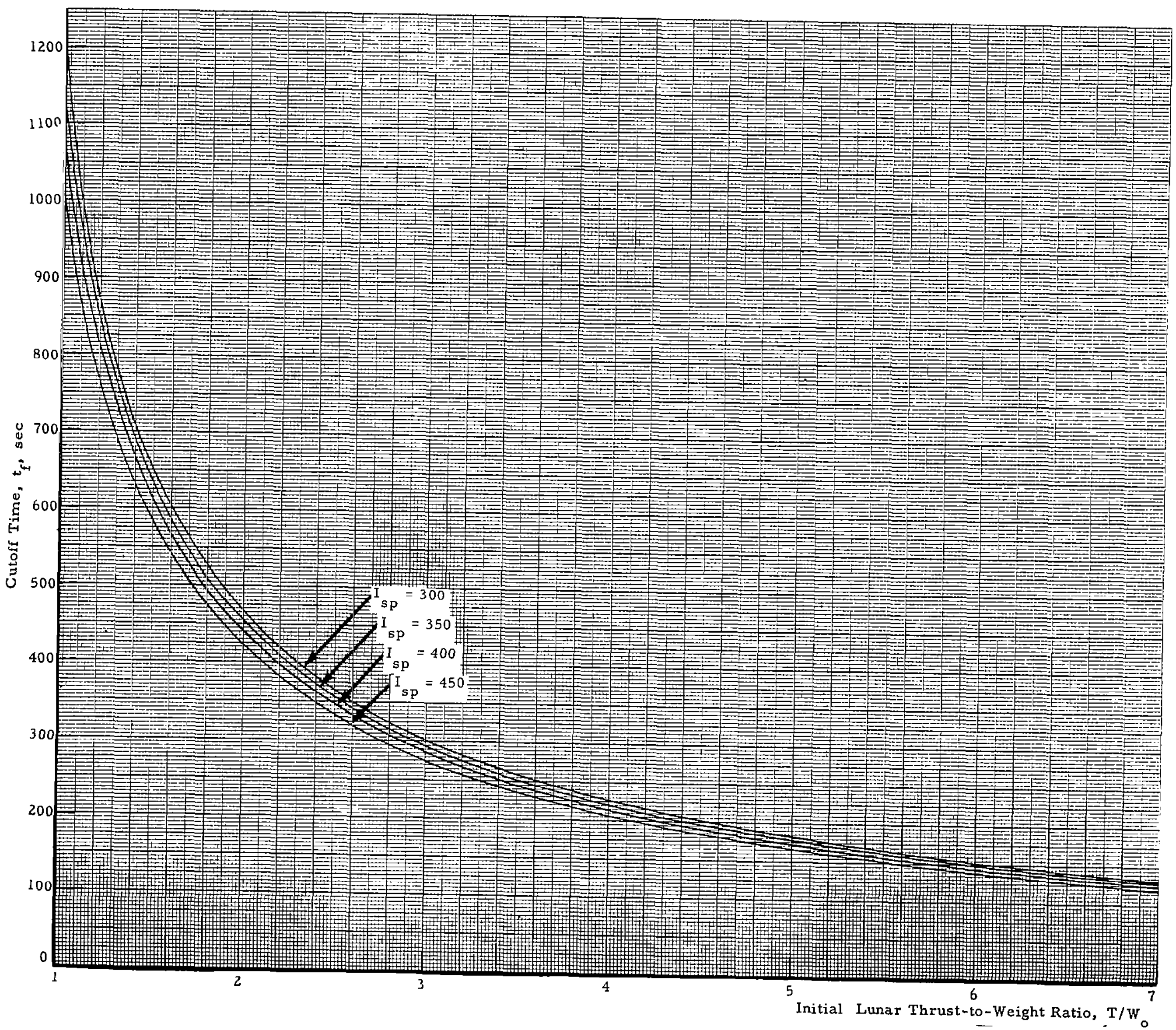

FIGURE 14. CUTOFF TIME VS INITIAL LUNAR THRUST-TO-WEIGHT RATIO FOR ASCENT TO 15 KILOMETER ORBIT (Δt=4 SEC)

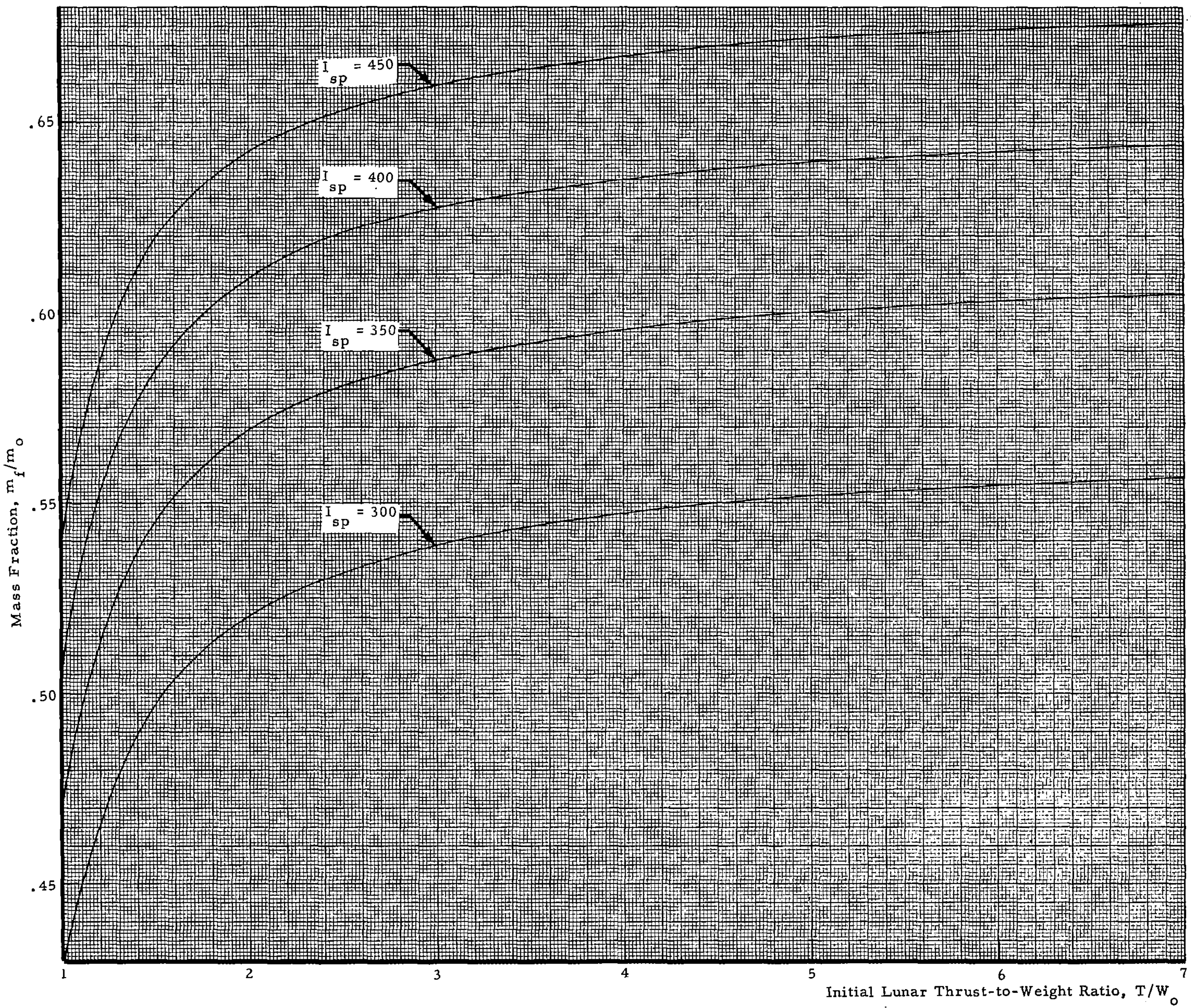

FIGURE 15. MASS FRACTION VS INITIAL LUNAR THRUST-TO-WEIGHT RATIO (γ_o=o, Δt=4 SEC)

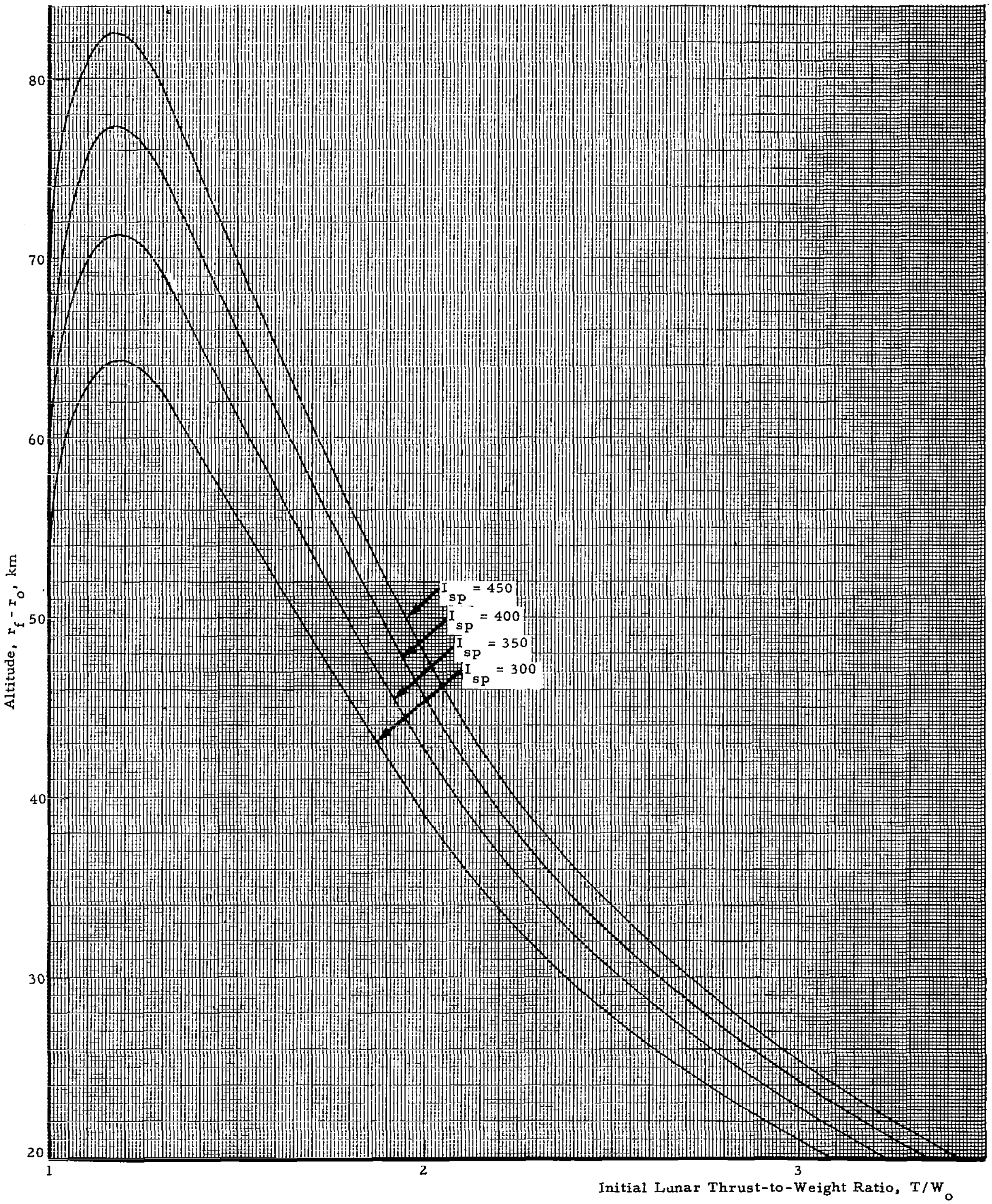

FIGURE 16. ALTITUDE VS INITIAL LUNAR THRUST-TO-WEIGHT RATIO (γ_o= o, Δt=4 SEC)

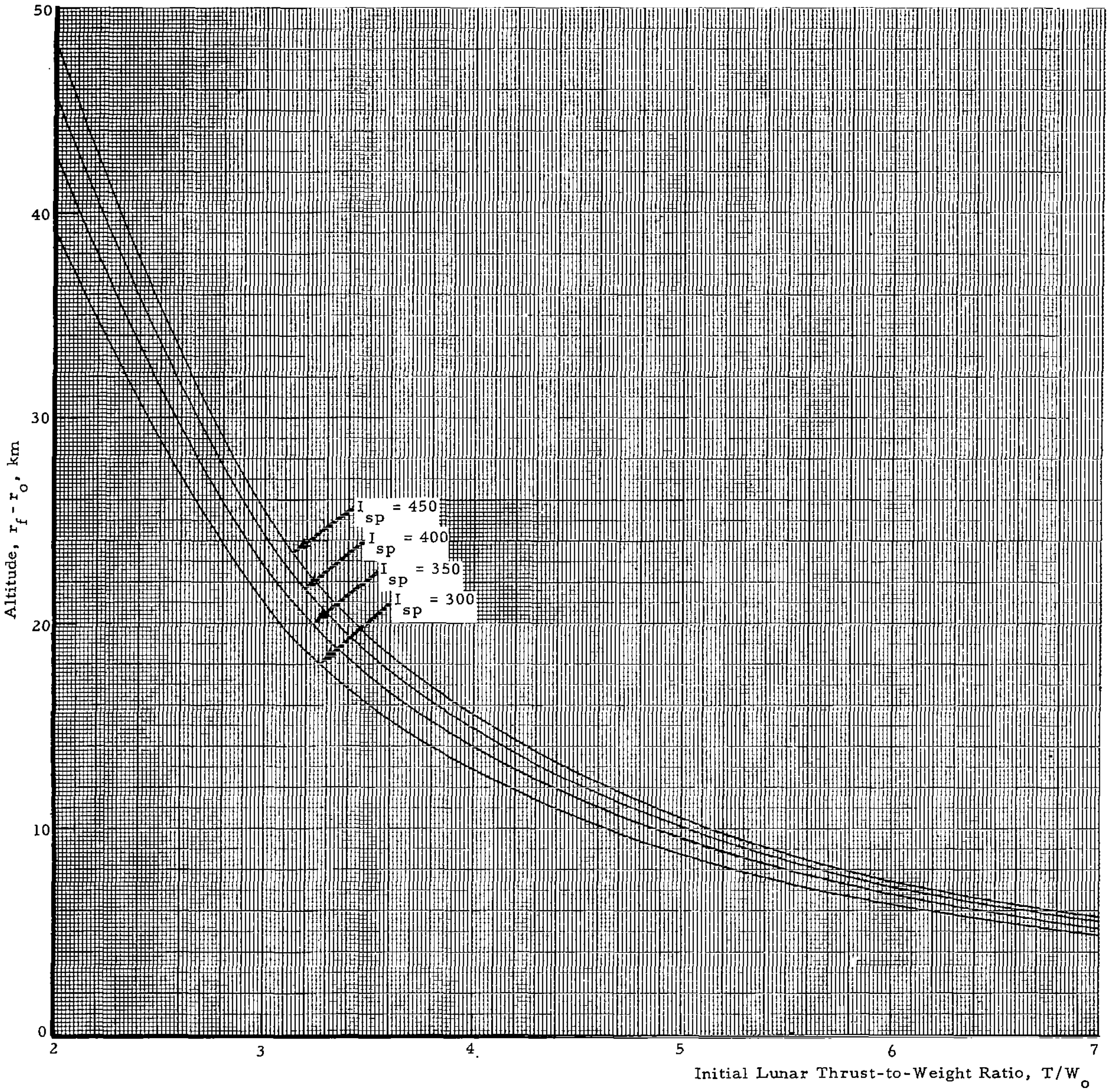

FIGURE 17. ALTITUDE VS INITIAL LUNAR THRUST-TO-WEIGHT RATIO ($\gamma_o = o$, $\Delta t = 4$ SEC)

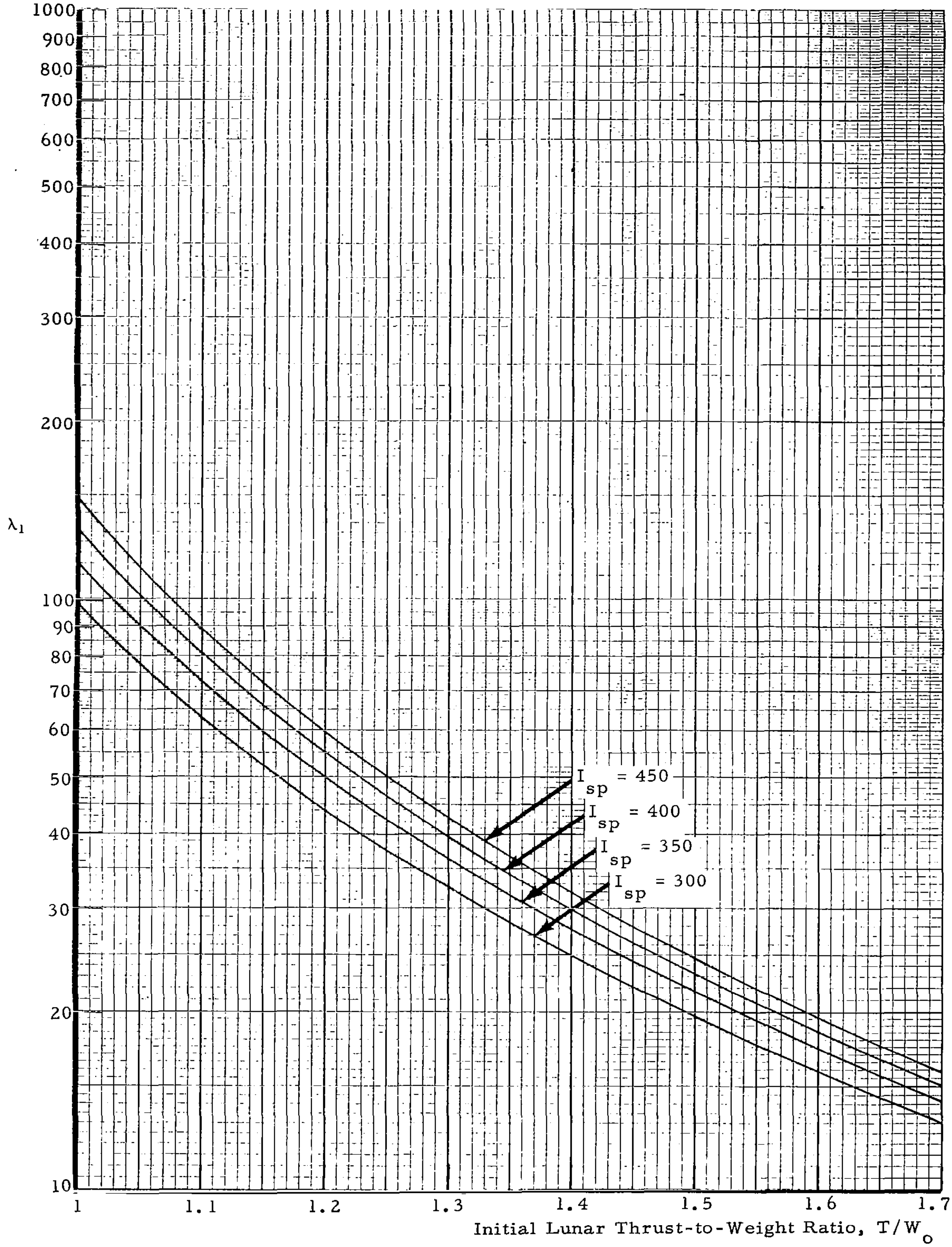

FIGURE 18. λ_1 VS INITIAL LUNAR THRUST-TO-WEIGHT RATIO (γ_o = o, Δt = 4 SEC)

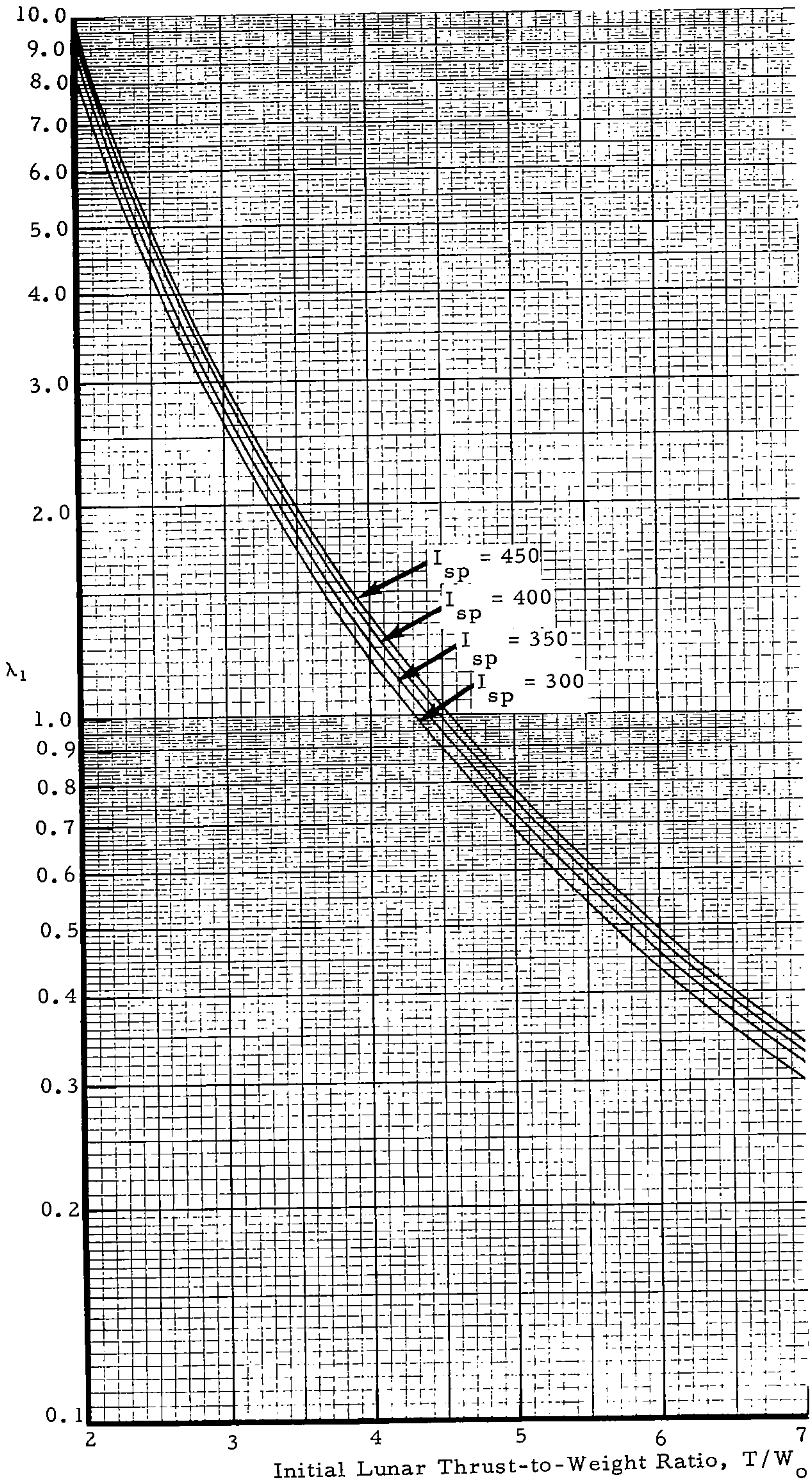

FIGURE 19. λ_1 VS INITIAL LUNAR THRUST-TO-WEIGHT RATIO (γ_o = o, Δt=4 SEC)

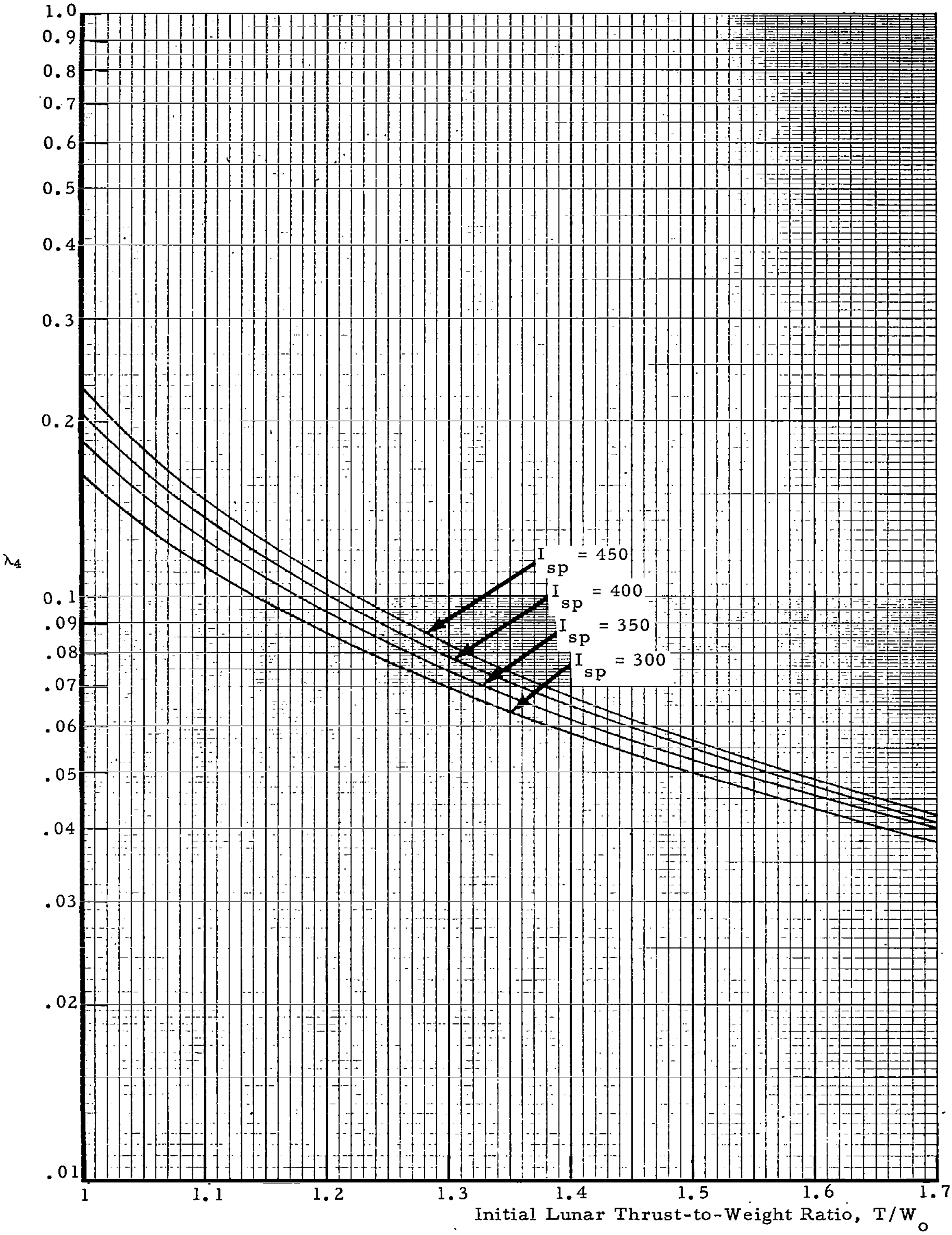

FIGURE 20. λ_4 VS INITIAL LUNAR THRUST-TO-WEIGHT RATIO
(γ_o = o, Δt=4 SEC)

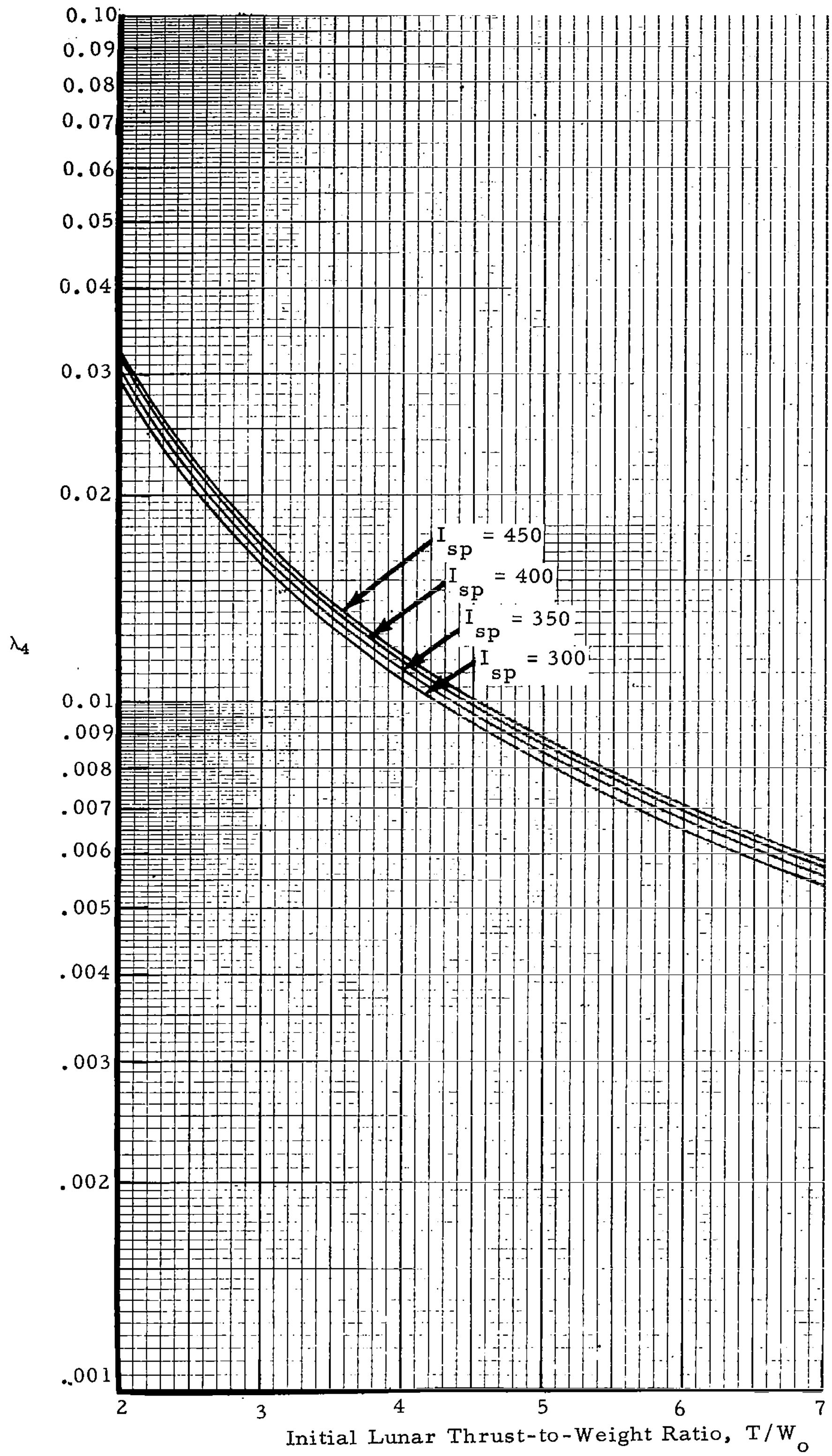

FIGURE 21. λ_4 VS INITIAL LUNAR THRUST-TO-WEIGHT RATIO (γ_o = o, Δt=4 SEC)

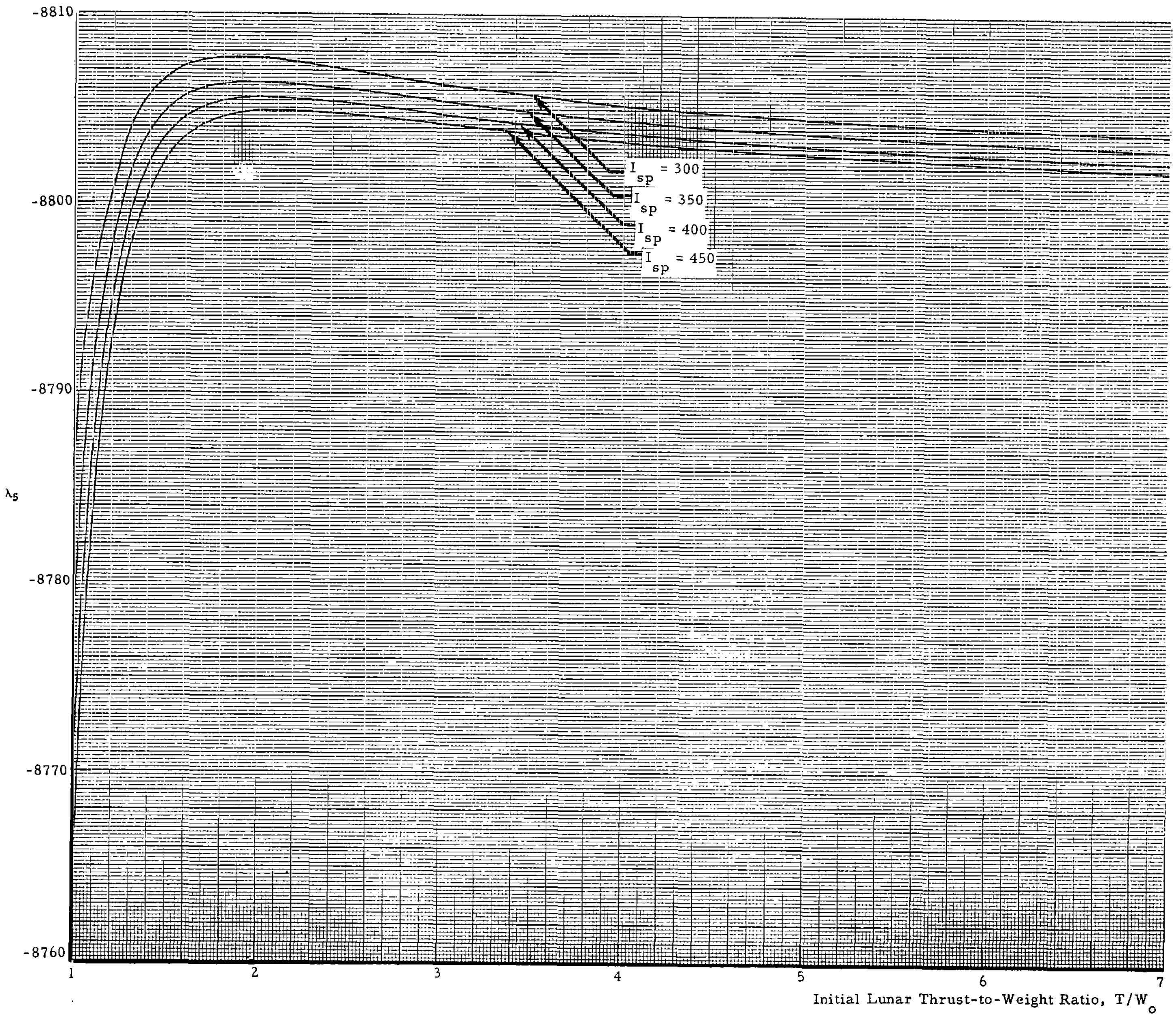

FIGURE 22. λ_5 VS INITIAL LUNAR THRUST-TO-WEIGHT RATIO (γ_o = o, Δt=4 SEC)

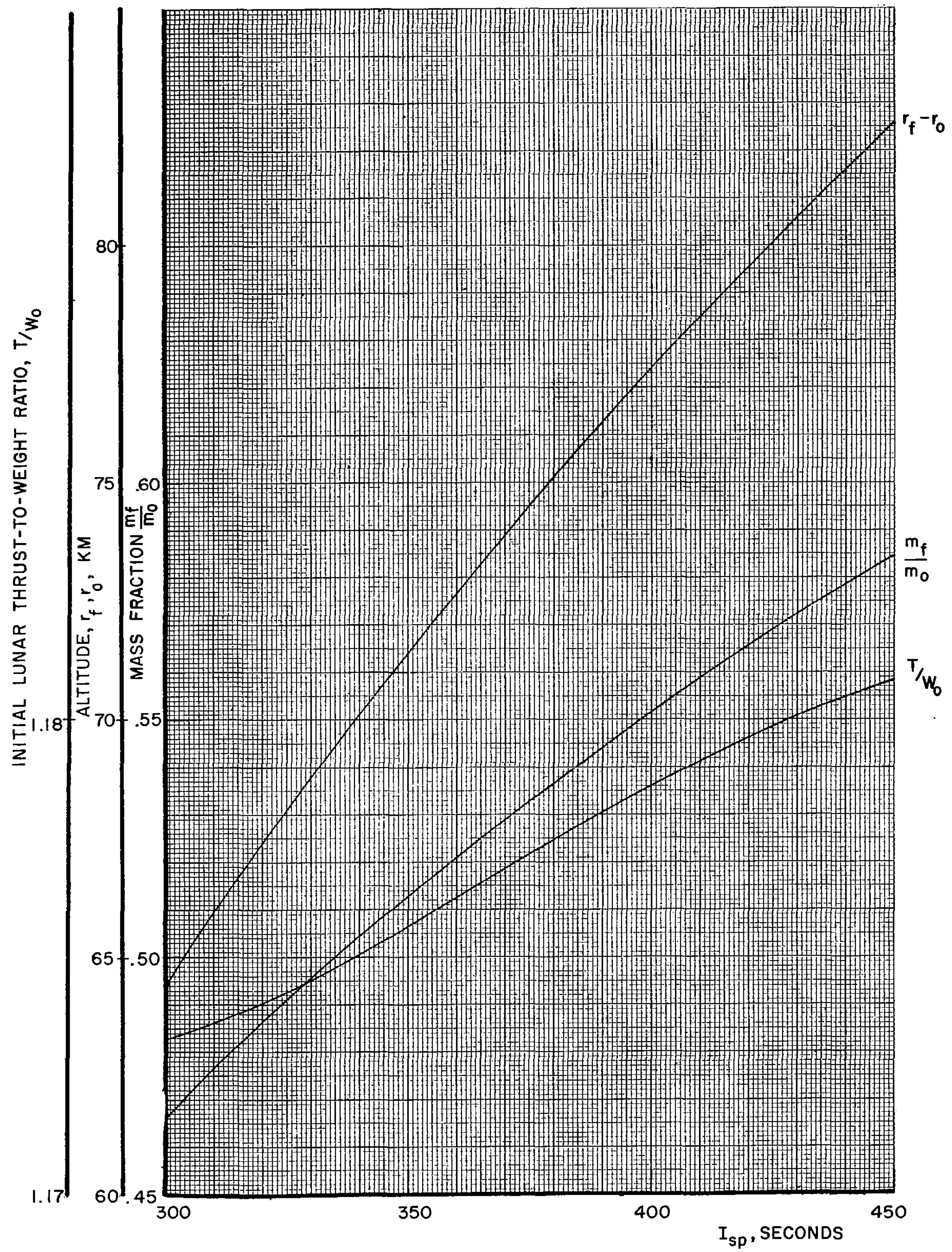

FIG 23. MASS FRACTION, ALTITUDE, AND INITIAL LUNAR THRUST-TO-WEIGHT RATIOS VS SPECIFIC IMPULSE FOR MAXIMUM FINAL ALTITUDES ($\gamma_0 = 0$)

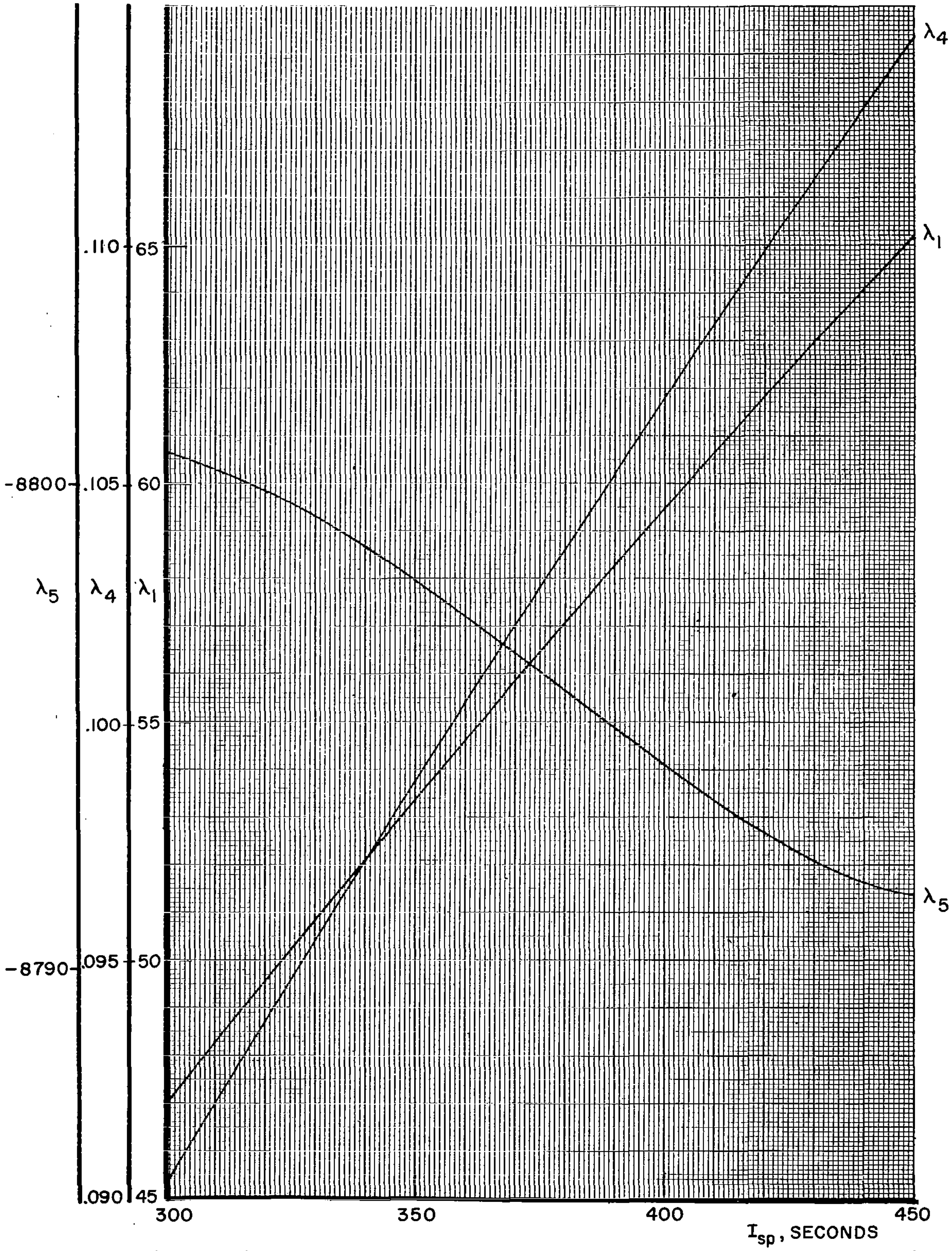

FIG.24. λ_1, λ_4, AND λ_5, VS SPECIFIC IMPULSE FOR MAXIMUM FINAL ALTITUDES (γ_0=0)

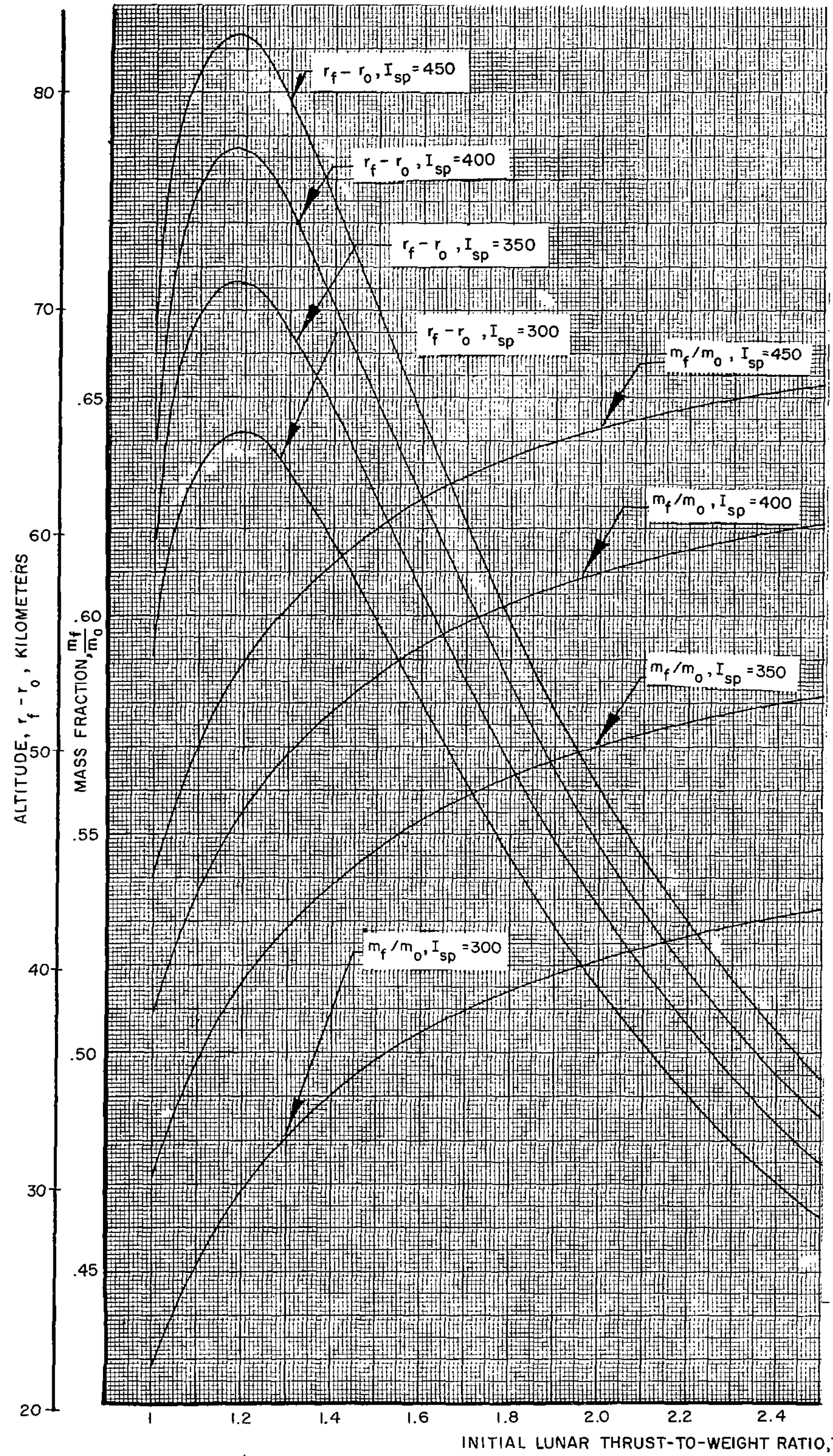

FIG 25. FINAL ALTITUDE AND MASS FRACTION VS INITIAL LUNAR THRUST-TO-WEIGHT RATIO ($\gamma_o = 0$)

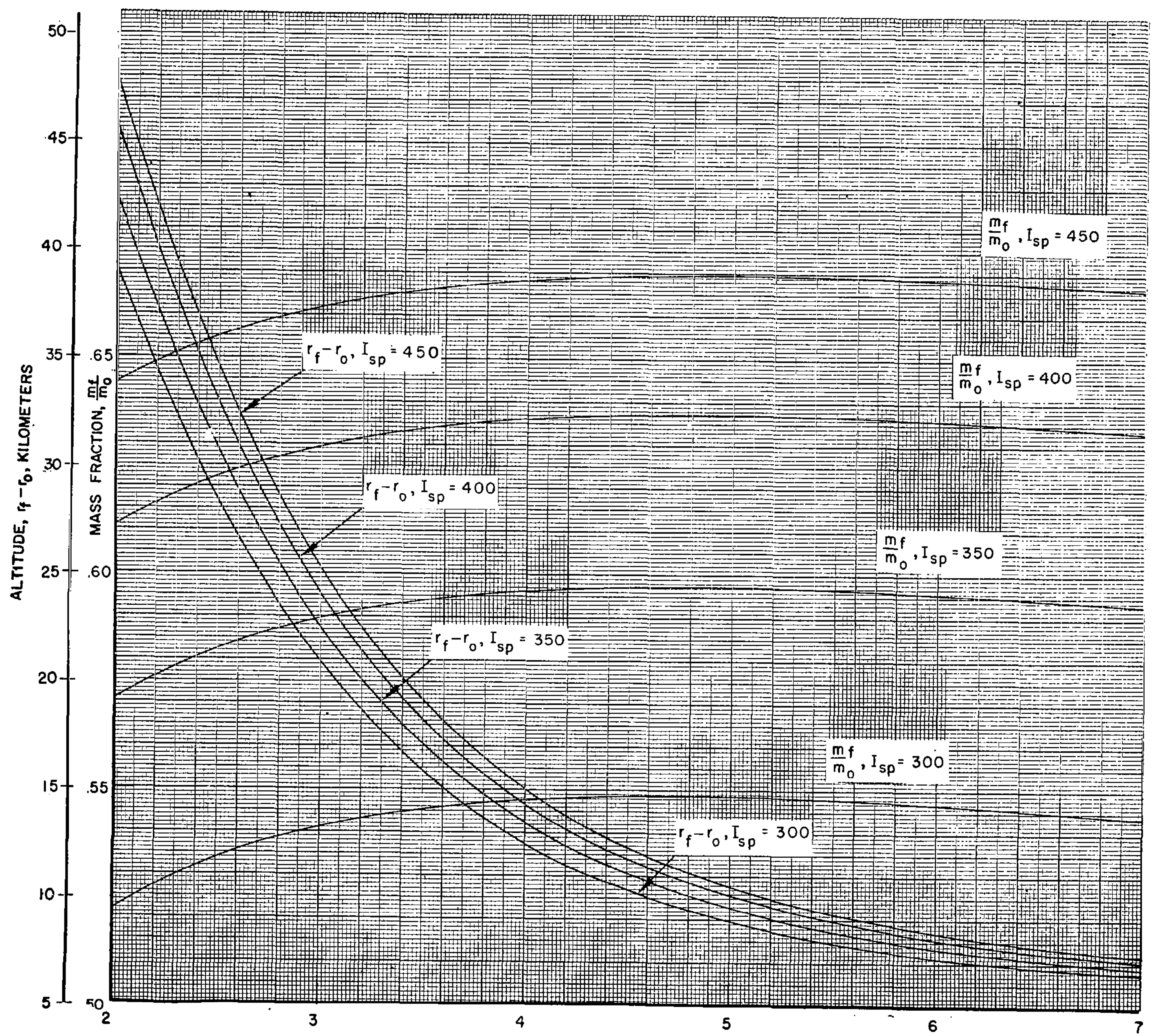

FIG 26. FINAL ALTITUDE AND MASS FRACTION VS INITIAL THRUST-TO-WEIGHT RATIO (γ_o=0°)

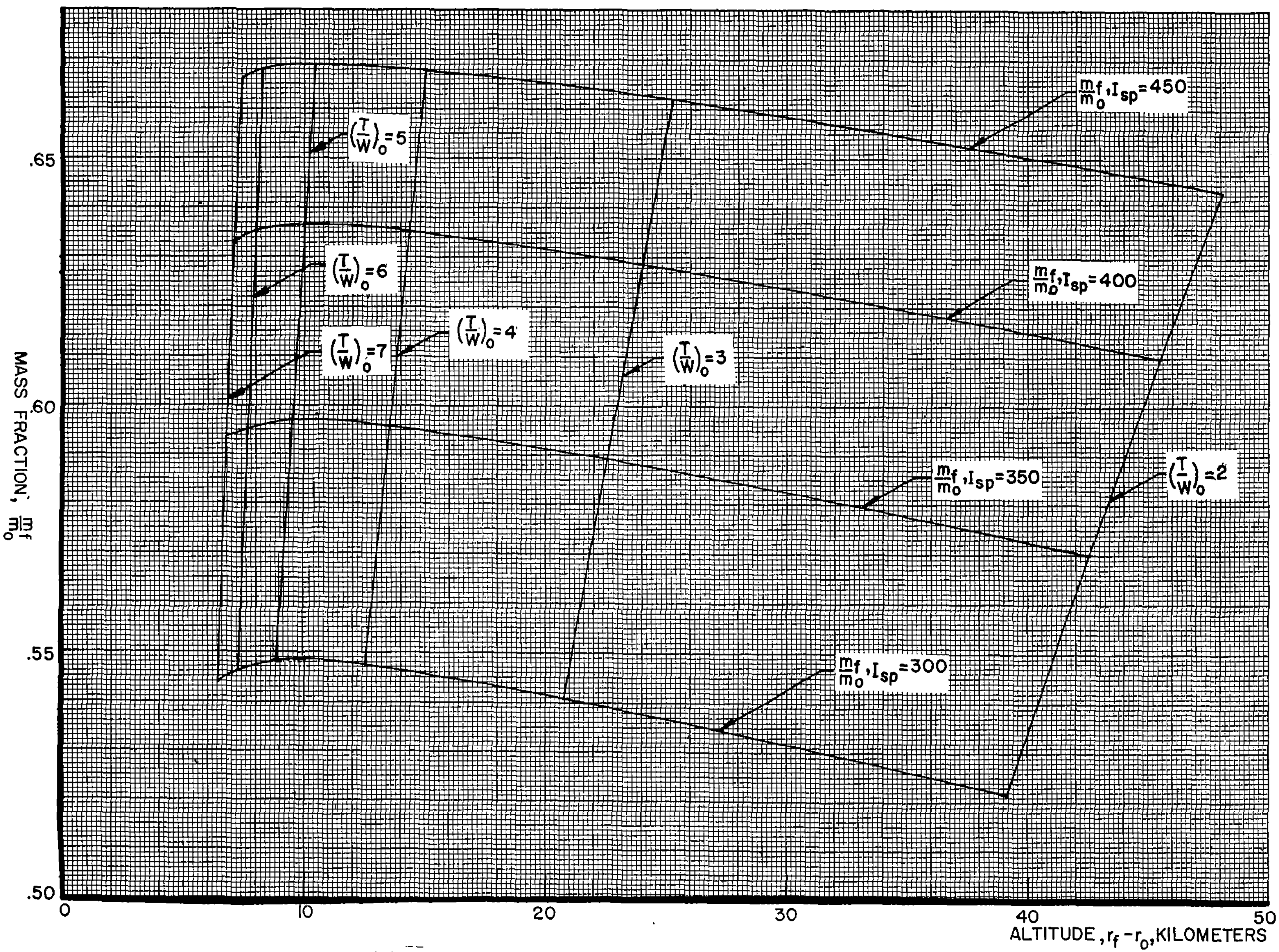

FIG 27. MASS FRACTION VS FINAL ALTITUDE ($\gamma_o=0°$)

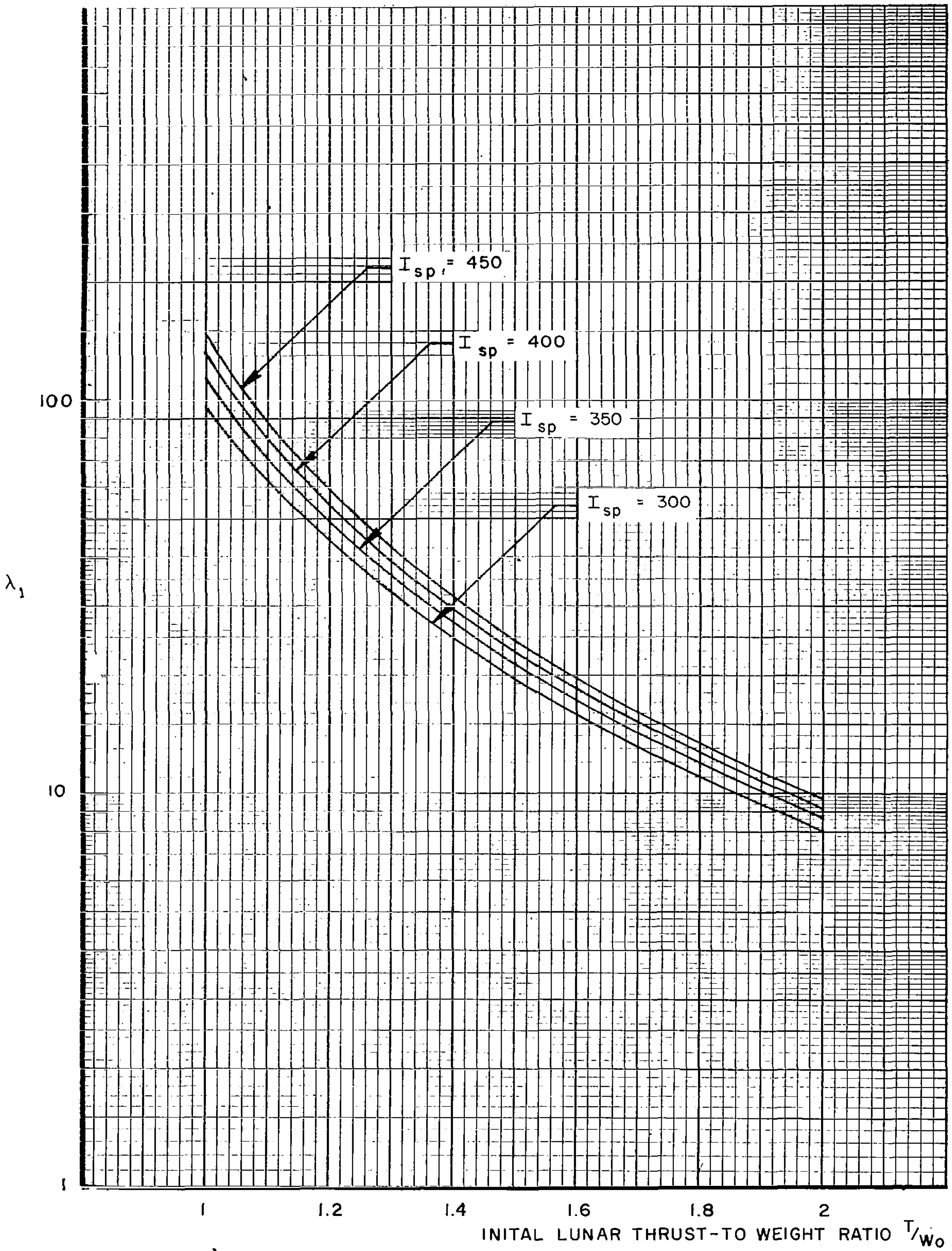

FIG 28. λ_1 VS INITAL LUNAR THRUST-TO-WEIGHT RATIO ($\gamma_0 = 0$)

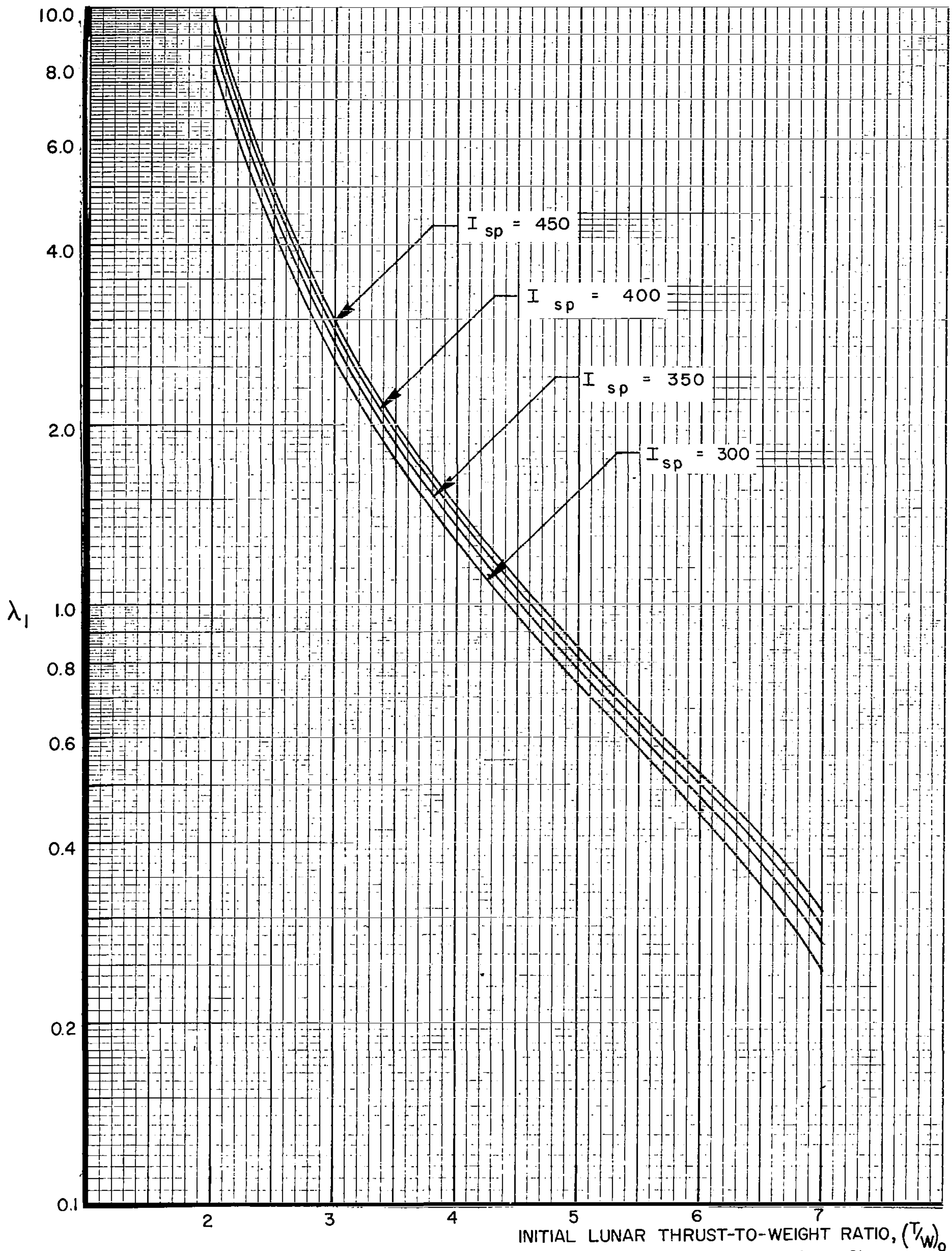

FIG 29. λ_1 VS INITIAL LUNAR THRUST-TO-WEIGHT RATIO (γ_0=0°)

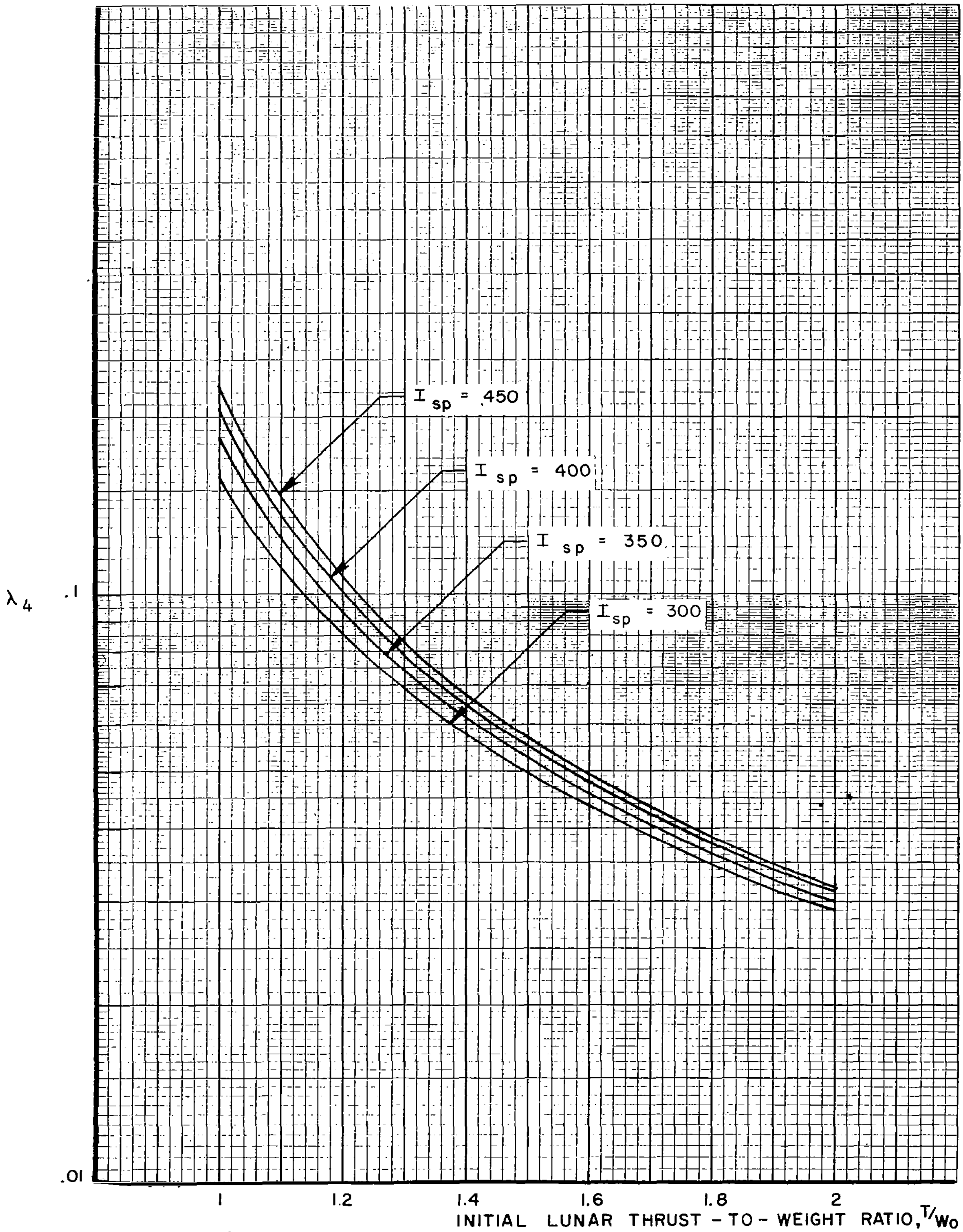

FIG 30. λ_4 VS INITIAL LUNAR THRUST-TO-WEIGHT RATIO ($\gamma_0 = 0$)

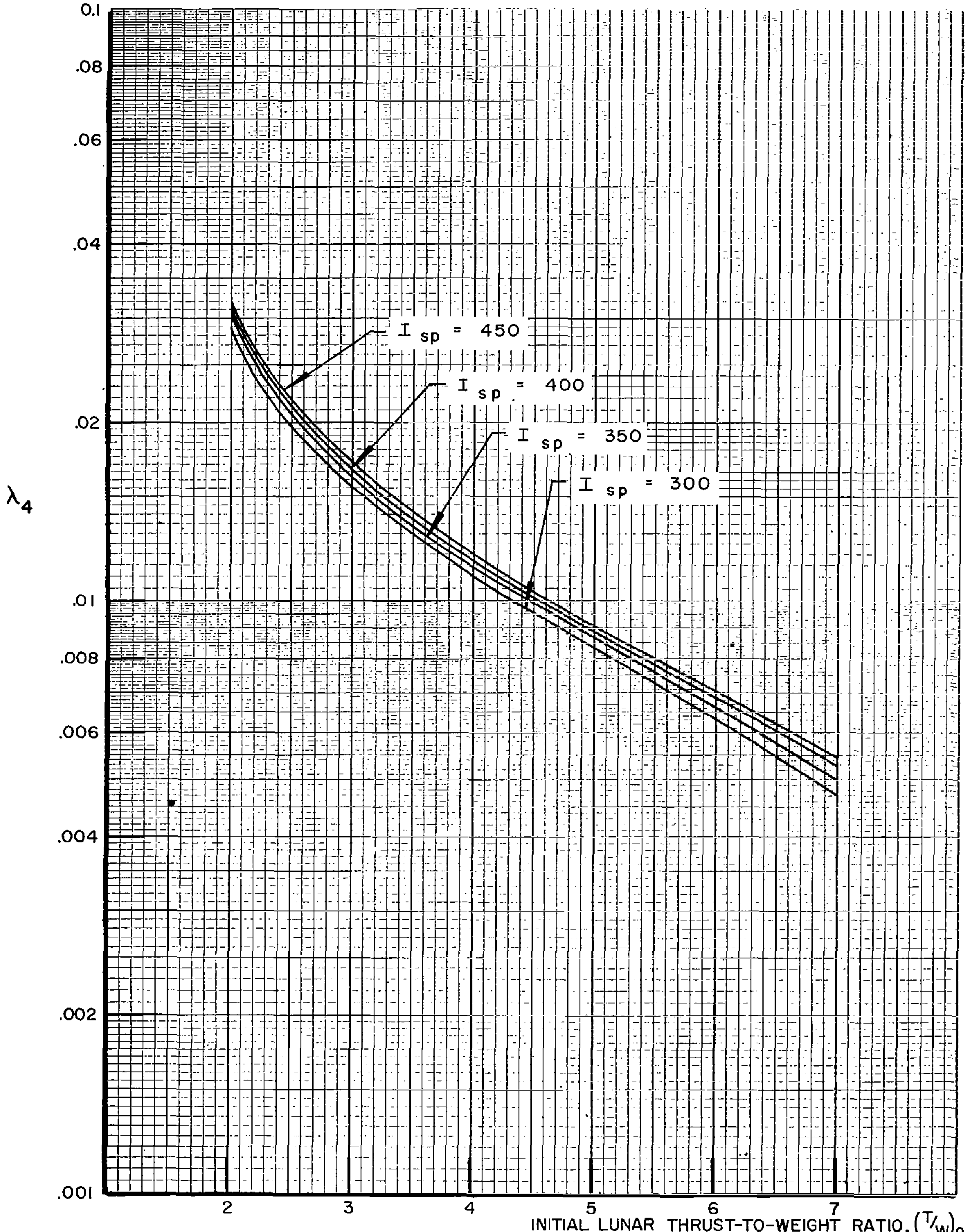

FIG 31. λ_4 VS INITIAL LUNAR THRUST-TO-WEIGHT RATIO (γ_0=0°)

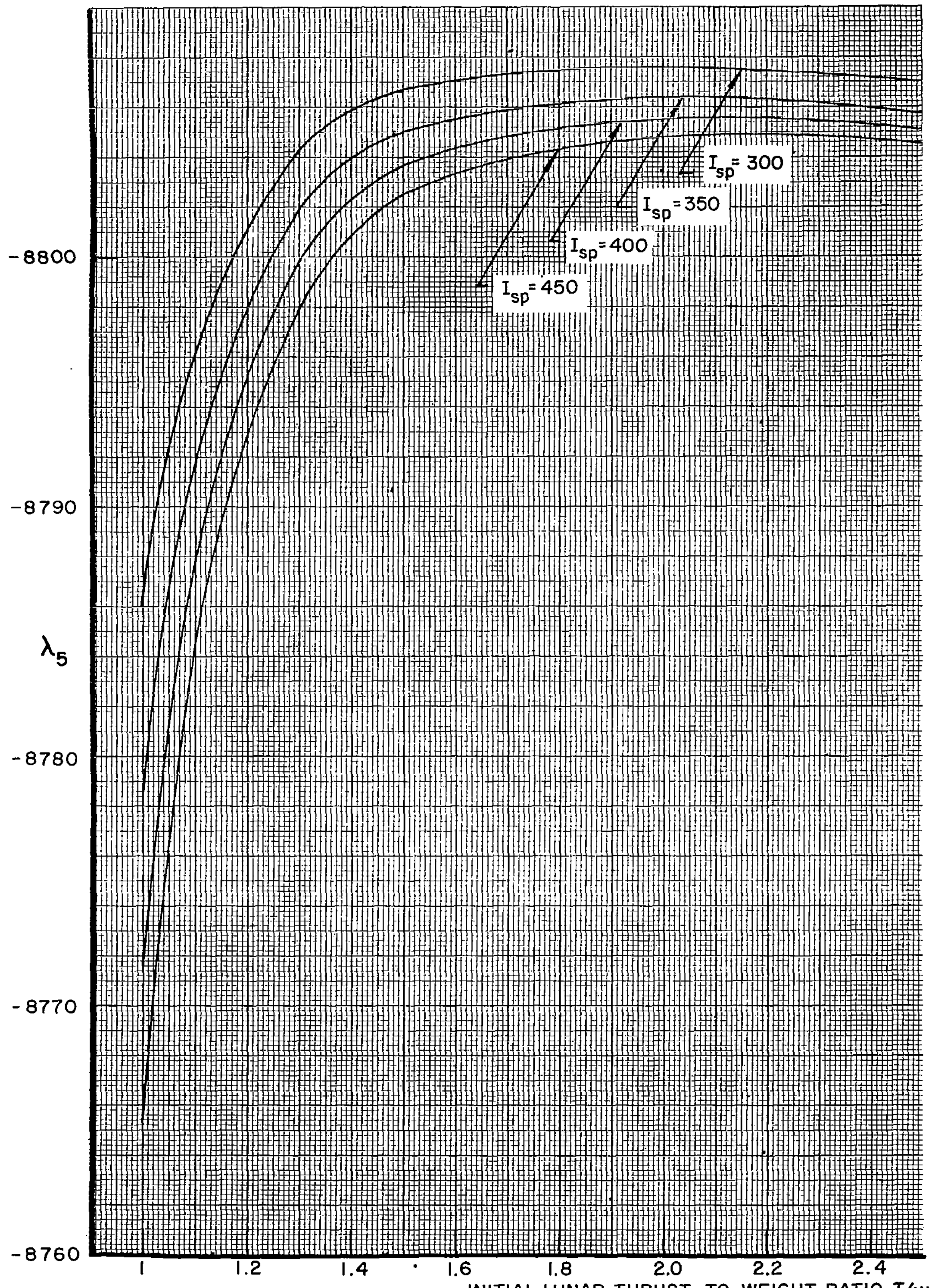

FIG. 32. λ_5 VS INITIAL LUNAR THRUST-TO-WEIGHT RATIO ($\gamma_0 = 0°$)

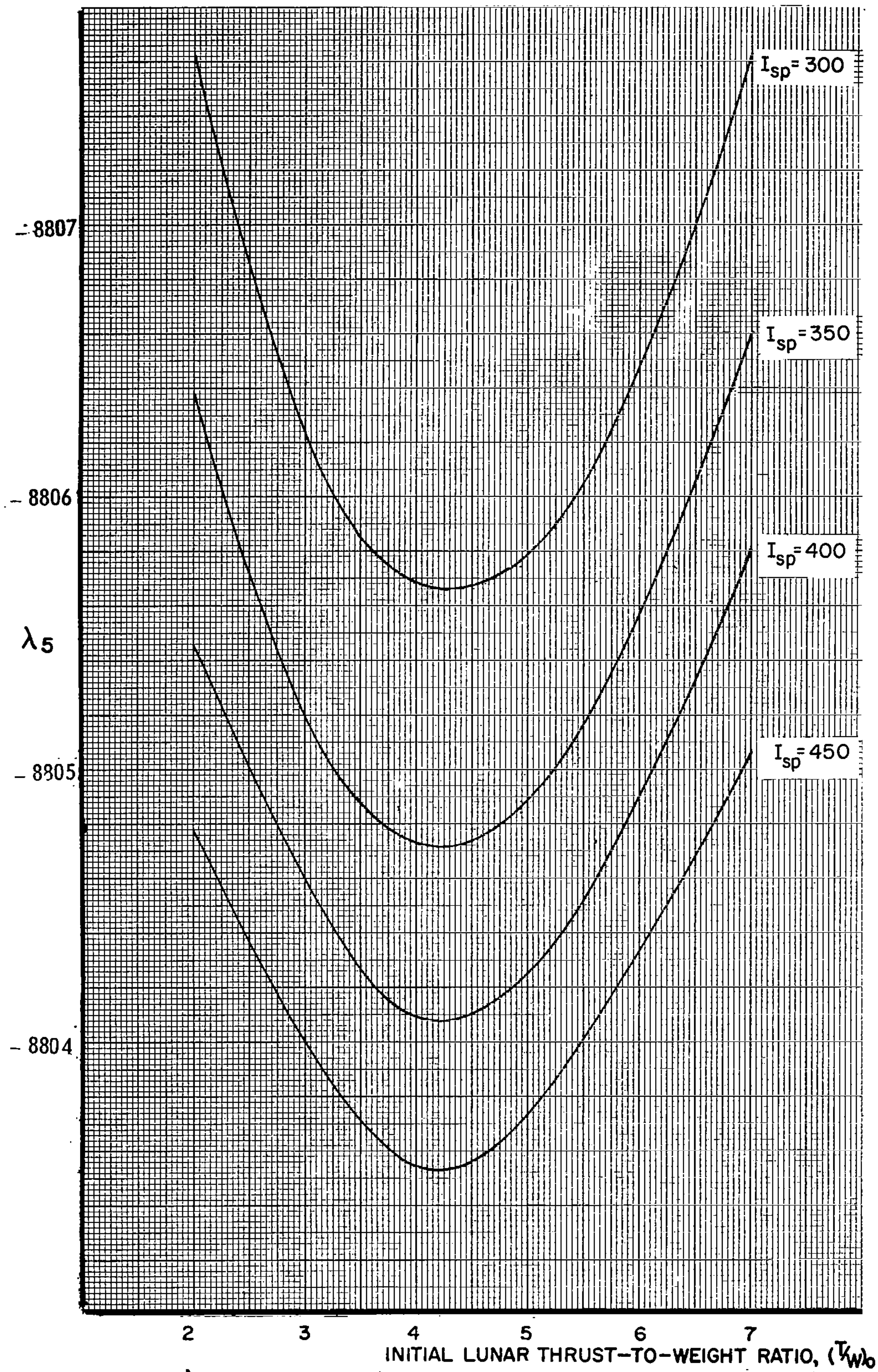

FIG 33. λ_5 VS INITIAL LUNAR THRUST-TO-WEIGHT RATIO $(\gamma_0 = 0°)$

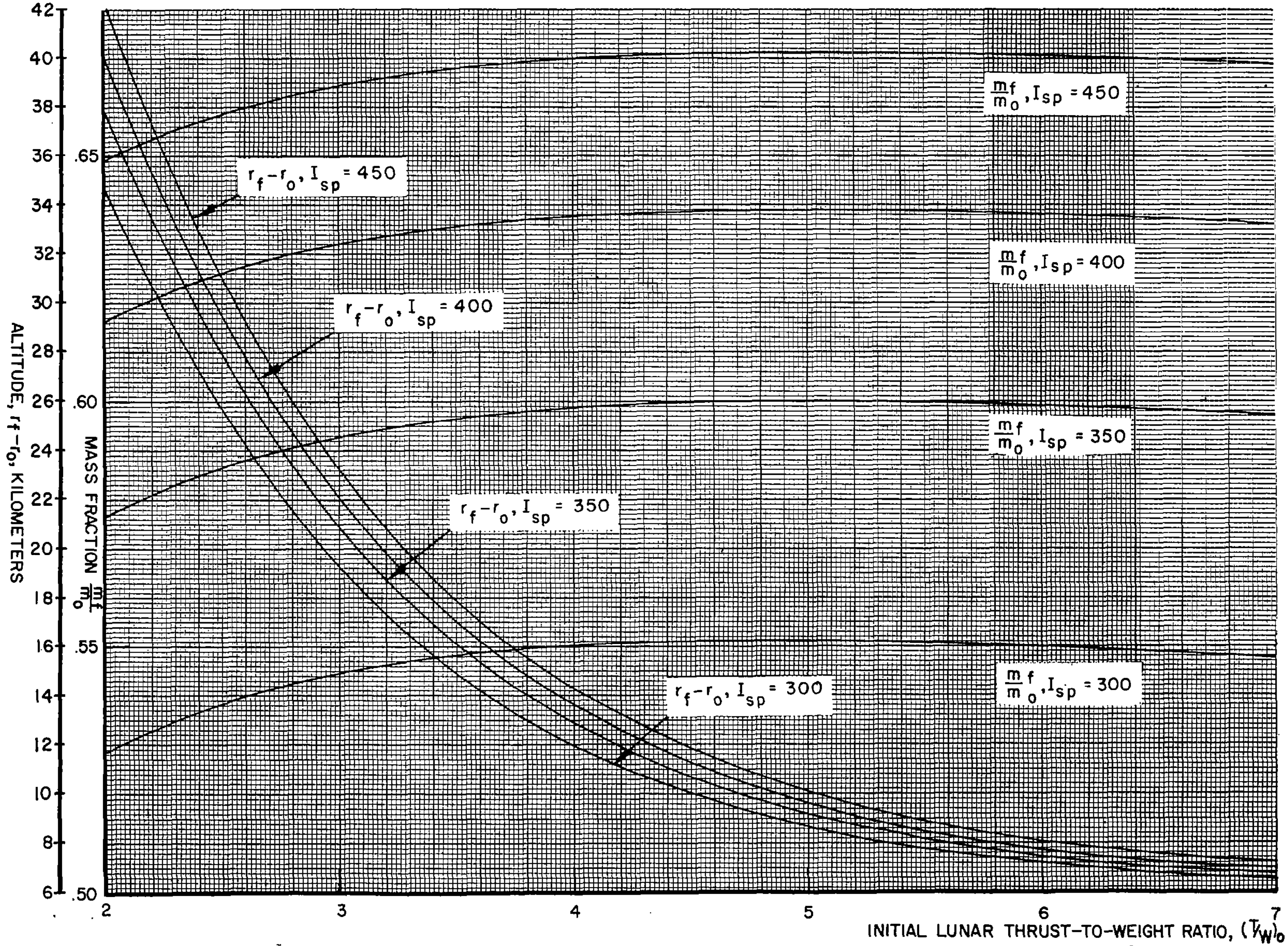

FIG 34. FINAL ALTITUDE AND MASS FRACTION VS LUNAR THRUST-TO-WEIGHT RATIO (γ_o=10°)

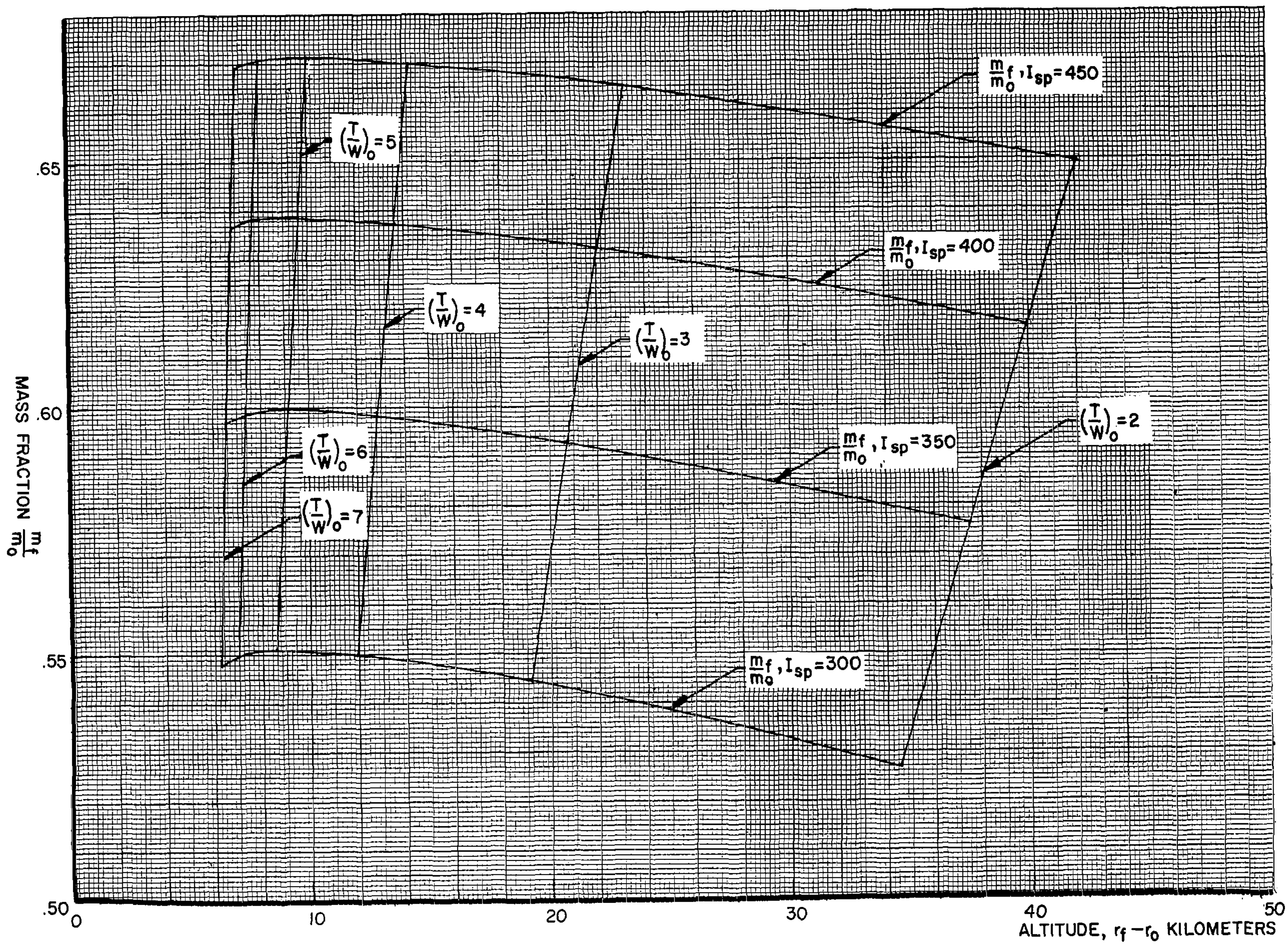

FIG 35. MASS FRACTION VS FINAL ALTITUDE (γ_o=10°)

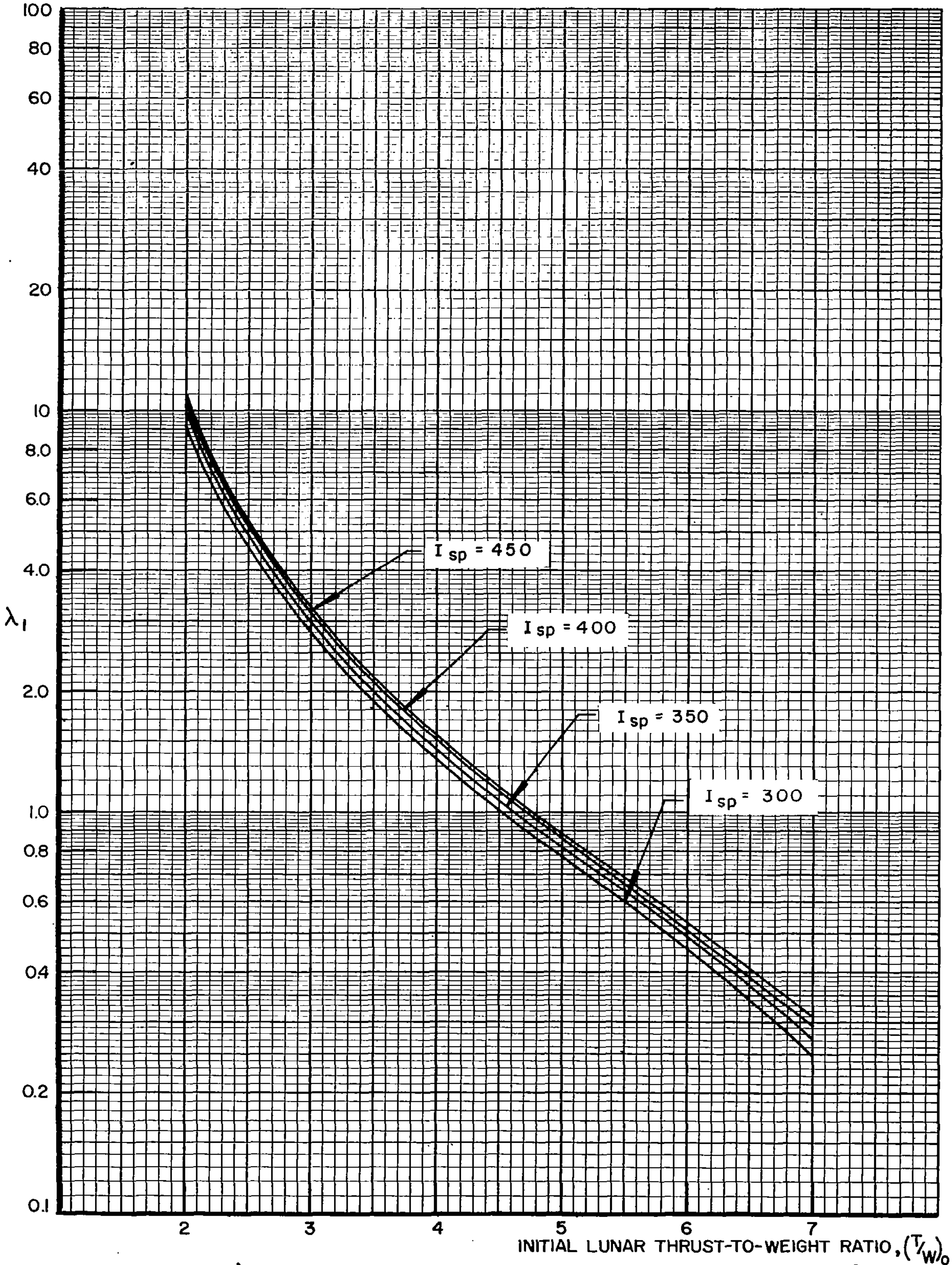

FIG 36. λ_1 VS INITIAL LUNAR THRUST-TO-WEIGHT RATIO (γ_0=10°)

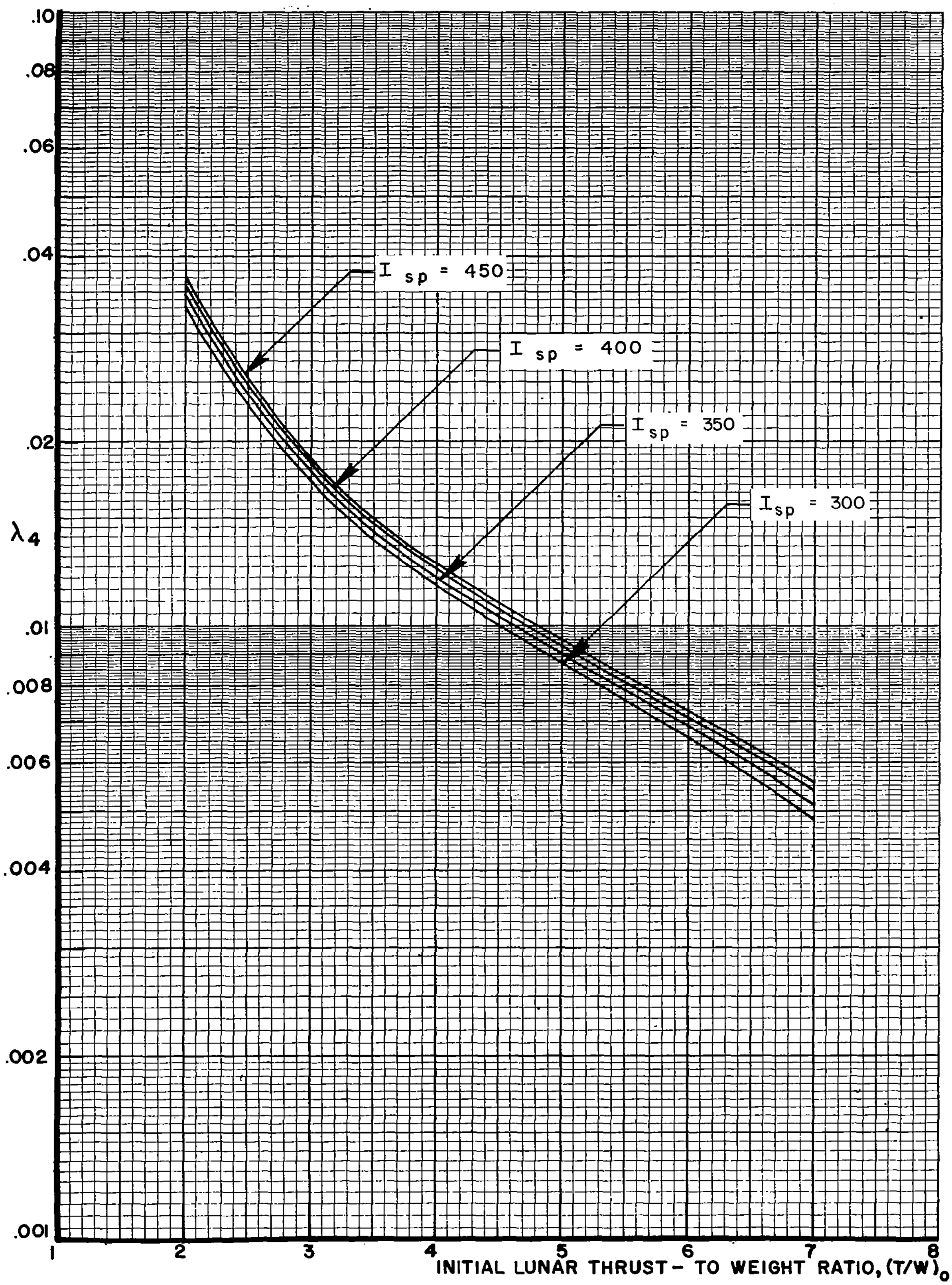

FIG 37. λ_4 VS INITIAL LUNAR THRUST – TO – WEIGHT RATIO, (γ_0 = 10°)

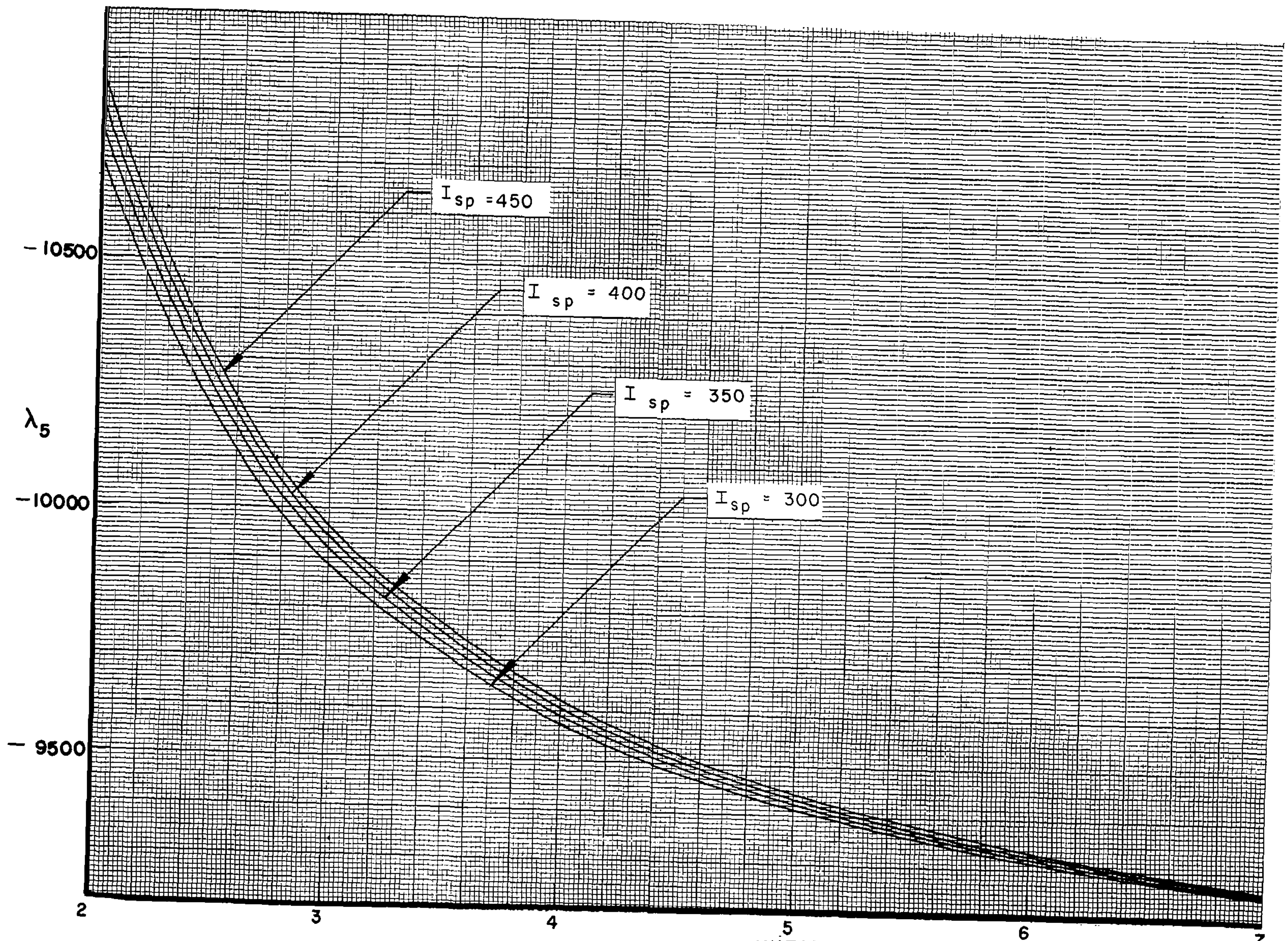

FIG 38. $\lambda 5$ VS INITIAL LUNAR THRUST-TO-WEIGHT RATIO, (γ_0 =10°)

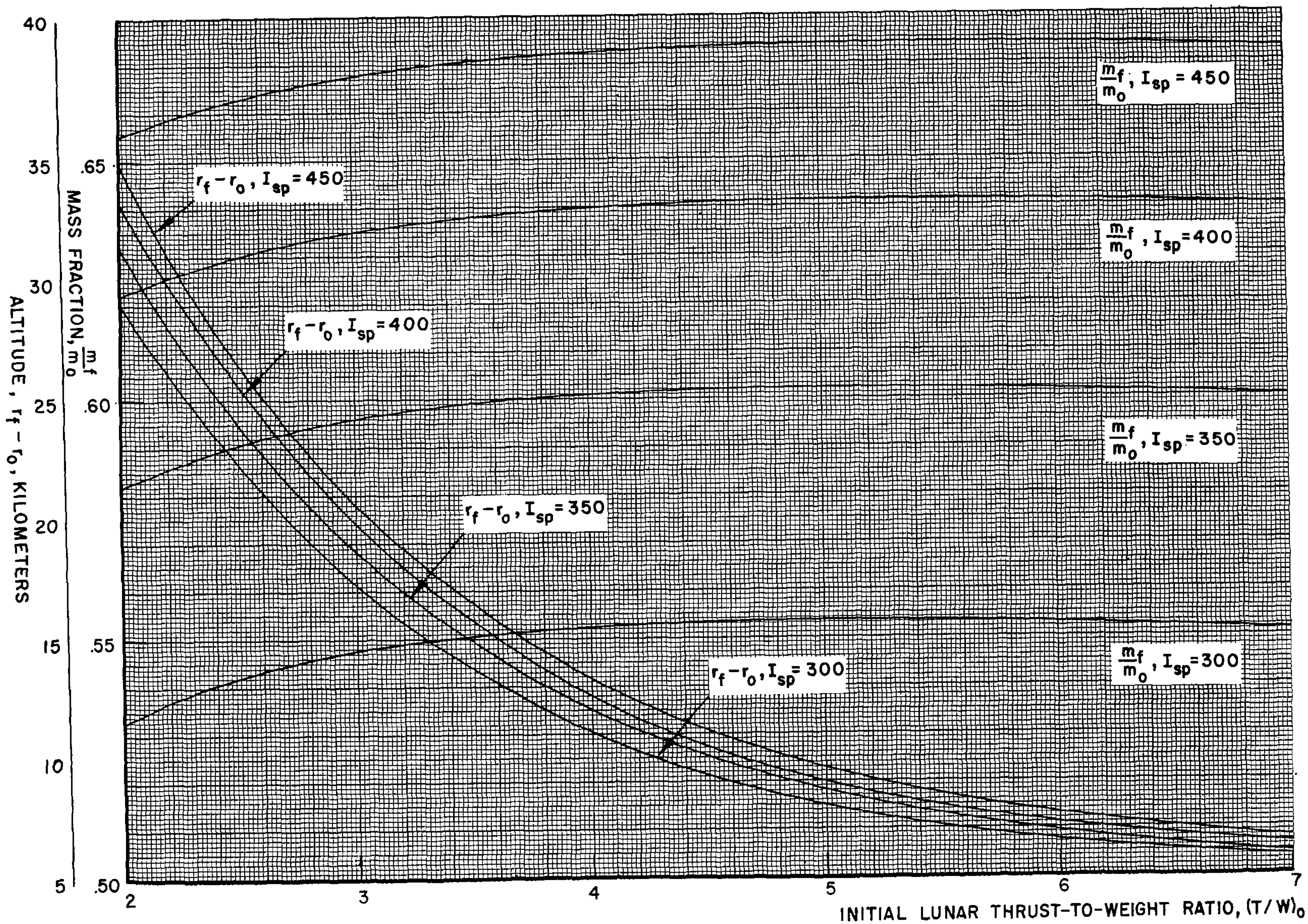

FIG 39. FINAL ALTITUDE AND MASS FRACTION VS INITIAL THRUST-TO-WEIGHT RATIO ($\gamma_o = 20°$)

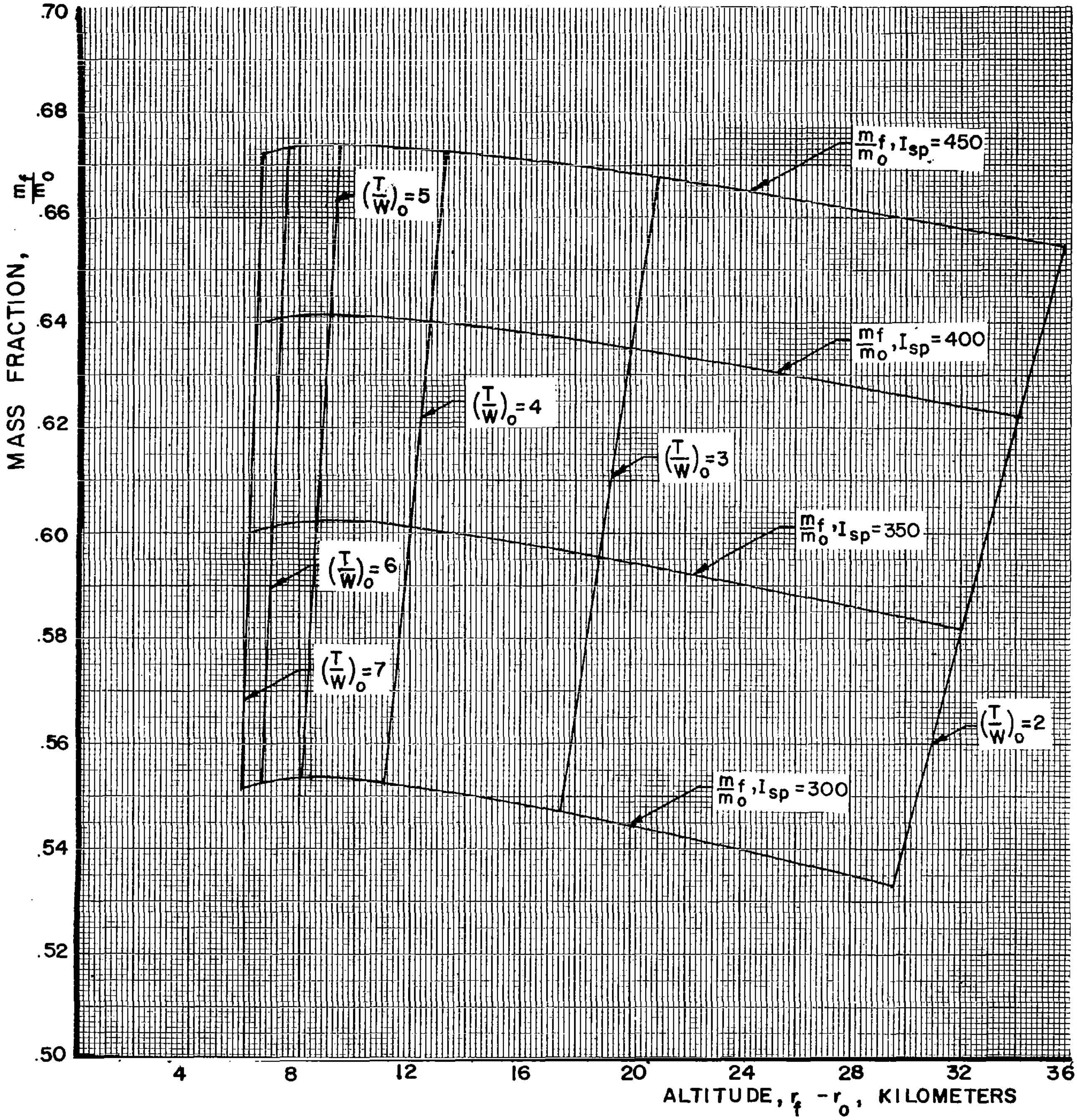

FIG 40. MASS FRACTION VS FINAL ALTITUDE (γ_o = 20°)

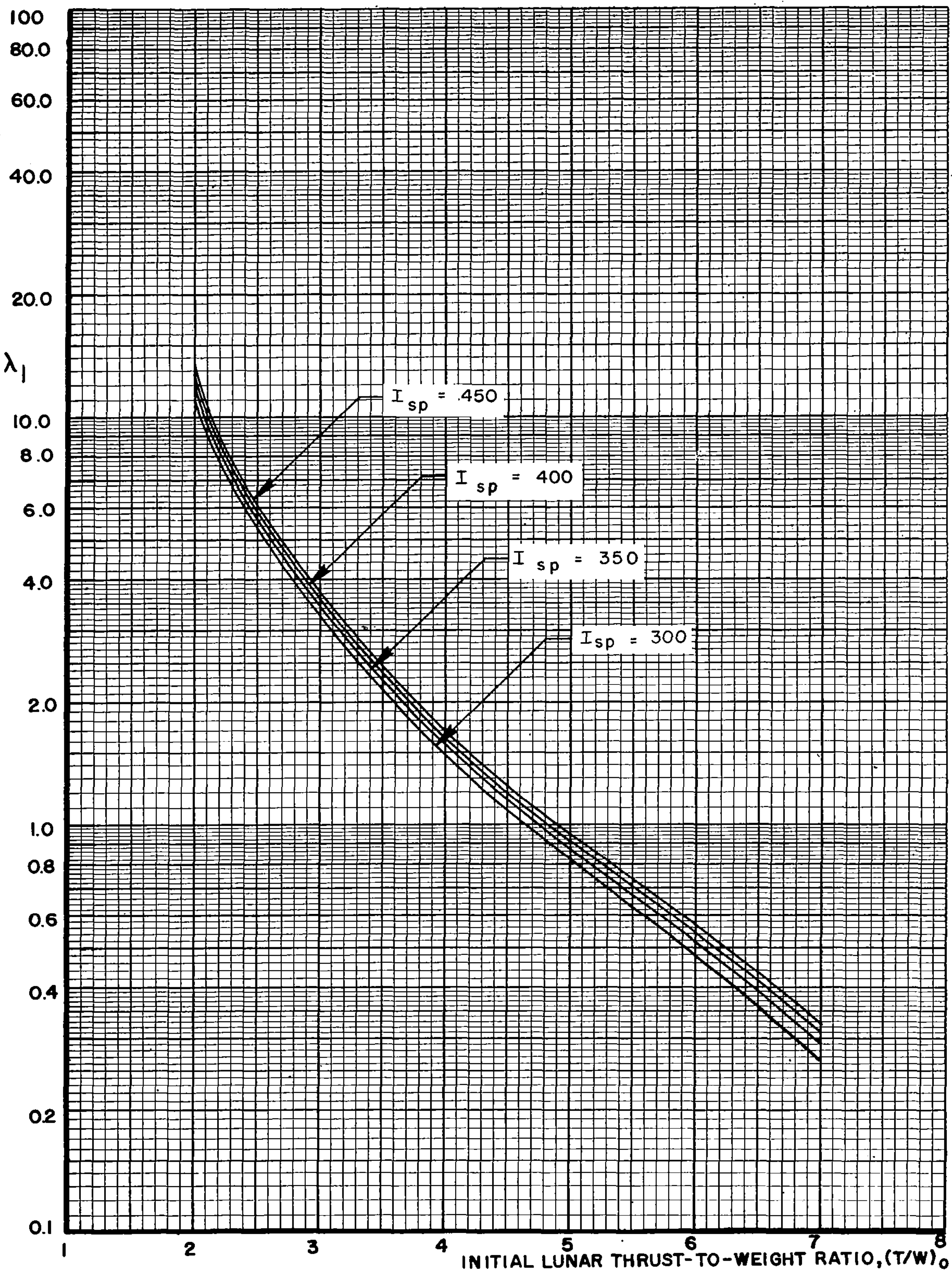

FIG 41 . λ_1 VS INITIAL LUNAR THRUST-TO- WEIGHT RATIO (γ_o = 20°)

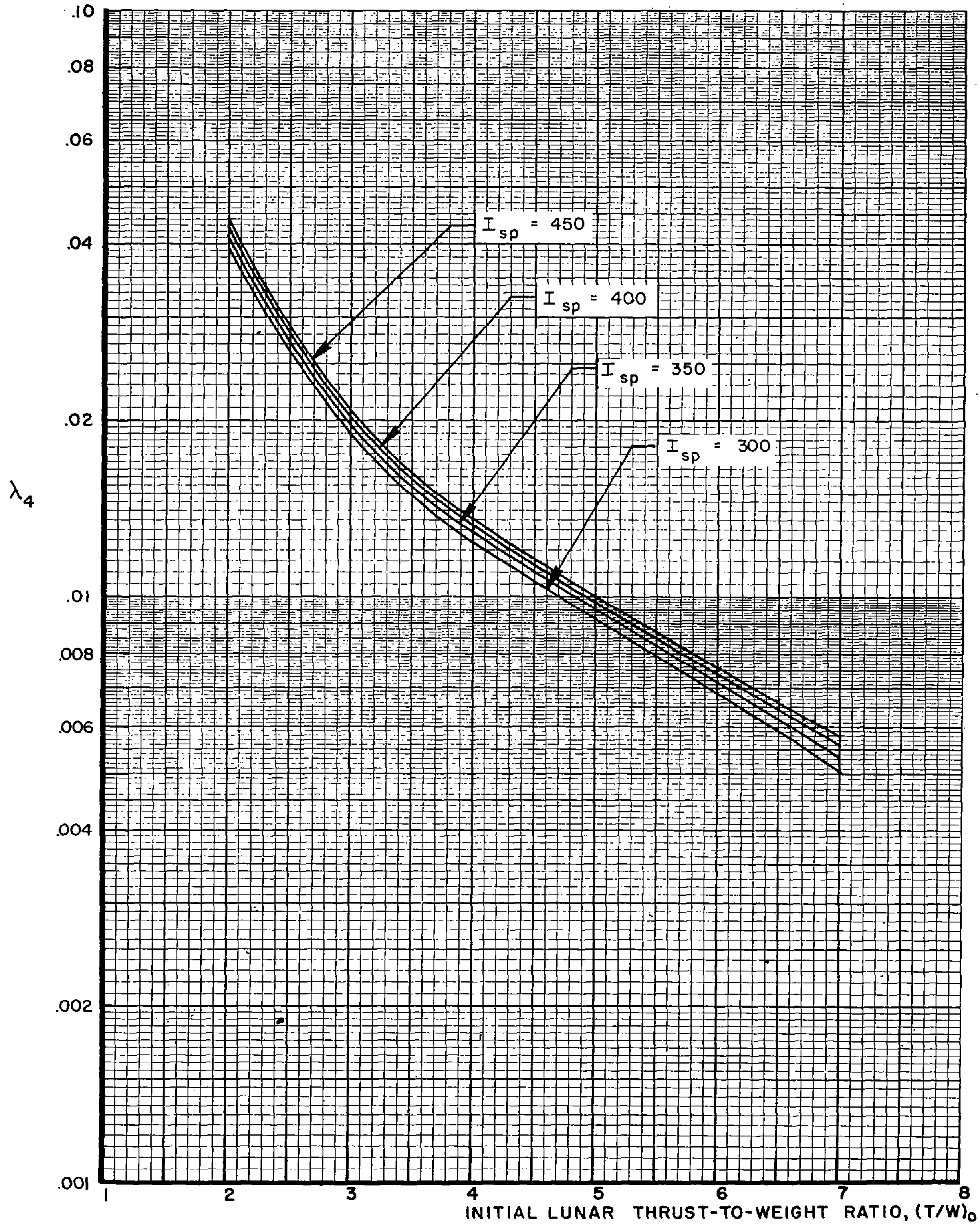

FIG. 12. λ_4 VS INITIAL LUNAR THRUST-TO-WEIGHT RATIO (γ_0 = 20°)

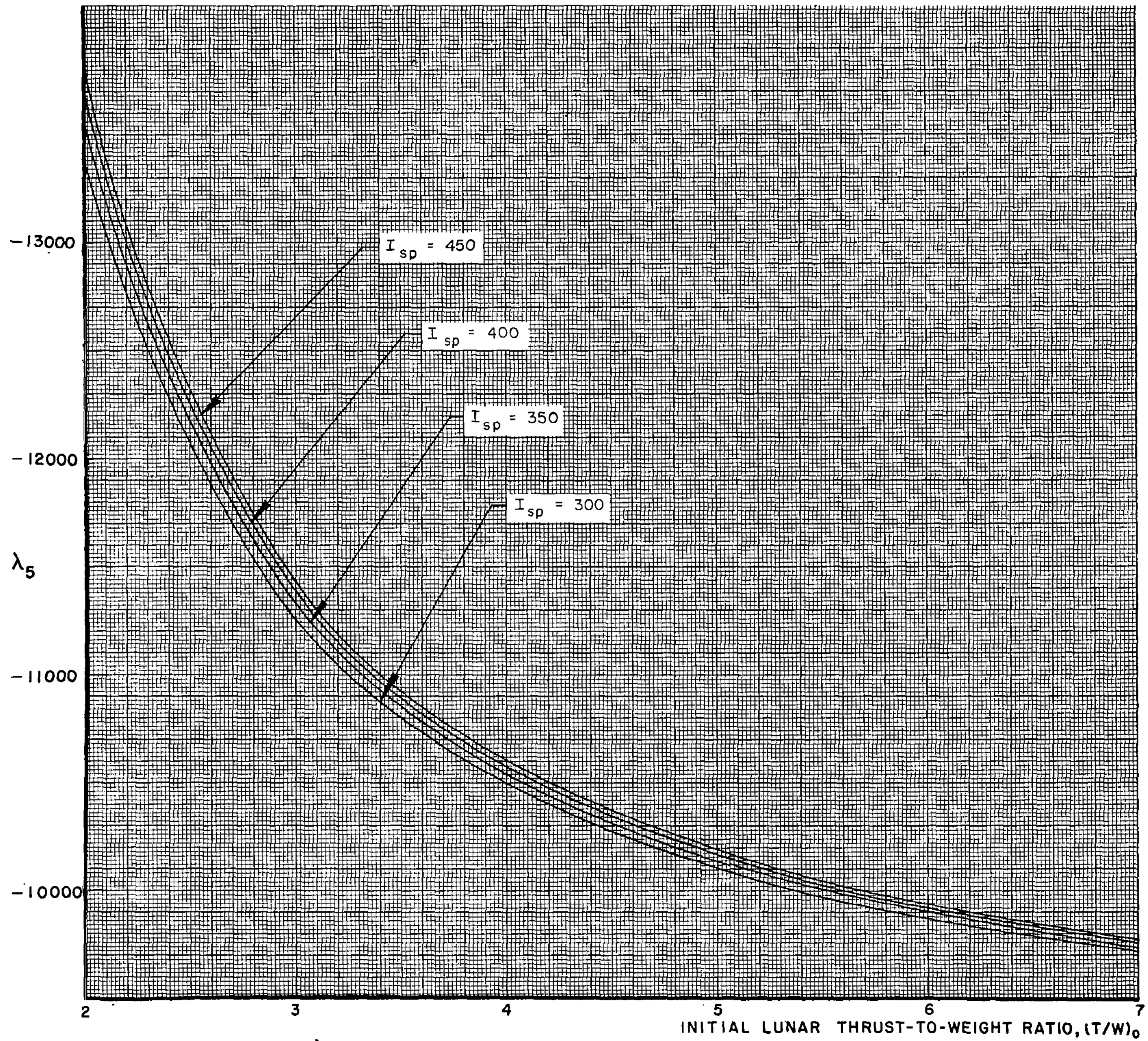

FIG 43. λ_5 VS INITIAL LUNAR THRUST-TO-WEIGHT RATIO ($\gamma_0 = 20°$)

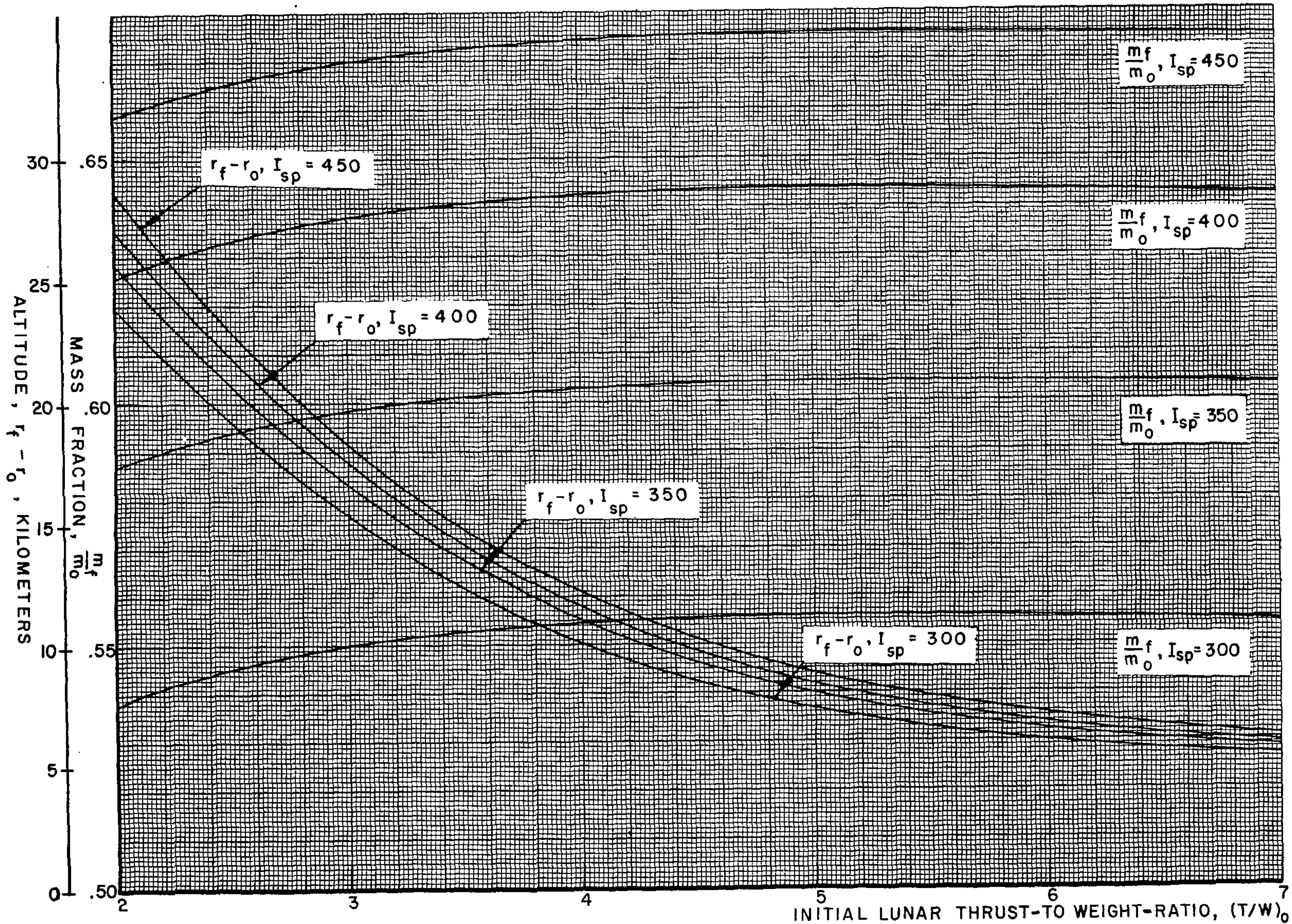

FIG 44. FINAL ALTITUDE AND MASS FRACTION VS INITIAL THRUST-TO-WEIGHT RATIO ($\gamma_o = 30°$)

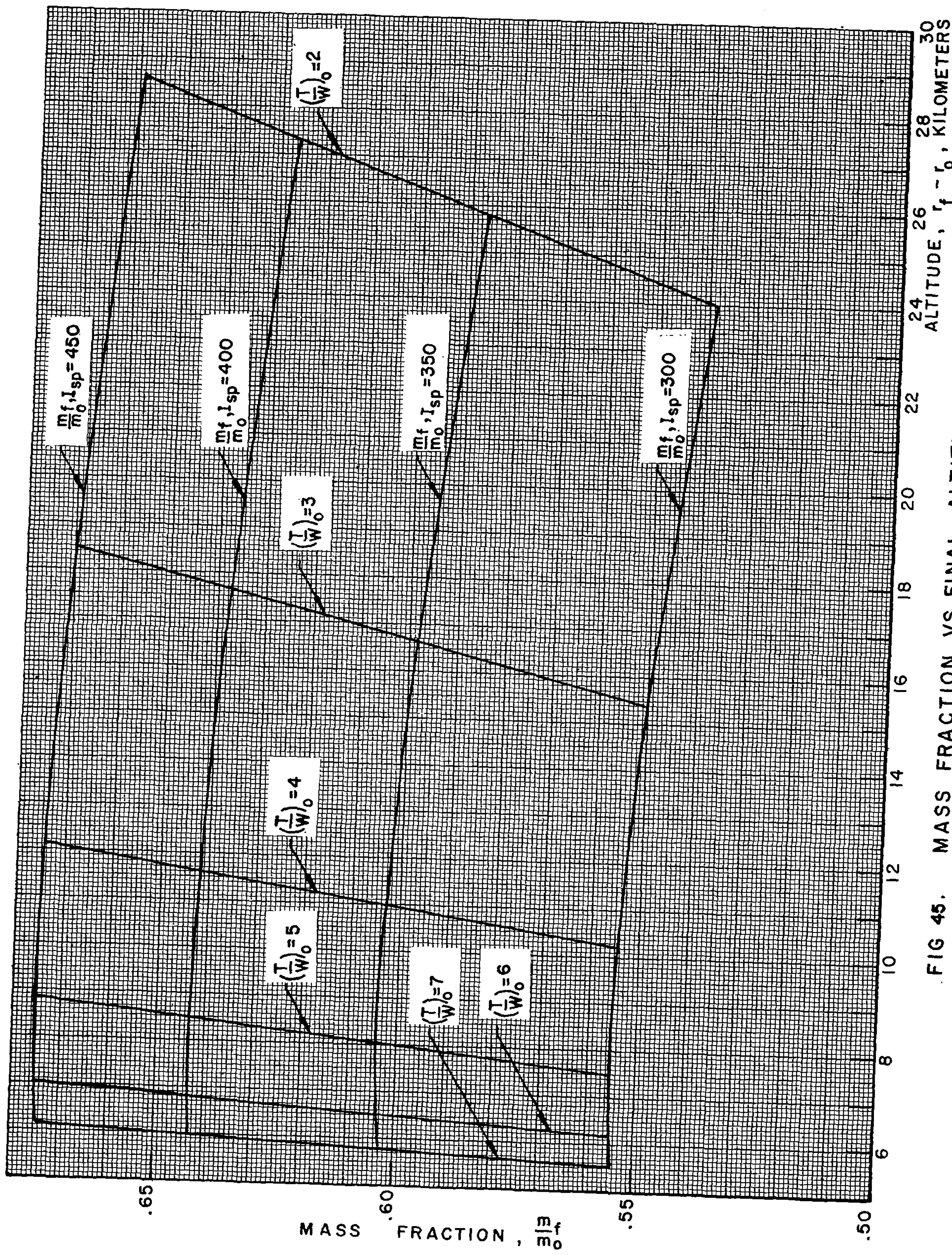

FIG 45. MASS FRACTION VS FINAL ALTITUDE (γ_o = 30°)

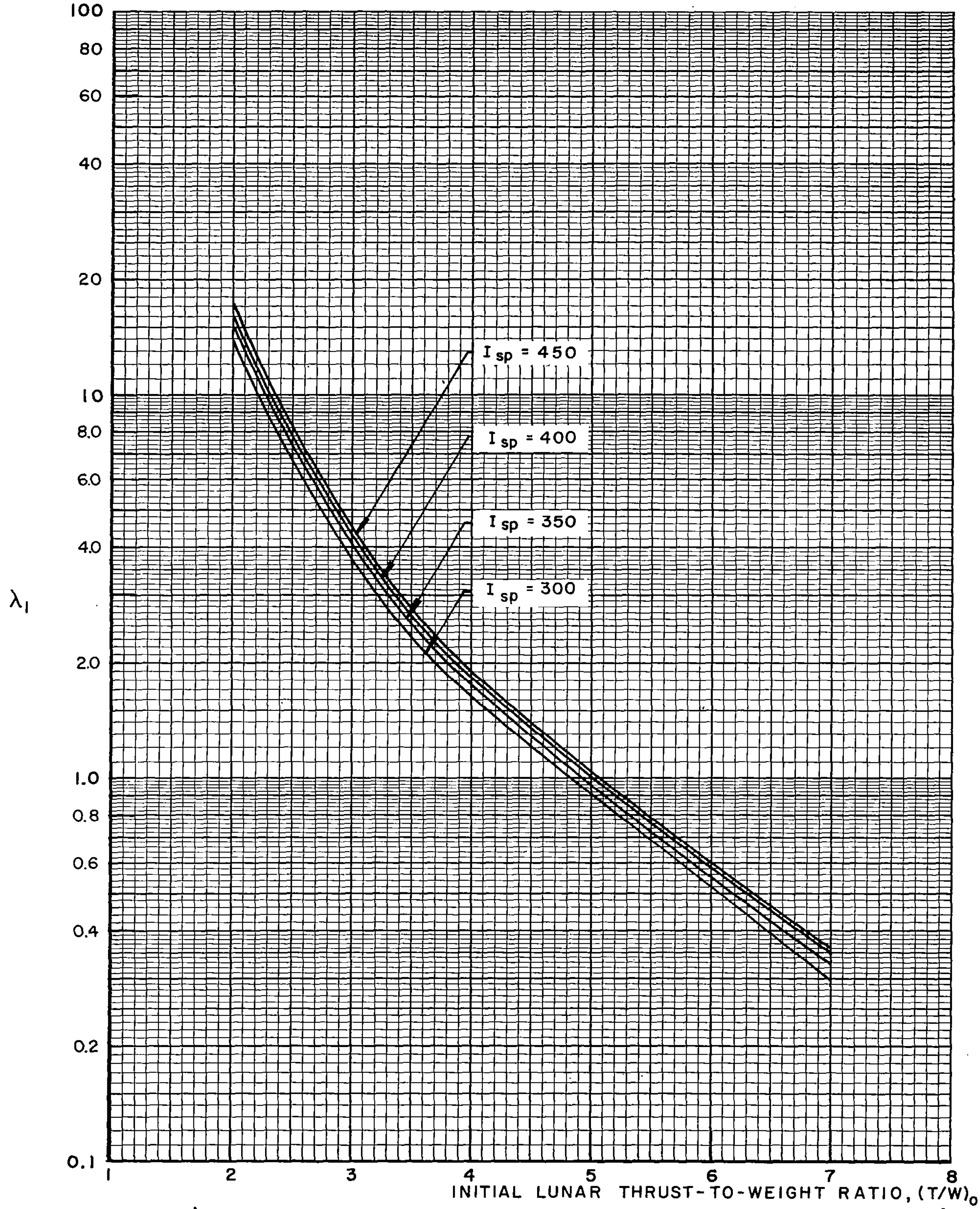

FIG 46. λ_1 VS INITIAL LUNAR THRUST-TO-WEIGHT RATIO ($\gamma_0 = 30°$)

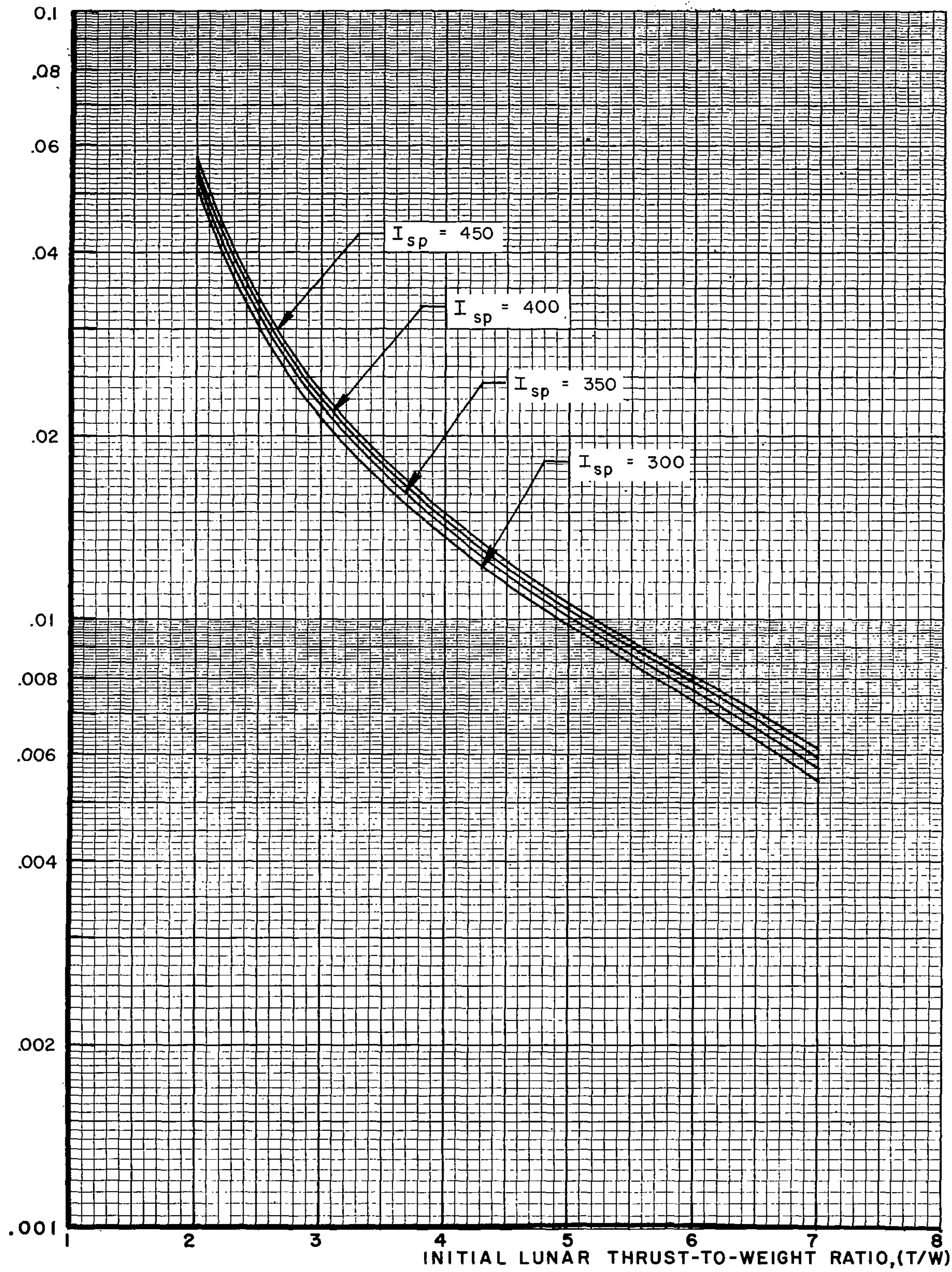

FIG 47. λ_4 VS INITIAL LUNAR THRUST-TO-WEIGHT RATIO ($\gamma_0 = 30°$)

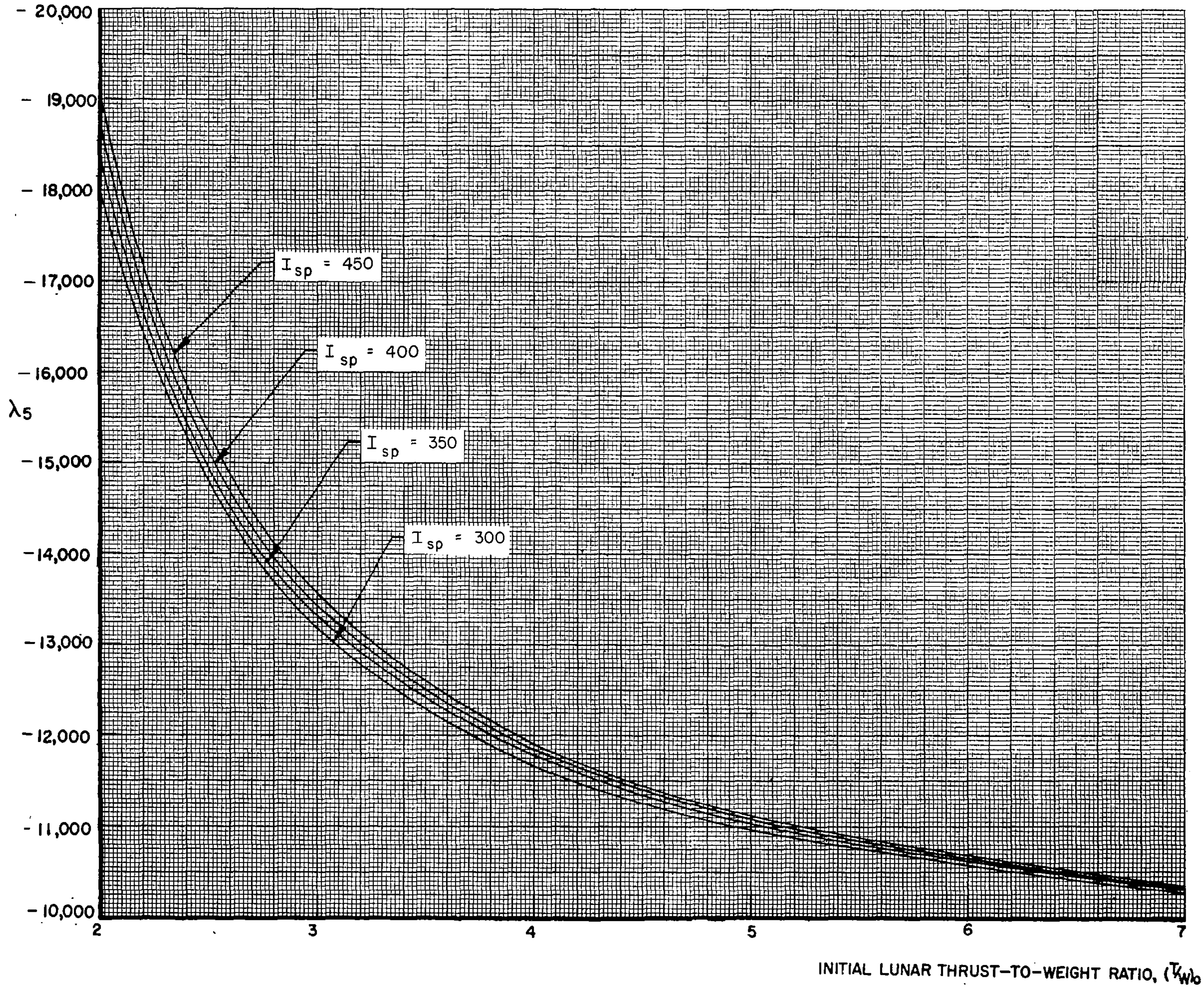

FIG 48. $\lambda 5$ VS INITIAL LUNAR THRUST-TO-WEIGHT RATIO (γ_o=30°)

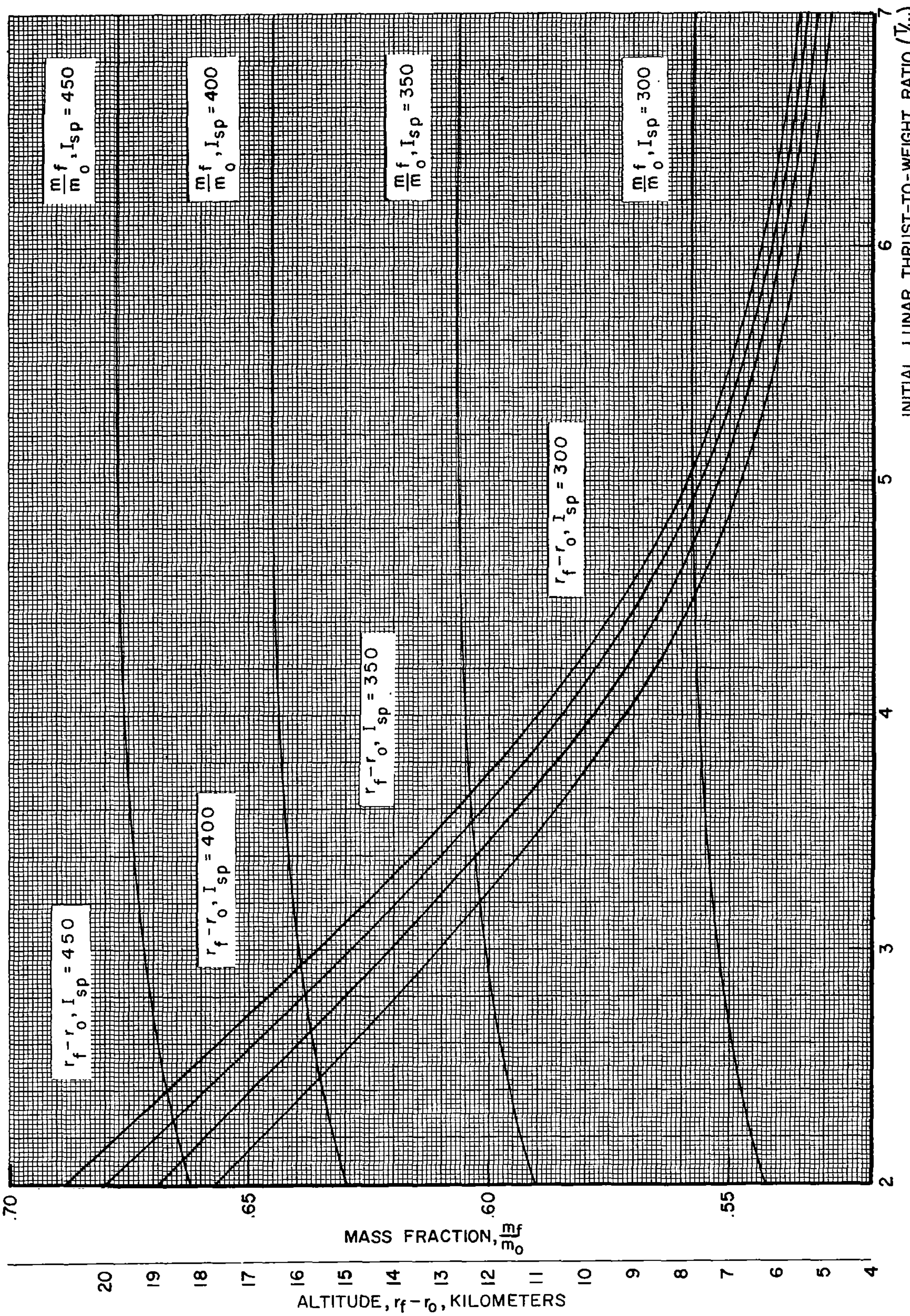

FIG 49 . FINAL ALTITUDE AND MASS FRACTION VS INITIAL THRUST-TO-WEIGHT RATIO (γ_o=40°)

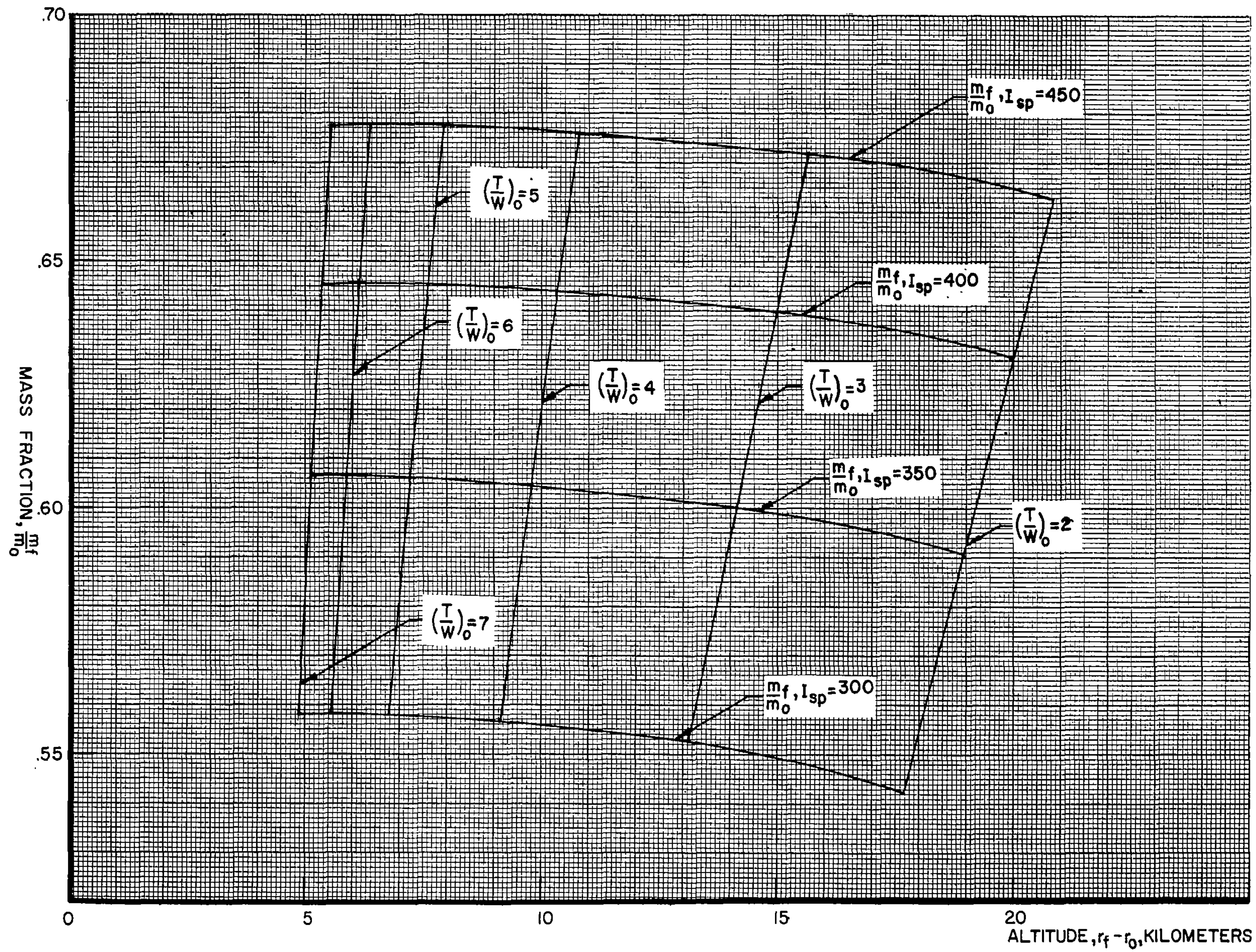

FIG 50. MASS FRACTION VS FINAL ALTITUDE ($\gamma_o=40°$)

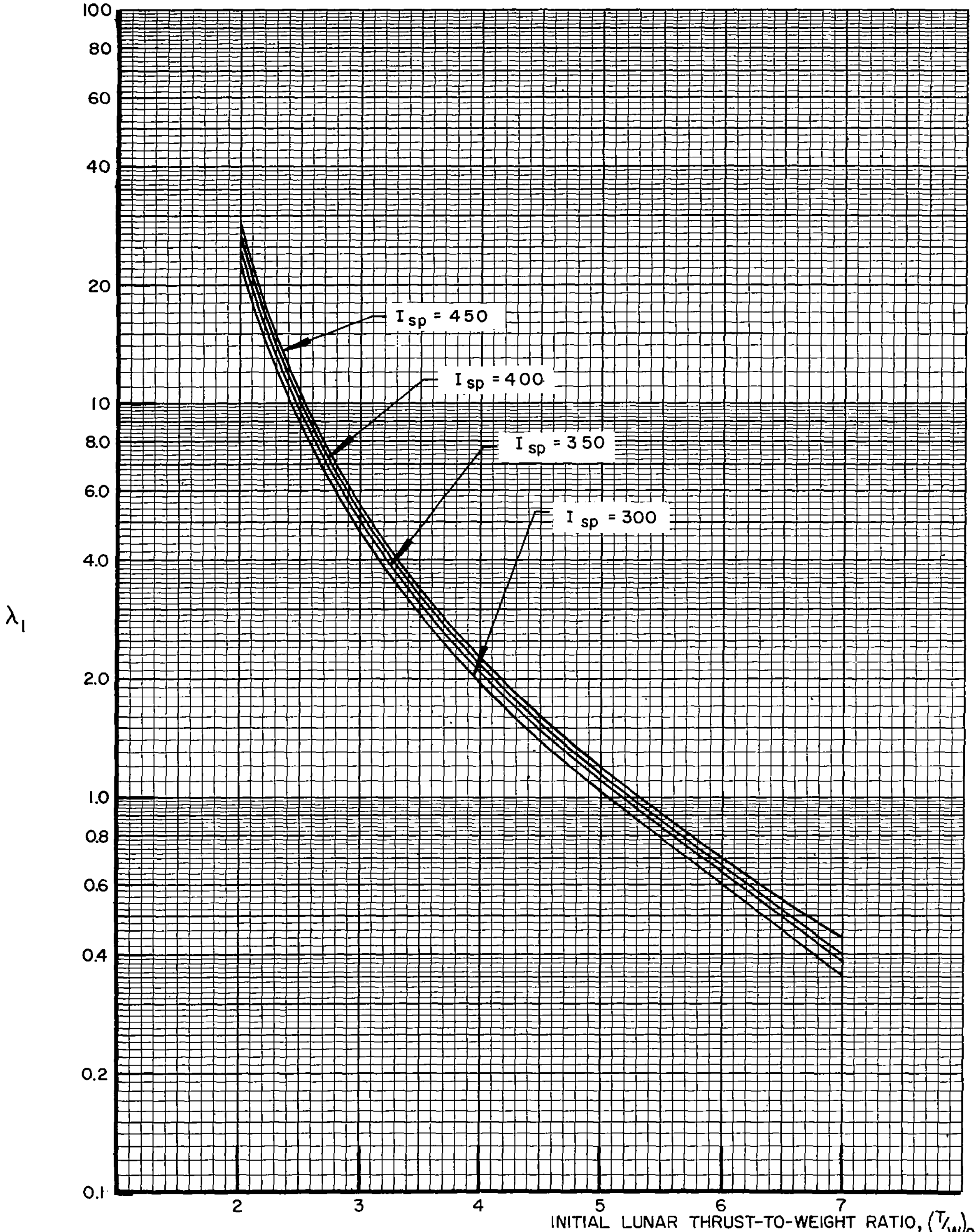

FIG 51. λ_1 VS INITIAL LUNAR THRUST-TO-WEIGHT RATIO (γ_o=40°)

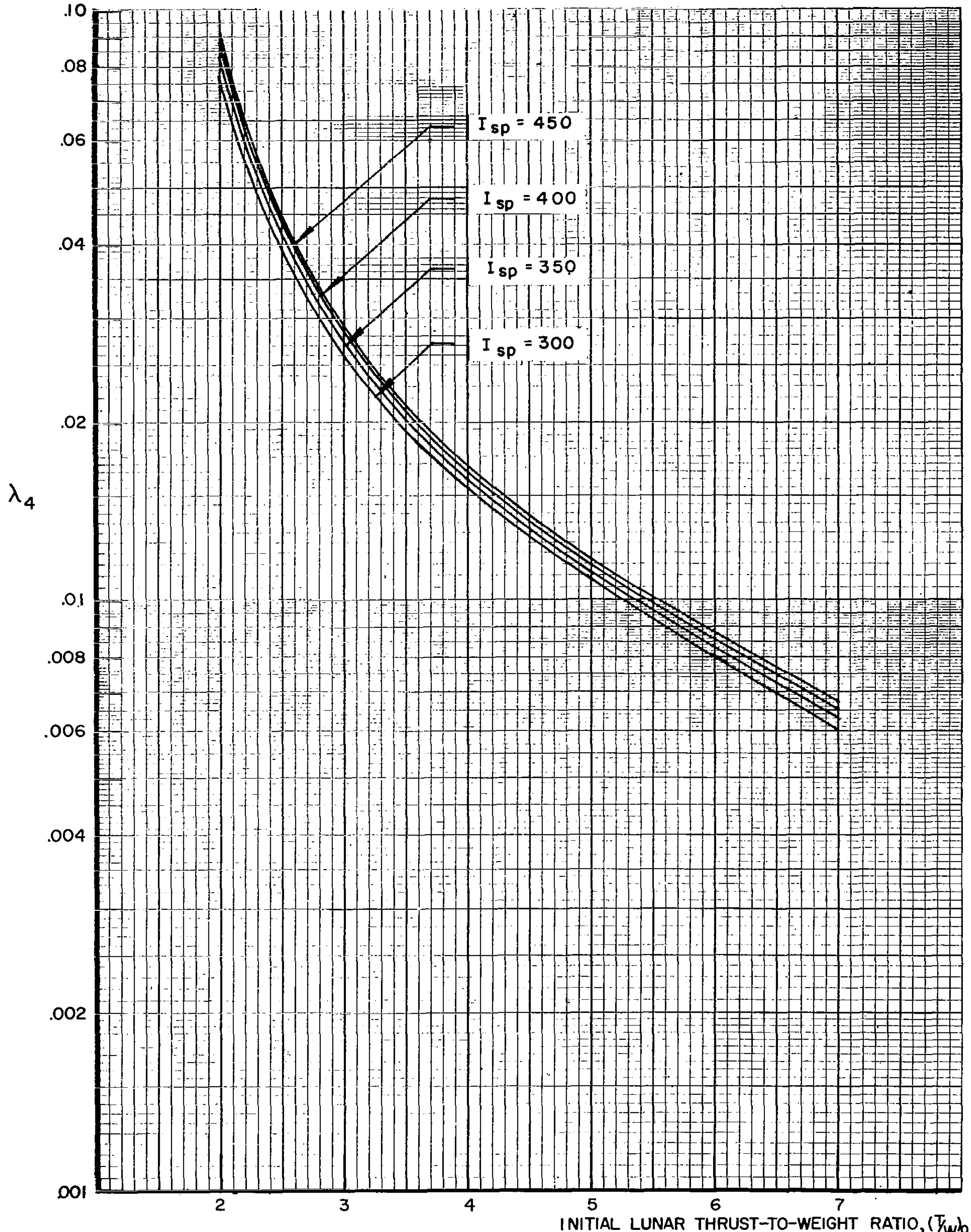

FIG 52 . λ_4 VS INITIAL LUNAR THRUST-TO-WEIGHT RATIO (γ_0=40°)

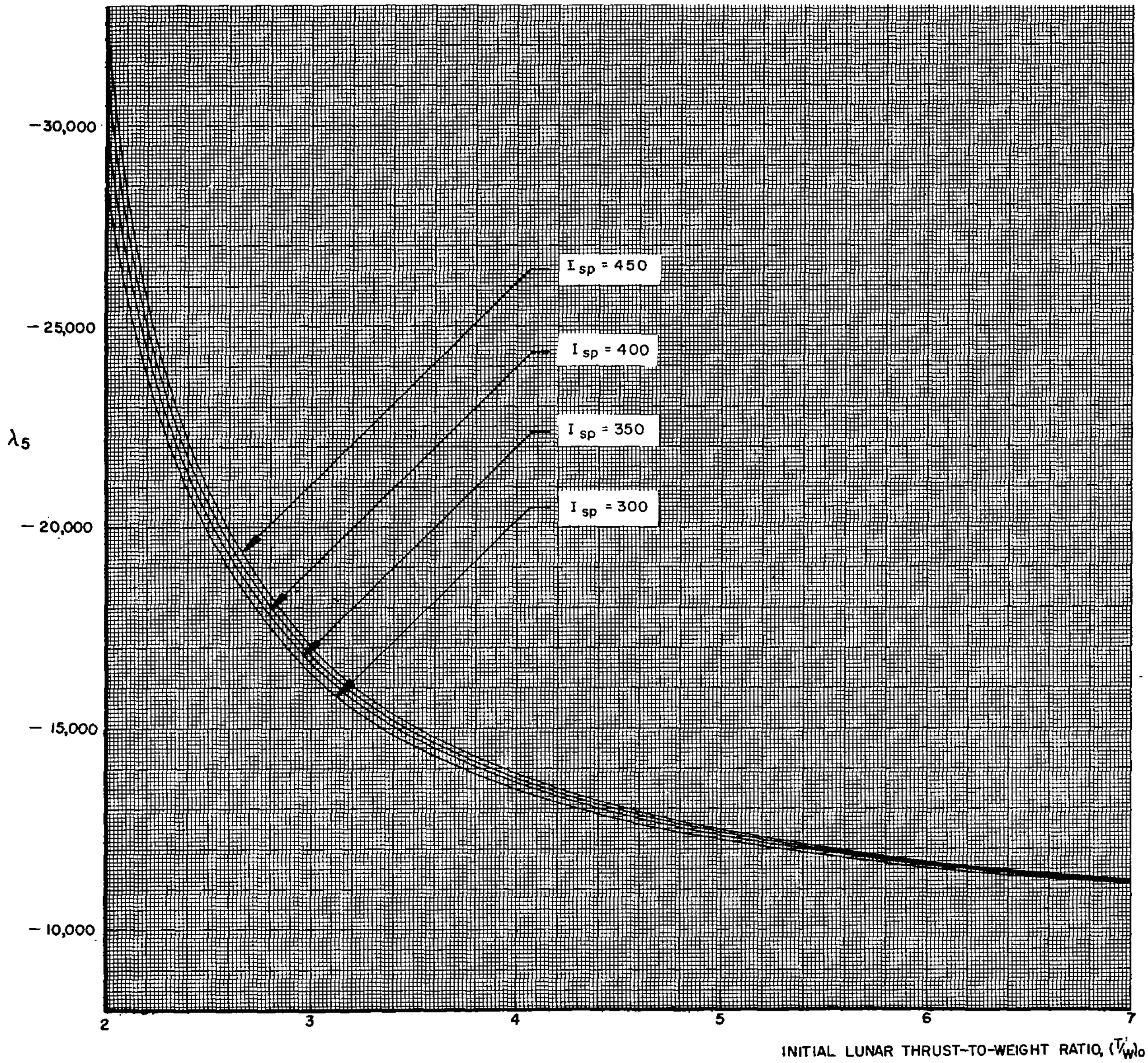

FIG 53. $\lambda 5$ VS INITIAL LUNAR THRUST-TO-WEIGHT RATIO (γ_o=40°)

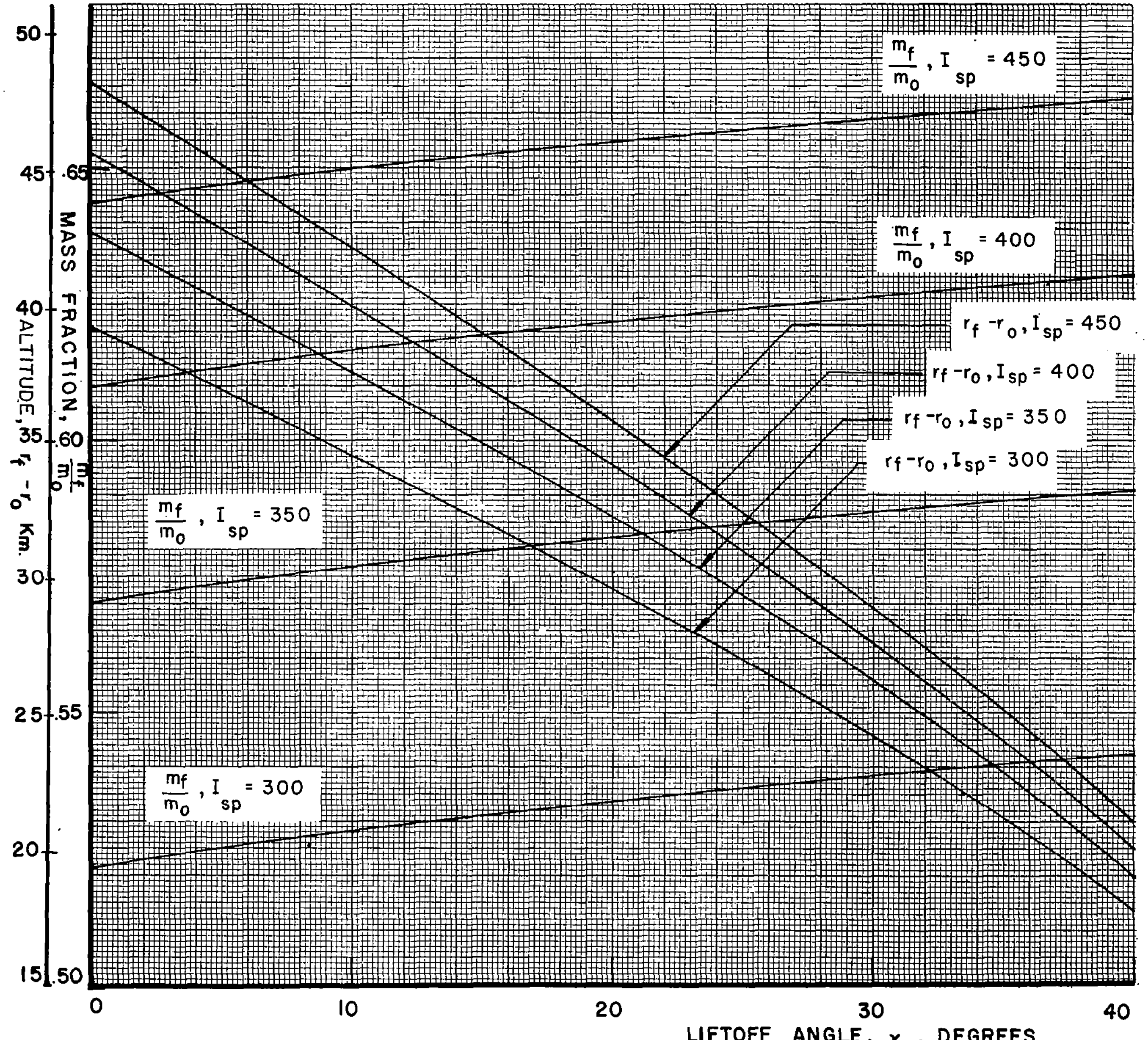

FIG 54. FINAL ALTITUDE AND MASS FRACTION VS LIFTOFF ANGLE FOR $(T/W)_o = 2$

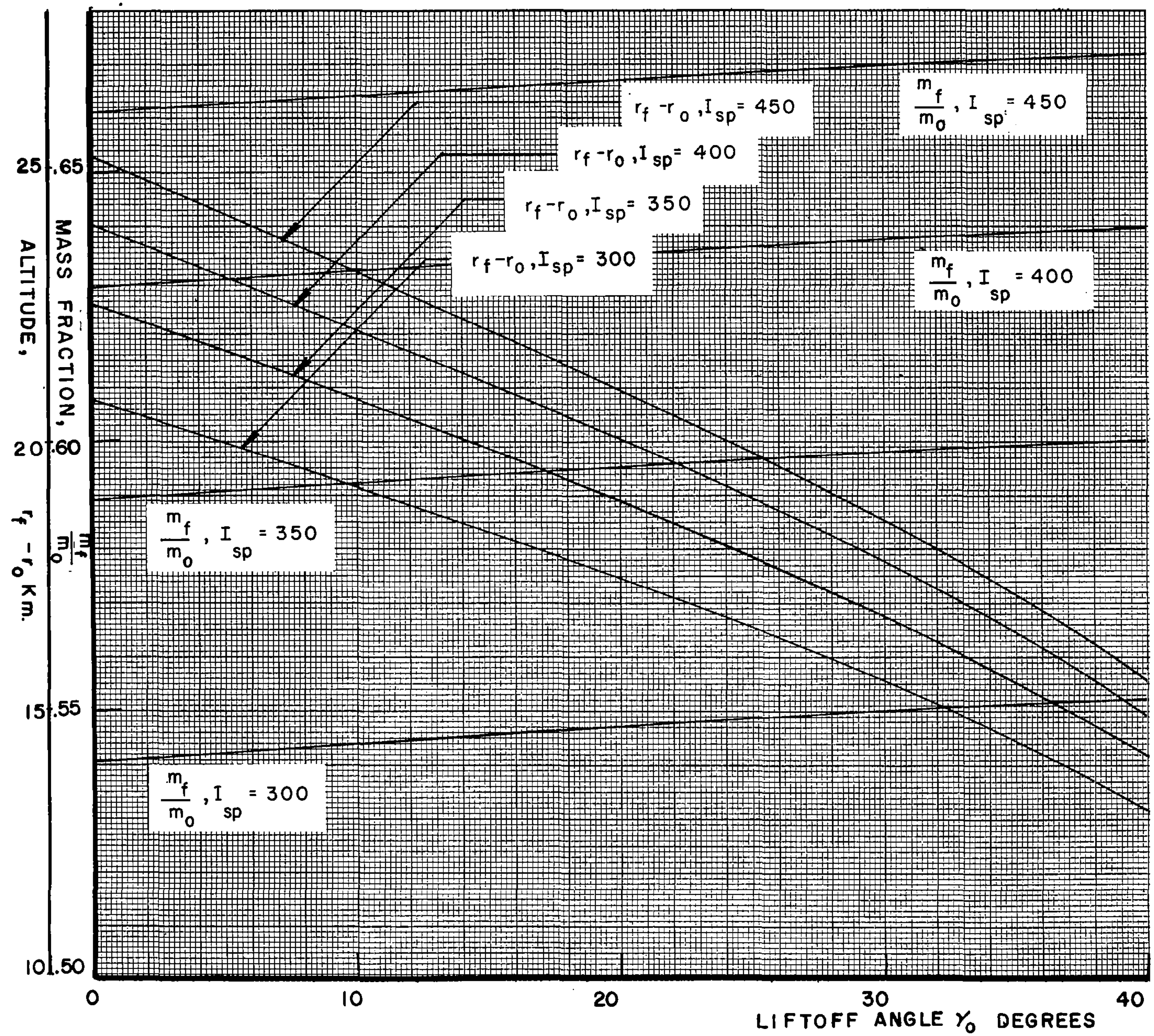

FIG 55. FINAL ALTITUDE AND MASS FRACTION VS LIFTOFF ANGLE FOR $(T/W)_o = 3$

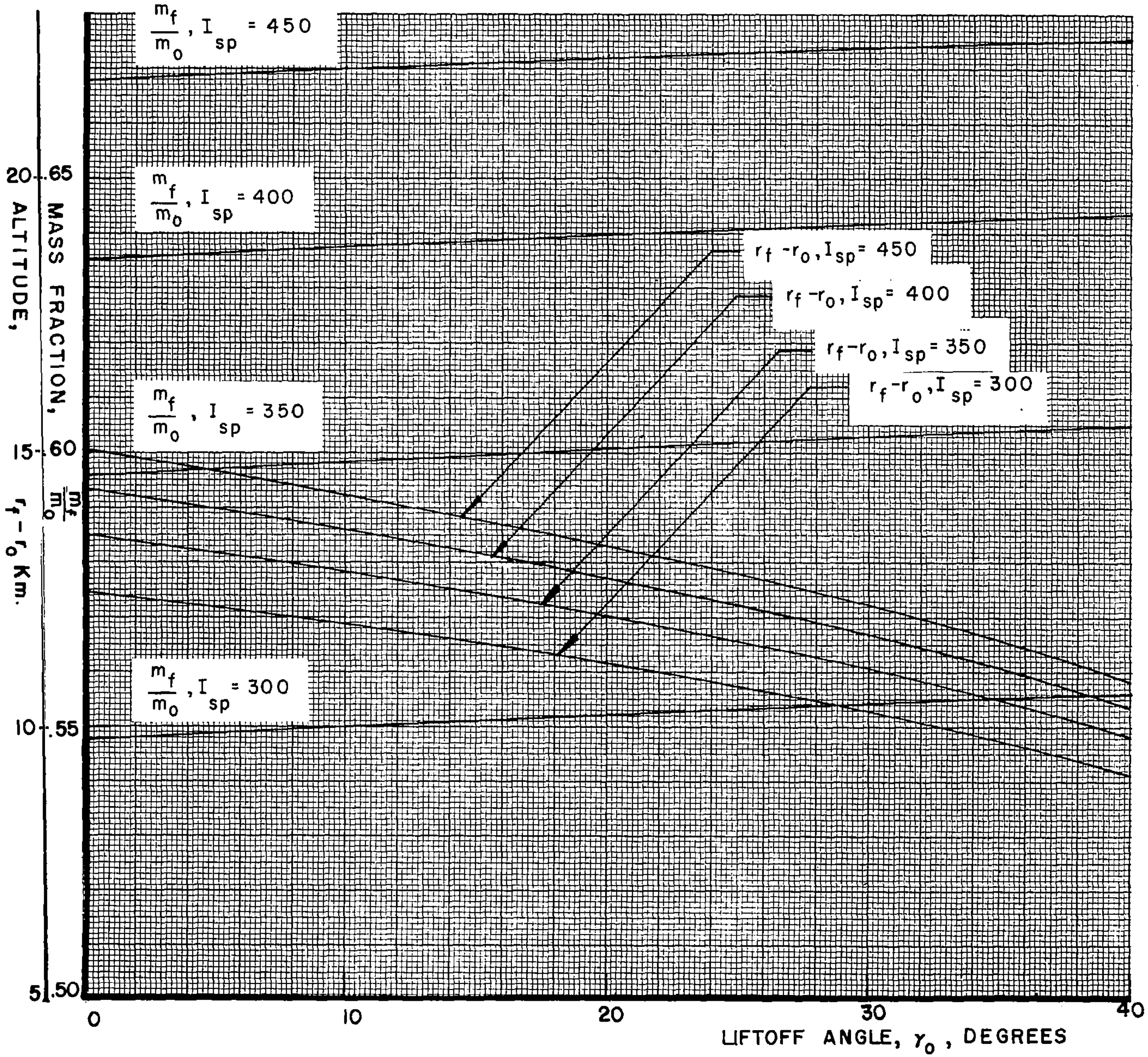

FIG 56. FINAL ALTITUDE AND MASS FRACTION VS LIFTOFF ANGLE FOR $(T/W)_o$ = 4

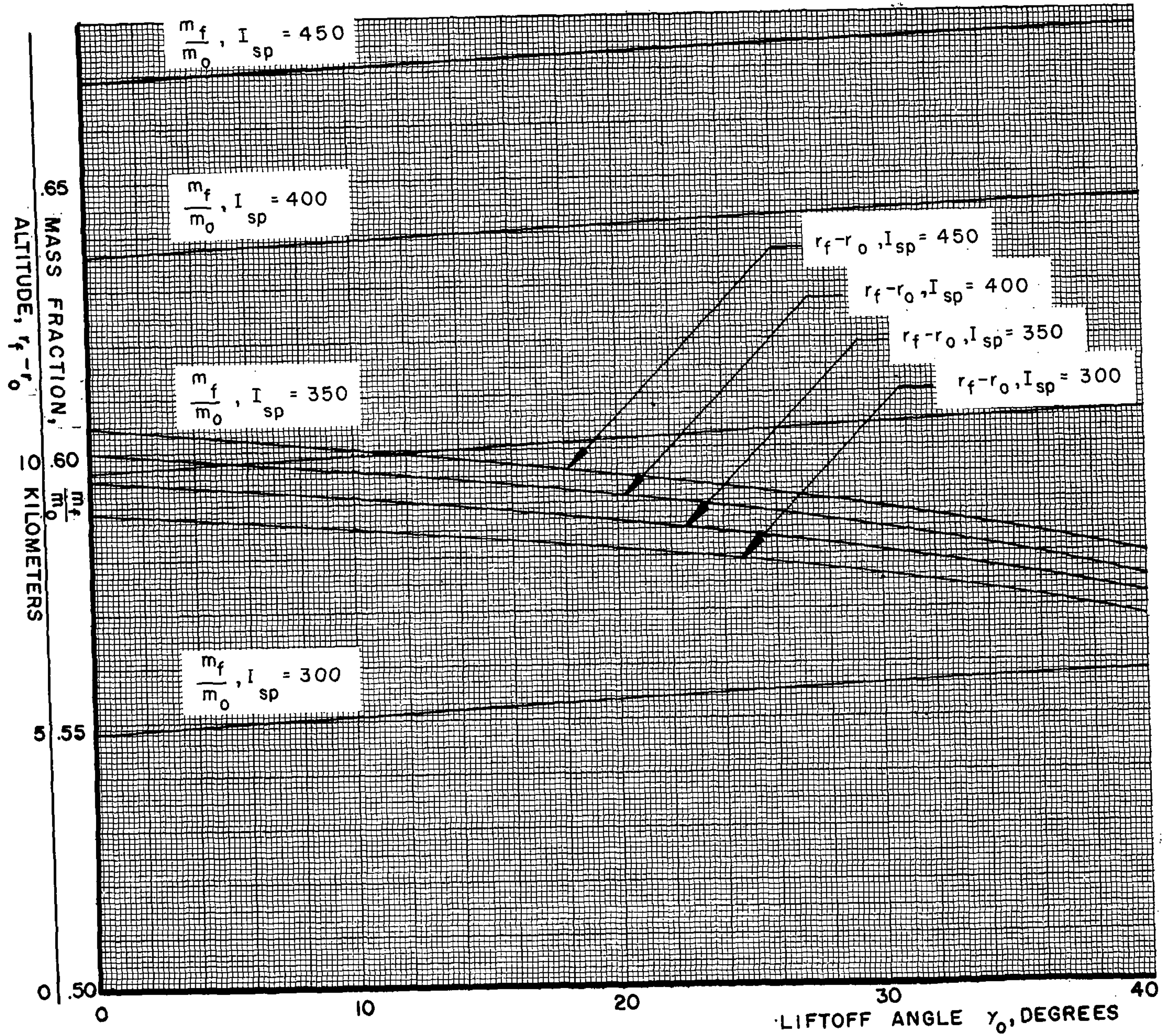

FIG 57. FINAL ALTITUDE AND MASS FRACTION VS LIFTOFF ANGLE FOR $(T/W)_o$ = 5

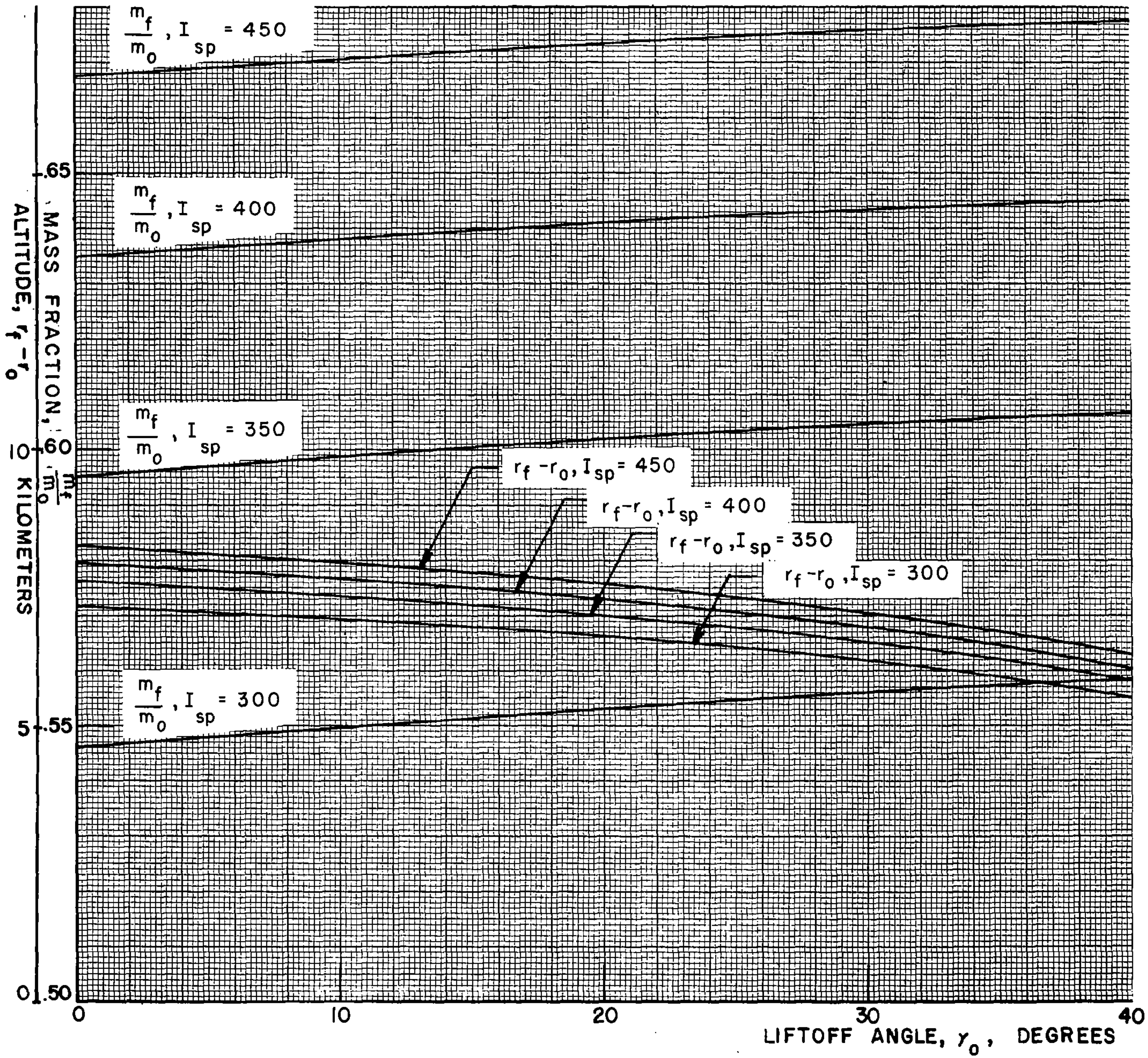

FIG 58. FINAL ALTITUDE AND MASS FRACTION VS LIFTOFF ANGLE FOR $(T/W)_o$ = 6

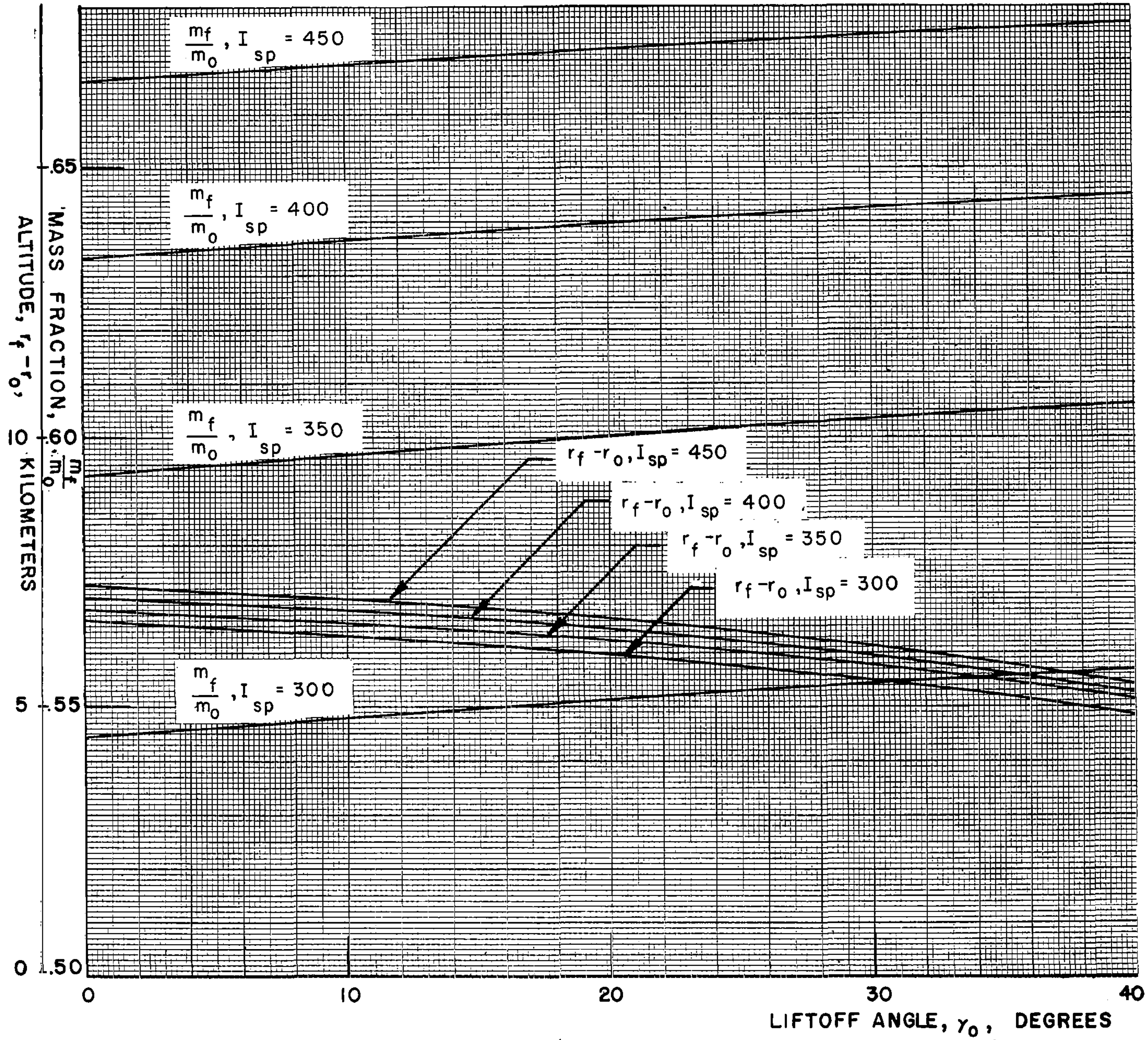

FIG 59. FINAL ALTITUDE AND MASS FRACTION VS LIFTOFF ANGLE FOR $(T/W)_o = 7$

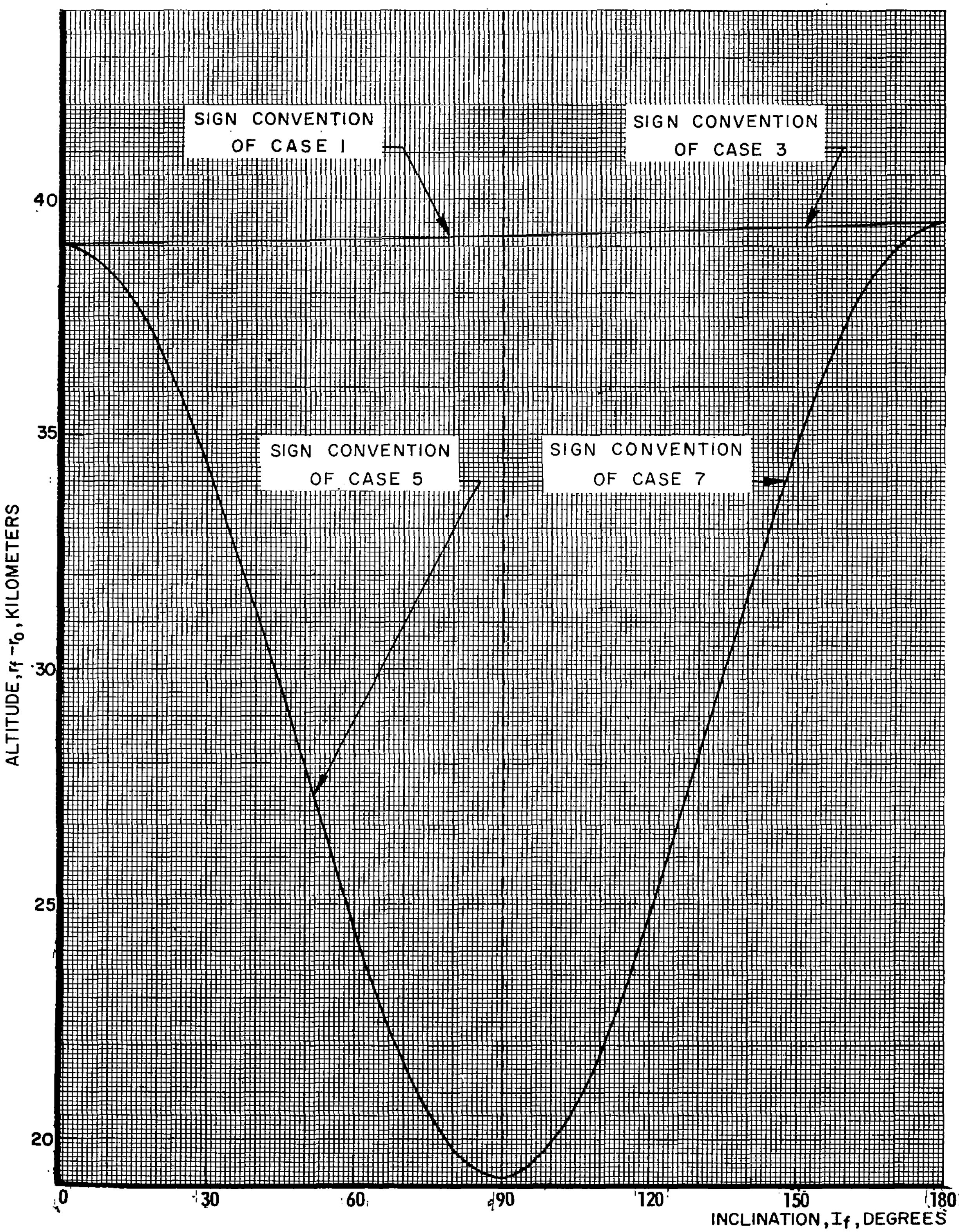

FIG. 60. FINAL ALTITUDE VS INCLINATION [$(T/W)_o = 2$ AND $I_{sp} = 300$ SEC.]

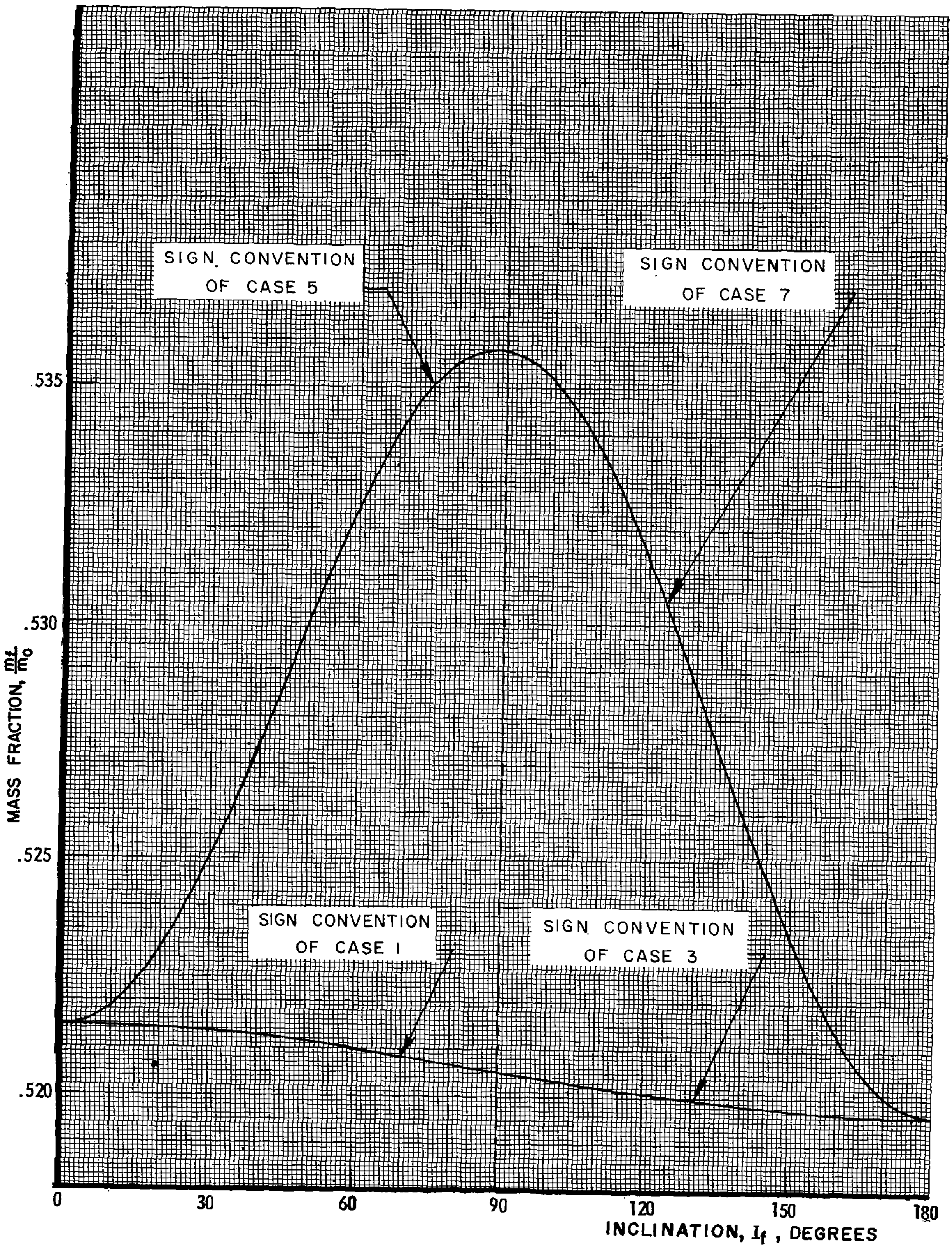

FIG. 61. MASS FRACTION VS INCLINATION $[(T/W)_0 = 2$ AND $I_{sp} = 300$ SEC$]$

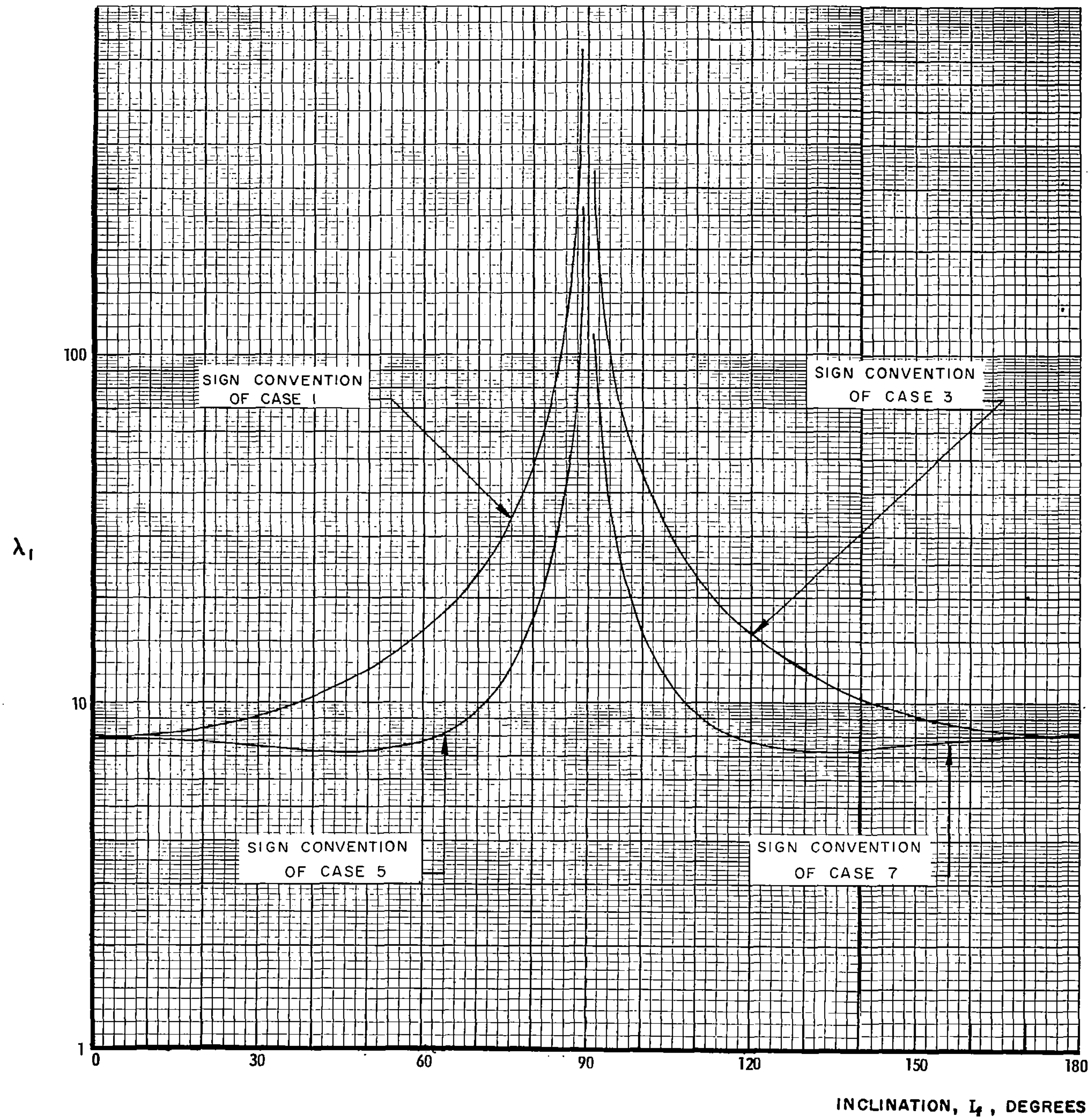

FIG 62. λ_1 VS INCLINATION $[(T/W)_0 = 2$ AND $I_{sp} = 300$ SECONDS$]$

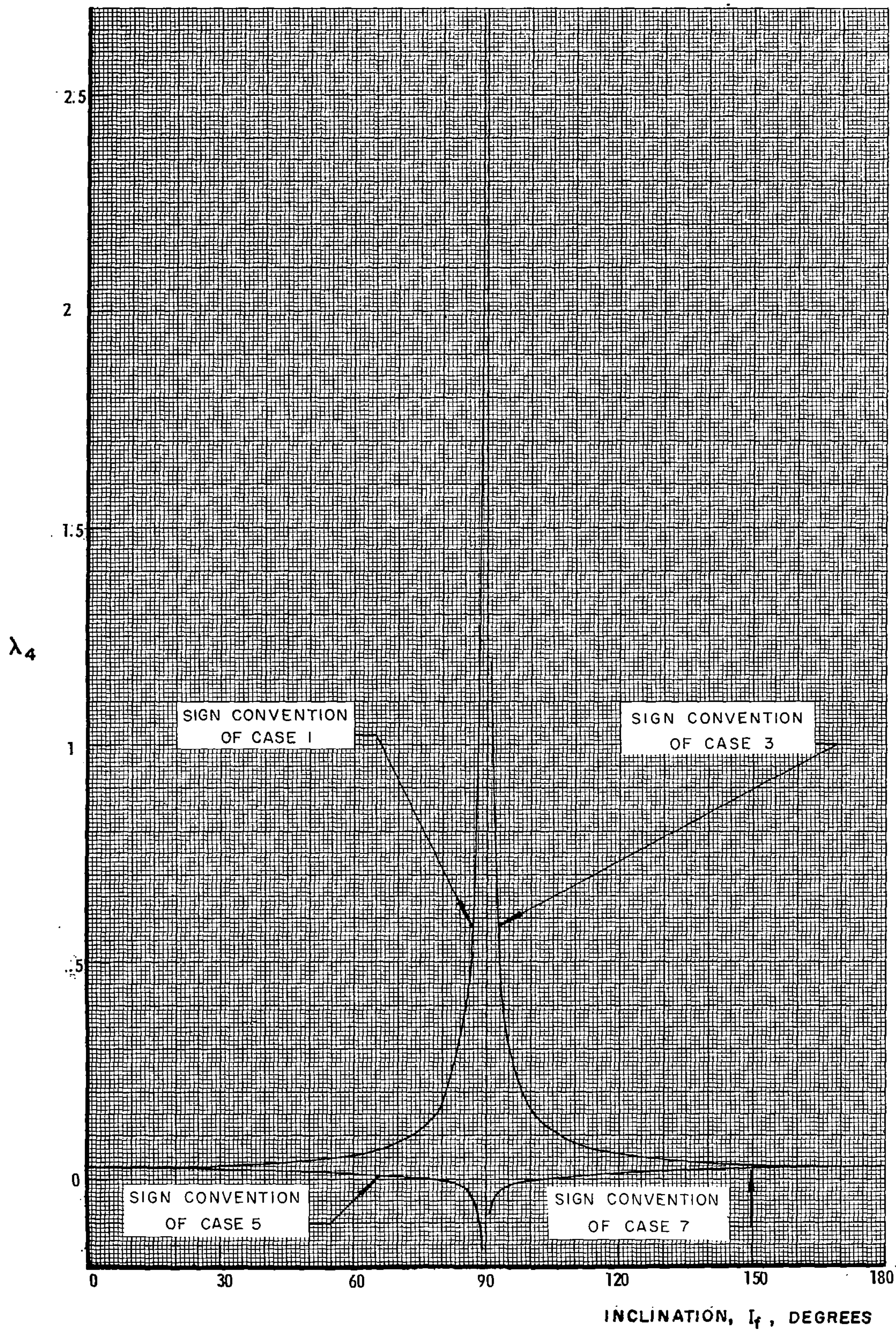

FIG 63. λ_4 VS INCLINATION $[(T/W)_0 = 2$ AND $I_{sp} = 300$ SECONDS$]$

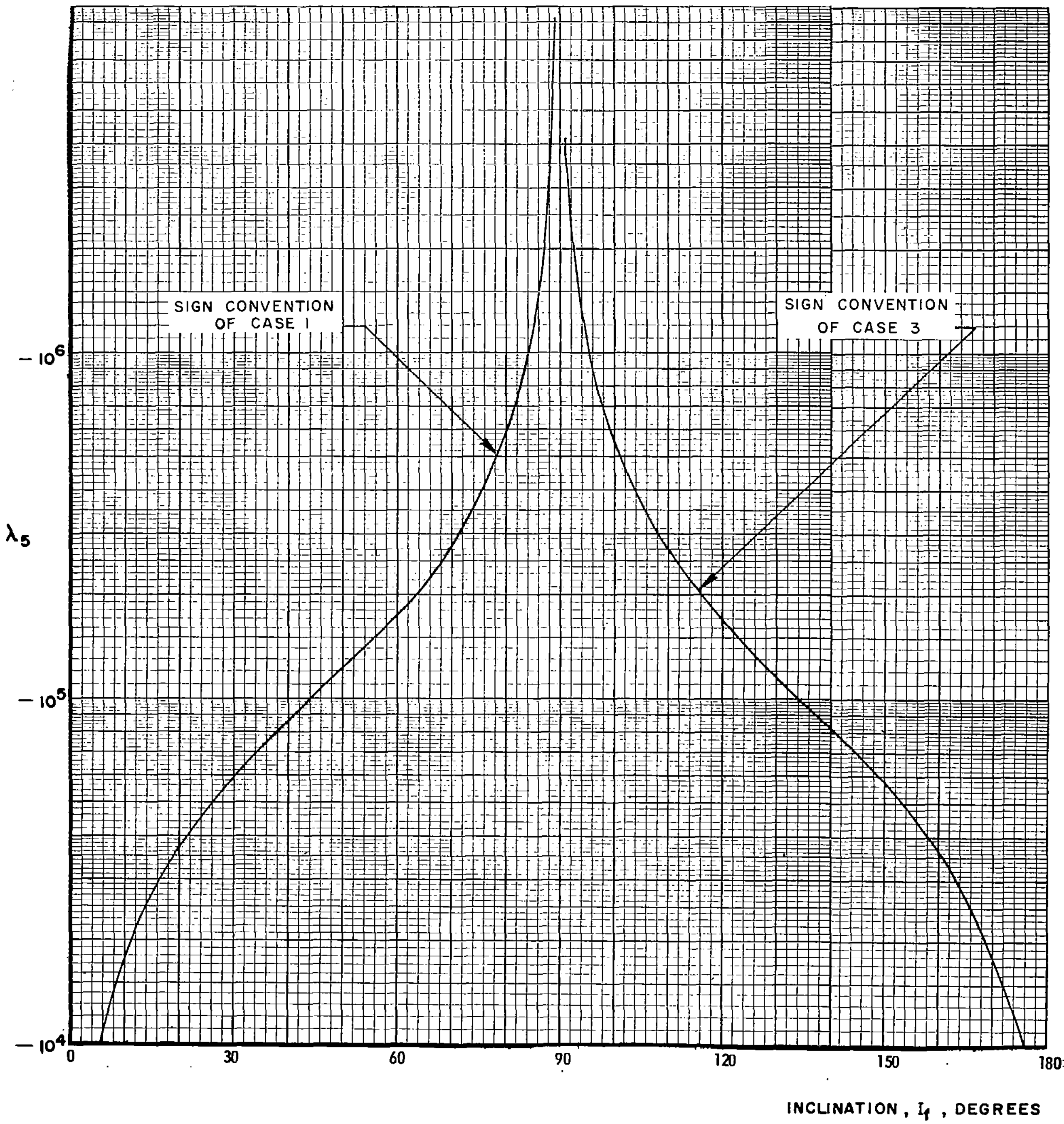

FIG 64. λ_5 VS INCLINATION $[(T/W)_0 = 2$ AND $I_{sp} = 300$ SEC.$]$

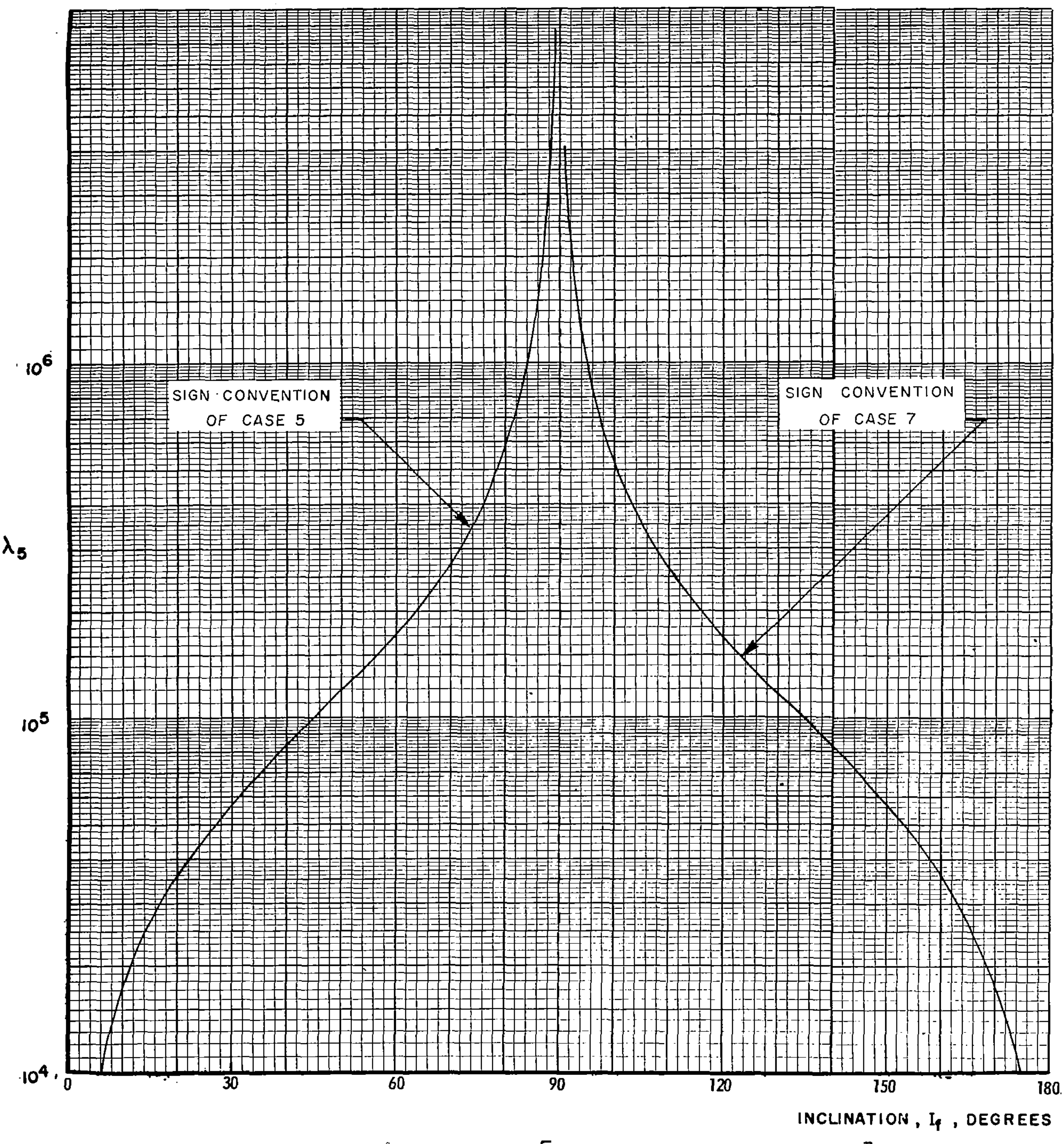

FIG 65. λ_5 VS INCLINATION $[(T/W)_0 = 2$ AND $I_{sp} = 300$ SEC.$]$

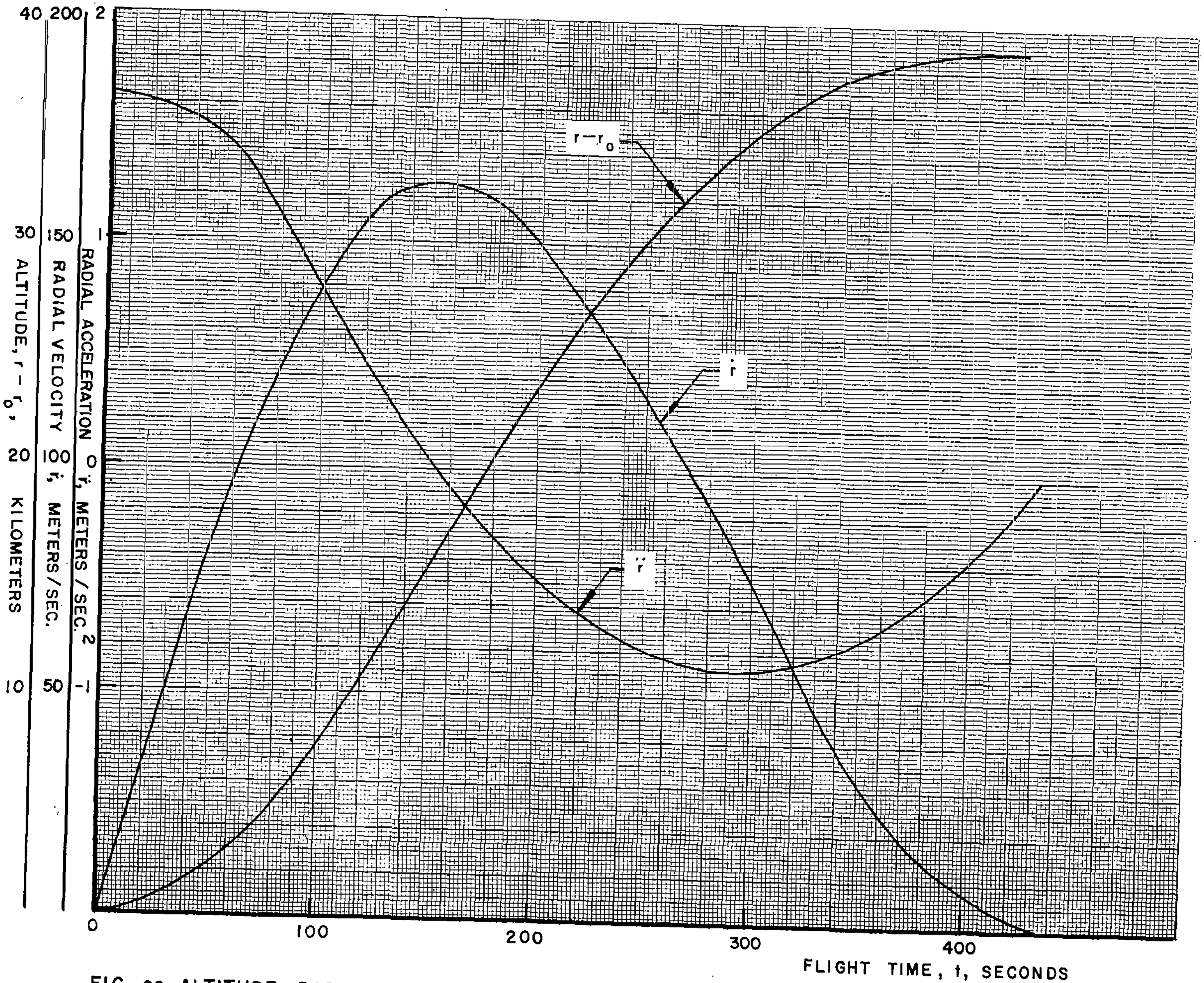

FIG 66. ALTITUDE, RADIAL VELOCITY, AND RADIAL ACCELERATION VS FLIGHT TIME $[(T/W)_0 = 2$ AND $I_{sp} = 300$ SEC.$]$

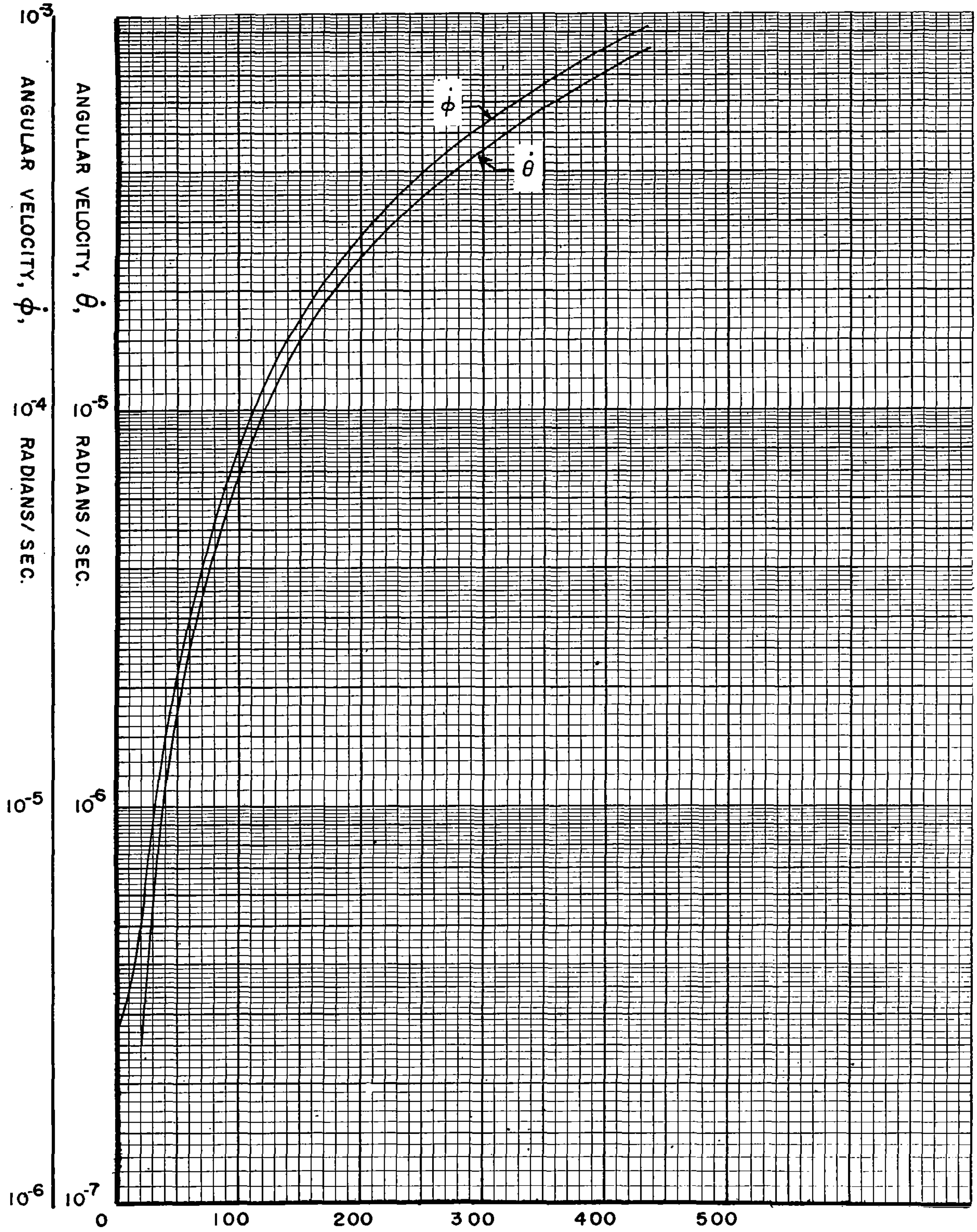

FIG 67. ANGULAR VELOCITY $\dot{\phi}$ AND $\dot{\theta}$ VS FLIGHT TIME $[(T/W)_0 = 2$ AND $I_{sp} = 300$ SEC.$]$

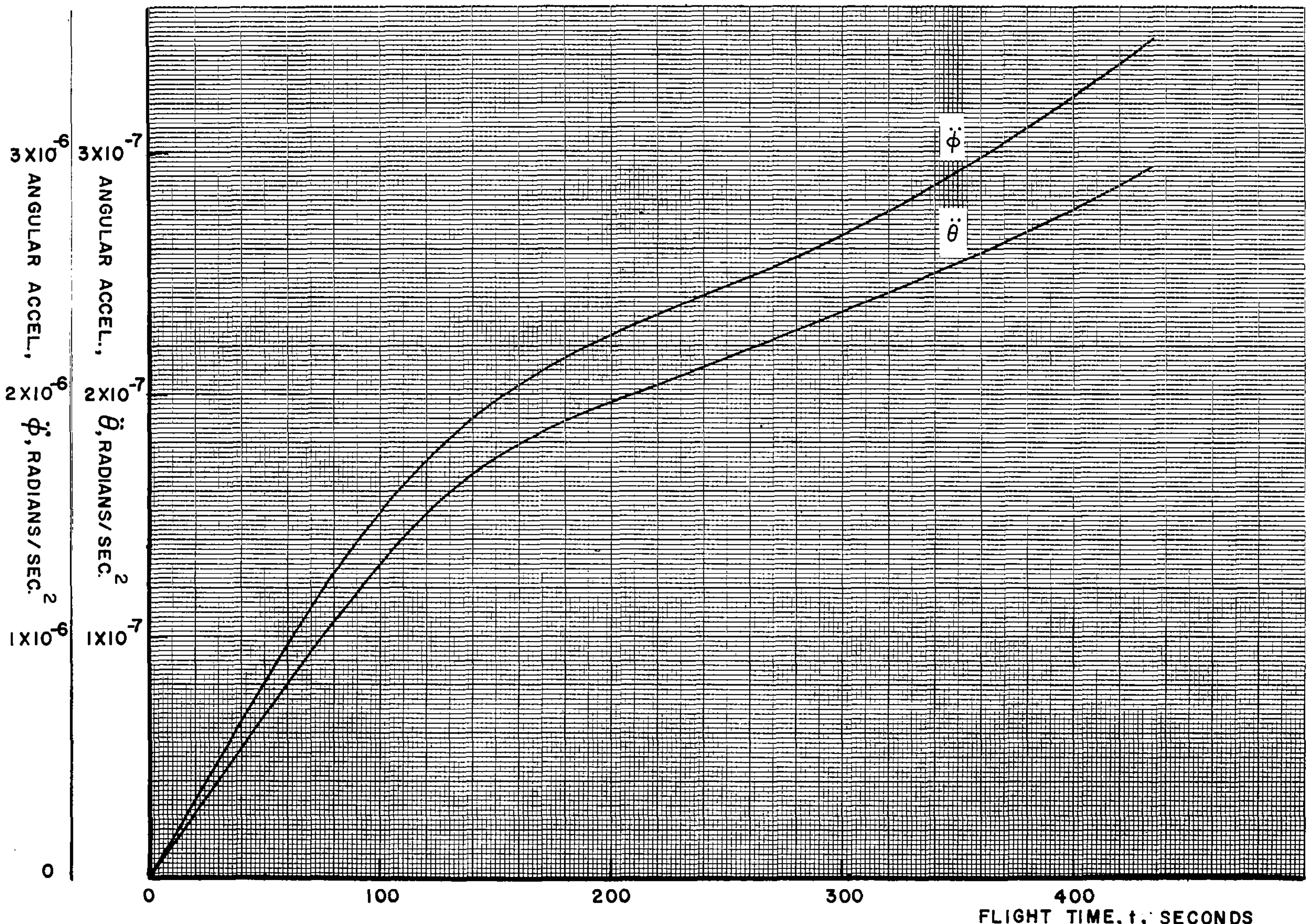

FIG 68. ANGULAR ACCELERATIONS $\ddot{\phi}$ AND $\ddot{\theta}$ VS FLIGHT TIME $\left[(T/W)_0 = 2 \text{ AND } I_{sp} = 300 \text{ SEC.}\right]$

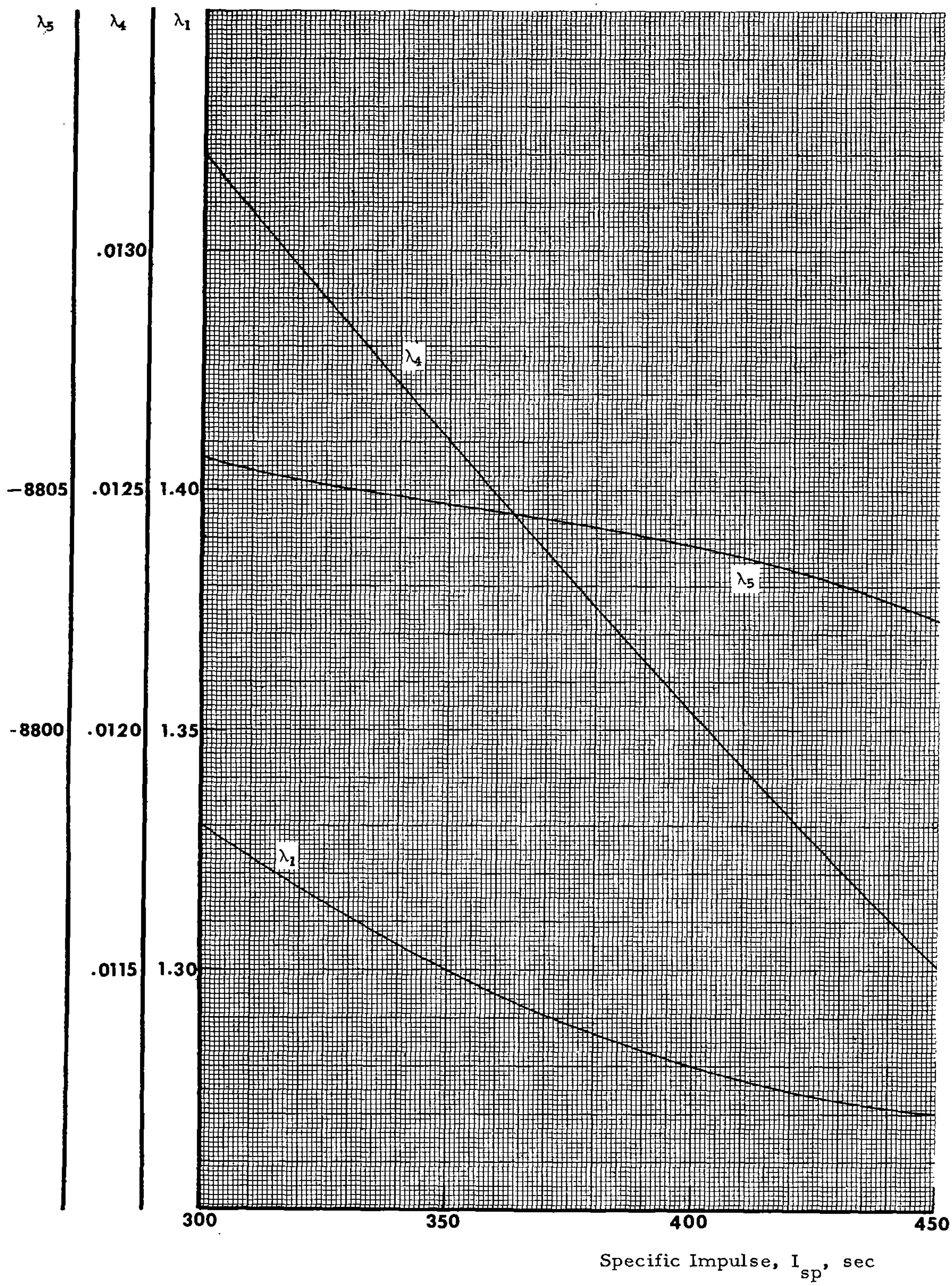

FIGURE 77. INITIAL VALUES OF LAGRANGIAN MULTIPLIERS VS SPECIFIC IMPULSE FOR INITIAL LUNAR THRUST-TO-WEIGHT RATIO OF 4.4796

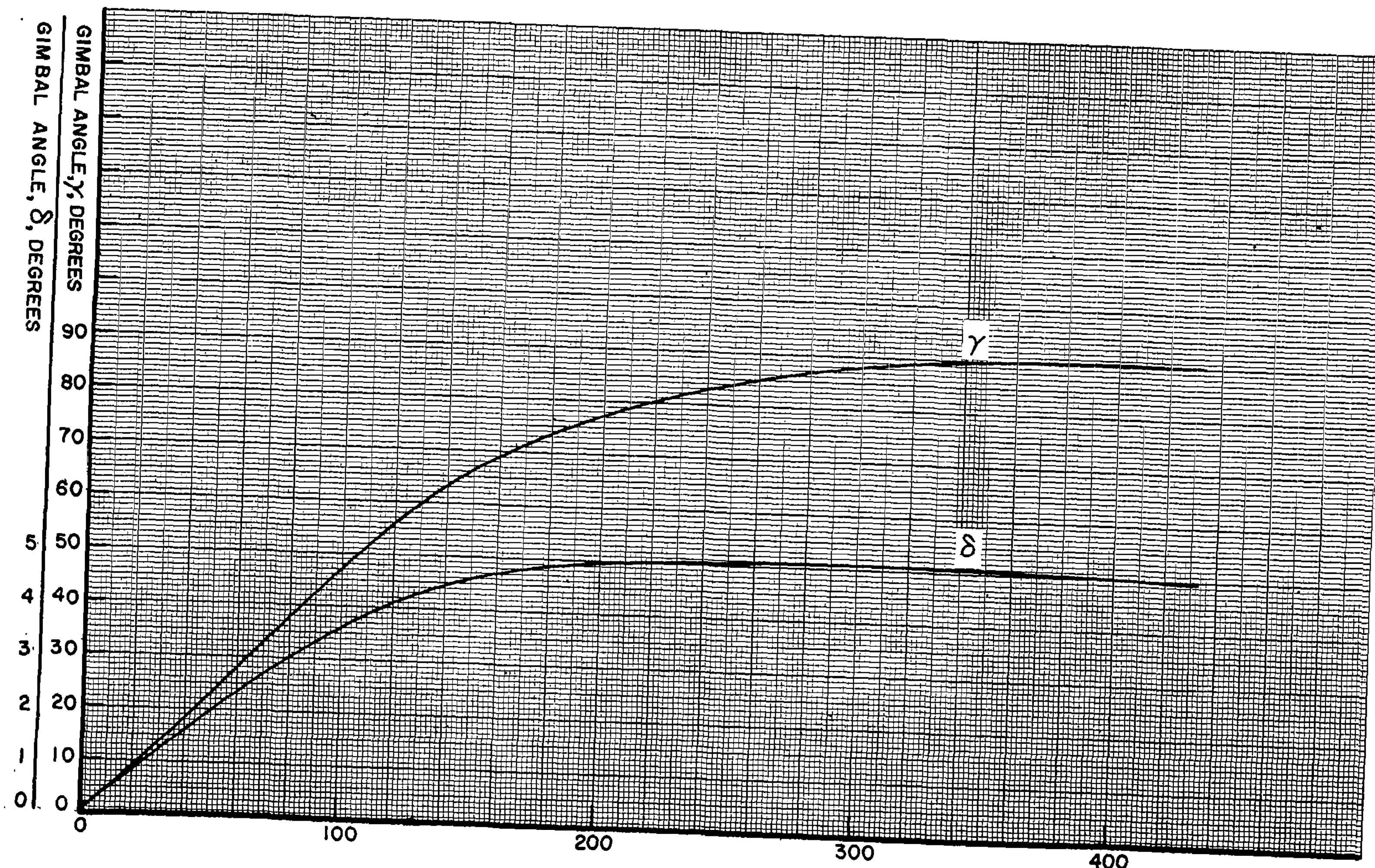

FIG 70 - GIMBAL ANGLES γ AND δ VS FLIGHT TIME $[(T/W)_0 = 2$ AND $I_{sp} = 300$ SECONDS$]$

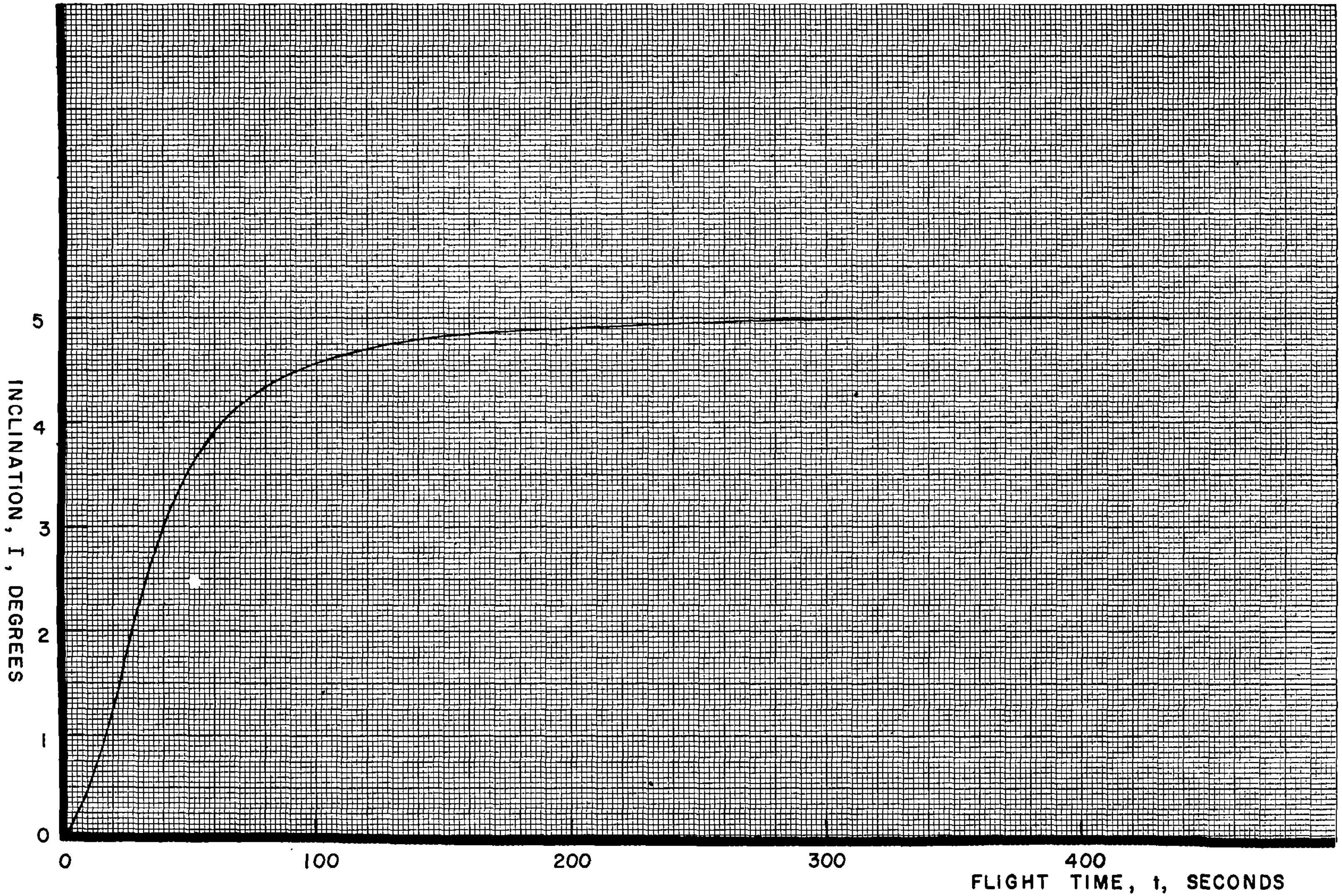

FIG 71. INCLINATION VS FLIGHT TIME $\left[(T/W)_0 = 2 \text{ AND } I_{sp} = 300 \text{ SECONDS}\right]$

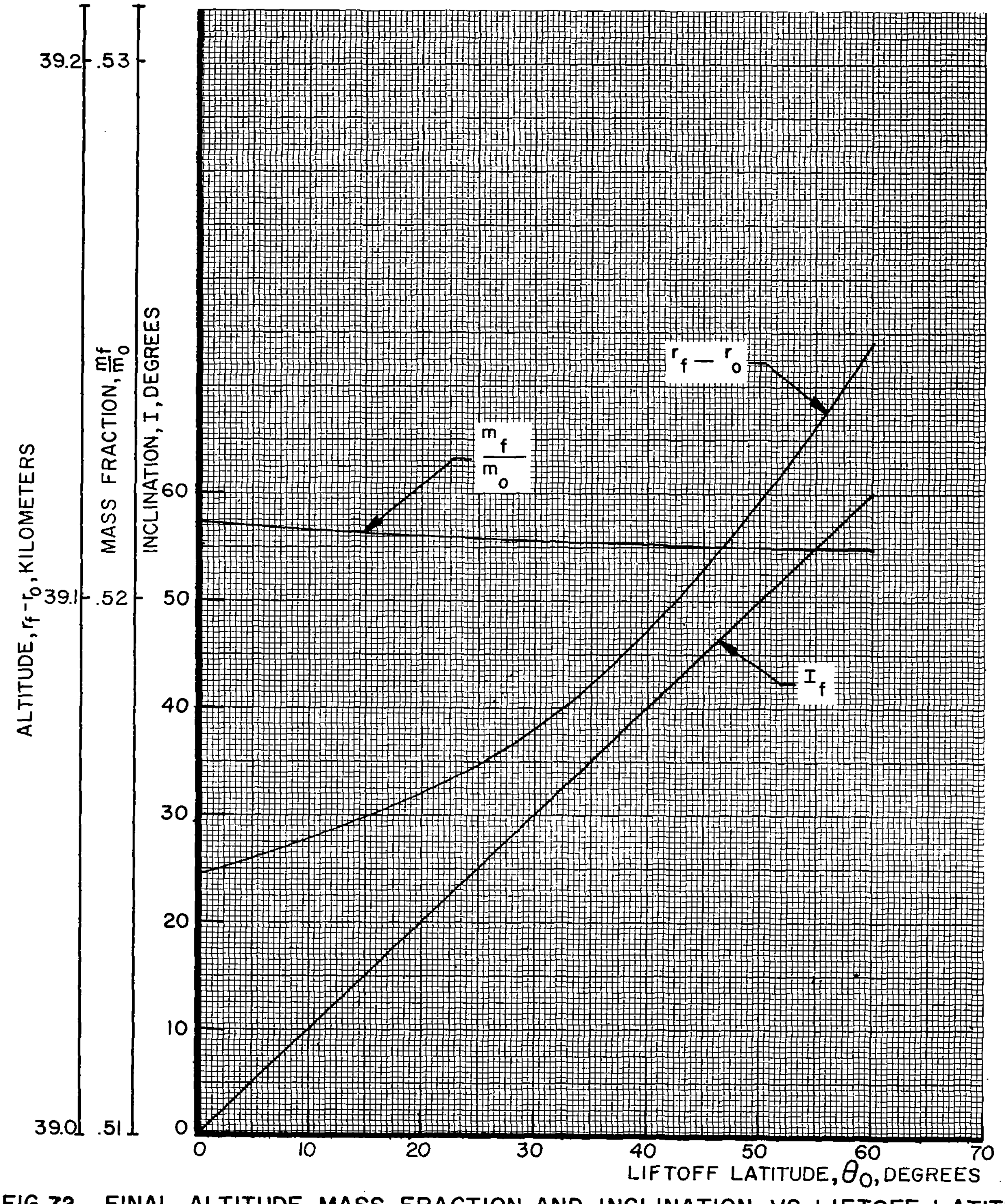

FIG 72 . FINAL ALTITUDE, MASS FRACTION, AND INCLINATION VS LIFTOFF LATITUDE
$[(T/W)_o = 2,\ I_{sp} = 300$ SEC., $\lambda_5 = 0]$

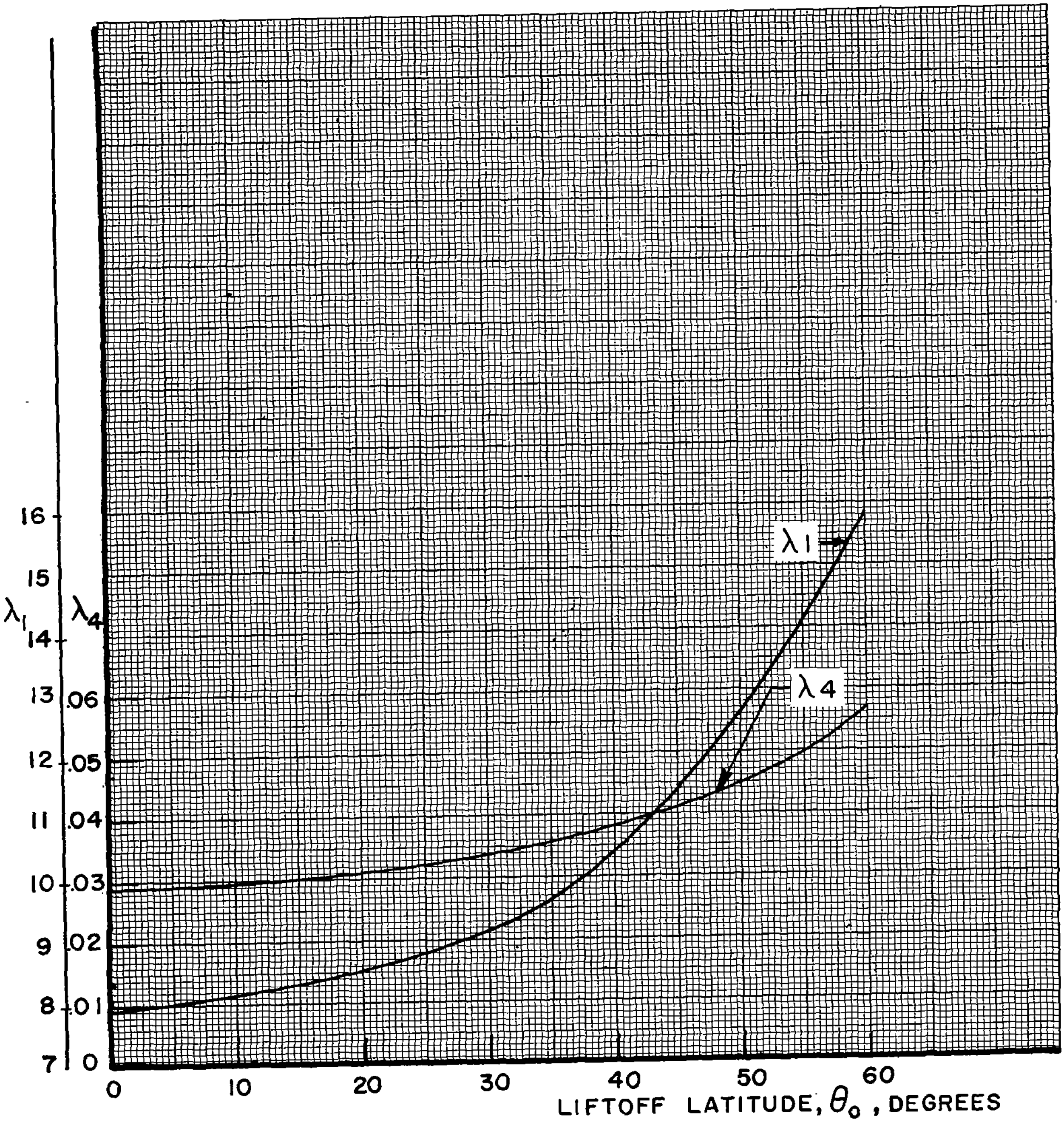

FIG 73. λ_1 AND λ_4 VS LIFTOFF LATITUDE $\left[(T/W)_0 = 2, I_{sp} = 300 \text{ SEC.}, \lambda_5 = 0\right]$

SECTION X. EXAMPLES

In order to illustrate a few of the possible methods of applying the preceding material to practical cases, a number of examples will be given. Since this entire report is unclassified, the following numbers do not correspond to real vehicles, but the methods of application carry over directly. While most cases below are treated graphically, one could use finite difference methods to interpolate directly from the tables.

Example 1. Suppose that we wish to determine the payload that an engine having 15,000 pounds of thrust and a specific impulse of 440 sec. can place in lunar orbit as a function of lift-off weight. Assume the lift-off weights to be studied are specified to be 25,000 pounds and 30,000 pounds (earth reference). Require that thrust and velocity vectors be aligned at orbit.

The first step is the construction of Table 53:

TABLE 53

I_{sp}	W_0	T	$(T/W_0)_\oplus$
440	25,000	15,000	.60000
440	27,500	15,000	.54545
440	30,000	15,000	.50000

The last column was obtained by dividing the thrust (T) by the initial weight (W_0). The next step is to convert the initial thrust-to-weight ratio from earth-reference to lunar-reference. This may be accomplished by taking the ratios of the earth value of the acceleration of gravity to the lunar value and multiplying the fourth column by this ratio.

Denoting the Moon by the subscript ☾ and the Earth by the subscript $\oplus$ we have

$$\frac{(g_0)_\oplus}{(g_0)_☾} = \frac{9.81\ m/\text{sec}^2}{1.622169\ m/\text{sec}^2} = 6.047459$$

Multiplying the earth-referenced thrust-to-weight by 6.047459, our table now looks as follows:

TABLE 54

I_{sp}	W_0	T	$(T/W_0)_\oplus$	$(T/W_0)_☾$
440	25,000	15,000	.60000	3.6285
440	27,500	15,000	.54545	3.2986
440	28,000	15,000	.50000	3.0238

Now we are in a position to use the material presented above. The bulk of the data given assumes launch from the lunar equator at the zero meridian into a plane of 5° inclination to the equator. A further assumption is called for about the lift-off angle. The data presented covers lift-off angles from vertical to 40° from vertical. While 40° lift-off angles give better performance, vertical ascent is probably a more reasonable assumption. With this in mind, we choose vertical ascent ($\gamma_0 = 0°$).

Since the thrust-to-weight is specified, we cannot choose an optimum value. FIG 15 shows the mass fraction and FIG 17 shows final altitude as functions of the initial lunar thrust-to-weight ratios covering the range of interest with parametric values of 300, 350, 400, and 450 under the assumption of vertical ascent and alignment of thrust and velocity vectors at orbit.

Using this figure, we begin by constructing a vertical line from $(T/W_0)_{\leftmoon} = 3.6285$, $(T/W_0)_{\leftmoon} = 3.2986$, and $(T/W_0)_{\leftmoon} = 3.0238$. The following table is obtained:

TABLE 55

$(T/W_0)_{\leftmoon}$	I_{sp}	m_f/m_0	$r_f - r_0$
3.6285	450	.6648	18.2
3.6285	400	.6325	17.4
3.6285	350	.5930	16.4
3.6285	300	.5449	15.1
3.2986	450	.6625	21.4
3.2986	400	.6320	20.5
3.2986	350	.5905	19.3
3.2986	300	.5420	17.7
3.0238	450	.6600	25.1
3.0238	400	.6278	23.9
3.0238	350	.5880	22.5
3.0238	300	.5390	20.7

We may now plot m_f/m_0 and $r_f - r_0$ vs. I_{sp} with parametric values of $(T/W_0) = 3.6285$, 3.2986, 3.0238. This has been done in FIG 74.

In order to obtain our final data, we now simply construct a vertical line from the specific impulse of interest, namely 440. Doing this we find:

TABLE 56

(T/W_0)	I_{sp}	m_f/m_0	$r_f - r_0$
3.6285	440	.6590	18.0
3.2986	440	.6568	21.2
3.0238	440	.6543	24.9

Inserting the data of Table 56 into Table 54, our accumulated data are

TABLE 57

I_{sp}	W_0	T	$(T/W_0)_{\oplus}$	$(T/W_0)_{\leftmoon}$	m_f/m_0	$r_f - r_0$
440	25,000	15,000	.60000	3.6285	.6590	18.0
440	27,500	15,000	.54545	3.2986	.6568	21.2
440	30,000	15,000	.50000	3.0238	.6543	24.9

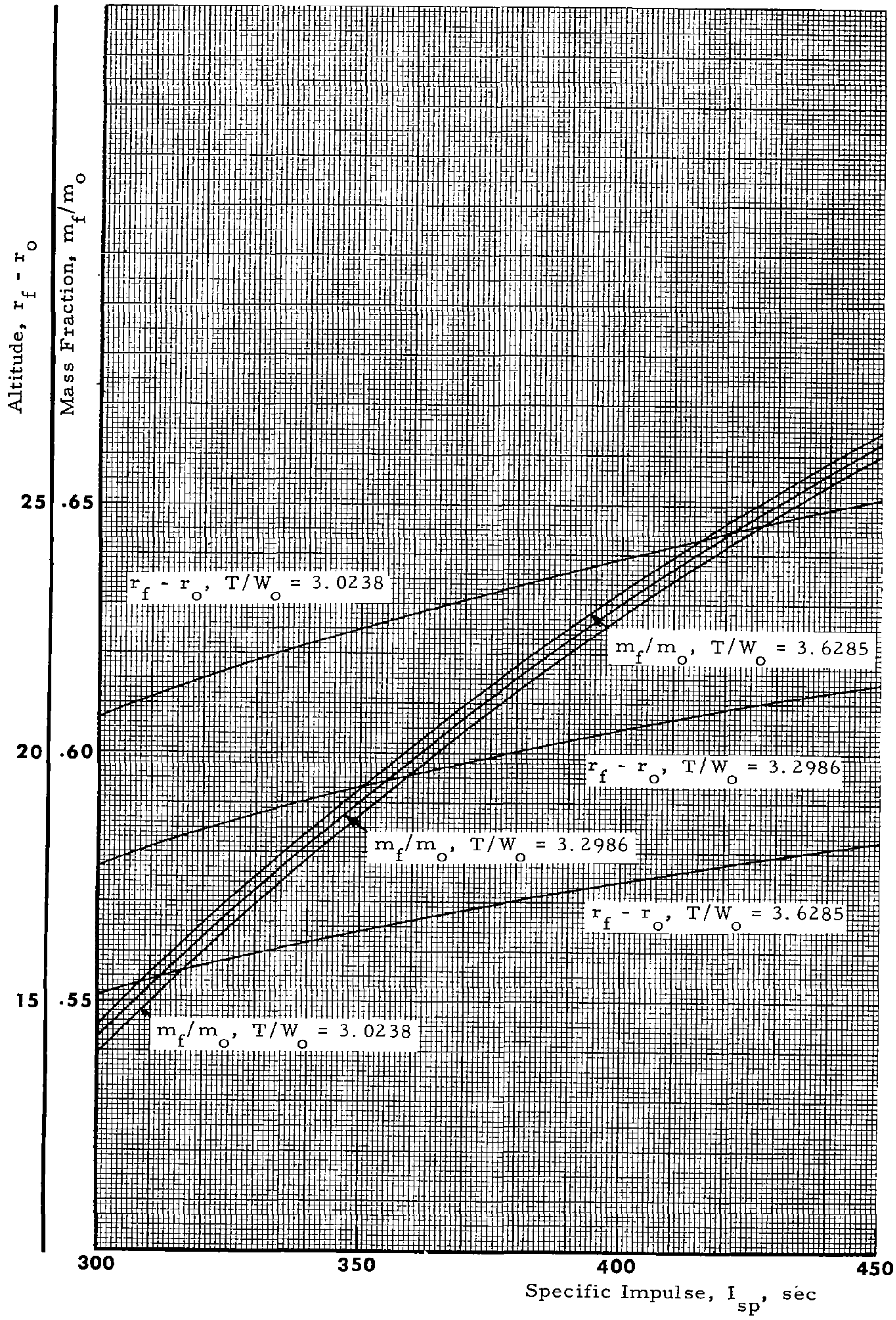

FIGURE 74. ALTITUDE AND MASS FRACTION VS SPECIFIC IMPULSE FOR INITIAL LUNAR THRUST-TO-WEIGHT RATIOS OF 3.0238, 3.2986, and 3.6285

The payload may now be found (in earth pounds) by multiplying the initial weight, W_0, by the mass fraction placed in orbit m_f/m_0. Doing this, we find the following:

TABLE 58

I_{sp} (sec.)	W_0 (pounds)	T (pounds)	$(T/W_0)_\oplus$ (Earth)	$(T/W_0)_☾$ (Moon)	m_f/m_0	$r_f - r_0$ (kilometers)	Payload (pounds)
440	25,000	15,000	.60000	3.6286	.6590	18.0	16,480
440	27,500	15,000	.54545	3.2986	.6568	21.2	18,060
440	30,000	15,000	.50000	3.0238	.6543	24.9	19,630

The last column of Table 58 gives the payload, in pounds, that can be delivered to the altitude listed in the next-to-last column.

Although this completes the solution, there is one other datum that is of interest. The characteristic velocity, u, may easily be derived from the mass fraction m_f/m_0. This quantity is defined as

$$u = g_0 I_{sp} \ln R$$

where R is the mass ratio [i.e., the reciprocal $1/(m_f/m_0) = m_f/m_0$]. We may then write

$$u = g_0 I_{sp} \ln \frac{m_0}{m_f} = (9.81)(440) \ln \left[\frac{1}{(m_f/m_0)}\right] = 4316.4 \ln \left[\frac{1}{(m_f/m_0)}\right]$$

Inserting values of m_f/m_0 from Table 58, we may calculate u as follows:

TABLE 59

m_f/m_0	$1/(m_f/m_0)$	$\ln\left[\left(1/\frac{m_f}{m_0}\right)\right]$	u
.6590	1.517	.4167	1799
.6568	1.523	.4207	1816
.6543	1.528	.4240	1830

The final table, including u is

TABLE 60

I_{sp} (sec)	W_0 (pounds)	T (pounds)	$(T/W_0)_\oplus$	$(T/W_0)_☾$	m_f/m_0	$r_f - r_0$ (kilometers)	Payload (pounds)	u (meters/sec)
440	25,000	15,000	.60000	3.6285	.6590	18.0	16,480	1799
440	27,500	15,000	.54545	3.2986	.6568	21.2	18,060	1816
440	30,000	15,000	.50000	3.0238	.6543	24.9	19,630	1830

Table 60 is reproduced using the approximate data of FIG 26 for purposes of comparison. It is shown below as Table 61.

TABLE 61

I_{sp} (sec)	W_0 (pounds)	T (pounds)	$(T/W_0)_\oplus$	$(T/W_0)_☾$	m_f/m_0	$r_f - r_0$ (kilometers)	Payload (pounds)	u (meters/sec)
440	25,000	15,000	.60000	3.6285	.6605	17.6	16,513	1790
440	27,500	15,000	.54545	3.2986	.6587	21.1	18,114	1802
440	30,000	15,000	.50000	3.0238	.6554	24.9	19,662	1824

Example 2. A second case which illustrates another interesting point of the theory is to assume a specific impulse of 395 seconds, and a thrust of 20,000 pounds. Let us consider lift-off weights of 27,000 pounds and 33,000 pounds. Assume that an orbital altitude of 15 kilometers is specified.

As before, we construct the following table

TABLE 62

I_{sp}	W_0	T	$(T/W_0)_\oplus$	$(T/W_0)_☾$
395	27,000	20,000	.74074	4.4796
395	30,000	20,000	.66667	4.0317
395	33,000	20,000	.60606	3.6651

Constructing vertical lines from $(T/W_0)_☾ = 4.4796$, 4.0317, and 3.6651 on FIG 7 we read the following values:

TABLE 63

$(T/W_0)_☾$	I_{sp} (seconds)	m_f/m_0
4.4796	450	.6688
4.4796	400	.6360
4.4796	350	.5958
4.4796	300	.5460
4.0317	450	.6687
4.0317	400	.6360
4.0317	350	.5958
4.0317	300	.5462
3.6651	450	.6684
3.6651	400	.6357
3.6651	350	.5955
3.6651	300	.5460

Interestingly enough, all values are so near the optimum thrust-to-weight value--an extremely flat region--that it is very difficult to resolve the three mass fraction curves. We thus study the thrust-to-weight value of 4.4796.

FIG 75 shows a plot of m_f/m_0 vs I_{sp} for $(T/W_0)_☾ = 4.4796$. From a vertical line at $I_{sp} = 395$ sec. we read

$$m_f/m_0 = .6328$$

Carrying through this one case (the other two values of thrust-to-weight may be carried through by the reader, if desired) we now find

TABLE 64

I_{sp} (seconds)	W_0 (pounds)	T (pounds)	$(T/W_0)_\oplus$	$(T/W_0)_☾$	m_f/m_0	Payload (lbs.)	u (m/sec.)
395	27,000	20,000	.74074	4.4796	.6328	17,090	1772

where u was calculated from

$$u = g_0 I_{sp} \ln \left[\frac{1}{(m_f/m_0)}\right] = (9.81)\ (395) \ln\left[\frac{1}{.6328}\right] =$$

$$3874.95 \ \ln\ (1.580) = (3874.95)\ (.4574) = 1772 \ \text{m/sec.}$$

It should be noted that this u, as in example 1, includes all gravity losses, plane change maneuvers, etc.

Example 3. Suppose next that we have the problem of determining the payload capability for final orbital altitude of 15 kilometers and characteristic velocity for a moon lift-off using $I_{sp} = 315$ sec. Let the engine thrust remain unspecified, for the moment, but consider lift-off weights of 16,000 pounds, 18,500 pounds, and 21,000 pounds.

Since we are essentially designing an engine around a specific impulse, we may as well choose an optimum thrust-to-weight for each of the above weights. FIG 5 of Section IX gives the data needed. This graph shows optimum thrust-to-weight ratios, final value of gamma, and mass fractions as a function of specific impulse for vertical ascent. These values may be read directly by constructing a vertical line from a specific impulse value of 315 sec.

Applying this procedure to FIG 5, we can directly read the following data;

$$(T/W_0)_☾ = 4.023 \text{ (Optimum)}$$

$$(m_f/m_0) = .5630$$

The (optimum) lunar thrust-to-weight ratio may now be converted to an earth-referenced value by dividing (rather than multiplying) by the factor $(g_0)_\oplus/(g_0)_☾ = 6.047459$. (The lunar thrust-to-weight ratio must always be larger than the earth thrust-to-weight ratio).

Doing this we find

$$\left(\frac{T}{W_0}\right)_\oplus = \left(\frac{T}{W_0}\right)_☾ \frac{(g_0)_☾}{(g_0)_\oplus} = \frac{4.023}{6.047459} = .6652$$

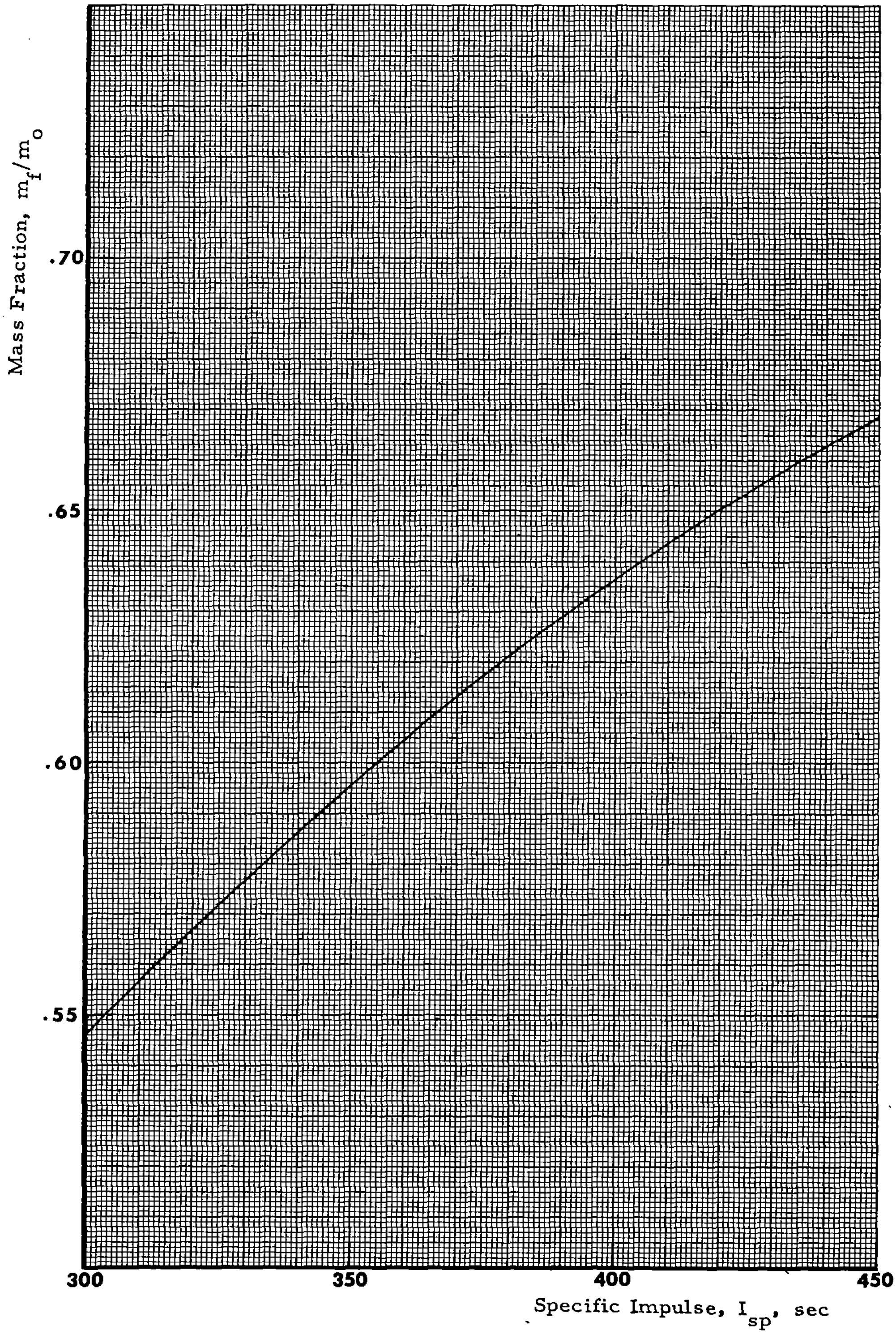

FIGURE 75. MASS FRACTION VS SPECIFIC IMPULSE FOR INITIAL LUNAR THRUST-TO-WEIGHT RATIO OF 4.4796

The engine thrust may now be found by multiplying the initial thrust-to-weight value by the lift-off weight. Thus we have

TABLE 65

W_0 (pounds)	$(T/W_0)_\oplus$	T (pounds)
16,000	.6652	10,640
18,500	.6652	12,310
21,000	.6652	13,970

The payload may now be found by multiplying the mass fraction (the same in each case, and equal to .5630) by the lift-off weight. Doing this gives

TABLE 66

W_0 (pounds)	Payload (pounds)
16,000	9,008
18,500	10,416
21,000	11,823

Since we have one mass fraction for all lift-off weights, we have only one characteristic velocity which is

$$u = g_0\, I_{sp} \ln\,[\,1/(m_f\,/m_0\,)] = (9.81)(315)\ \ln\,[1/.5630] = 1775 \text{ m/sec.}$$

Example 4. Consider the problem of delivering a payload to a prespecified altitude with thrust and velocity vectors aligned at orbit. Let us assume a specific impulse of 375 sec. and an altitude of 30 km. The initial thrust-to-weight ratio is necessarily unspecified since we have fixed the final altitude and final value of gamma.

We begin by construction of a horizontal line at an altitude of 30 km on FIG 16. This line then cuts the various altitude curves which correspond to various specific impulses at a definite thrust-to-weight ratio. The mass fractions for these thrust-to-weight ratios, and the same specific impulse values, may then be read as usual from FIG 15. We obtain the following data:

TABLE 67

$r_f - r_0$ (km)	I_{sp}(sec)	$(T/W_0)_{☾}$	$m_f\,/m_0$
30.0	300	2.37	.5295
30.0	350	2.52	.5810
30.0	400	2.63	.6260
30.0	450	2.71	.6560

FIG 76 shows a plot of initial lunar thrust-to-weight ratio and mass fraction vs specific impulse for a final altitude of 30 km.

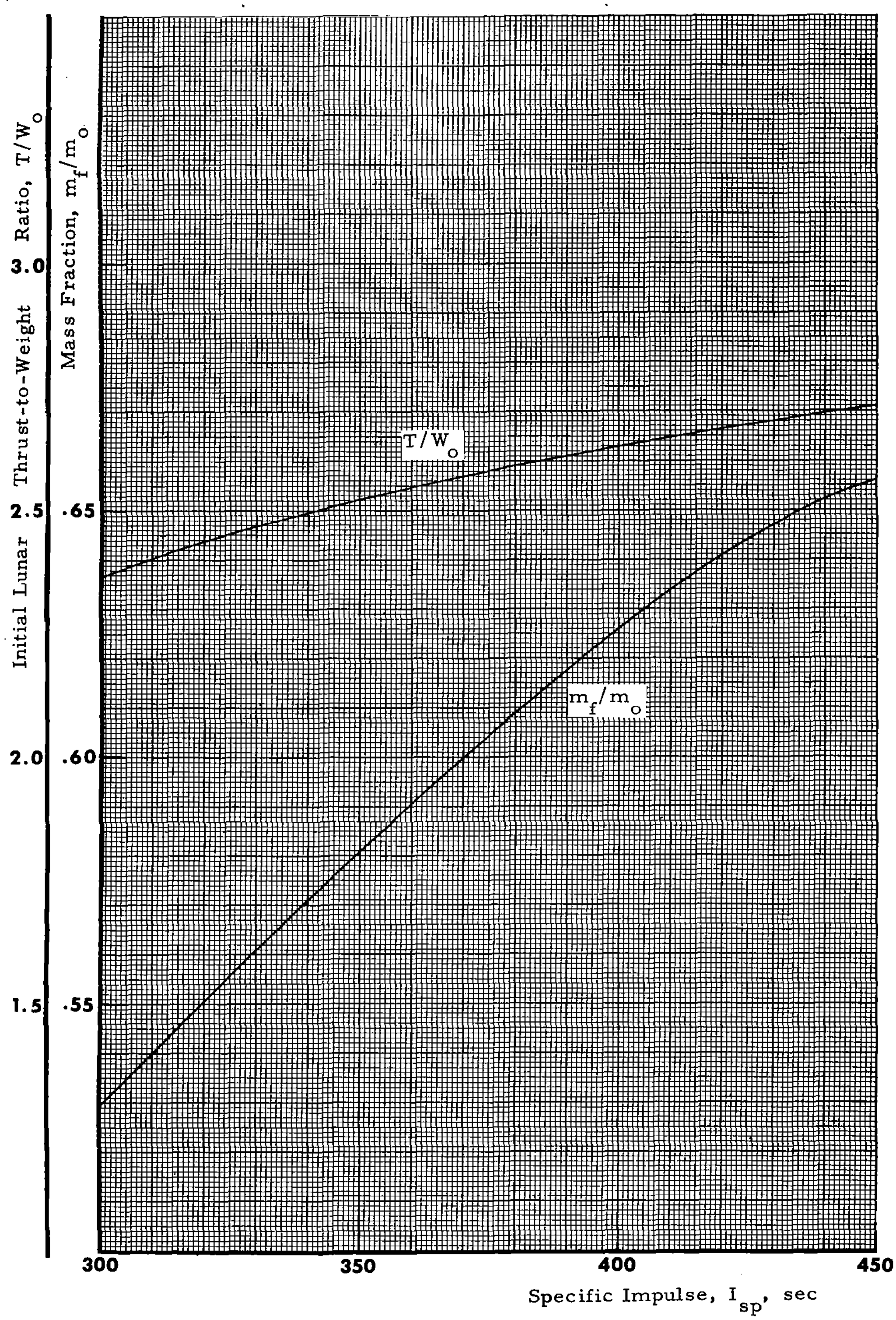

FIGURE 76. INITIAL LUNAR THRUST-TO-WEIGHT RATIO AND MASS FRACTION VS SPECIFIC IMPULSE FOR A FINAL ALTITUDE OF 30 KILOMETERS

The information we desire may now be obtained by constructing a vertical line from a specific impulse value of 375 sec., and reading the mass fraction and initial thrust-to-weight ratio from the vertical scales. This procedure yields

$$(T/W_0) = 2.58$$

$$m_f/m_0 = .6042$$

This result shows that any vehicle with an initial thrust-to-weight ratio of 2.58, and a specific impulse of 375 sec. will place a mass fraction of .6042 into an orbit of 30 km altitude.

If the initial engine thrust was specified to be, say, 10,000 pounds, then

$$(W_0) = \frac{10,000}{2.58} = 3875 \text{ lunar pounds}$$

The corresponding earth weight is

$$(W_0)_\oplus = 23,430 \text{ earth pounds}$$

The payload can now be found, in earth pounds as

$$\text{Payload} = (W_0)_\oplus\ (m_f/m_0) = (23,430)\ (.6042) = 14,160 \text{ pounds}$$

Example 5. Example 3 considered the problem of designing an engine of prespecified specific impulse to place a maximum percentage of a given lift-off weight into orbit. Suppose, now, that an engine thrust and specific impulse are given, and we wish to place a maximum payload into lunar orbit by variation of the lift-off weight. Suppose, finally, that thrust and velocity vectors must be aligned at orbit.

This problem, at first sight, appears to be equivalent to Example 3. Further consideration shows that a basic distinction exists. The reasoning is as follows: If we fix the specific impulse and thrust, and there is a certain lift-off weight that produces the optimum thrust-to-weight ratio and maximizes the mass fraction placed in orbit; if we load the vehicle more heavily at lift-off, then the final mass fraction decreases, but to find the payload, we multiply the mass fraction by the lift-off weight. Although the mass fraction is *decreasing*, the product of mass fraction and lift-off weight (which is *increasing*) may be either increasing, decreasing, or even constant as initial thrust-to-weight ratio varies.

We propose to investigate this for a specific example. Suppose that the thrust is fixed at 15,000 pounds, and the specific impulse is chosen to be 350 sec. (this value can be read directly from the tables and will serve for purposes of illustration).

Let us choose our initial values of the lift-off weight, in lunar pounds, such that the initial thrust-to-weight ratios are covered in the tables of Section VIII. The following table is obtained:

TABLE 68

I_{sp}	T (pounds)	$(W_0)_ℂ$ (pounds)	$(T/W_0)_ℂ$
350	15,000	15,000	1.0
350	15,000	13,636	1.1
350	15,000	11,538	1.3
350	15,000	10,000	1.5
350	15,000	7,500	2.0
350	15,000	5,000	3.0
350	15,000	3,750	4.0
350	15,000	3,000	5.0
350	15,000	2,500	6.0
350	15,000	2,143	7.0

The mass fractions may now be read directly from Tables 12 through 21 of Section VIII by choosing the entries with $I_{sp} = 350$. This yields

TABLE 69

$(W_0)_\zeta$ (pounds)	$(T/W_0)_\zeta$	m_f/m_0	$(W_0)_\zeta(m_f/m_0)$
15,000	1.0	.4729	7094
13,636	1.1	.4981	6792
11,538	1.3	.5286	6099
10,000	1.5	.5465	5465
7,500	2.0	.5701	4276
5,000	3.0	.5888	2944
3,750	4.0	.5967	2238
3,000	5.0	.6009	1803
2,500	6.0	.6036	1509
2,143	7.0	.6054	1297

where the last column was found from taking the indicated product. This column shows that the payload is continually increasing with decreasing thrust-to-weight ratio, and terminates in an end point maximum at $(T/W_0)_\zeta = 1$.

The implication of the above Table is that a given engine should always be loaded until the thrust-to-weight is one to achieve maximum payload. This is a different problem than achieving maximum mass fraction.*

The question of the usefulness of the "optimum" initial lunar thrust-to-weight ratios now arises, and we continue our investigation along slightly different lines. Since there exists no optimum for this case, we proceed by choosing an initial thrust-to-weight ratio of 7 for comparative purposes.

The problem may be approached by considering that the payload was prespecified at 7094 lunar pounds. Using the above engine, we would then find a necessary initial lunar thrust-to-weight ratio of 1.

But now consider what happens if the above requirement on choice of initial thrust is relaxed, and we are able to choose another engine of arbitrary thrust and the same specific impulse. The payload must still be 7094 pounds.

Table 49 shows that for a specific impulse of 350 sec. the mass fraction corresponding to an initial thrust-to-weight ratio of 7 is .6054. The lift-off weight must then be

$$(W_0)_\zeta = (W_f)_\zeta \left(\frac{m_0}{m_f}\right) = \frac{(W_f)_\zeta}{(m_f/m_0)} = \frac{7094}{.6054} = 11{,}718 \text{ pounds}$$

$$T = (T/W_0)_\zeta (W_0)_\zeta = (7)(11{,}718) = 82{,}026 \text{ pounds}$$

So far we have merely attained the same payload using two different engines. Now let us consider the propellant expenditure used in each case. For the 15,000 pound thrust case, we have

$$(W_{prop})_1 = (W_0)_\zeta - (W_f)_\zeta = 15{,}000 - 7{,}094 = 7{,}906 \text{ pounds}$$

* The reader must bear in mind that the earlier remarks about maximization of payload by trajectory shaping are not modified by this discussion.

While for the 82,026 pound thrust case

$$(W_{prop})_2 = (W_0)_4 - (W_f)_4 = 11{,}718 - 7{,}094 = 4{,}624 \text{ pounds}$$

The difference in propellant expenditures is

$$(W_{prop})_1 - (W_{prop})_2 = 3282 \text{ pounds}$$

This figure, converted to earth pounds, is

$$(W_{prop})_1 - (W_{prop})_2 = 19{,}848 \text{ (earth) pounds}$$

This difference is the price that must be paid, in this particular example, for a poor choice of engine. Since all propellant used for ascent from the lunar surface must first be propelled to escape from the earth and braked onto the Moon, the cost is even higher than this example illustrates.

The above example illustrates quite markedly the difference between various maxima. For the first thrust level considered, the payload placed in lunar orbit was a maximum; the second thrust level placed the same payload in orbit with a better thrust (referred to mission viewpoint). Similar results are obtained for a comparison between the optimal thrust-to-weight ratio in comparison to a thrust-to-weight ratio of unity for the case of ascent to a prespecified altitude.

It might be objected that the higher thrust engine would weigh a good deal more, and thus offset much of our gain. Consider that both engines have a thrust-to-engine-weight of 25:1. In practice, we can do much better on the higher thrust engines (aside from clustering), but disregard this to obtain an upper bound.

Thus, in the first case we have an (earth referenced) engine weight of

$$W_{engine} = \frac{15{,}000}{25} = 600 \text{ pounds}$$

while in the second case

$$W_{engine} = \frac{82{,}026}{25} = 3281 \text{ pounds}$$

Thus, the upper bound of weight gain due to our engine is 2681 pounds while the propellant that has been saved is about an order of magnitude greater.

Example 6. The above cases have been determined from graphical data or read directly from the prepared tables. It will often happen that these methods do not yield sufficiently accurate results or the required data falls outside the scope of the material presented.

We shall illustrate the two preceding situations as follows: Suppose that an improved value of the final results of Example 2 are required. The initial thrust-to-weight ratio is 4.4796, and the specific impulse is 395 sec. The initial problem is to obtain initial values of the various Lagrange multipliers which correspond to these initial conditions.

FIG 9, 11, and 12 show λ_1^0, λ_4^0, and λ_5^0 (respectively) as functions of initial thrust-to-weight ratio. Constructing a vertical line on each of these graphs from a thrust-to-weight ratio of 4.4796, the following data are found:

TABLE 70

I_{sp}	λ_1^0	λ_4^0	λ_5^0
300	1.28	.01390	−8805.7
350	1.25	.01320	−8804.7
400	1.23	.01267	−8803.9
450	1.22	.01220	−8802.3

FIG 77 shows a cross plot of these data as a function of specific impulse. A vertical line from the I_{sp} value of 395 sec. now yields the values

$$\lambda_1^o = 1.28$$

$$\lambda_4^o = .01209$$

$$\lambda_5^o = -8803.9$$

which can be used along with the values $I_{sp} = 395$ and $T/W_0 = 4.8380$ as input data to a computer (as well as $\lambda_2^o = \lambda_3^o = 0$ and $C_1 = -10^5$).

Another problem of interest is to vary the inputs to obtain higher values of the inclination than 5°. For instance, we might wish to launch a vehicle into an orbit of 40° inclination. The guessing procedure might proceed as follows: Table 33 and the corresponding entry of Table 26 show that, for the vehicle used, λ_1^o increased by

$$\frac{(\lambda_1^o)_{40^o}}{(\lambda_1^o)_{5^o}} = \frac{10.44}{7.99} = 1.31$$

To obtain a 40° inclination orbit we could make a first guess at λ_1^o as

$$(\lambda_1^o)_{40^o} = (1.31)(\lambda_1^o)_{5^o}$$

with similar scalings for the other multipliers.

Similarly, if we wish to vary the lift-off latitude from 0° to 60°, Table 34 gives a scaling factor of

$$\frac{(\lambda_1^o)_{60^o}}{(\lambda_1^o)_{0^o}} = \frac{15.955}{7.963} = 2.0$$

Thus, we could make a first guess at latitude variation of λ_1^o as

$$(\lambda_1^o)_{60^o} = (2)(\lambda_1^o)_{0^o}$$

etc.

An alternative procedure would be to converge the initial guesses (as was done above) and then iterate in small steps for final inclinations; for example, iterate for 10°, 20°, 30°, and 40° with the converged initial values for each case fed in an initial data for the following case. Similar procedures can be used to extend the ranges of lift-off latitude, thrust-to-weight ratios, specific impulses, etc.

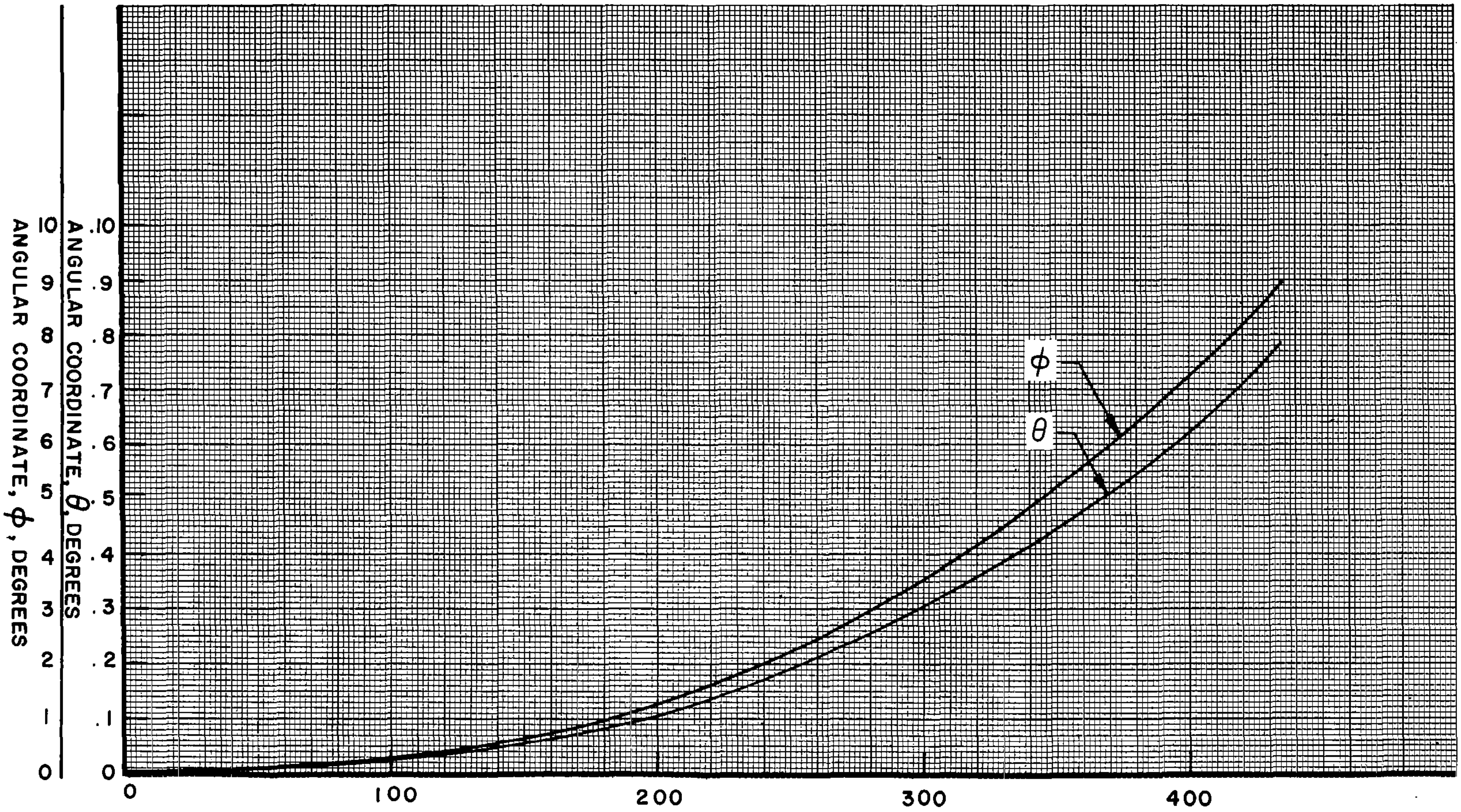

FIG 69. ANGULAR COORDINATES ϕ AND θ VS FLIGHT TIME $\left[(T/W)_0 = 2 \text{ AND } I_{sp} = 300 \text{ SEC.}\right]$

The above guessing game probably appears quite crude to anyone who has not attempted an actual isolation of the initial values of the Lagrange multipliers for a case of interest. Those who have worked in this area will find it more acceptable.

SECTION XI. CONCLUSIONS

The preceding material has covered, of necessity, a rather limited range of problems. This restriction is due to the requirement of obtaining all solutions numerically rather than analytically. The material presented will, hopefully, aid in initial estimates of the various multipliers necessary to obtain other cases of interest. The restriction of constant thrust is contrary to most material dealing with variational trajectory shaping, but is more acceptable to present day state-of-the-art considerations.

The necessary end-point conditions were stated symbolically and pursued no further since various engineering constraints usually leave no free end point. However, as was demonstrated in the numerical results, it is possible to maximize the mass fraction placed into orbit (for the case of prespecified orbital altitude) or maximize final altitude (if an angle of attack is specified at cutoff) by choice of the initial lunar thrust-to-weight ratio.

The orbit of maximum mass fraction is of interest from both academic and engineering considerations. This study was originally undertaken to verify the existence of this orbit. The problem is subtler than previously stated (Ref.3) in that a false maximum is predicted if the final angle of attack is specified to be zero; the predicted optima, however, depends upon the numerical integration step size. On the other hand, prespecification of the altitude that must be achieved at orbit predicts a thrust-to-weight ratio that maximizes the mass fraction injected into orbit independently of the numerical integration step size.

The orbit of maximum altitude occurs for low values of the initial thrust-to-weight ratio if the angle of attack is specified to be zero at cutoff. These trajectories are quite difficult to isolate due to the long burning times and instability with respect to the initial values of the multipliers. For thrust-to-weight ratios of less than four (or thereabouts), the altitudes for this type of trajectory become prohibitively low.

The cases which investigate an optimal value of the liftoff angle gamma produce very low orbits for a very small increase in mass fraction. Attempts to optimize mass fraction with respect to the initial value of the angle delta produced extremely unstable trajectories.

The first two sets of tables are more accurate than the following data since the integration stepsize is smaller. It is interesting to note that the later tables are internally consistent.

A final point with respect to the choice of initial thrust-to-weight ratio is that *maximum mass fraction does not correspond to maximum payload* (see example 5, Section X). The thrust-to-weight ratios that are labeled "optimum" refer to the overall mission viewpoint and not to the local viewpoint.

The problem of a choice of sign convention was numerically investigated for four cases; two of these four were treated in detail. The most important of these four is the sign convention of case number one (see Section VI). This particular sign convention is most important from an engineering viewpoint.

APPENDIX A

DERIVATION OF SECOND ORDER EULER EQUATIONS

The system of five first-order differential equations for λ_1, λ_2, λ_3, λ_4, λ_5 may be converted in a system of two second-order equations (for λ_1 and λ_2) and one first-order differential equation for λ_3 by either of two methods.

The first of these methods involves neglecting the kinematical substitutions for $\dot{r}$, $\dot{\theta}$, $\dot{\phi}$ and writing

$$F = \lambda_1 \left[\ddot{r} - \frac{T}{(m_0 - \dot{m}\, t)} \cos\delta \cos\gamma + \frac{M\,G}{r^2} - r\,(\dot{\theta}^2 + \dot{\phi}^2 \cos^2\theta) \right]$$

$$+ \lambda_2 \left[\ddot{\theta} - \frac{T}{(m_0 - \dot{m}\, t)\, r} \sin\delta + \frac{2\,\dot{r}\,\dot{\theta}}{r} + \dot{\phi}^2 \sin\theta \cos\theta \right]$$

$$+ \lambda_3 \left[\ddot{\phi} - \frac{T}{(m_0 - \dot{m}\, t)\, r \cos\theta} \cos\delta \sin\gamma - 2\,\dot{\theta}\,\dot{\phi} \tan\theta + \frac{2\dot{r}\,\dot{\phi}}{r} \right] \qquad \text{(A-1)}$$

The equations for λ_1, λ_2, λ_3 are now given by the second-order Euler equation

$$\frac{d^2}{dt^2}\left(\frac{\partial F}{\partial \ddot{y}_s}\right) - \frac{d}{dt}\left(\frac{\partial F}{\partial \dot{y}_s}\right) + \left(\frac{\partial F}{\partial y_s}\right) = 0 \quad (y_s = r,\ \theta,\ \phi) \qquad \text{(A-2)}$$

Note that

$$\frac{\partial F}{\partial \ddot{y}_s} = \lambda_s \qquad \text{(A-3)}$$

Thus, equation (A I-2) becomes

$$\ddot{\lambda}_s - \frac{d}{dt}\left(\frac{\partial F}{\partial \dot{y}_s}\right) + \left(\frac{\partial F}{\partial y_s}\right) = 0 \qquad \text{(A-4)}$$

Note that

$$\frac{\partial F}{\partial \phi} = 0 \qquad \text{(A-5)}$$

Thus, the Euler equation for λ_3 becomes

$$\ddot{\lambda}_3 - \frac{d}{dt}\left(\frac{\partial F}{\partial \dot{\phi}}\right) = \frac{d}{dt}\left(\dot{\lambda}_3 - \frac{\partial F}{\partial \dot{\phi}}\right) = 0$$

or

$$\dot{\lambda}_3 - \frac{\partial F}{\partial \dot{\phi}} = \text{constant} \qquad \text{(A-6)}$$

A second method of obtaining the second-order equations for λ_1 and λ_2 is to differentiate equations (88) and (89) with respect to time, and eliminate $\dot{\lambda}_3$, $\dot{\lambda}_4$, $\dot{\lambda}_5$, $\ddot{r}$, $\ddot{\theta}$, $\ddot{\phi}$ from the resulting equations by the use of equations (90), (91), (92), (85), (86) and (87).

By either of these methods we find the following:

$$\ddot{\lambda}_1 - \frac{2}{r}\dot{\lambda}_2\dot{\theta} - \lambda_1\left[\frac{2MG}{r^3} + (\dot{\theta}^2 - 3\dot{\phi}^2\cos^2\theta)\right] + \frac{2\lambda_2}{r}\left[\frac{2\dot{r}\dot{\theta}}{r} - \dot{\phi}^2\sin\theta\cos\theta\right]$$

$$+ \frac{2C_1\dot{\phi}}{r} - \frac{a(g_0)_{\text{\leftmoon}}(g_0)_{\oplus} I_{sp}}{[(g_0)_{\oplus} I_{sp} - a(g_0)_{\text{\leftmoon}} t]\, r^2\cos\theta}\left[\frac{\lambda_3^2 + \lambda_2^2\cos^2\theta}{\sqrt{(\lambda_1^2 r^2 + \lambda_2^2)\cos^2\theta + \lambda_3^2}}\right] = 0 \qquad \text{(A-7)}$$

$$\ddot{\lambda}_2 + 2\left(\dot{\lambda}_1 r\dot{\theta} - \frac{\dot{\lambda}_2\dot{r}}{r}\right) + \lambda_2\left[\frac{2MG}{r^3} + \frac{2\dot{r}^2}{r^2} + \dot{\phi}^2(4\sin^2\theta - 1) - 2\dot{\theta}^2\right]$$

$$- 2\lambda_1[\dot{r}\dot{\theta} + 2r\dot{\phi}^2\sin\theta\cos\theta] + 2\lambda_3\dot{\phi}\tan\theta(\dot{\theta}\tan\theta - \dot{r}/r)$$

$$- 2C_1\dot{\phi}\tan\theta + \frac{a(g_0)_{\text{\leftmoon}}(g_0)_{\oplus} I_{sp}}{[(g_0)_{\oplus} I_{sp} - a(g_0)_{\text{\leftmoon}} t]\, r}\left[\frac{\lambda_3^2\tan\theta\sec\theta}{\sqrt{(\lambda_1^2 r^2 + \lambda_2^2)\cos^2\theta + \lambda_3^2}}\right] = 0 \qquad \text{(A-8)}$$

$$\dot{\lambda}_3 + 2[(\lambda_1 r\cos\theta - \lambda_2\sin\theta)\dot{\phi}\cos\theta + \lambda_3(\dot{\theta}\tan\theta - \dot{r}/r)] + C_1 = 0 \qquad \text{(A-9)}$$

The set of equations listed above may be used as an alternative set to equations (88) - (92) in determining λ_1, λ_2, λ_3 (the only λ's that appear in the equations of motion). The initial value problem is no simpler in this case since we now must guess values of λ_1, $\dot{\lambda}_1$, λ_2, $\dot{\lambda}_2$, λ_3, C_1 to begin integration.

APPENDIX B

FREE-FLIGHT TRANSFER

Integration of the equations of motion under the assumption of zero thrust will be carried out in this Appendix. Although this assumption is contrary to the preceding development, it may often be desirable to assume that cutoff occurs at some condition other than a circular orbit. We might, for example, burn to parabolic velocity via a circular orbit or burn until an elliptical orbit of prespecified parameters is obtained. The following equations will aid in the choice of various cutoff conditions for such problems.

A number of the following equations are, in reality, nothing more than the Kepler equations in three dimensions, referenced to the equatorial plane. The standard techniques for integration of the two-body equations carry over almost directly. For this reason, no detailed developments will be included.

Under the assumption of zero thrust, the equations of motion may be written:

$$\ddot{r} = -\frac{MG}{r^2} + r\,(\dot{\theta}^2 + \dot{\phi}^2 \cos^2\theta) \tag{B-1}$$

$$\ddot{\theta} = -\frac{2\dot{r}\dot{\theta}}{r} - \dot{\phi}^2 \sin\theta\cos\theta \tag{B-2}$$

$$\ddot{\phi} = 2\,\dot{\theta}\,\dot{\phi}\,\tan\theta - \frac{2\dot{r}\dot{\phi}}{r} \tag{B-3}$$

Multiplying (B-3) by $r^2 \cos^2\theta$ an exact differential results and upon integration we find

$$r^2 \cos^2\theta\,\dot{\phi} = l_1 \tag{B-4}$$

where l_1 (an angular momentum) is a constant of integration.

Solving equation (B-4) for $\dot{\phi}^2$, substituting it into equation (B-2) and multiplying the result by $2r^4\dot{\theta}$ another exact differential results. Upon integration of this expression we find that

$$r^4\dot{\theta}^2 + \frac{l_1^2}{\cos^2\theta} = l_2^2 \tag{B-5}$$

where l_2 is the total angular momentum per unit mass.

Solving equation (B-5) for $\dot{\theta}^2$ and substituting it in equation (B-1), along with the expression for $\dot{\phi}^2$ derived above, we find

$$\ddot{r} = -\frac{MG}{r^2} + \frac{l_2^2}{r^3} \tag{B-6}$$

Multiplying this equation by $\dot{r}$ and integrating yields

$$\frac{1}{2}\dot{r}^2 = \frac{MG}{r} - \frac{1}{2}\frac{l_2^2}{r^2} + E \qquad \text{(B-7)}$$

where E is the total energy per unit mass.

The final integrations may now be undertaken. From equation (B-4) we can write

$$\frac{r^2 \cos^2\theta \, d\phi}{l_1} = dt \qquad \text{(B-8)}$$

and from this form the operator $\frac{d}{dt}$ as

$$\frac{d}{dt} = \frac{l_1}{r^2 \cos^2\theta} \frac{d}{d\phi} \qquad \text{(B-9)}$$

Writing equation (B-2) as

$$\frac{1}{r^2}\frac{d}{dt}\left[r^2 \frac{d}{dt}(\theta)\right] + \dot{\phi}^2 \sin\theta\cos\theta = 0 \qquad \text{(B-10)}$$

and substituting for $\dot{\phi}^2$ and $\frac{d}{dt}$ we find

$$\frac{l_1}{r^4\cos^2\theta}\frac{d}{d\phi}\left[\frac{l_1 r^2}{r^2\cos^2\theta}\frac{d\theta}{d\phi}\right] + \frac{l_1^2}{r^4\cos^4\theta}\sin\theta\cos\theta = 0 \qquad \text{(B-11)}$$

Noting that

$$\frac{1}{\cos^2\theta}\frac{d\theta}{d\phi} = \frac{d\tan\theta}{d\phi} \qquad \text{(B-12)}$$

equation (B-11) becomes

$$\frac{d^2(\tan\theta)}{d\phi^2} + \tan\theta = 0 \qquad \text{(B-13)}$$

which immediately yields

$$\tan\theta = A\sin(\phi + \phi_1) \qquad \text{(B-14)}$$

where ϕ_1 is an integration constant which determines the position of the vehicle in orbit. The amplitude constant A may be readily evaluated at the cutoff point as

$$A = \frac{\tan\theta_c}{\sin(\phi_c + \phi_1)} = \tan I \qquad \text{(B-15)}$$

The other constant of integration, ϕ_1, may be determined by the use of equation (40).

Solving equation (B-7) for

$$dt = \frac{dr}{\sqrt{2E + \frac{2MG}{r} - \frac{l_2^2}{r^2}}} \tag{B-16}$$

and equating dt to equation (B-8) we find

$$\frac{dr}{\sqrt{2E + \frac{2MG}{r} - \frac{l_2^2}{r^2}}} = \frac{r^2 \cos^2 \theta \, d\phi}{l_1} \tag{B-17}$$

The θ term appearing in the last equation may now be eliminated by equation (B-14) yielding

$$\frac{dr}{\sqrt{2E + \frac{2MG}{r} - \frac{l_2^2}{r^2}}} = \frac{r^2 d\phi}{l_1 (1 + \tan^2 \theta)} = \frac{r^2 d\phi}{l_1 [1 + A^2 \sin^2 (\phi + \phi_1)]}$$

Thus

$$\int \frac{dr}{r^2 \sqrt{2E + \frac{2MG}{r} - \frac{l_2^2}{r^2}}} = \int \frac{d\phi}{l_1 \, [1 + A^2 \sin^2 (\phi + \phi_1)]} \tag{B-18}$$

Equation (B-18) may now be integrated by setting $u = 1/r$. Carrying out the integrations yields

$$- \cos^{-1} \left[+ \frac{l_2^2 / r - MG}{\sqrt{(MG)^2 + 2E l_2^2}} \right] = \frac{l_2}{l_1 \sqrt{1 + A^2}} \tan^{-1} \left[\sqrt{1 + A^2} \, \tan (\phi + \phi_1) \right] \tag{B-19}$$

Solving for r gives

$$r = \frac{l_2^2}{MG + \sqrt{(MG)^2 + 2E l_2^2} \cos \left\{ \frac{l_2}{l_1 \sqrt{1 + A^2}} \tan^{-1} \left[\sqrt{1 + A^2} \, \tan (\phi + \phi_1) \right] \right\}} \tag{B-20}$$

Rearranging equation (B-20) into standard form

$$r = \frac{l_2^2 / MG}{1 + \sqrt{1 + \frac{2E l_2^2}{(MG)^2}} \cos \left\{ \frac{l_2}{l_1 \sqrt{1 + A^2}} \tan^{-1} \left[\sqrt{1 + A^2} \tan (\phi + \phi_1) \right] \right\}} \tag{B-21}$$

Two of the orbital parameters, the semi-major axis, a, and eccentricity, e, can be immediately recognized from equation (B-21) by requiring the orbit to be a conic section.

$$e = \sqrt{1 + \frac{2E l_2^2}{(MG)^2}} \tag{B-22}$$

$$a (1 - e^2) = \frac{l_2^2}{MG} \tag{B-23}$$

$$a = -\frac{MG}{2E} \tag{B-24}$$

The inclination may still be found by applying equation (40) to the cutoff values of ϕ_c and θ_c. These parameters will be required to study rendezvous techniques.

If no orbital inclination change is to occur during free-flight transfer, the above system of equations reduce to the more familiar Keplerian description; however, *the reference plane must be chosen as the same plane in which the vehicle achieves cutoff (i. e., circular) conditions.*

Equation (B-21) is far more complicated than necessary. We may begin the simplification by noting that, from (B-15)

$$\frac{l_2}{l_1 \sqrt{1 + A^2}} = \frac{l_2}{l_1 \sec I} \tag{B-25}$$

From equations (B-4) and (B-5), we have

$$\frac{l_2}{l_1 \sec I} = \frac{\sqrt{\dot\theta^2 + \dot\phi^2 \cos^2\theta}}{\cos^2\theta \sec I \cdot \dot\phi} \tag{B-26}$$

Differientating (B-14) with respect to time and substituting the value of A from (B-15) yields

$$\dot\theta = \frac{\tan I \cos(\phi + \phi_1)\dot\phi}{1 + \tan^2 I \sin^2(\phi + \phi_1)} \tag{B-27}$$

Eliminating $\dot\theta$ in equation (B-26) via equation (B-27) and the function of θ by

$$\cos\theta = \frac{1}{\sqrt{1 + \tan^2 I \sin^2(\phi + \phi_1)}} \tag{B-28}$$

yields

$$\frac{l_2}{l_1 \sec I} = 1 \tag{B-29}$$

The resultant trigonometric function appearing in equation (B-21) may now be readily simplified. We begin by noting that, for any argument, s,

$$\cos s = \frac{1}{\sqrt{1 + \tan^2 s}} \tag{B-30}$$

Thus, replacing $s \rightarrow \tan^{-1} s$ we find

$$\cos(\tan^{-1} s) = \frac{1}{\sqrt{1 + [\tan(\tan^{-1} s)]^2}} = \frac{1}{\sqrt{1 + s^2}} \tag{B-31}$$

From this

$$\cos\{\tan^{-1}[\sec I \tan(\phi + \phi_1)]\} = \frac{1}{\sqrt{1 + \sec^2 I \tan^2(\phi + \phi_1)}} \tag{B-32}$$

Replacing $\sec^2 I$ by its expression from equation (B-14) gives

$$\cos\{\tan^{-1}[\sec I \tan(\phi + \phi_1)]\} = \cos\theta \cos(\phi + \phi_1) \tag{B-33}$$

Assembling the results yields the final form of equation (B-21) as

$$r = \frac{a(1-e^2)}{1+e\cos\theta\cos(\phi+\phi_1)} \tag{B-34}$$

Equation (B-7) may be regarded as an expression for $\dot{r}$ in theory only. Numerical work with this equation shows that it is almost useless due to loss of significant figures. For this reason, we differentiate equation (B-34) with respect to time to obtain a useable equation for $\dot{r}$. Thus

$$\dot{r} = \frac{a(1-e^2)\,e\,[\sin\theta\cos(\phi+\phi_1)\,\dot{\theta} + \cos\theta\sin(\phi+\phi_1)\,\dot{\phi}]}{[1+e\cos\theta\cos(\phi+\phi_1)]^2}$$

$$= \frac{r^2 e\,[\sin\theta\cos(\phi+\phi_1)\,\dot{\theta} + \cos\theta\sin(\phi+\phi_1)\,\dot{\phi}]}{a(1-e^2)^2} \tag{B-35}$$

Eliminating θ and $\dot{\theta}$ as before we find

$$\dot{r} = \frac{(r^2\dot{\phi}\cos^2\theta)\,e\cos\theta\sec^2 I\sin(\phi+\phi_1)}{a(1-e^2)} \tag{B-36}$$

Substituting for $r^2\,\dot{\phi}\cos^2\theta$ from equation (B-4) and $a(1-e^2)$ from equation (B-23) gives

$$\dot{r} = e\left(\frac{l_1\sec I}{l_2}\right)\left(\frac{MG}{l_2}\right)\cos\theta\sec I\sin(\phi+\phi_1)$$

$$= e\left(\frac{MG}{l_2}\right)\cos\theta\sec I\sin(\phi+\phi_1) \tag{B-37}$$

by equation (B-29). A convenient form for this equation may be obtained if we eliminate sin $(\phi+\phi_1)$ by use of equation (B-14). For $I \neq 0$ we have

$$\dot{r} = e\left(\frac{MG}{l_2}\right)\sin\theta\csc I \tag{B-38}$$

For the case of $I = 0$ equation (B-37) becomes

$$\dot{r} = e\left(\frac{MG}{l_2}\right)\sin(\phi+\phi_1) \tag{B-39}$$

Another datum of importance along the trajectory is time. To obtain an expression for this quantity which retains significant figures during numerical manipulations, we write equation (B-16) in the form

$$dt = \frac{r\,dr}{\sqrt{2Er^2+2MGr-l_2^2}} \tag{B-40}$$

Substituting expressions for E and l_2^2 from equations (B-24) and (B-23), respectively, gives

$$dt = \sqrt{\frac{a}{MG}}\;\frac{r\,dr}{\sqrt{a^2e^2-(a-r)^2}} \tag{B-41}$$

The eccentric anomaly, $\mathfrak{E}$, may be introduced by defining

$$a - r = a\,e \cos \mathfrak{E} \tag{B-42}$$

From this definition comes

$$r = a\,(1 - e \cos \mathfrak{E}) \tag{B-43}$$

and

$$d r = a\,e \sin \mathfrak{E}\; d\,\mathfrak{E} \tag{B-44}$$

Substituting these expressions into equation (B-41) we find

$$d t = \sqrt{\frac{a^3}{M G}}\,(1 - e \cos \mathfrak{E})\; d\,\mathfrak{E} \tag{B-45}$$

or

$$t - t_1 = \sqrt{\frac{a^3}{M G}}\;(\mathfrak{E} - e \sin \mathfrak{E}) \tag{B-46}$$

The eccentric anomaly may now be related to a combination of the angles ϕ and θ as follows: Let us define

$$\cos \eta = \cos \theta \cos (\phi + \phi_1) \tag{B-47}$$

The geometrical significance of η is shown in FIG 78.

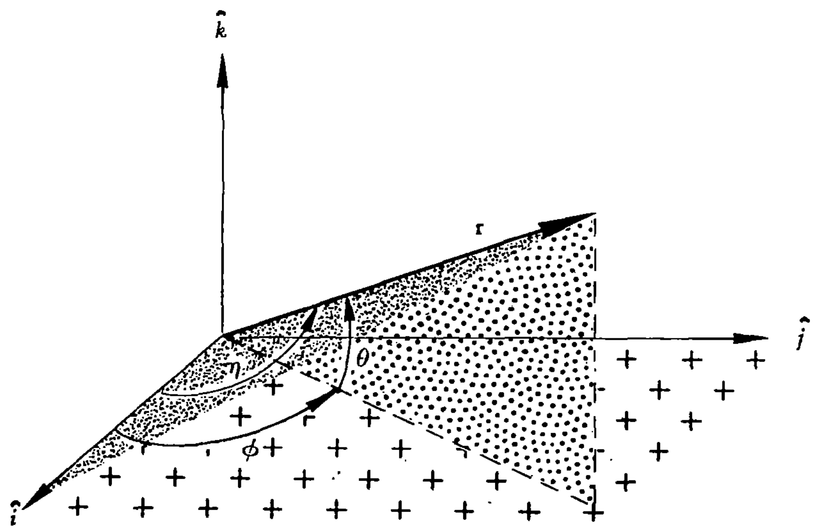

FIG 78. Geometrical Significance of η

Equating the expression for r from equations (B-34) and (B-43) and solving for $\cos\eta$ results in

$$\cos\eta = \frac{\cos\mathcal{E} - e}{1 - e\cos\mathcal{E}} \tag{B-48}$$

From this comes

$$1 + \cos\eta = \frac{(1-e)(1+\cos\mathcal{E})}{1 - e\cos\mathcal{E}} \tag{B-49}$$

and

$$1 - \cos\eta = \frac{(1+e)(1-\cos\mathcal{E})}{1 - e\cos\mathcal{E}} \tag{B-50}$$

Then

$$\sqrt{\frac{1-\cos\eta}{1+\cos\eta}} = \tan\frac{\eta}{2} = \sqrt{\frac{1+e}{1-e}}\tan\frac{\mathcal{E}}{2} \tag{B-51}$$

The preceding equations of this Appendix will be used to illustrate the method of attack that may be used to transfer from a circular orbit to another conic section.

At any point along the powered trajectory that occurs after passing through circular orbit, the values of r, $\dot{r}$, θ, $\dot{\theta}$, ϕ, $\dot{\phi}$ are known by numerical integration of equations (85) through (92). Thus, the function represented by equation (B-7).

$$E = \frac{1}{2}\left[\dot{r}^2 + r^2(\dot{\theta}^2 + \dot{\phi}^2\cos^2\theta)\right] - \frac{MG}{r} \tag{B-52}$$

serves to determine E. The eccentricity can now be specified from equations (B-4), (B-5), and (B-22) as

$$e = \sqrt{1 + \frac{2Er^4}{(MG)^2}(\dot{\theta}^2 + \dot{\phi}^2\cos^2\theta)} \tag{B-53}$$

and the semi-major axis as in equation (B-24)

$$a = -\frac{MG}{2E}$$

At each point the apogee altitude may be found from

$$r_a = a(1+e) \tag{B-54}$$

and the perigee altitude from

$$r_p = a(1-e) \tag{B-55}$$

If a "pseudo-Hohmann" transfer from circular orbit to a higher circular orbit is desired, the value of r_a will probably be prespecified (as well as the requirement that $r_p > r$). Several options are possible, such as requiring that the final altitude of the final circular orbit be equal to r_a. Or, one might require an elliptical orbit of period equal to that of the circular orbit. In any case, the powered flight continues until such time as the specified orbital parameters are attained. For a direct parabolic escape one would merely require that cutoff occurs at $E = 0$ ($r_a = \infty$).

APPENDIX C

COMPUTER FLOW DIAGRAMS

GENERAL DATA FLOW

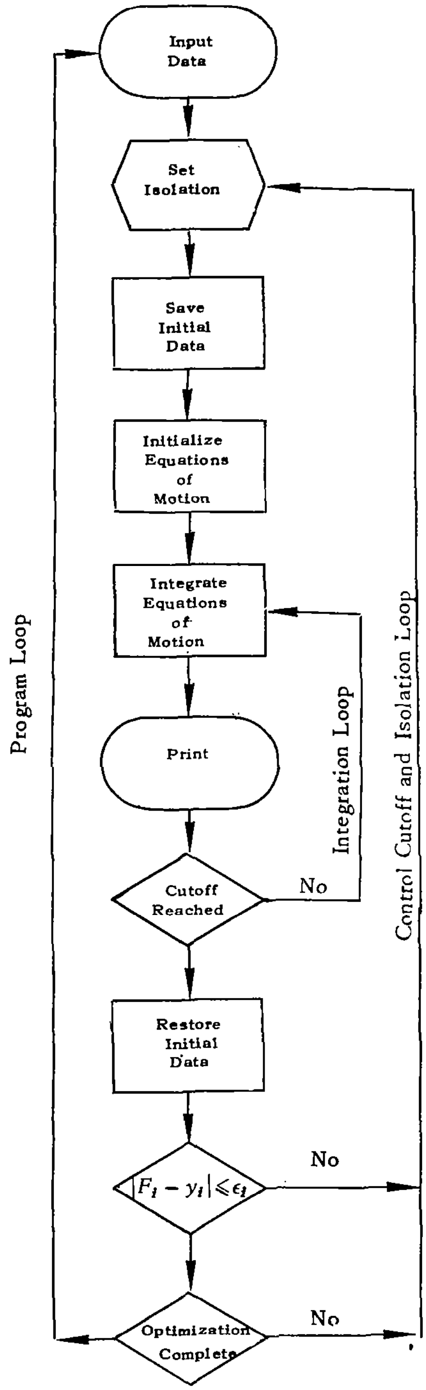

GENERAL DATA FLOW FOR COMPUTER

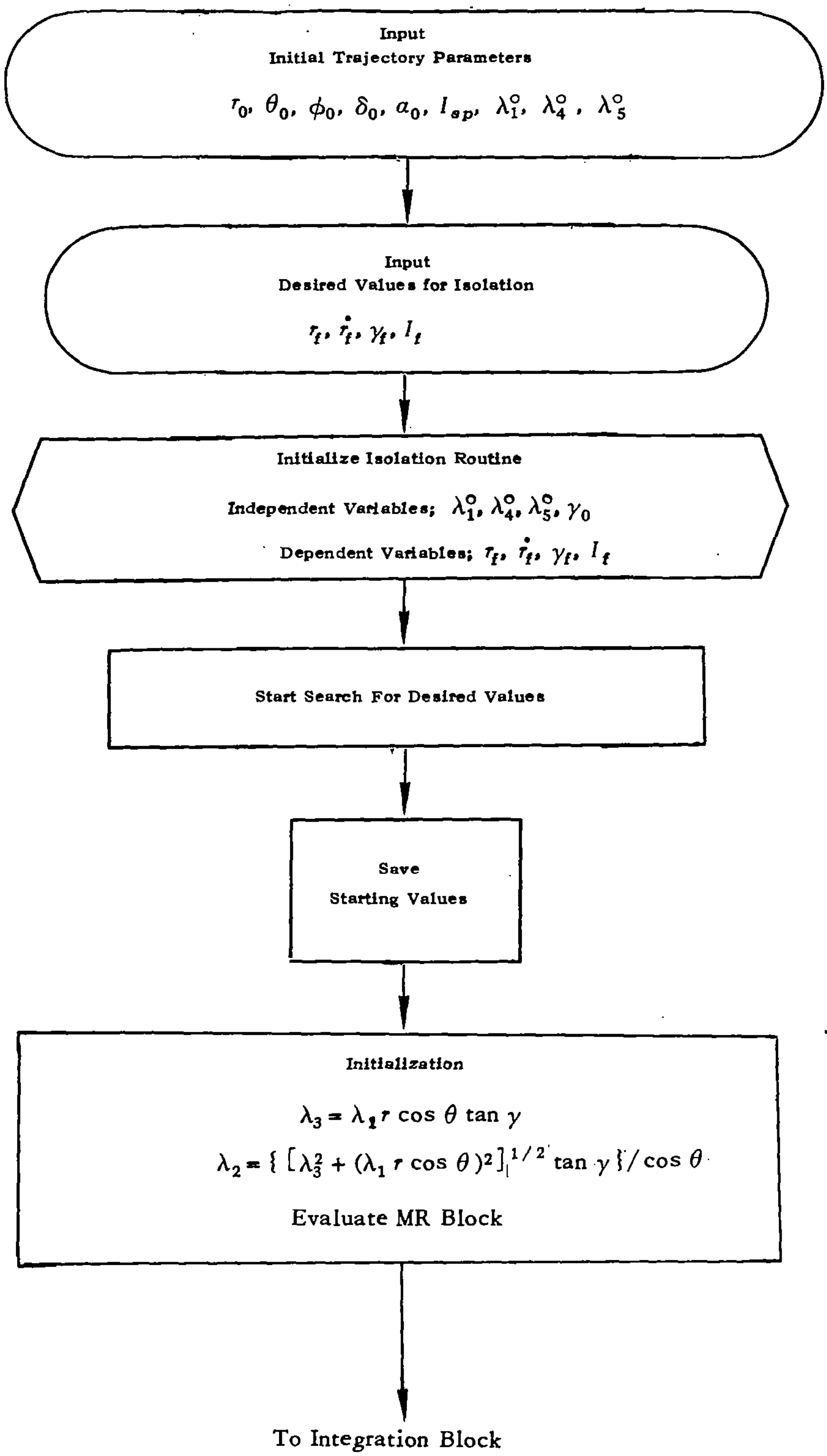

INTEGRATION BLOCK

n = Typical Time Step and m = 1, 2, 3, 4, 5

Save

$$r_n \to r_0;\ \theta_n \to \theta_0;\ \phi_n \to \phi_0;\ (\lambda_m)_n \to (\lambda_m)_0$$
$$\dot{r}_n \to \dot{r}_0;\ \dot{\theta}_n \to \dot{\theta}_0;\ \dot{\phi}_n \to \dot{\phi}_0;\ t_n \to t_0$$

↓

Compute

$$r_1 = r_0 + \dot{r}_0\ \Delta t/2$$
$$\dot{r}_1 = \dot{r}_0 + \ddot{r}_0\ \Delta t/2$$
$$\theta_1 = \theta_0 + \dot{\theta}_0\ \Delta t/2$$
$$\dot{\theta}_1 = \dot{\theta}_0 + \ddot{\theta}_0\ \Delta t/2$$
$$\phi_1 = \phi_0 + \dot{\phi}_0\ \Delta t/2$$
$$\dot{\phi}_1 = \dot{\phi}_0 + \ddot{\phi}_0\ \Delta t/2$$
$$(\lambda_m)_1 = (\lambda_m)_0 + (\dot{\lambda}_m)_0\ \Delta t/2$$
$$t_1 = t_0 + \Delta t/2$$

↓

Evaluate MR Block

$$\ddot{r} = f(r_1, \dot{r}_1, t_1);\ \ddot{\theta} = f(\theta_1, \dot{\theta}_1, t_1);\ \ddot{\phi} = f(\phi_1, \dot{\phi}_1, t_1);\ \dot{\lambda}_m = f[(\lambda_m)_1, t_1]$$

↓

Compute

$$r_2 = r_0 + \dot{r}_1\ \Delta t/2$$
$$\dot{r}_2 = \dot{r}_0 + \ddot{r}_1\ \Delta t/2$$
$$\theta_2 = \theta_0 + \dot{\theta}_1\ \Delta t/2$$
$$\dot{\theta}_2 = \dot{\theta}_0 + \ddot{\theta}_1\ \Delta t/2$$
$$\phi_2 = \phi_0 + \dot{\phi}_1\ \Delta t/2$$
$$\dot{\phi}_2 = \dot{\phi}_0 + \ddot{\phi}_1\ \Delta t/2$$
$$(\lambda_m)_2 = (\lambda_m)_0 + (\dot{\lambda}_m)_1\ \Delta t/2$$
$$t_2 = t_0 + \Delta t/2$$

↓

Evaluate MR Block

$$\ddot{r} = f(r_2, \dot{r}_2, t_2);\ \ddot{\theta} = f(\theta_2, \dot{\theta}_2, t_2);\ \ddot{\phi} = f(\phi_2, \dot{\phi}_2, t_2);\ \dot{\lambda}_m = f[(\lambda_m)_2, t_2]$$

Compute

$$r_3 = r_0 + \dot{r}_2 \, \Delta t$$
$$\dot{r}_3 = r_0 + \ddot{r}_2 \, \Delta t$$
$$\theta_3 = \theta_0 + \dot{\theta}_2 \, \Delta t$$
$$\dot{\theta}_3 = \dot{\theta}_0 + \ddot{\theta}_2 \, \Delta t$$
$$\phi_3 = \phi_0 + \dot{\phi}_2 \, \Delta t$$
$$\dot{\phi}_3 = \dot{\phi}_0 + \ddot{\phi}_2 \, \Delta t$$
$$(\lambda_m)_3 = (\lambda_m)_0 + (\dot{\lambda}_m)_2 \Delta t$$
$$t_3 = t_0 + \Delta t$$

↓

Evaluate MR Block

$$\ddot{r} = f(r_3, \dot{r}_3, t_3); \quad \ddot{\theta} = f(\theta_3, \dot{\theta}_3, t_3); \quad \ddot{\phi} = f(\phi_3, \dot{\phi}_3, t_3); \quad \dot{\lambda}_m = f[(\lambda_m)_3, t_3]$$

↓

Compute

$$r_{n+1} = r_0 + (\dot{r}_0 \Delta t + 2 \dot{r}_1 \Delta t + 2 \dot{r}_2 \Delta t + \dot{r}_3 \Delta t)/6$$
$$\dot{r}_{n+1} = \dot{r}_0 + (\ddot{r}_0 \Delta t + 2 \ddot{r}_1 \Delta t + 2 \ddot{r}_2 \Delta t + \ddot{r}_3 \Delta t)/6$$
$$\theta_{n+1} = \theta_0 + (\dot{\theta}_0 \Delta t + 2 \dot{\theta}_1 \Delta t + 2 \dot{\theta}_2 \Delta t + \dot{\theta}_3 \Delta t)/6$$
$$\dot{\theta}_{n+1} = \dot{\theta}_0 + (\ddot{\theta}_0 \Delta t + 2 \ddot{\theta}_1 \Delta t + 2 \ddot{\theta}_2 \Delta t + \ddot{\theta}_3 \Delta t)/6$$
$$\phi_{n+1} = \phi_0 + (\dot{\phi}_0 \Delta t + 2 \dot{\phi}_1 \Delta t + 2 \dot{\phi}_2 \Delta t + \dot{\phi}_3 \Delta t)/6$$
$$\dot{\phi}_{n+1} = \dot{\phi}_0 + (\ddot{\phi}_0 \Delta t + 2 \ddot{\phi}_1 \Delta t + 2 \ddot{\phi}_2 \Delta t + \ddot{\phi}_3 \Delta t)/6$$
$$(\lambda_m)_{n+1} = (\lambda_m)_0 + [(\dot{\lambda}_m)_0 \Delta t + 2 (\dot{\lambda}_m)_1 \Delta t + 2 (\dot{\lambda}_m)_2 \Delta t + (\dot{\lambda}_m)_3 \Delta t]/6$$
$$t_{n+1} = t_0 + \Delta t$$

↓

Evaluate MR Block

$$\ddot{r} = f(r_{n+1}, \dot{r}_{n+1}, t_{n+1}); \quad \ddot{\theta} = f(\theta_{n+1}, \dot{\theta}_{n+1}, t_{n+1}); \quad \ddot{\phi} = f(\phi_{n+1}, \dot{\phi}_{n+1}, t_{n+1}); \quad \dot{\lambda}_m = f[(\lambda_m)_{n+1}, t_{n+1}]$$

↓

To Control Block

CONTROL BLOCK

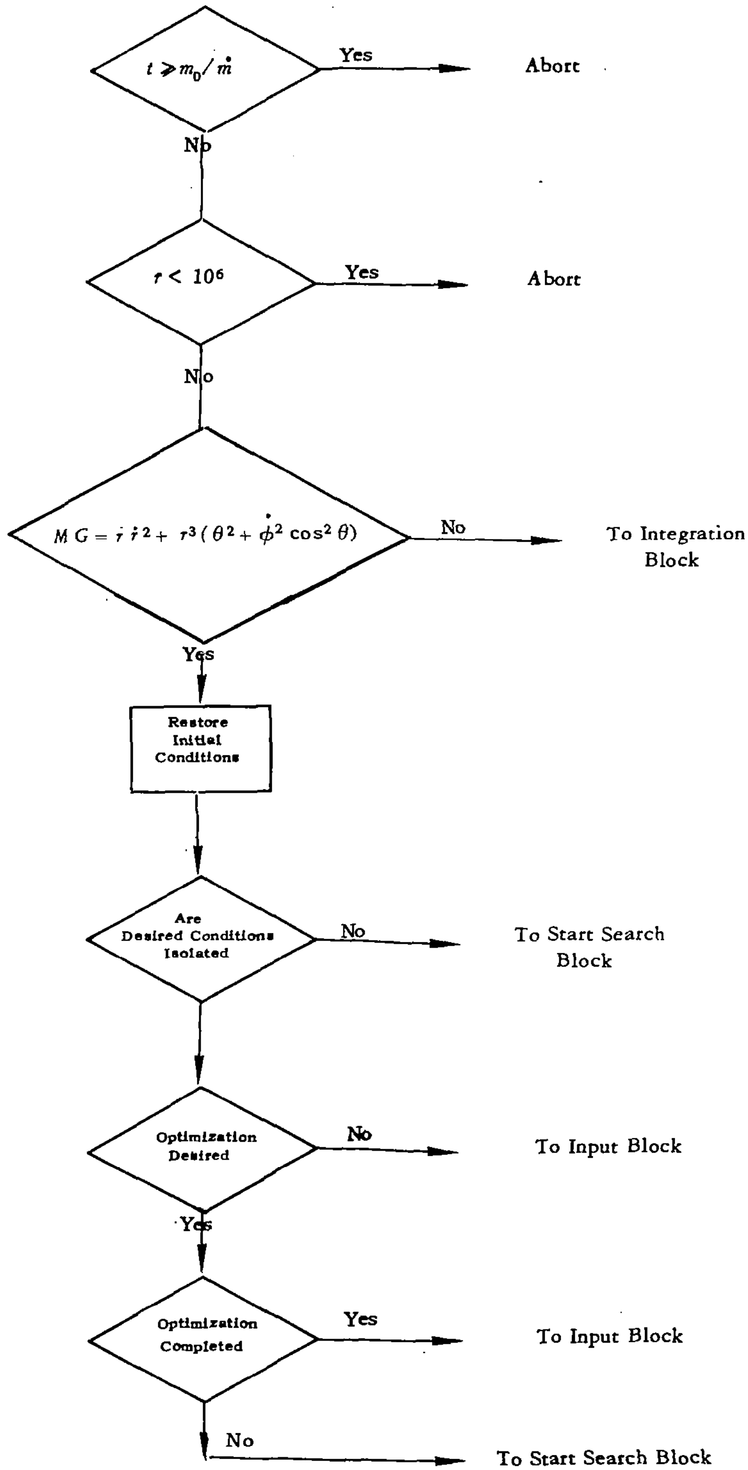

MR BLOCK

Compute

$$\ddot{r} = \left[\frac{a\,(g_0)_{\text{\(}}\,(g_0)_{\oplus}\,I_{sp}}{(g_0)_{\oplus}\,I_{sp} - a\,(g_0)_{\text{\(}}\,t}\right]\left[\frac{\lambda_1\,r\cos\theta}{\sqrt{(\lambda_1^2 r^2 + \lambda_2^2)\cos^2\theta + \lambda_3^2}}\right] - \frac{MG}{r^2} + r\,(\dot{\theta}^2 + \dot{\phi}^2\cos^2\theta)$$

$$\ddot{\theta} = \left[\frac{a(g_0)_{\text{\(}}\,(g_0)_{\oplus}\,I_{sp}}{(g_0)_{\oplus}\,I_{sp} - a\,(g_0)_{\text{\(}}\,t}\right]\left[\frac{\lambda_2\cos\theta}{r\sqrt{(\lambda_1^2\,r^2 + \lambda_2^2)\cos^2\theta + \lambda_3^2}}\right] - \frac{2\dot{r}\dot{\theta}}{r} - \dot{\phi}^2\sin\theta\cos\theta$$

$$\ddot{\phi} = \left[\frac{a\,(g_0)_{\text{\(}}\,(g_0)_{\oplus}\,I_{sp}}{(g_0)_{\oplus}\,I_{sp} - a\,(g_0)_{\text{\(}}\,t}\right]\left[\frac{\lambda_3}{r\cos\theta\sqrt{(\lambda_1^2\,r^2 + \lambda_2^2)\cos^2\theta + \lambda_3^2}}\right] + 2\dot{\theta}\dot{\phi}\tan\theta - \frac{2\,\dot{r}\,\dot{\phi}}{r}$$

$$\dot{\lambda}_1 = \frac{2}{r}\quad(\lambda_2\,\dot{\theta} + \lambda_3\,\dot{\phi}) - \lambda_4$$

$$\dot{\lambda}_2 = -2\,(\lambda_1 r\,\dot{\theta} - \frac{\lambda_2\dot{r}}{r} + \lambda_3\dot{\phi}\tan\theta) - \lambda_5$$

$$\dot{\lambda}_3 = -2[(\lambda_1 r\cos\theta - \lambda_2\sin\theta)\,\dot{\phi}\cos\theta + \lambda_3(\dot{\theta}\tan\theta - \frac{\dot{r}}{r})] - C_1$$

$$\dot{\lambda}_4 = -\lambda_1\left[\frac{2MG}{r^3} + (\dot{\theta}^2 + \dot{\phi}^2\cos^2\theta)\right] - \frac{2\dot{r}}{r^2}\,(\lambda_2\dot{\theta} + \lambda_3\dot{\phi})$$
$$- \left[\frac{a\,(g_0)_{\text{\(}}\,(g_0)_{\oplus}\,I_{sp}}{(g_0)_{\oplus}\,I_{sp} - a\,(g_0)_{\text{\(}}\,t}\right]\left[\frac{(\lambda_2^2\cos^2\theta + \lambda_3^2)}{r^2\cos^2\theta\sqrt{(\lambda_1^2 r^2 + \lambda_3^2)\cos^2\theta + \lambda_3^2}}\right]$$

$$\dot{\lambda}_5 = \dot{\phi}^2(\lambda_1 r\sin 2\theta + \lambda_2\cos 2\theta) - 2\lambda_3\dot{\theta}\dot{\phi}\sec^2\theta - \left[\frac{a(g_0)_{\text{\(}}(g_0)_{\oplus}\,I_{sp}}{(g_0)_{\oplus}\,I_{sp} - a(g_0)_{\text{\(}}\,t}\right]\left[\frac{\lambda_3^2\tan\theta\sec\theta}{r\sqrt{(\lambda_1^2 r^2 + \lambda_2^2)\cos^2\theta + \lambda_3^2}}\right]$$

George C. Marshall Space Flight Center
National Aeronautics and Space Administration
Huntsville, Alabama, 1963

REFERENCES

1. Breakwell, John V.: *The Optimization of Trajectories.* NAA, Adv. Engng. AL-2706, Aug. 24, 1957; also, J. Soc. Indust. and App. Math., V. 7, No. 2, June, 1959, p. 215-247; also, Chapter 12, General Research in Flight Science, January 1959 - January 1960, Vol. III, Flight Dynamics and Space Mechanics, LMSD-288139, Jan., 1960; also, AD-209 092.

2. Burns, Rowland E.: *Correlative Survey Report on Powered Flight Trajectory Optimization Including an Extensive Critical Bibliography.* ARS Space Flight Report to the Nation, October 9-15, 1961, No. 2071-61.

3. Burns, Rowland E. and Singleton, Larry G.: *Ascent From the Lunar Surface.* NASA TN D-1644, June, 1963.

4. Krause, Helmut G. L.: *The Secular and Periodic Perturbations of the Orbit of an Artificial Earth Satellite.* Presented at the VII International Astronautical Congress, Rome, Sept. 17-22, 1956. Translated by Army Ballistic Agency, Huntsville, Alabama as ABMA Misc. 75; also, AD-208 900.

5. Krause, Helmut G. L.: *Comparison of Precalculated Orbital Elements of the Army Explorer Satellites With the Actual Elements Derived From Observations.* Army Ballistic Missile Agency Report DSP-TR-2-60, June 20, 1960.

6. Silver, Sidney: Share; Book no. D-3, Installation JPL, Title, SRCH.